https://ntrs.nasa.gov/search.jsp?R=19730024093 2020-03-23T01:19:09+00:00Z

NASA CR 121216
MDC E0784

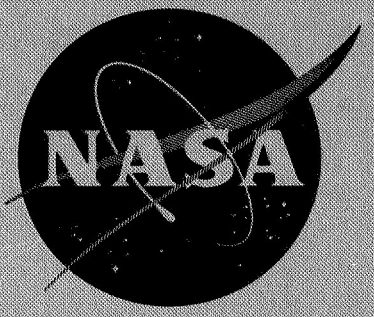

CASE FILE COPY

FINAL REPORT

FUSED SLURRY SILICIDE COATINGS FOR COLUMBIUM ALLOY REENTRY HEAT SHIELDS

Volume I Evaluation Analysis

by

Barry Fitzgerald

MCDONNELL DOUGLAS ASTRONAUTICS COMPANY - EAST

Saint Louis, Missouri

August 1973

prepared for

NATIONAL AERONAUTICS AND SPACE ADMINISTRATION

NASA LEWIS RESEARCH CENTER

CONTRACT NAS3-14307

John P. Merutka, Project Manager

1. Report No.	2. Government Accession No.	3. Recipient's Catalog No.
CR-121216		

4. Title and Subtitle	5. Report Date
Fused Slurry Silicide Coatings for Columbium Alloy Reentry Heat Shields, Volume I , Evaluation Analysis	August 1973
	6. Performing Organization Code: Evaluation Analysis
7. Author(s): Barry Fitzgerald	8. Performing Organization Report No.: MDC E0784
9. Performing Organization Name and Address: McDonnell Douglas Astronautics Company - East, St. Louis, Missouri 63166	10. Work Unit No.
	11. Contract or Grant No.: NAS3-14307
12. Sponsoring Agency Name and Address: National Aeronautics and Space Administration, Washington, D. C. 20546	13. Type of Report and Period Covered: Contractor Report
	14. Sponsoring Agency Code

15. Supplementary Notes

Project Manager, John P. Merutka, NASA Lewis Research Center, Cleveland, Ohio

16. Abstract

The R-512E (Si-20Cr-20Fe) fused slurry silicide coating process was optimized to coat full size (20" x 20") single face rib and corrugation stiffened panels fabricated from FS-85 columbium alloy for 100 mission Space Shuttle heat shield applications. Structural life under simulated Space Shuttle lift-off stresses and reentry conditions demonstrated reuse capability well beyond 100 flights for R-512E coated FS-85 columbium heat shield panels. Demonstrated coating damage tolerance showed no immediate structural failure on exposure. The FS-85 columbium alloy was selected from five candidate alloys (Cb-752, C-129Y, WC-3015, B-66 and FS-85) based on the evaluation tests which were designed to:

1. Determine the change in material properties due to coating and reuse,
2. Determine the alloy tolerance to coating damage,
3. Determine the coating emittance characteristics under reuse conditions, and
4. Determine new coating chemistries for improved coating life.

The experimental and coating process details of this work is presented in CR-134483, Vol. II, Experimental and Coating Process Details

17. Key Words (Suggested by Author(s))	18. Distribution Statement
oxidation resistant coatings columbium alloys fused slurry silicide coatings heat shields	unclassified - unlimited

19. Security Classif. (of this report)	20. Security Classif. (of this page)	21. No. of Pages	22. Price*
unclassified	unclassified	144	$3.00

* For sale by the National Technical Information Service, Springfield, Virginia 22151

Copy No. 6

FOREWORD

This is the Final Technical Report on NASA-Lewis Research Center Contract NAS3-14307. The program, "Fused Slurry Silicide Coatings for Columbium Alloy Reentry Heat Shields," was conducted between June 1970 and February 1973. Mr. John P. Merutka of NASA-Lewis Research Center's Material and Structures Division was the Project Manager. The McDonnell Douglas Astronautics Company - East Study Manager was Mr. Barry Fitzgerald.

The subcontract work on slurry process optimization was performed by HiTemCo under the technical direction of Barry Reznik with Sy Priceman assisting. Mr. Larry Sama is the Manager of Operations at HiTemCo and assisted in the preparation of the final report.

The contributions of the following individuals at MDAC-E are acknowledged: Dr. R. G. Gregory and J. K. Lehman, Strength Analysis and Rib Stiffened Panel Optimization Study; F. S. Pogorzelski, Panel Fabrication; M. B. Munsell, Reentry Simulation; and R. J. Schmitt, Emittance Measurements.

This report is divided into two volumes. Volume I, CR-121216, is the evaluation analysis summary; Volume II, CR-134483, presents the experimental and coating process details.

TABLE OF CONTENTS

TABLE OF CONTENTS (Continued)

LIST OF PAGES

Title Page

ii -- viii

1 -- 144

ILLUSTRATIONS

ILLUSTRATIONS (Continued)

ILLUSTRATIONS (Continued)

TABLES

I

SUMMARY

In this program, studies were conducted to optimize the coating process and more fully characterize fused slurry silicide coated columbium alloys for use as heat shields on Space Shuttle vehicles. Much of the characterization effort was performed concurrently with the slurry process scaleup optimization.

1.0 EVALUATION OF COATED COLUMBIUM SHEET AND HEAT SHIELD PANELS

Test conditions for reuse evaluation of fused slurry silicide coated columbium alloys were selected to be representative of a Space Shuttle operational system. The selected conditions of temperature, pressure and stress were not representative of a particular point on a specific vehicle but were designed to encompass the severe elements of any probable trajectory.

Five columbium alloys (Cb-752, C-129Y, FS-85, B-66, and WC-3015) were evaluated in a series of tests to determine the optimum alloy for Space Shuttle heat shields. Evaluations included a weldability and ductile to brittle transition temperature test, mechanical property changes due to coating and reuse, and the effect of reuse on emittance.

Fabrication Tests - All five alloys successfully passed a welding test in which a circular weld was made on a restrained sheet of material and visually examined for cracking.

Ductile to brittle transition temperature (DBTT) tests were conducted as a measure of fabricability. The high DBTT for the WC-3015 alloy makes fabrication and handling of thin gage heat shields of this alloy very difficult. The moderately low DBTT for the B-66 alloy was not as low as desired since slight variations in chemistry or annealing temperature could raise the DBTT above room temperature. The other three alloys, Cb-752, FS-85, and C-129Y, had DBTT's that were low enough to allow variations in the parameters that affect DBTT and still remain below room temperature.

Mechanical Properties - The effects of coating and reuse on the mechanical properties of the five columbium alloys were determined by tensile testing standard sheet specimens that were coated and conditioned. Exposure was representative of the reentry flight of Space Shuttle Orbiter vehicle temperature and pressure profiles. Coated tensile specimens were exposed in both a defected and nondefected condition. Defecting consisted of removing a spot of coating 0.030" (0.076 cm) in

diameter from one side of the 0.25" (0.6 cm) wide by 1.0" (2.5 cm) specimen gage length. In the nondefected condition coated tensile specimens were exposed to 50 and 100 reentry cycles. Defected specimens were exposed for 5 to 10 cycles in the external pressure environment and 50 cycles in the internal pressure environment. The coating caused no loss of ultimate or yield strength for any of the five alloys when the metal consumed during coating formation was accounted for. There was a loss in tensile elongation for all alloys. The effects of reuse cycling and defecting plus reuse cycling on ultimate tensile strength of the five alloys are shown in Figures 5-13 through 5-17, Section 5.0. Reuse cycling caused no significant loss in mechanical properties except for the WC-3015 at room temperature. Defecting produced significant loss in room temperature properties after reuse cycling, but elevated temperature properties were not significantly degraded.

Emittance Tests - Specimens of the five columbium alloys were coated with the R-512E coating and then exposed to 2400°F (1300°C) external pressure reentry cycling to determine the effects of reuse on emittance. Three specimens of each alloy were removed after 9, 24, 49 and 99 cycles of exposure. An additional cycle of exposure using resistance heating was accomplished in the emissometer during emittance measurements. Because of difficulties encountered in attaching thermocouples directly to the thin sheet samples, a new method using ultraviolet pyrometry was developed to measure specimen time temperature. Temperature and emittance were calculated by iteration from the thermopile infrared detector and the optical pyrometer outputs. The emittance at 2400°F (1300°C) is approximately 0.9 and is affected very little by reentry cycling or reuse (see Figures 3-5 through 3-9, Section 3.0, Volume II).

Analytical Testing - X-ray diffraction, x-ray fluorescence, and electron microprobe techniques were used to study the effects of reuse on coating chemistry. There were no major effects or differences in chemistry due to reuse. The major conclusion that can be drawn from the electron microprobe analysis is the excellent stability of the elements in the R-512E coating on FS-85 with respect to furnace simulated reentry cycling.

Reuse Studies - Test results from mechanical property, coating chemistry optimization, chemistry and structure, and emittance studies were reviewed to choose the three alloys most suitable for heat shield panel applications. The three columbium alloys selected were: FS-85, Cb-752 and C-129Y. Five panels

(1" x 4") each of R-512E coated FS-85 and Cb-752 and four panels (1" x 4") of C-129Y were tested. One hundred cycle reuse capability was successfully demonstrated for all three alloy/coating systems. The overall screening test results showed that FS-85 was the best alloy; therefore coated FS-85 was selected for the coating/alloy evaluations to be performed in the remainder of the program.

Subsize 3" x 12" (7.5 cm x 30 cm) rib stiffened FS-85 heat shield panels coated with 3.0 mils (75 μm) of R-512E coating were subjected to the temperature, pressure, and stress representative of reentry flight profile conditions for a Space Shuttle Orbiter for this study. Eight panels were exposed to flight simulation conditions for 200 cycles. Evidence of the first incipient coating failure for the eight panels tested did not become apparent until after 66 flight simulation cycles. Two panels showed no evidence of coating failures until after 200 flight simulation cycles had been completed. All incipient coating failures, which occurred prior to 176 flight simulation cycles, were edge failures. One surface failure occurred after 176 flight simulation cycles. Times to incipient coating failures were examined statistically utilizing Weibull distribution. Rank tables were used because of the small sample size. Median rank values for the incipient times to failure are shown plotted on Weibull probability paper in Figure 1. Also shown are the 5% and 95% rank curves which encompass 90% of the total population of test data for an infinite number of samples.

Structural life for seven of the eight panels exceeded 200 reentry cycles for the test conditions employed. The one structural failure was a fatigue failure which occurred during the last acoustic exposure (simulating lift-off conditions) after the panel had been reentry cycled 200 times. The panel had successfully passed 176 complete flight simulations. The fatigue failure started at a coating failure site on one of the rib stiffeners. This coating failure site was first evident after 176 reentry cycles. Other edge incipient coating failures (some of which occurred at 66 reentry cycles) had no effect on structural integrity up to 200 reentry cycles.

Localized Coating Damage - An investigation was conducted to determine the effect of local coating damage on the structural integrity of coated FS-85 rib and corrugation stiffened panels. The panels and test conditions were identical to those utilized in the coating reuse life studies. Prior to reentry simulation, each panel was intentionally defected at one to three sites to simulate coating damage. An area of coating approximately 1/8" (0.32 cm) in diameter was removed by grit blasting at each site.

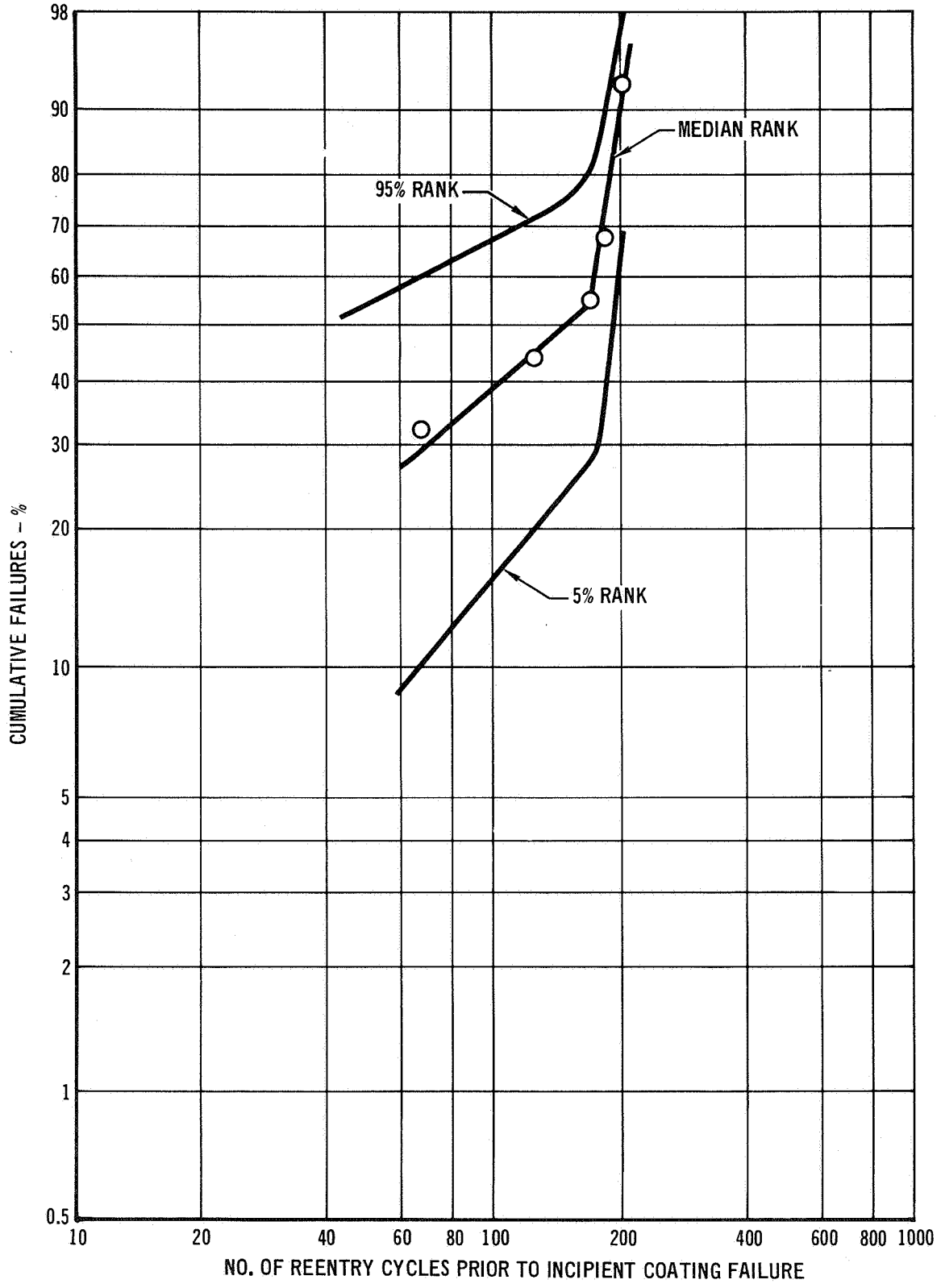

WEIBULL PLOT OF INCIPIENT COATING FAILURE ON 3" x 12" PANELS

NOTE: SAME AS TEXT FIGURE 11-12

FIGURE 1

The performance of all of the defected panels, considering the acoustic condition and defect size utilized, showed that FS-85 columbium alloy heat shields are quite tolerant of local coating damage. No immediate catastrophic failures occurred. Even under the severe acoustic conditions and worst case defect location, the defected heat shields survived a minimum of 20 reentry flights.

The results of creep and elastic deflection measurements made during reentry testing of defected panels did not vary appreciably from those obtained on non-defected panels.

The defecting showed no effect of the ability of the panels to withstand static design loads. Depending on defect location, the fatigue life was reduced as much as 80%, by the defecting and subsequent contamination and oxidation during exposure.

2.0 COATING PROCESS OPTIMIZATION AND SCALEUP STUDIES

The objective of this study was to optimize a slurry or slurries, so that full size 20" x 20" (50 cm x 50 cm) rib and corrugation stiffened panels could be coated uniformly and reproducibly. The basic R-512E (Si-20Cr-20Fe) coating was used throughout the study.

Screening - Thirty-two slurry compositions were prepared and evaluated on a basis of dipping and drying rates, coating thickness, coating uniformity top to bottom, streaking, sagging, and edge pull back. Twenty-seven of the slurries used an acrylic resin for a binder and five slurries used a nitrocellulose lacquer.

One nitrocellulose based and one acryllic based slurry was selected for coating process optimization and the coating of the full size rib and corrugation stiffened panels respectively.

Chemistry Variations - Possible variation in coating chemistry obtained with the dipping process were determined by coating a 20" x 20" (50 cm x 50 cm) flat stainless steel mockup. Samples from the green coating were selectively removed from 2" (5 cm) square areas in nine locations on the panel. The coating powder obtained was analyzed for chromium and iron by x-ray fluorescence techniques, the results are shown in Figure 2. The iron content was found to vary from 19.0 to 20.0%, chromium from 19.5 to 22%, and silicon from 58.6 to 61.0%. Since the nominal slurry composition is 60% Si, 20% Cr, and 20% Fe, the analyzed values indicate the effectiveness of the process and stability of the slurry.

Edge Coating Methods - Several edge coating methods were evaluated. A paint striping tool method of applying a bead of slurry directly to the edges was developed which significantly improved coating life. Cb-752 samples were evaluated by slow oxidation testing at one atmosphere in the as-dipped, oversprayed, and beaded edge conditions. The results of these tests are shown in Figure 3. In another slow cycle, one atmosphere test, Cb-752 coated panel segments with the edge bead coating had lives in excess of 100 cycles.

Composition Optimization - A study was performed to select a coating chemistry for the C-129Y and FS-85 alloys that would offer better protection than the R-512E (Si-20Cr-20Fe) coating. Several basic compositions (Si-20Ti-10Mo; Si-20Cr-20Fe; Si-20Cr-5Ti; Si-40Cr-10Mo; Si-20Cr-10W; and Si-20Ti-3V) were applied to the C-129Y and FS-85 alloys and screened at 2400°F (1300°C) through slow cycle oxidation and reduced pressure profile tests to determine their protectibility. Coating compositions with higher than 20% Cr showed the most promise. The best performing coating on FS-85 was Si-40Cr-20Fe and the best performing coating on C-129Y was Si-35Cr-20Fe. The decision was made not to change to the 35 or 40% Cr content coatings for the remainder of the program because the improvement in life was not considered significant enough to warrant a change.

Subsize Panel Tests - Ten subsize, 3" x 12" (7.5 cm x 30 cm), rib and corrugation stiffened FS-85 panels were used to verify the effectiveness and reproducibility of the coating produced from the optimized acrylic and nitrocellulose slurries and application processes. These panels were evaluated like the 1" x 4" panels under the simulation of temperature, pressure, and stress conditions representing a Space Shuttle Orbiter reentry with the addition of an acoustic simulation of the lift-off environment. Panels were evaluated up to 100 reentry flight cycles. There was no breakdown of coating produced by the environment. Structural failures were experienced on all panels due to fatigue from the acoustic testing. The acoustic environment was designed to cause fatigue failures at approximately 100 flight cycles. Based on the results of the test, the fatigue life at 10,000 psi (69 MN/m^2) is somewhere between 650,000 and 760,000 cycles (100 flight cycles).

Scaleup Test - As final verification of the coating application process, full size 20" x 20" (50 cm x 50 cm) rib and corrugation stiffened FS-85 columbium alloy heat shield panels were coated. An average green coating weight of 24 mg/cm^2 was achieved with a range as determined by Dermitron NDT of 21 to 27 mg/cm^2. The edges

of the panels were coated by the edge beading technique and diffusion treated for one hour at 2580°F (36 hsec at 1420°C). After firing the panels, the coating was found to have local thickness variations that were within the program goal of ± 3 mg/cm^2. This is better than a 50% reduction in the ± 7 mg/cm^2 variation typical prior to this process optimization study.

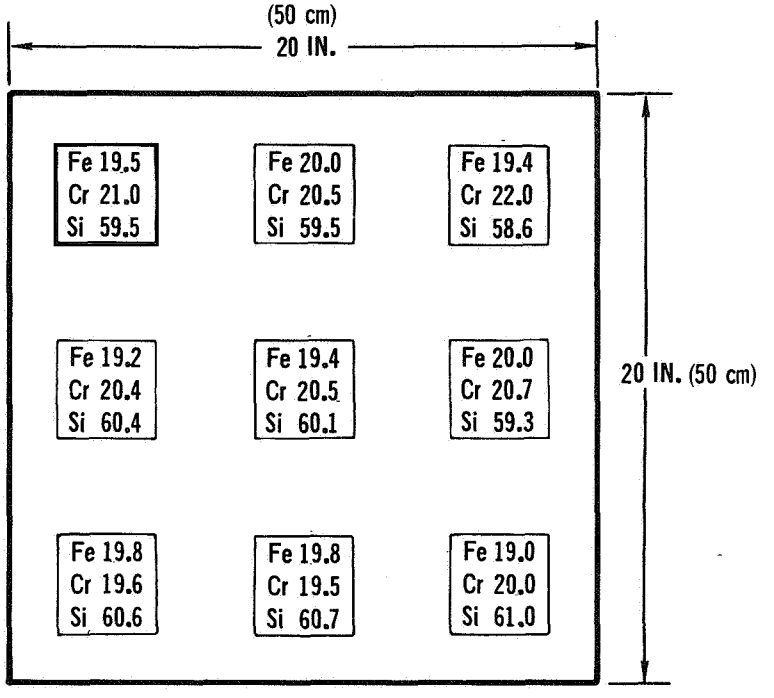

COATING COMPOSITION UNIFORMITY ON 20 IN. x 20 IN. (50 CM x 50 CM) FLAT STAINLESS MOCKUP

NOTE: SAME AS TEXT FIGURE 8-3

FIGURE 2

CONDITION	EDGE THICKNESS NDT (MILLIVOLTS) COPPER PROBE	1 ATMOSPHERE SLOW CYCLIC OXIDATION LIFE
AS DIPPED	-0.2	2 CYCLES
AS DIPPED AND OVERSPRAYED	+0.2	20-50 CYCLES
AS DIPPED AND SLURRY BEADED	+0.4	75-150 CYCLES

EFFECT OF EDGE COATING METHOD ON PERFORMANCE R-512E COATING

NOTE: SAME AS TEXT TABLE 8-4

FIGURE 3

II

INTRODUCTION

Continued exploration and utilization of Outer Space will depend on development of economical manned vehicle systems. A NASA System, Space Shuttle, currently being developed is relying heavily on reusability for economy. The Space Shuttle will have the aerodynamic maneuvering characteristics of an airplane for horizontal earth landing and still possess the capability of withstanding spacecraft reentry temperatures. A fully reusable thermal protection system (TPS) capable of withstanding static and dynamic loading as well as the heat of reentry will be a major factor in the success of the Space Shuttle vehicles.

Coated columbium is a prime candidate for reusable Space Shuttle heat shielding because of its efficient structural capability between 2000°F (1100°C) and 2600°F (1425°C). Contributing to its prime candidacy is availability, fabricability, and prior use history. Before coated columbium can be used with full confidence for Space Shuttle heat shielding, performance areas requiring further study and evaluation are reuse capability and effects of local loss of coating.

In June 1970, the NASA Lewis Research Center authorized McDonnell Douglas Astronautics Company - East to conduct a program to optimize and more fully characterize fused slurry silicide coatings on columbium alloys. A prime objective of this program was the characterization of fused slurry silicide coated B-66, C-129Y, Cb-752, WC-3015, and FS-85 columbium alloys including a determination of the change in material properties due to coating and reuse, the reuse capability of coated material, coating damage tolerance, general fabricability, and evaluation of nondestructive techniques. An additional objective which was pursued under subcontract at HiTemCo was to optimize the fused slurry silicide coating process and to scale-up this process to coat full size columbium alloy heat shields.

Characterization and evaluation of the five columbium alloys B-66, C-129Y, Cb-752, WC-3015, and FS-85 coated with the R-512E fused slurry silicide coating also served as a screening test to select the optimum alloy for Space Shuttle heat shield panels. Evaluation studies involving all five alloys included the effects of coating, the effects of cyclic reentry exposure on mechanical properties (ultimate, yield and elongation) and emittance. From these tests three alloys (Cb-752, C-129Y, and FS-85) were selected for further evaluation. The coating/base metal reuse capability was determined for the three selected alloys

utilizing miniature heat shield panels and applying a realistic failure criterion of structural life.

Concurrent with the alloy screening tests, HiTemCo optimized the coating process which they had previously developed under Air Force sponsorship to apply the R-512E fused slurry silicide coating. Optimization studies included slurry formulation preparation, and application parameters. Progress was measured by the uniformity of the coating before and after firing and by the resistance of the coating to oxidation. Both acrylic and lacquer based slurries were optimized for application to full size hardware. Verification of coating uniformity, oxidation performance, and reproducibility was checked by coating and evaluating subsize 3" x 12" (7.5 cm x 30 cm) rib and corrugation stiffened FS-85 heat shield panels. Evaluation included metallographic examination and flight simulation testing for 100 cycles. After acceptable performance had been demonstrated in the subsize panel evaluation, full size 20" x 20" (50 cm x 50 cm) rib and corrugation stiffened panels (two of each) were coated and inspected.

Other investigations were designed to add to the technology required to make coated columbium a reliable long life heat shield for vehicles such as Space Shuttle. The effect of local loss of coating on heat shield performance was investigated, and the structural life of heat shields was studied.

Subsized FS-85 rib and corrugation stiffened heat shield panels were utilized in determining the effects of local loss of coating on heat shield performance. Small areas of coating were intentionally removed from the panels prior to exposing them to flight simulation. The effects of this coating damage on the structural integrity and life of the heat shield panels were determined.

The structural lives of columbium heat shields were studies using subsize 3" x 12" (7.5 cm x 30 cm) rib stiffened FS-85 panels. Panels were exposed to flight simulation testing for 200 cycles or structural failure whichever occurred first.

III

EXPERIMENTAL

1.0 MATERIAL CHARACTERIZATION AND PROCESS SCALE-UP STUDIES

Materials and experimental activities are described in this section.

2.0 INTERNATIONAL UNITS

The International System of Units, SI Units, is used as the secondary system of units in this report, parenthetically following the customary English Units. In the case of figures and tables, separate abscissa and ordinate scales or columns are given, one in SI Units, and one in customary English Units.

The SI Units used in this report, together with their symbols, are listed below:

Physical Quantity	Name of Unit	Symbol
Length	meter	m
Mass	gram	g
Time	second	s
Area	square meter	m^2
Volume	cubic meter	m^3
Density	grams per cubic meter	g/m^3
Force	newton	N ($kg \cdot m/s^2$)
Pressure	newton per square meter	N/m^2
Dynamic Viscosity	newton-second per square meter	$N \cdot s/m^2$
Work	joule	J (N·m)

The names of multiples and submultiples of the SI Units used were formed by the application of the following prefixes:

Multiplying Factor	Prefix	Symbol
10^6	mega	M
10^3	kilo	k
10^2	hecto	h
10^{-2}	centi	c
10^{-3}	milli	m
10^{-6}	micro	μ

3.0 PROCUREMENT OF COLUMBIUM ALLOYS

3.1 Selection of Alloys - The selection of the sheet columbium alloys for evaluation in this program was based on the available knowledge about their strength, formability, weldability, reusability and coatability.

Mechanical properties was one of the more important considerations in alloy selection. Strength to density ratio as a function of temperature and creep properties were taken into consideration. The ability of the alloys to retain ductility and strength after fusion welding and their ability to be bent around sharp radii without cracking were considered. Coatability was evaluated in terms of the effects that the fused slurry silicide coating fusion cycle would have on alloy behavior.

Five columbium alloys were selected on the basis of possessing the best combination of properties for performing as reusable heat shields for a Space Shuttle vehicle. The five alloys and their nominal chemistries were:

Designation	Nominal Chemistry
Cb-752	Cb-10W-2.5 Zr
C-129Y	Cb-10W-10Hf-0.1Y
FS-85	Cb-28Ta-10W-1 Zr
B-66	Cb-5V-5Mo-1 Zr
WC-3015	Cb-30Hf-15W-5Ti-1Zr-0.05C

The columbium alloys that were studied in this program were procured to the applicable McDonnell Douglas or suppliers' specifications. In addition, all of the suppliers were instructed to supply only material representative of today's state-of-the-art. This is particularly applicable to the new developmental alloy WC-3015; the original composition was developed for a casting or bar product. Since we were requesting sheets, the alloy developer (Wah Chang Albany Corporation) modified the alloy composition to yield a lower strength but a more fabricable alloy. This new alloy has a lower tungsten and carbon content than the original alloy in addition to increased concentrations of titanium and zirconium. A small amount of yttrium was also added.

The B-66 alloy was obtained from the Bureau of Naval Weapons in the form of 0.050" (0.127 cm) sheet which remained in their storage from an earlier program (NoW-63-023/c). The material was produced by Westinghouse Astronuclear Laboratory. This material was rerolled to the required gages. All rolling and annealing was accomplished in a refractory metal supplier's (Fansteel) plant to insure that the material would be processed with the same equipment and techniques that are used in the manufacture of other refractory metals.

The C-129Y alloy was procured from Wah Chang Albany Corporation.

FS-85 and Cb-752 alloys were procured from Fansteel Corporation.

Since all of these alloys were being considered for use as heat shield panels, which will require a material with good fabrication characteristics, they were procured in the fully annealed condition.

3.2 Material Certifications - The suppliers were required to submit certified test reports outlining the typical method of manufacture, including final annealing temperature, and carbon, oxygen, nitrogen and hydrogen interstitial analyses which which tend to inhibit fabricability.

A typical method of manufacture used for production of the columbium alloy sheet was to arc melt, extrude into sheet bar, and vacuum anneal, followed by conditioning (cleaning) and a thickness reduction process of rolling and annealing. Three or four conditioning, rolling, and annealing sequences were required depending on final sheet thickness desired.

The interstitial content was controlled because a high interstitial content can seriously affect the ductility and weldability of columbium alloys.

A summary of the certifications received with C-129Y, Cb-752, FS-85, B-66 and WO-3015 is presented in Table 3-1. The chemical analyses shown in this table were on the final products. It can be seen that the interstitials are representative of current sheet technology, and the mechanical properties are representative of fully annealed material except for the WC-3015 alloy.

TABLE 3-1
SUMMARY OF VENDOR CERTIFICATIONS
Chemical Analysis (1)

ALLOY DESIGNATION	PPM				% BY WEIGHT											R.T. MECHANICAL PROPERTIES			ASTM GRAIN SIZE
	C	O	H	N	Fe	Si	Ti	Y	Hf	V	Zr	Mo	Ta	W	Cb	FTU KSI (MN/m^2)	FTY KSI (MN/m^2)	e %	
FS-85	84	55	5	48	0.0005	0.001	0.00005	–	0.01	–	0.92	0.005	26.50	10.20	BAL	88(607)	66(455)	24(2)	7
CB-752	92	44	5	70	0.001	0.001	0.005	–	–	–	2.65	0.1740	0.43	9.80	BAL	79(545)	56(386)	28(2)	8
C-129Y	50	110	3.5	56	0.005	0.005	0.004	0.12	10.05	–	0.39	0.0125	0.37	9.40	BAL	87.5(603)	72(496)	27(3)	9.5
WC-3015	470	330	1.5	60	0.015	0.005	4.47	0.0755	31.3	–	1.4	0.0130	0.65	15.3	BAL	145(1000)	140(965)	12(3)	–
B-66	96	56	5	90	0.005	–	0.001	–	–	4.90	0.90	4.40	–	–	BAL	106(731)	81(558)	25(2)	6.5

(1) INTERSTITIAL ANALYSIS (COHN) FOR FINAL PRODUCT
(2) ELONGATION OVER 1" (2.5 cm) GAUGE LENGTH
(3) ELONGATION OVER 2" (2.5 cm) GAUGE LENGTH

4.0 CONSPECTUS OF THE TEST CONDITIONS

Reuse evaluation of fused slurry silicide coated columbium alloys involving tabs, tensile, and panel specimens required the selection of a set of test conditions for the profile simulation testing. These test conditions were selected to represent a Space Shuttle operational system. Instead of selecting a particular trajectory and point on a specific vehicle, the necessary parameters of time, temperature, pressure, and stress were studied separately. An attempt was made to insure that the full effect of each parameter would be imposed upon the test specimen in a realistic manner. The test conditions had to be representative of the general environmental conditions of the several Shuttle vehicles and missions under consideration, as well as of probable future vehicles.

The initial test conditions selected are shown in Figure 4-1 and were used for evaluation of tabs, tensile specimens, and miniature heat shield panels.

The temperature, pressure, and stress relationships for subsize panels were maintained throughout as shown in Figure 4-2.

The flight simulation testing of a subsize rib stiffened panel required the use of a 7" (18 cm) diameter tube furnace. Since this furnace would not cool at the required rate, the profile was extended to 3600 sec elapsed time.

A part of the flight simulation which was performed on each subsize heat shield panel and not shown in Figure 4-2 was acoustic exposure to simulate the noise environment experienced during lift-off. Peak acoustic loading conditions are experienced for approximately 30 sec during each lift-off. Each of the test parameters will be discussed separately and the rationale for its definition is given in Volume II.

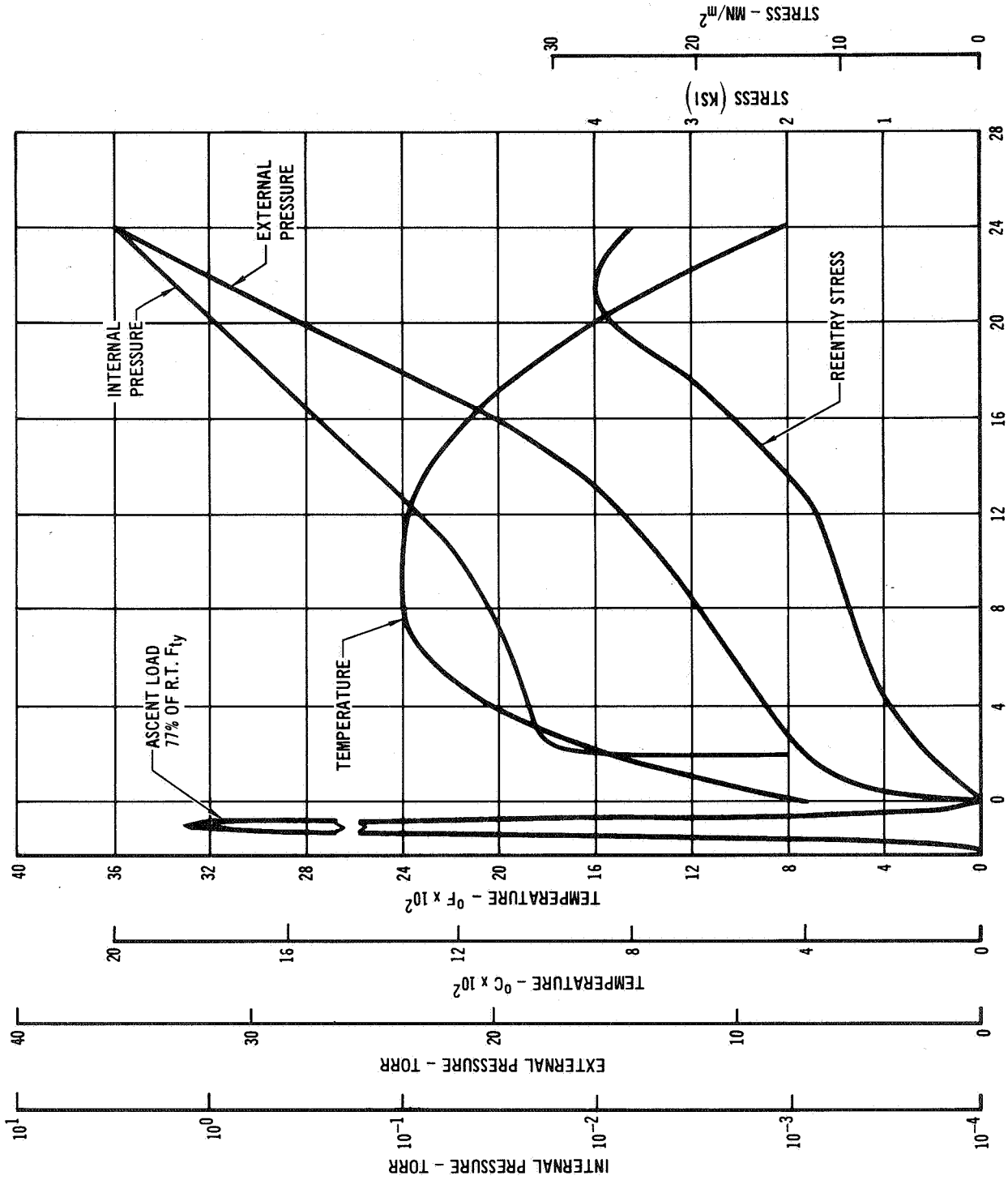

REENTRY PROFILE TEST CONDITIONS FOR TABS, TENSILE, AND MINIATURE HEAT SHIELD PANELS

FIGURE 4-1

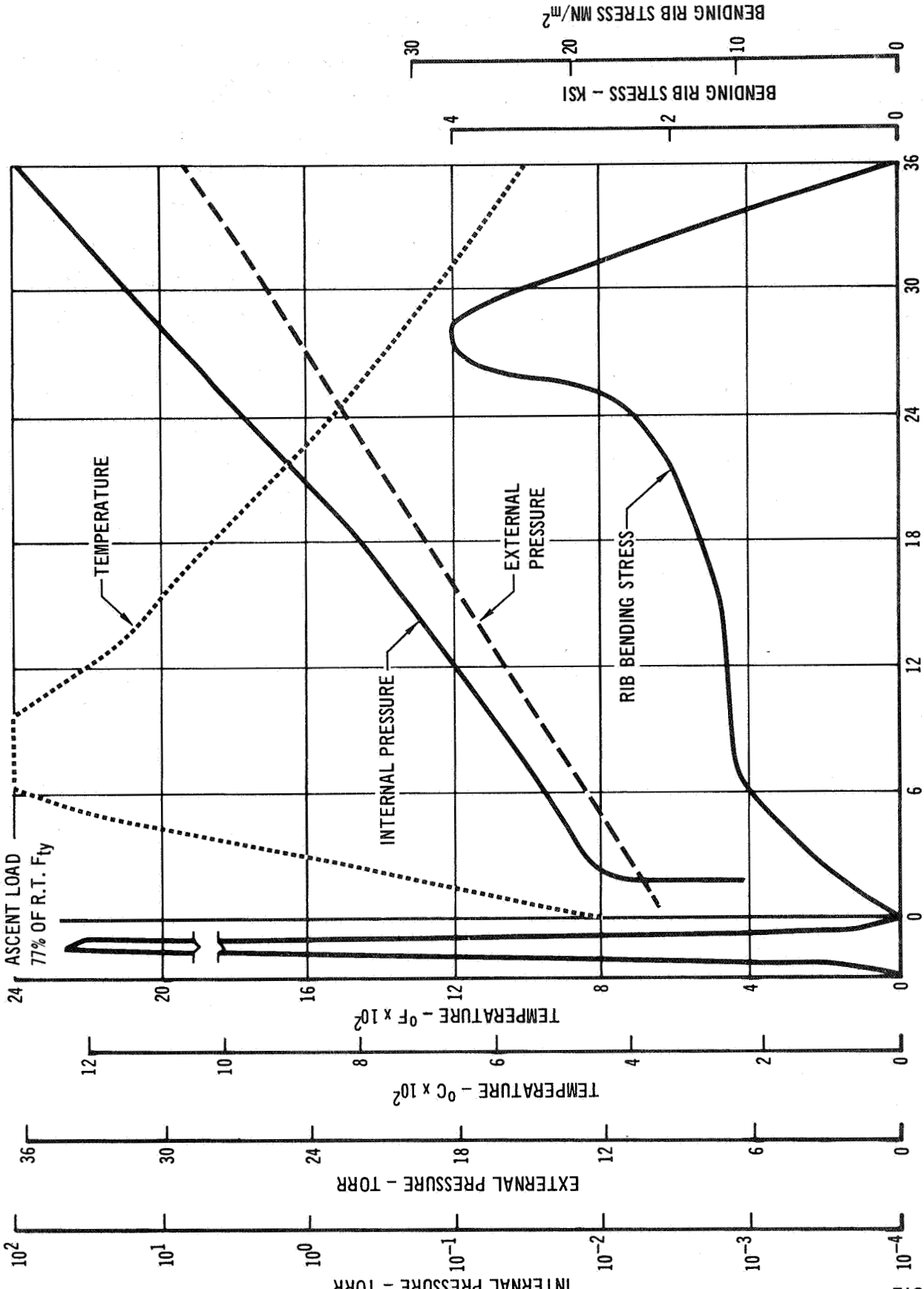

REENTRY PROFILE TEST CONDITIONS FOR SUB-SIZE PANELS

FIGURE 4-2

5.0 CHARACTERIZATION AND EVALUATION OF COLUMBIUM ALLOYS

The five columbium alloys were given a series of evaluation tests to determine the optimum alloy for Space Shuttle heat shields. Evaluation included general fabricability and change in material properties due to coating and reuse.

5.1 Fabricability - Weldability was initially determined by performing a circular patch or a restraint weld on the 0.012" (0.03 cm) thick material. Restraint was accomplished by clamping an 8" (20 cm) ring over the sheet and then electron beam welding a 2" (5 cm) circle. The test fixture with one of the welded specimens is shown in Figure 5-1. All of the alloys were successfully welded with no evidence of cracking.

Samples of each of the five columbium alloys, Cb-752, FS-85, C-129Y, WC-3015 and B-66, were prepared for determination of the ductile to brittle transition temperature (DBTT). In this test the DBTT is defined as that temperature at which a 120° bend can be successfully made (without cracking) in a material over a 1T radius using a 1 x 2" (2.5 x 5.0 cm) specimen and a 2R + 2-1/2T span (T is the sheet material thickness and R is the bend radius which in this case is equal to T). Using this test the DBTT was determined for all 5 columbium alloys in the "as received" and the "welded and stress relieved" condition. To determine if any asymmetry existed in the "as received" material, test samples were included with the grain running longitudinally, transversely, and on a 45° angle. The results of these tests are presented in Figure 5-2.

From this figure it can be seen that the WC-3015 alloy possessed the highest transition temperature in both the "as received" and "welded and stress relieved condition." The postweld heat treatment caused a significant increase in the transition temperature, making this alloy unacceptable for welded structures. In the case of the B-66 and Cb-752 alloys, the transition temperatures are lower than normally expected. This is primarily due to modifications in the alloy's final annealing temperature and the selection of a postweld thermal cycle that allowed overaging to occur. Previous in-house studies involving the Cb-752 alloy have shown that the conventional practice of annealing this alloy for 1 hour at 2200-2300°F (1200-1260°C) generally resulted in a transition temperature of +50°F (10°C) while anneals conducted above 2300°F (1260°C) usually caused lowering of this temperature. Based on this data a decision was made to request the material supplier to use a final annealing temperature of 1 hour at 2550°F (1400°C), which resulted in the lower transition temperature. The use of this technique is not

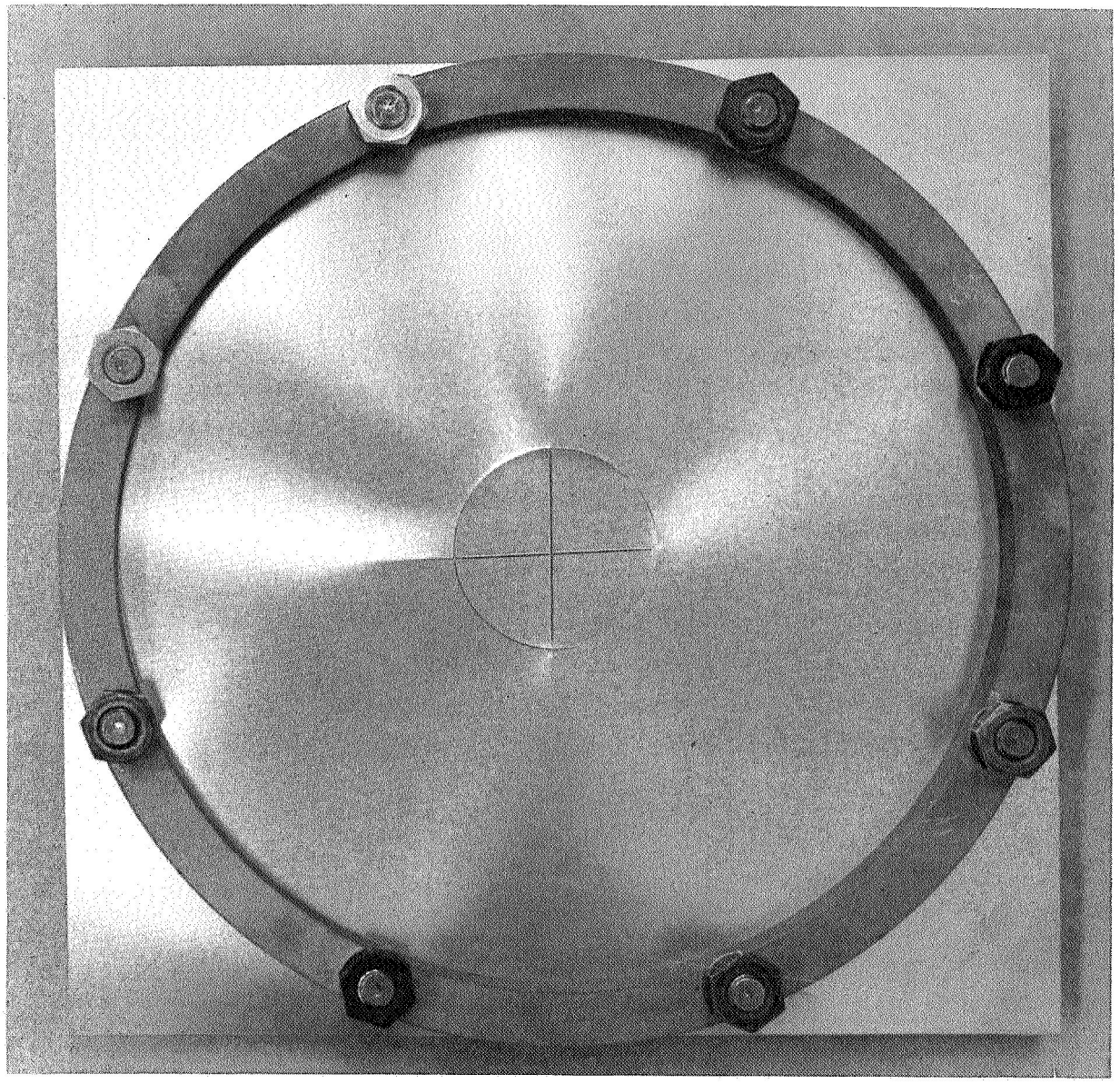

F5–85 WELD RESTRAINT SPECIMEN

FIGURE 5–1

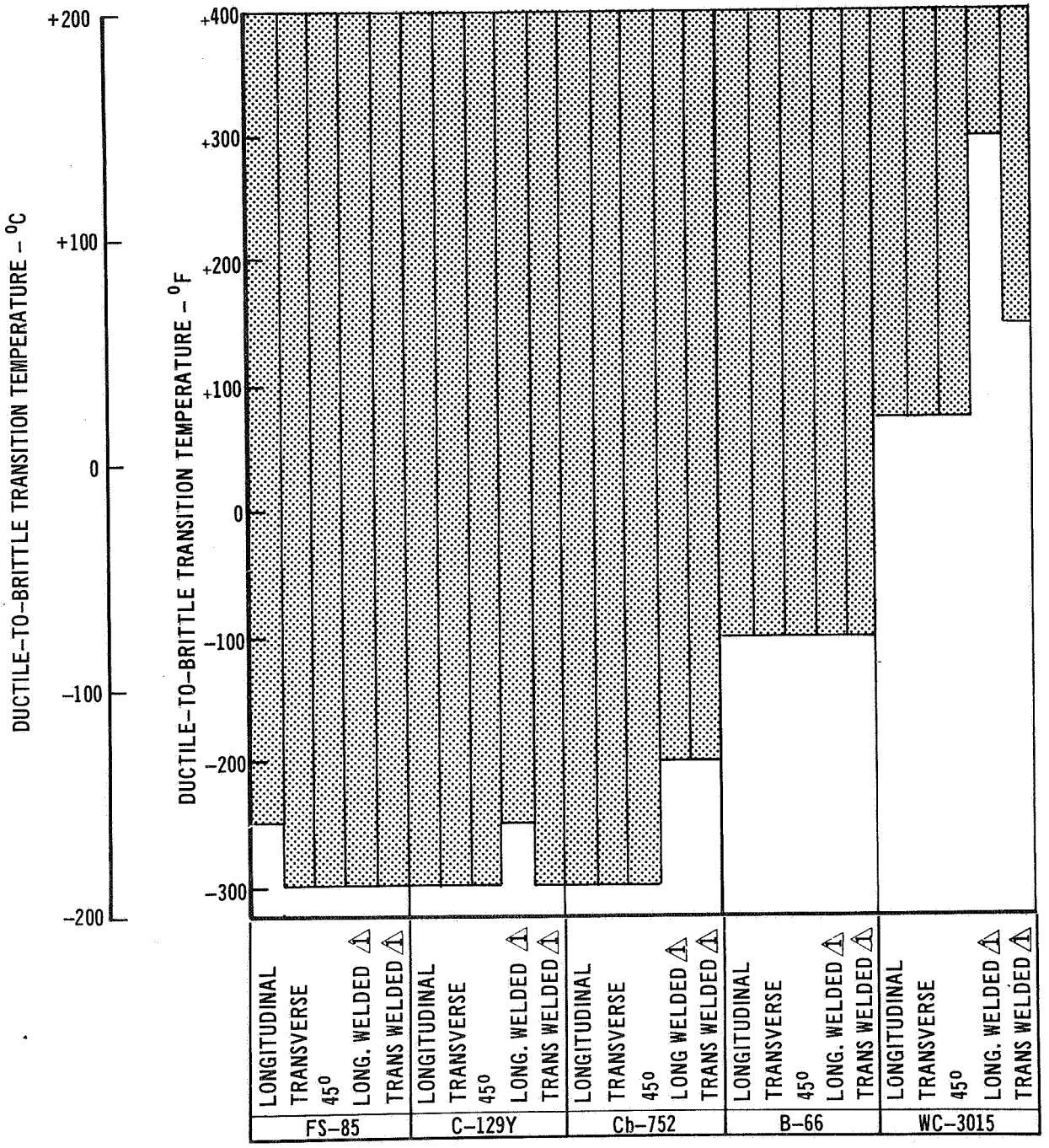

1 WELDS GIVEN POST WELD HEAT TREATMENT OF 1 HOUR AT 2450°F

2 SHADED AREA IS DUCTILE REGION

DUCTILE-BRITTLE TRANSITION TEMPERATURE

FIGURE 5-2

without its associated penalties since it tends to reduce the tensile strength. The same technique was used on the B-66 alloy which was final annealed for 1 hour at 2450°F (1340°C).

5.2 Mechanical Properties - Utilizing 0.012" (0.03 cm) sheet material of the five columbium alloys (Cb-752, C-129Y, FS-85, B-66, and WC-3015) tensile specimens were prepared. Evaluation testing using these tensile specimens included determining the effects of fused slurry silicide coating, thermal reuse cycling, and coating damage on the mechanical properties.

Tensile specimens were sheared so that the rolling and grain direction of the sheet would be parallel to the major axis of the tensile specimen. Longitudinal test specimens were used in an effort to provide tensile data that would be representative of the type of tensile loading experienced by the heat shield panels.

The tensile specimen shown in Figure 5-3 is slightly smaller than the standard ASTM specimen, but it is in agreement with the tensile specimens described in the Materials Advisory Board Report MAB-216M, "Evaluation Test Methods for Refractory Metal Sheet Materials." This specimen is preferable to the standard ASTM specimen because it requires less material, allows more rapid heating, improves gage length temperature uniformity and reduces grip loads. After machining, the edges of the specimens were carefully deburred (slightly rounded parallel to the direction of specimen loading) and a number stamped on the end tab in the location, as shown in Figure 5-3, to maintain specimen identity.

The manufactured tensile specimens were inspected for dimensional tolerances, and thicknesses and widths were recorded for each accepted specimen. Four hundred specimens were manufactured. Thirty were retained for tensile testing in the bare condition and the remaining 370 were coated by HiTemCo with a nominal 19 mg/cm^2 R-512E (60Si-20Cr-20Fe) coating.

After coating and prior to reentry exposure cycling approximately 40% of the coated specimens had coating defect (damage) sites intentionally induced. Specimens were locally defected by grit blasting with a microblaster to remove, down to the base metal, a 0.030" (0.076 cm) diameter spot of coating, from one side only, in the center of the gage length. For each coated alloy a time-pressure setting relationship was developed for the microblaster to obtain complete coating removal.

All except 60 of the coated tensile specimens were exposed to reentry cycling. Reentry cycling consisted of exposure to the temperature and pressure profiles of Figure 4-1. Stress profiling was not used on the tensile specimens. Tensile

specimens were exposed to reentry cycling and tensile tested according to the test plan presented in Table 5-1.

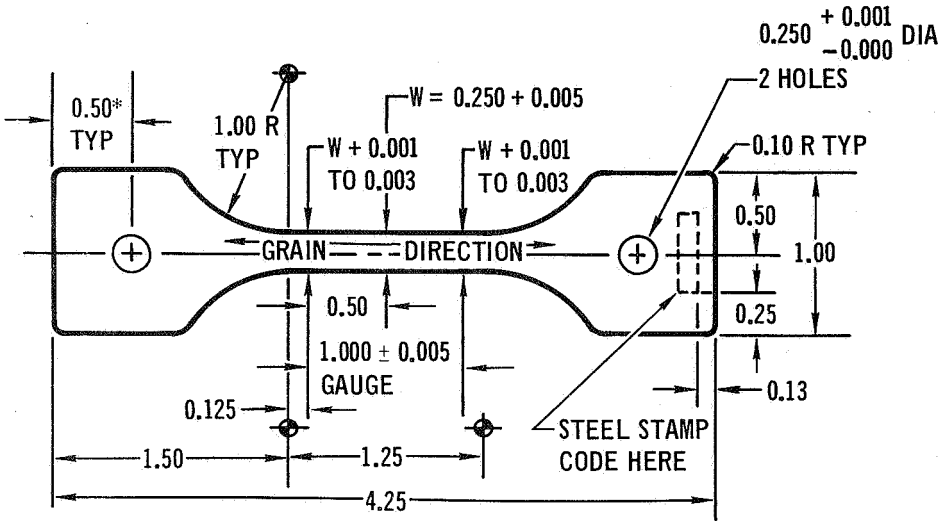

NOTE:

IN		CM
0.001	=	0.0025
0.003	=	0.0076
0.005	=	0.0127
0.125	=	0.318
0.13	=	0.33
0.25	=	0.63
0.50	=	1.27
1.00	=	2.54
1.25	=	3.18
1.50	=	3.81
4.25	=	10.80

*DIMENSIONS ARE IN INCHES

TENSILE SPECIMEN

FIGURE 5-3

TABLE 5-1

TEST PLAN FOR TENSILE TESTS PERFORMED ON EACH OF THE 5 COLUMBIUM ALLOYS

SPECIMEN CONDITION	NUMBER OF REENTRY EXPOSURE CYCLES	PRESSURE	TEST TEMPERATURE				
			R.T.	760°C 1400°F	1100°C 2000°F	1300°C 2400°F	1400°C 2600°F
UNCOATED	0	–	X		X		
COATED	0	–	X	X	X	X	X
DEFECTED	5	EXTERNAL	(X)*	X	(X)	X	
DEFECTED	10	EXTERNAL	(X)	X	(X)	X	
DEFECTED	50	INTERNAL	(X)	X	(X)	X	
UNDEFECTED	50	EXTERNAL	X	X	X	X	X
UNDEFECTED	100	EXTERNAL	X	X	X	X	X

*(X): TESTS CONDUCTED ON C-129Y, Cb-752 AND FS-85 ALLOYS ONLY.

5.2.1 Coating and Coating Effects - Upon removal from the reentry simulator, tensile specimens were visually inspected.

Approximately one-third of the R-512E coated Cb-752 tensile specimens had incipient coating failures at edges after 50 and 100 cycles of reentry exposures. For the remaining 4 alloys no coating failures were observed; however, after reentry simulation, the WC-3015 specimens were severely distorted and embrittled to the extent that many specimens were broken trying to load them in the tensile machine.

Metallographic examination was conducted to determine coating uniformity, microstructural changes due to cycling and base metal consumption due to coating and reentry cycling. Photomicrographs of each coated alloy, "as coated" and after 100 reentry cycles, are shown in Figures 5-4, 5-5, 5-6, 5-7 and 5-8.

The coating thicknesses for B-66, C-129Y, Cb-752, FS-85, and WC-3015 in the "as coated" condition were nominally 3.0, 3.2, 3.2, 3.2, and 3.8 mils per side (76, 81, 81, 81, and 96 μm), respectively. These coating thicknesses were produced from approximately the same weight of applied slurry (19.3 mg/cm^2). Base metal consumptions in mils per side, due to coating, 50 cycles, and 100 cycles of reentry exposure for all 5 alloys are presented in Figure 5-9. From this figure it can be seen that even though Cb-752 had the lowest base metal consumption as a result of coating, it also had the second highest consumption as a result of thermal cycling. Both the C-129Y and FS-85 had the lowest total base metal consumption for 100 cycles. The highest base metal consumption both before and after cycling occurred in WC-3015. The high reaction rate between WC-3015 and the coating (R-512E) resulted in the rounding of tensile specimen edges. This did not occur with the other alloys. However, it does bring to light the possibility that reaction rate controlled via temperature and slurry composition may be used to help produce uniform coating coverage on edges.

Two nondestructive coating thickness measurement techniques were employed to determine and monitor coating thickness during cyclic reentry exposure of coated tensile specimens. A thermoelectric device was used to determine coating thicknesses on edges in the "as coated" condition. The Dermitron, or eddy current device, was used for surface thickness measurements. Calibration curves for both devices were developed for each coating-metal system. Because electrical continuity is required

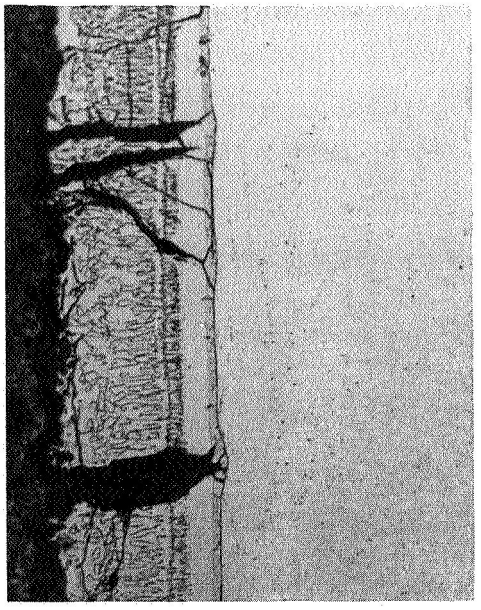

250 X

After 100 Cycles

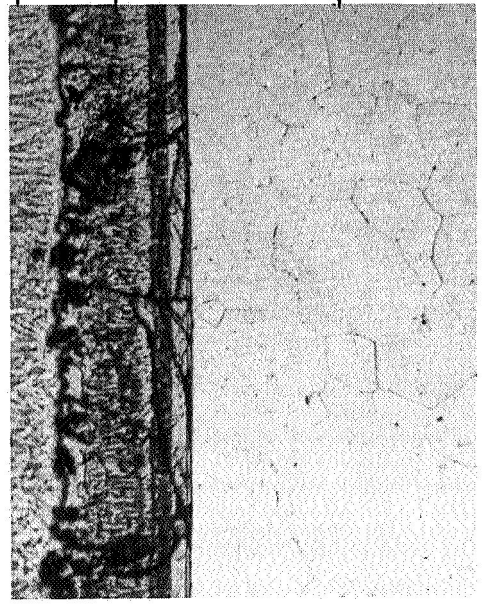

250 X

As Coated

R-512E COATED B-66 COLUMBIUM ALLOY

FIGURE 5-4

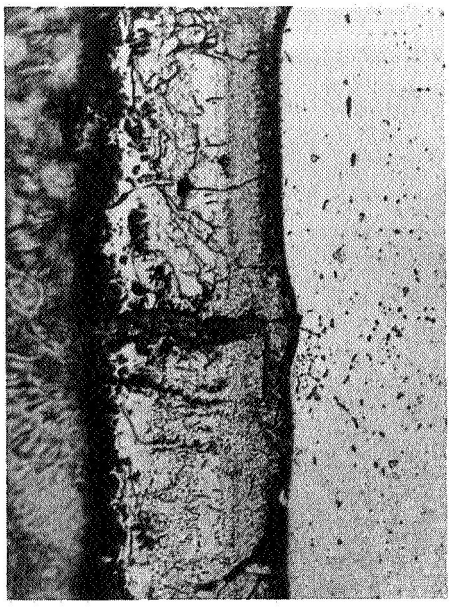

250 X

After 100 Cycles

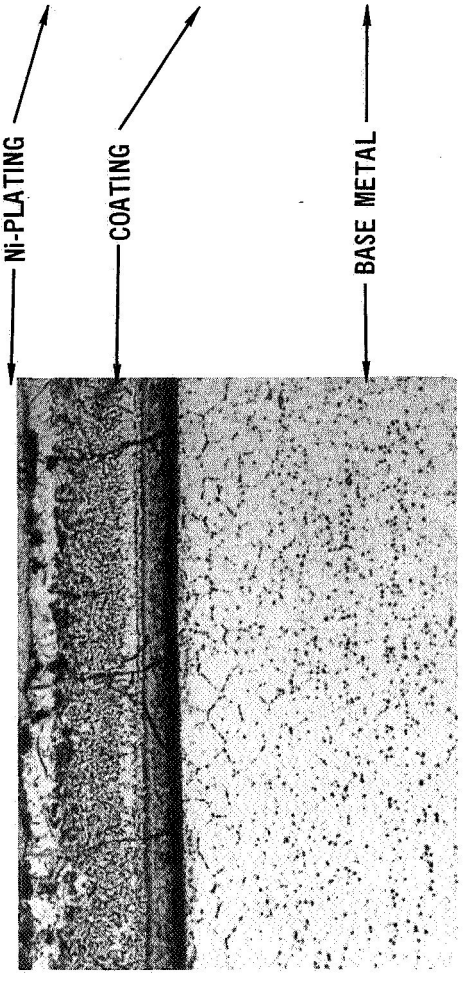

250 X

As Coated

R-512E COATED WC-3015 COLUMBIUM ALLOY

FIGURE 5-5

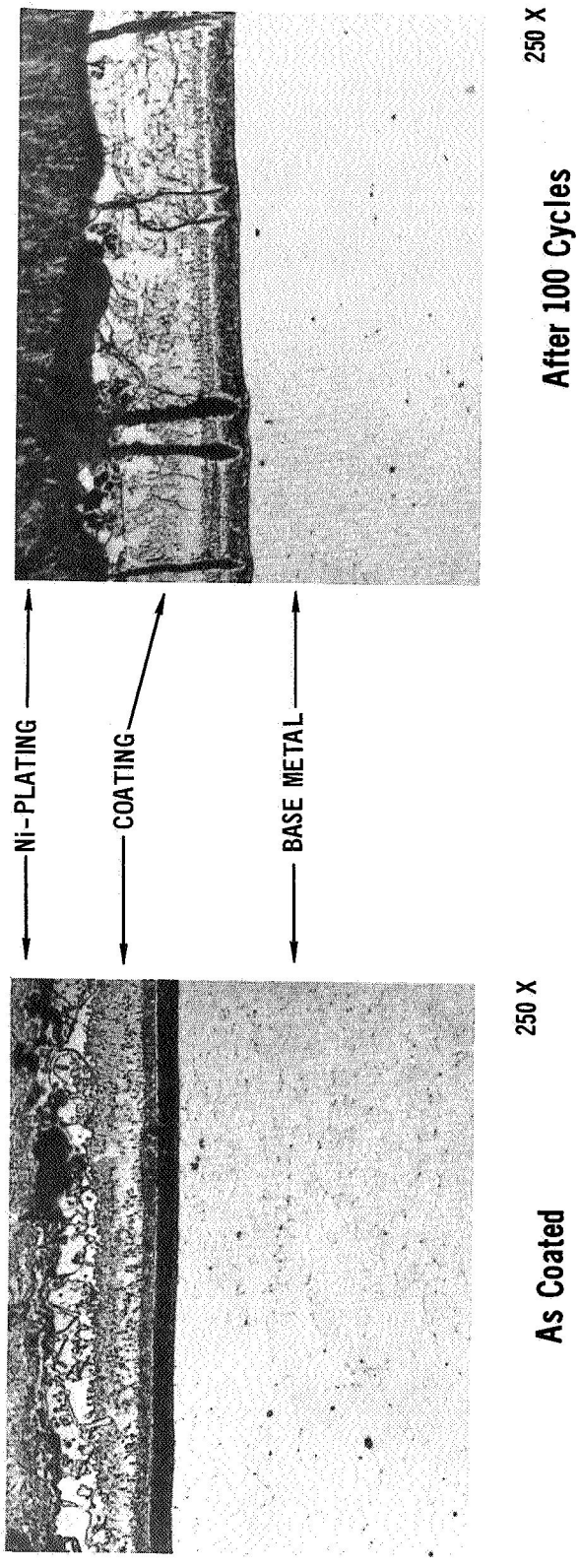

FIGURE 5-6

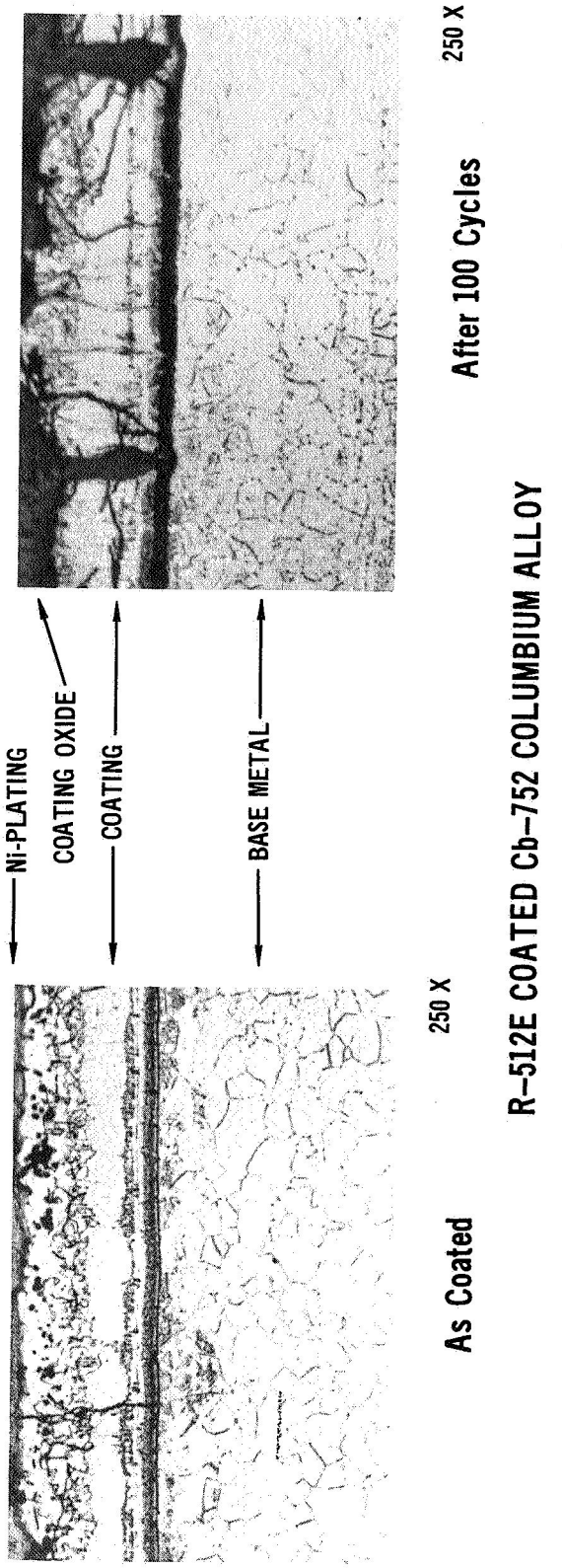

FIGURE 5-7

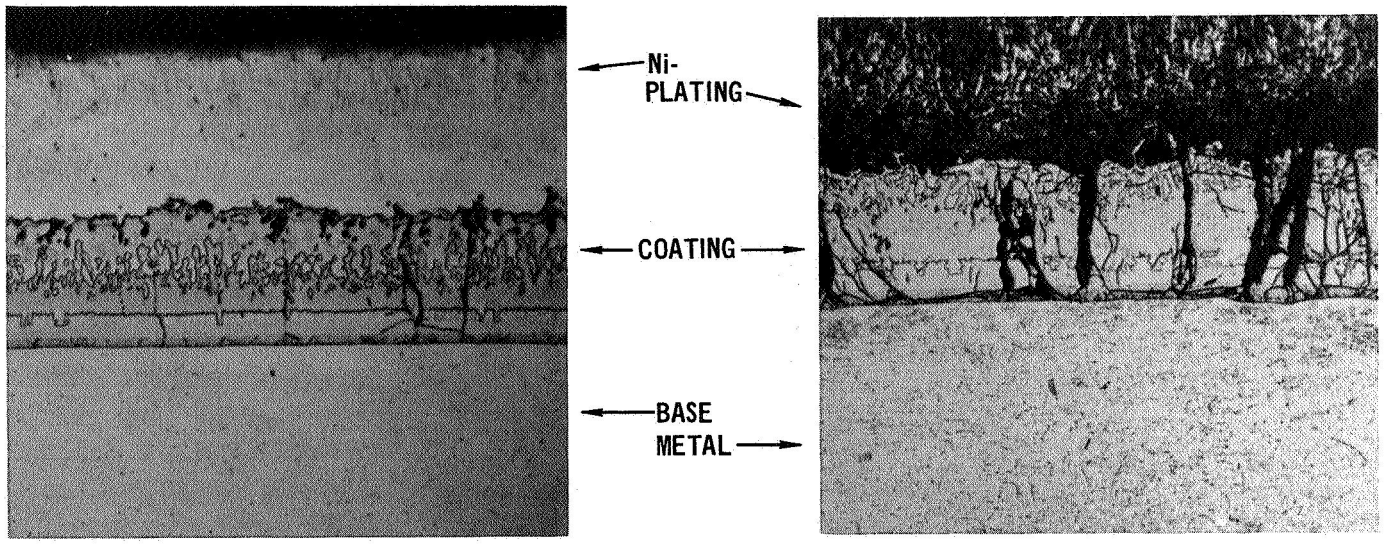

250 X
As Coated

250 X
After 100 Cycles

R-512E COATED FS-85 COLUMBIUM ALLOY

FIGURE 5-8

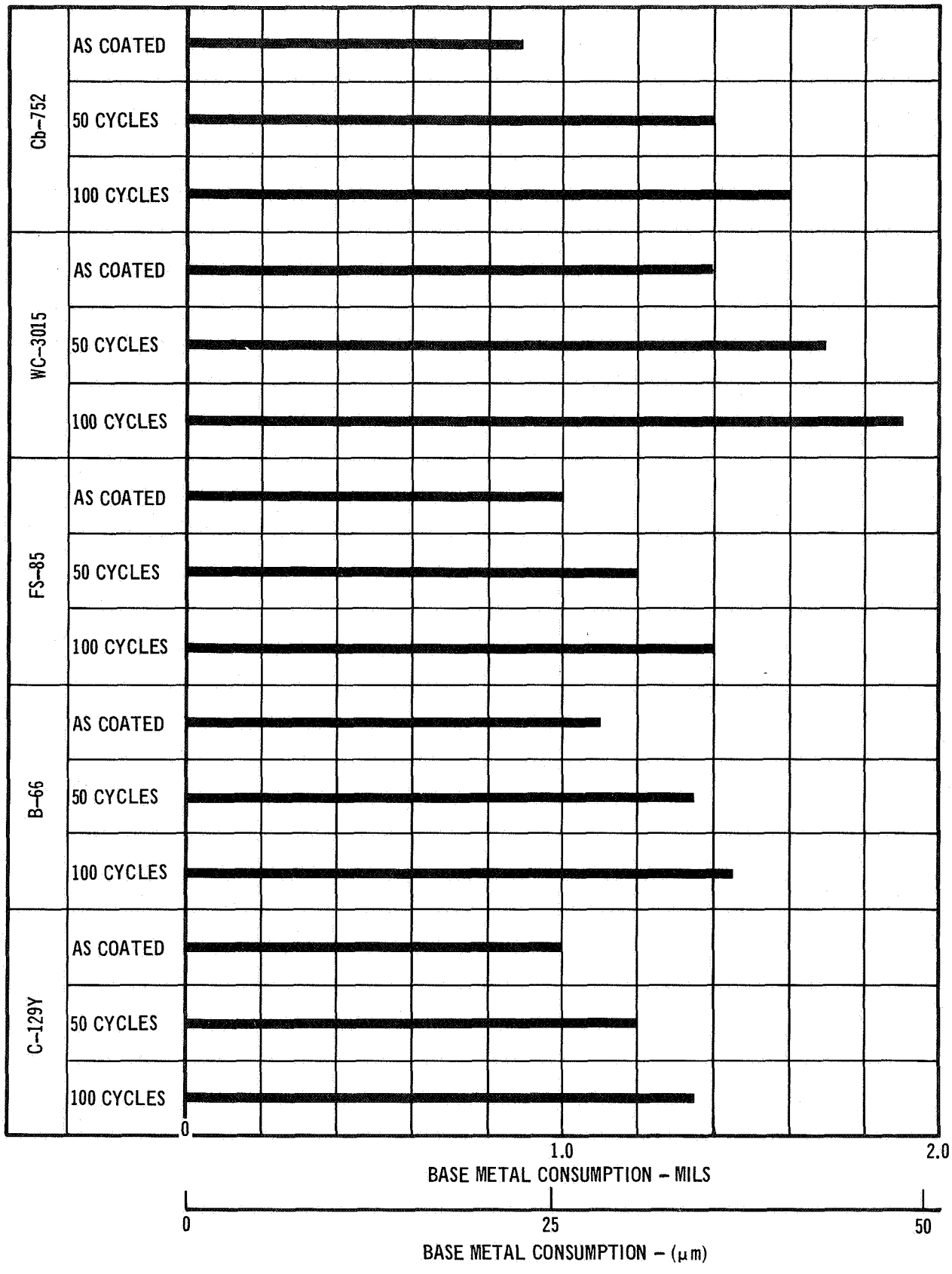

COMPARISON OF ALLOY BASE METAL CONSUMPTION PER SIDE

FIGURE 5-9

for the thermoelectric device, it could only be used on specimens in the "as coated" condition. The tensile specimens of the five R-512E coated columbium alloys - Cb-752, FS-85, C-129Y, B-66, and WC-3015 - that were exposed to a various number of reentry cycles up to 100 and used for determination of reuse effects on mechanical properties were also utilized to monitor coating thickness changes during reentry exposure.

Table 5-2 presents a breakdown of the NDT data accumulated for the five R-512E/ alloy systems. The "as coated" high, low, and average coating thicknesses as determined by the Dermitron and the thermoelectric devices are shown in mils per side. All thickness numbers except the high and low, shown for each location before and after cycling, represent the average of a minimum of six specimens.

Both the Dermitron and the thermoelectric devices showed a distinct taper in the coating thickness from one end to the other. Based on Dermitron readings, the R-512E coated C-129Y showed the most taper, 0.4 mil (10 μm) per side. This taper results from the dip application of the slurry. It should be remembered that these tensile specimens were coated prior to optimization of the slurry coating process.

The thermoelectric readings showed very thin coating on edges for the R-512E/ Cb-752 and R-512E/WC-3015 systems. However, the R-512E/Cb-752 was the only system to show edge failures during the reentry exposures.

The change in coating thickness which occurred due to reentry exposures was monitored with the Dermitron. The negative change in thickness for the specimens which were exposed for 50 cycles in the internal pressure environment may be accounted for by a larger loss due to oxidation/vaporization mechanisms than growth due to diffusion at the coating-base metal interface. All coating-base metal systems showed a loss in thickness when exposed for 50 cycles to the internal pressure environment (approximately 5×10^{-2} torr).

All specimens exposed in the external pressure environment showed a considerable growth in thickness. This was due to the combined diffusion zone growth and growth associated with oxide formation on the surface of the coating. The growth rate did not appear consistent with an expected diffusion rate controlled function. The R-512E/C-129Y had the largest total growth per side after 100 cycles, 2.25 mils (57 μm).

After simulated reentry thermal cycling, mechanical property tests were conducted on B-66, C-129Y, Cb-752, FS-85 and WC-3015 to determine the effects of coating and coating damage on the reuse properties of the columbium alloys. A

TABLE 5–2

TYPICAL NDT COATING THICKNESS R–512E COATED COLUMBIUM ALLOY TENSILE SPECIMENS

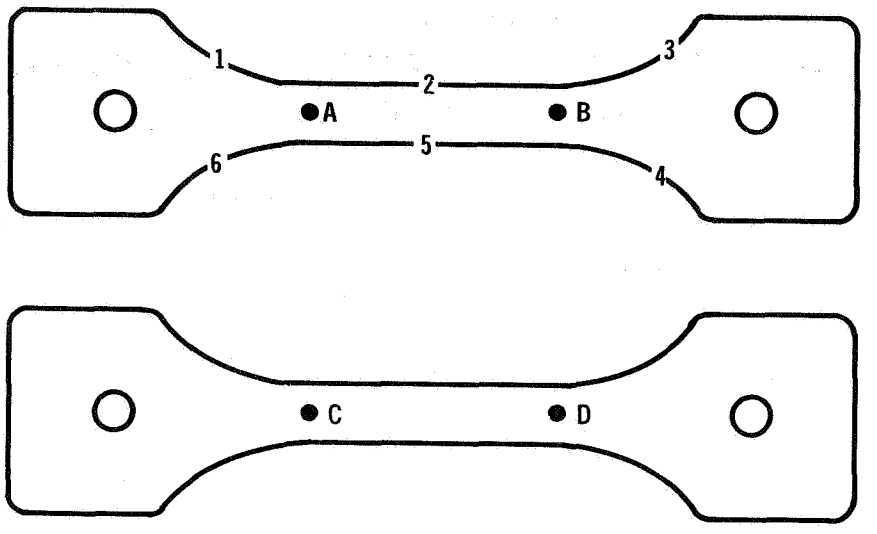

*SEE TABLE 5–2 (Continued)

ALLOY/ COATING	NDT DEVICE	LOCATION	AS COATED THICKNESS (MILS)*			CHANGE FROM AS COATED THICKNESS (MILS/SIDE)* DUE TO REENTRY CYCLING				
						INTERNAL PRESSURE	EXTERNAL PRESSURE			
			LO	AVG	HI	50 CYCLES	5 CYCLES	10 CYCLES	50 CYCLES	100 CYCLES
FS–85/ R-512E	DERMITRON	A	3.1	3.3	3.5	–0.1	+1.1	+1.2	+1.3	+2.0
		B	3.0	3.2	3.3	–0.3	+0.9	+1.2	+1.3	+2.3
		C	3.1	3.3	3.6	–0.2	+1.0	+1.3	+1.8	+1.9
		D	3.0	3.2	3.4	–0.6	+0.8	+1.1	+1.1	+2.2
	THERMOELECTRIC	1	4.6	5.0	5.6	–	–	–	–	–
		2	3.7	4.4	5.6	–	–	–	–	–
		3	4.1	4.5	4.8	–	–	–	–	–
		4	4.1	4.3	4.7	–	–	–	–	–
		5	3.8	4.2	5.0	–	–	–	–	–
		6	4.4	5.0	6.5	–	–	–	–	–
C–129Y/ R-512E	DERMITRON	A	3.4	3.6	3.7	–0.5	+1.0	+0.8	+1.0	+2.5
		B	3.0	3.1	3.3	–0.3	+0.6	+0.8	+0.8	+1.9
		C	3.3	3.5	3.7	–0.6	+0.5	+0.9	+0.9	+2.5
		D	2.9	3.2	3.3	–0.3	+0.9	+0.8	+0.7	+2.1
	THERMOELECTRIC	1	5.5	6.0	7+	–	–	–	–	–
		2	4.1	4.6	7.0	–	–	–	–	–
		3	3.2	4.0	6.5	–	–	–	–	–
		4	3.4	5.0	5.6	–	–	–	–	–
		5	3.9	5.3	6.8	–	–	–	–	–
		6	5.6	6.0	7+	–	–	–	–	–
Cb-252/ R-512E	DERMITRON	A	2.8	3.0	3.3	–0.4	+0.8	+1.0	+1.4	+2.2
		B	2.3	2.7	3.0	–0.2	+0.3	+0.8	+1.3	+1.9
		C	2.7	3.2	3.4	–0.3	+0.8	+0.8	+1.4	+2.1
		D	2.7	2.8	3.0	–0.2	+0.5	+1.0	+1.2	+2.0
	THERMOELECTRIC	1	2.3	3.5	3.8	–	–	–	–	–
		2	1.0	2.5	3.3	–	–	–	–	–
		3	0.2	1.0	2.4	–	–	–	–	–

TABLE 5–2 (Continued)

TYPICAL NDT COATING THICKNESS R–512E COATED COLUMBIUM ALLOY TENSILE SPECIMENS

ALLOY/ COATING	NDT DEVICE	LOCATION	AS COATED THICKNESS (MILS)*			CHANGE FROM AS COATED THICKNESS (MILS/SIDE)* DUE TO REENTRY CYCLING				
						INTERNAL PRESSURE	EXTERNAL PRESSURE			
			LO	AVG	HI	50 CYCLES	5 CYCLES	10 CYCLES	50 CYCLES	100 CYCLES
		4	0.6	1.5	2.5	–	–	–	–	–
		5	1.4	2.4	3.4	–	–	–	–	–
		6	2.2	3.2	3.8	–	–	–	–	–
B-66/R-512E	DERMITRON	A	3.8	4.0	4.4	–0.2	+0.8	+1.0	+1.2	+1.3
		B	3.7	4.0	4.2	–0.2	+0.6	+0.9	+1.4	+1.7
		C	3.8	4.0	4.3	–0.2	+0.6	+1.3	+1.4	+1.5
		D	3.6	3.9	4.4	–0.2	+0.5	+0.8	+1.2	+1.0
	THERMOELECTRIC	1	5.0	5.7	6.1	–	–	–	–	–
		2	4.0	5.0	5.8	–	–	–	–	–
		3	4.0	4.8	5.4	–	–	–	–	–
		4	3.7	4.7	5.7	–	–	–	–	–
		5	4.4	4.9	5.7	–	–	–	–	–
		6	5.0	5.5	5.9	–	–	–	–	–
WC3015/R-512E	DERMITRON	A	3.2	3.8	4.6	–0.2	+0.8	+0.9	+1.0	+1.2
		B	3.0	3.9	4.5	0	+0.5	+0.7	+0.9	+1.1
		C	3.5	4.2	4.9	–0.4	+0.7	+0.9	+1.6	+1.5
		D	3.4	4.3	4.9	–0.1	+0.6	+0.8	+1.0	+1.4
	THERMOELECTRIC	1	1.3	1.8	2.3	–	–	–	–	–
		2	0.7	1.5	2.5	–	–	–	–	–
		3	0.1	1.0	1.9	–	–	–	–	–
		4	0.1	1.5	2.3	–	–	–	–	–
		5	0.5	1.7	2.5	–	–	–	–	–
		6	1.5	2.0	3.8	–	–	–	–	–

* THICKNESS CONVERSIONS TO METERS
1.0 MILS = 25 μm
2.0 MILS = 50 μm
3.0 MILS = 75 μm
4.0 MILS = 100 μm
5.0 MILS = 125 μm
6.0 MILS = 150 μm
7.0 MILS = 175 μm

summary of tensile tests performed is shown in Table 5-1. The individual results of all mechanical property tests for the five alloys are presented in Appendix A. The values reported include tensile elongation over a 1" (2.5 cm) span, tensile ultimate, and tensile yield (cross head travel for elevated temperature tests). The Ftu and Fty were calculated two ways - using before coating dimensions (base-line) and dimensions of the remaining metal (effective) at the time of the tensile test, determined from the base metal consumption information in Figure 5-9. Base metal consumption was determined from cross section photomicrographs of two specimens from each exposure condition. Base metal consumption due to coating was assumed to be the same on all specimens of a given alloy exposed to the same conditions.

A comparison of the room temperature and 2000°F (1100°C) bare and coated mechanical properties prior to flight simulation exposure is shown in Figure 5-10. The coated strengths are based on metal remaining after coating (effective). Coated Ftu and Fty in most all cases show an increase over the bare strength. The increase is much more evident at 2000°F (1100°C) and can best be explained by the fact that the coating is carrying some of the load being put into the tensile specimen. Load bearing cross section dimensions used for stress calculations are based only on the metal remaining. The most pronounced observation is the large decrease in elongation due to coating, particularly for the B-66 and WC-3015 alloys.

5.2.2 Cycling Effects - A comparison of the effective ultimate strengths and elongations versus number of reentry exposure cycles of the five columbium alloys is presented in Figure 5-11. The comparisons were made at 4 different temperatures: room temperature, 1400°F (760°C), 2000°F (1093°C) and 2600°F (1425°C). Ultimate strengths and elongations are shown for the following specimen conditions; "as coated" (0 cycles), 50 cycles, and 100 cycles of reentry exposure, which consisted of temperature and external pressure profiles as shown in Figure 4-1. The strength values reported are based on effective base metal thicknesses. There is no apparent significant effect of cycling on the ultimate strengths and elongations of the columbium alloys with the exception of WC-3015 alloy which showed strength losses up to 38% due to cycling. The FS-85 showed the next largest strength losses of 15 and 18% but only at the intermediate temperatures of 1400°F (760°C) and 2000°F (1100°C), respectively.

The elongation did not show much change due to cycling from the "as coated" condition.

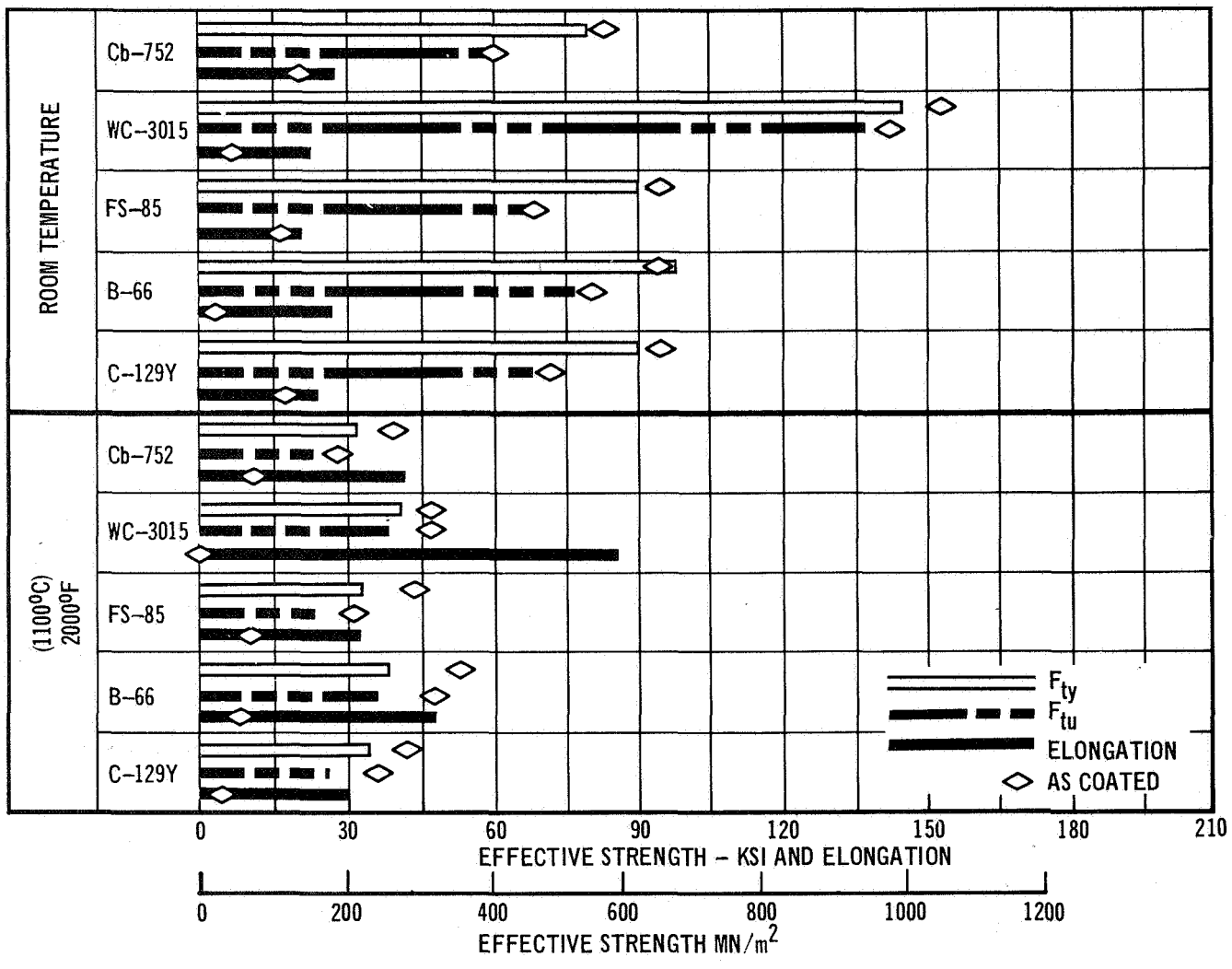

COMPARISON OF ALLOY MECHANICAL PROPERTIES (BARE AND AS COATED)

FIGURE 5-10

COMPARISON OF ALLOY ULTIMATE STRENGTHS AND ELONGATIONS (AFTER REENTRY CYCLING AND AS COATED)

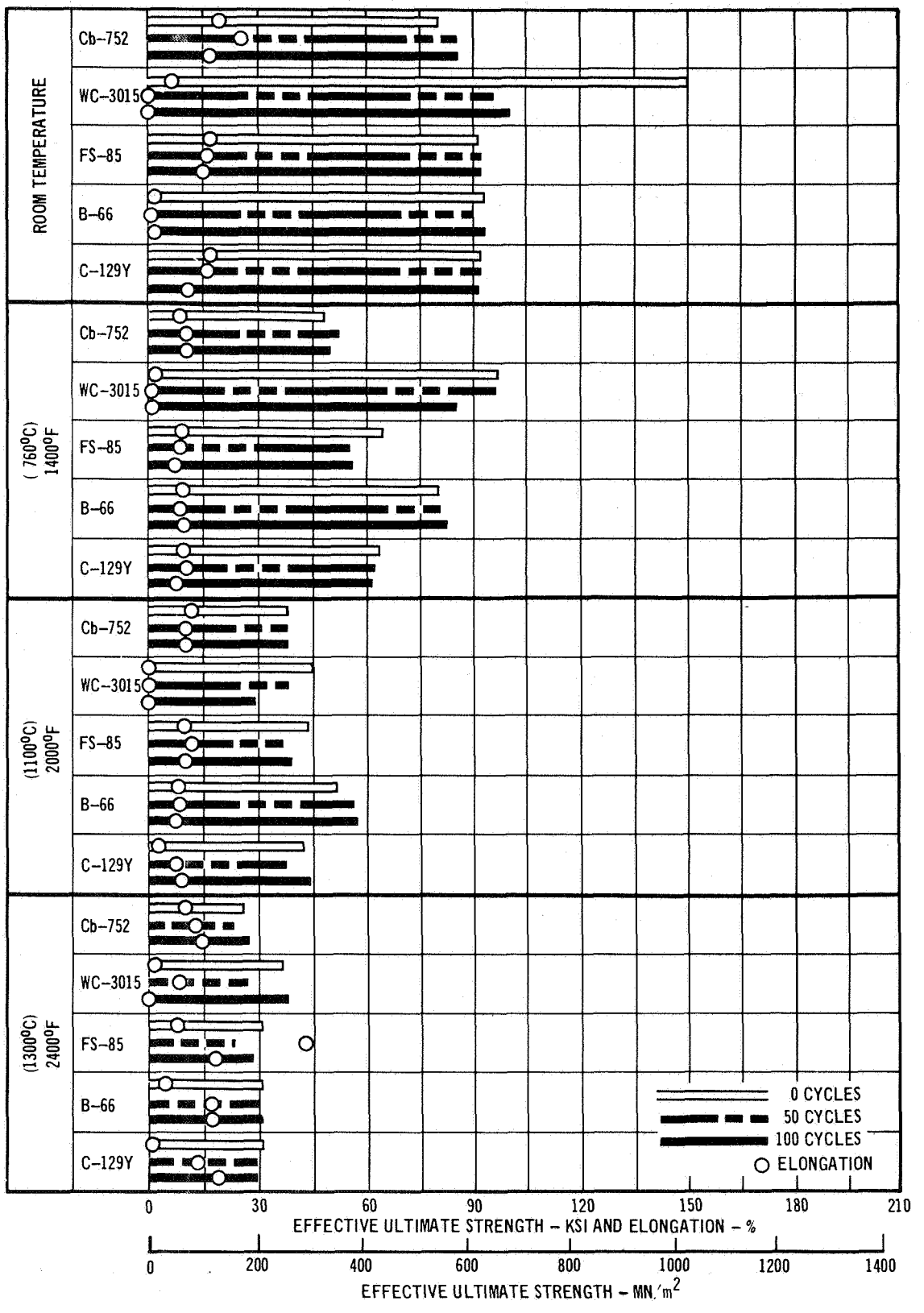

FIGURE 5-11

A comparison of the effective yield strengths for the "as coated" and cycled alloys is shown in Figure 5-12. The same trends that were evident in comparing the ultimate strengths are evident in the yield strengths. The general conclusion is that thermal cycling for up to 100 simulated shuttle reentries has very little effect on the mechanical properties of R-512E coated Cb-752, FS-85, B-66 and C-129Y.

5.2.3 Coating Damage (Defect) Effects - Tensile specimens from each alloy were intentionally damaged as previously described and exposed to 5 and 10 simulated shuttle reentries in the external pressure environment and 50 simulated reentries in the internal pressure environment. Tensile tests were then conducted and a comparison of results with undamaged specimens is shown in Figures 5-13, 5-14, 5-15, 5-16 and 5-17.

Effective ultimate strength losses at room temperature for the Cb-752, WC-3015, FS-85, B-66 and C-129Y defected and exposed for 10 cycles external pressure were 42%, 52%, 44%, 50%, and 30%, respectively. At 1400°F (760°C) the changes in effective ultimate strength for the same order of alloys were +2.6%, -15.6%, -41.0%, -44.2%, and -24.8%. At 2400°F (1300°C) changes in effective ultimate strengths were -12.5%, -4.1%, -17.6%, -15.1% and -9.3%.

The yield strength losses were in general approximately one-half of the ultimate strength losses.

The elongation properties for all of the alloys in the damaged condition after 10 reentry cycles were almost totally destroyed at room temperature and 1400°F (760°C). At 2400°F (1300°C) elongation properties were fully restored. At room temperature, the elongations were so low that yield strengths at .2% offset could not be determined except for the Cb-752 and C-129Y alloys which still showed elongations of less than 1%. The effects of local coating removal and reentry exposure for 10 cycles on tensile elongation are presented in Figure 5-18.

Coating damage specimens were exposed for 5 reentry cycles (external pressure) and tensile tested at 1400°F (760°C) and 2400°F (1300°C). Changes in strength were very close to the same for the specimens which were exposed for 10 cycles, indicating that strength deterioration in damaged specimens is not a linear function with respect to time. Room temperature strengths however were always lower for the specimen which were exposed for 10 cycles.

Coating damage specimens areas were exposed to 50 reentry cycles (internal pressure) and tensile tested at 1400°F (760°C) and 2400°F (1300°C). Changes in strength and elongation were very similar to those for the specimens which were

COMPARISON OF ALLOY YIELD STRENGTHS (AFTER REENTRY CYCLING AND AS COATED)

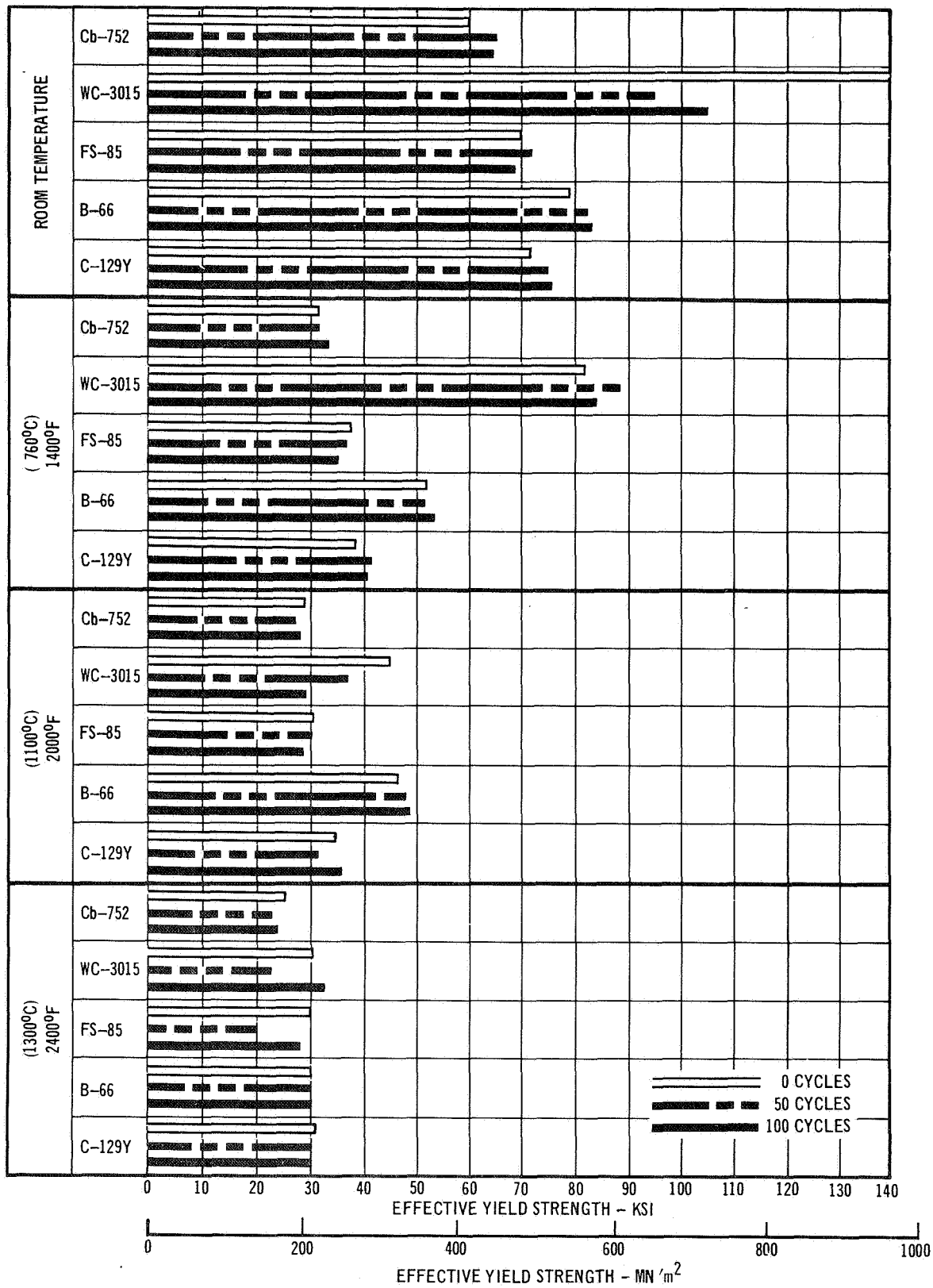

FIGURE 5-12

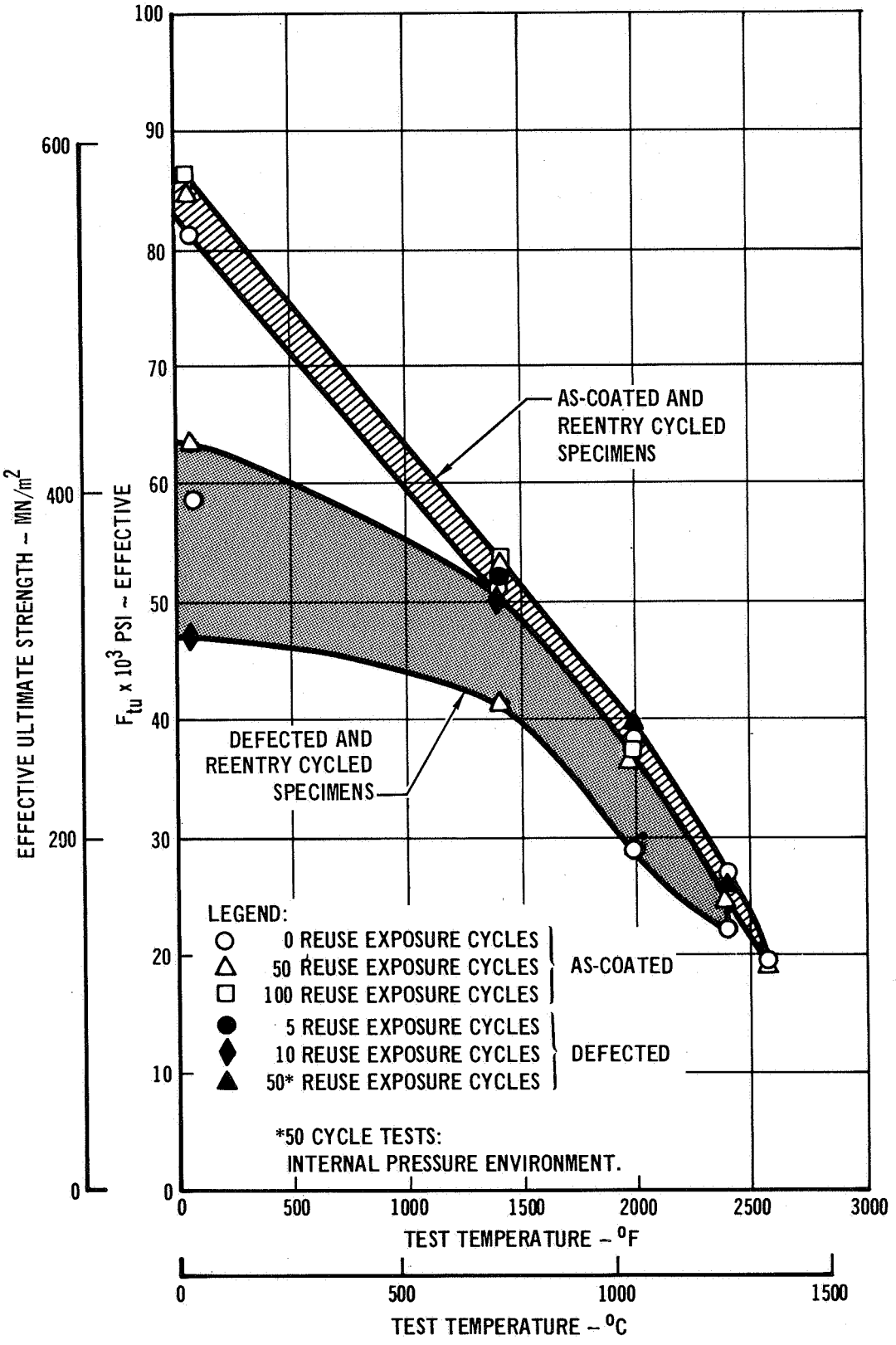

R–512E COATED Cb–752: EFFECTIVE ULTIMATE TENSILE STRENGTH AS A FUNCTION OF REUSE AND COATING DAMAGE

FIGURE 5–13

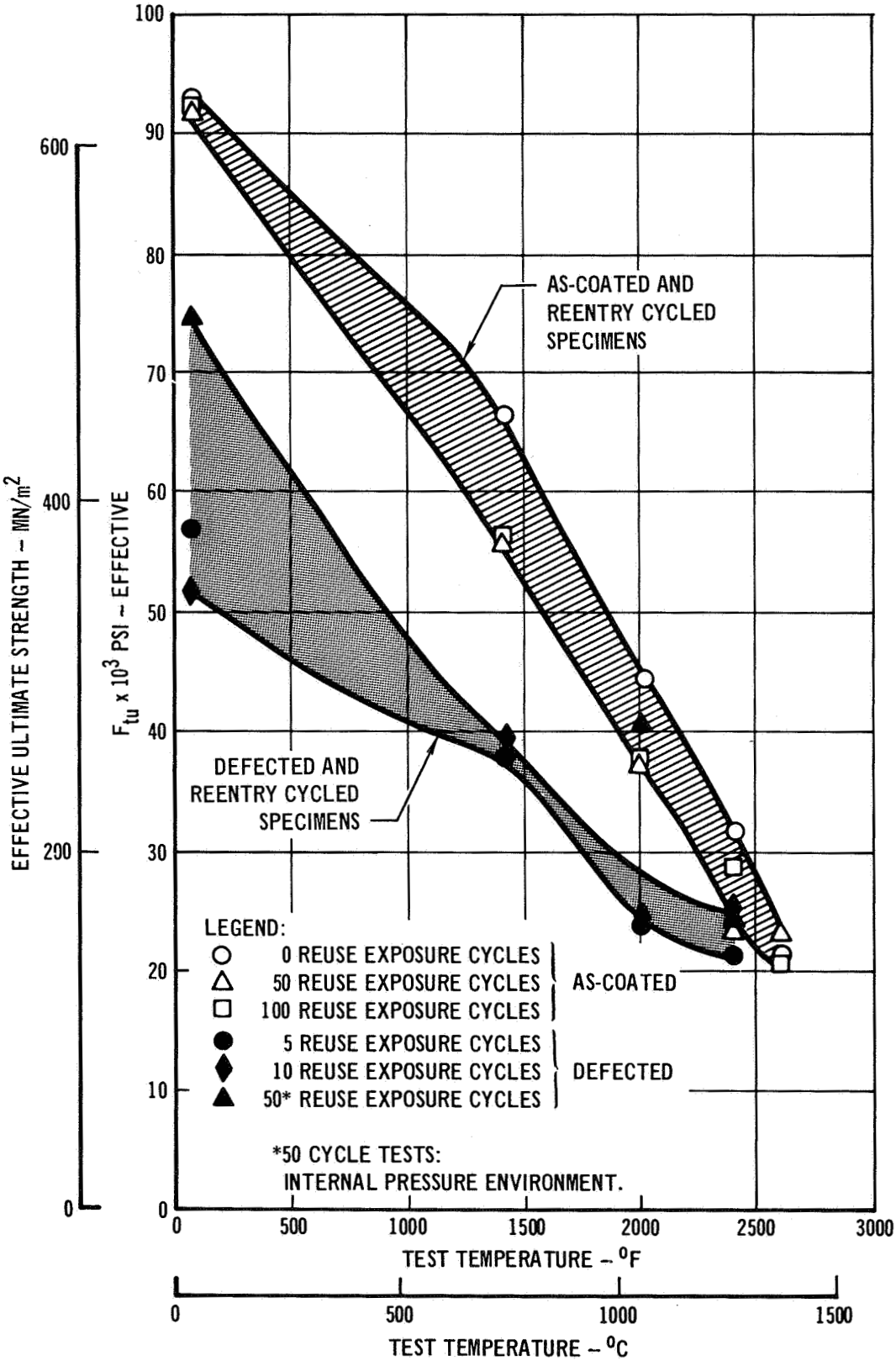

R-512E COATED FS-85: EFFECTIVE ULTIMATE TENSILE STRENGTH AS A FUNCTION OF REUSE AND COATING DAMAGE

FIGURE 5-14

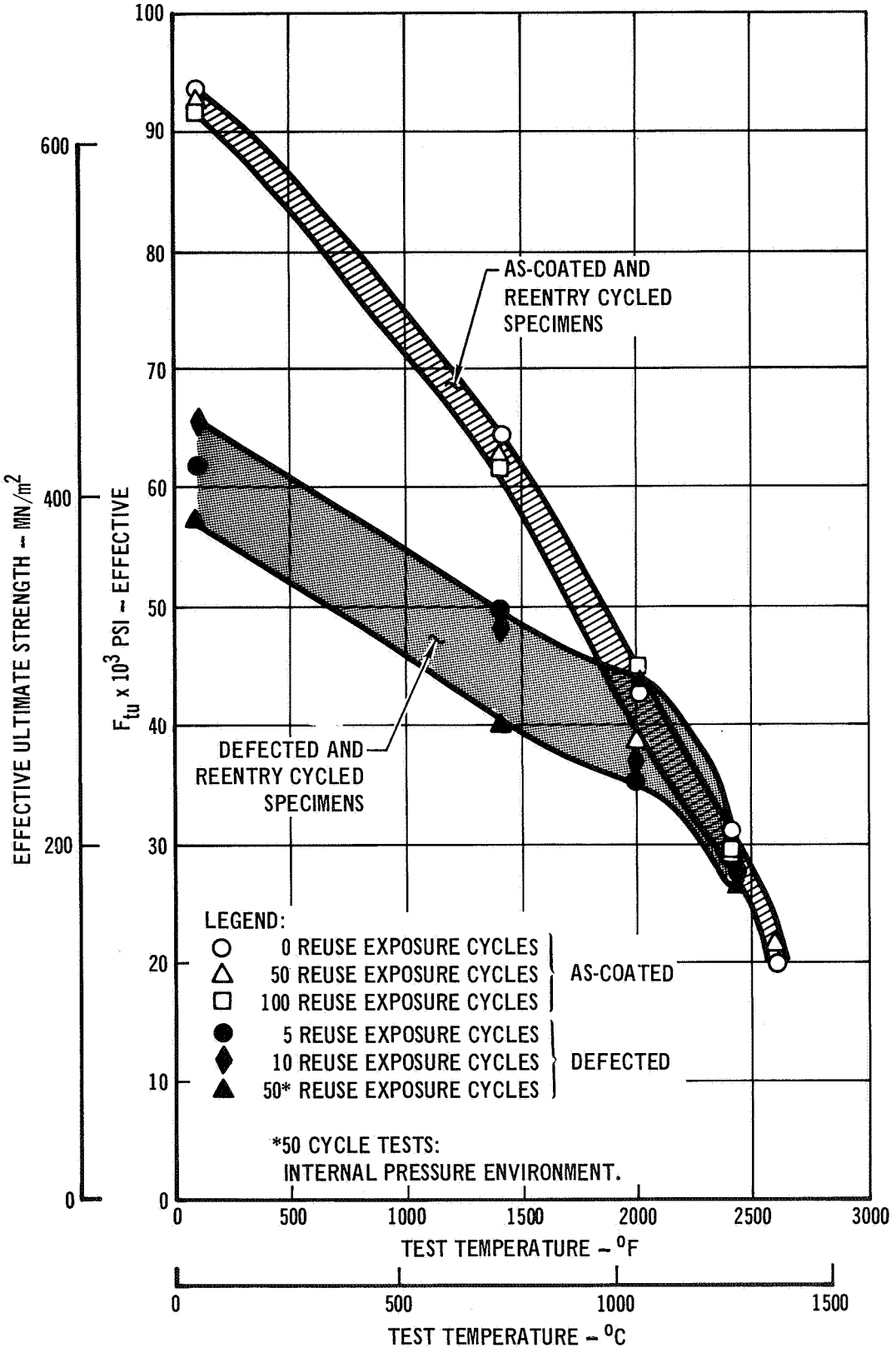

R-512E COATED C-129Y: EFFECTIVE ULTIMATE TENSILE STRENGTH AS A FUNCTION OF REUSE AND COATING DAMAGE

FIGURE 5-15

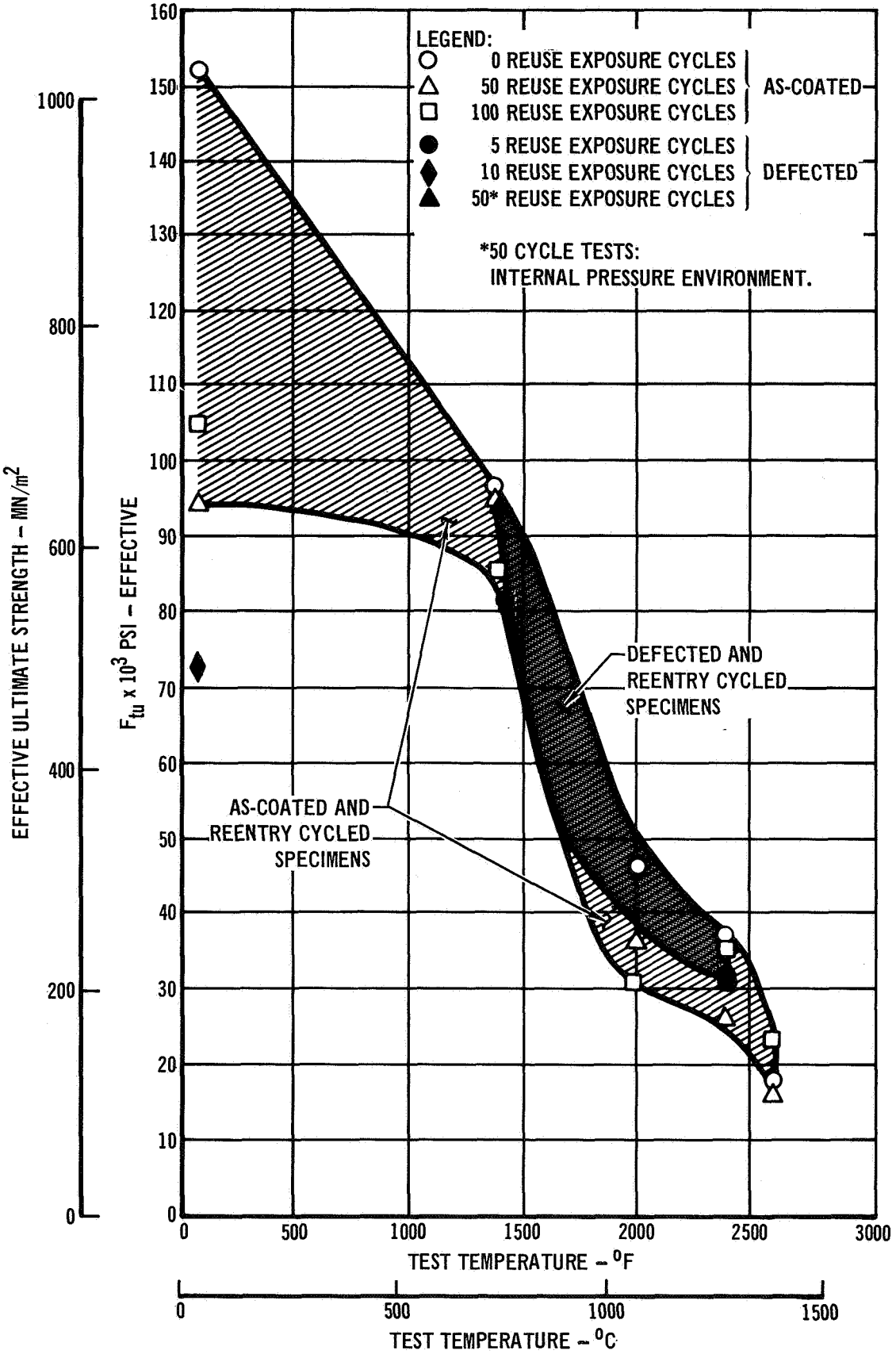

R-512E COATED WC-3015: EFFECTIVE ULTIMATE TENSILE STRENGTH AS A FUNCTION OF REUSE AND COATING DAMAGE

FIGURE 5-16

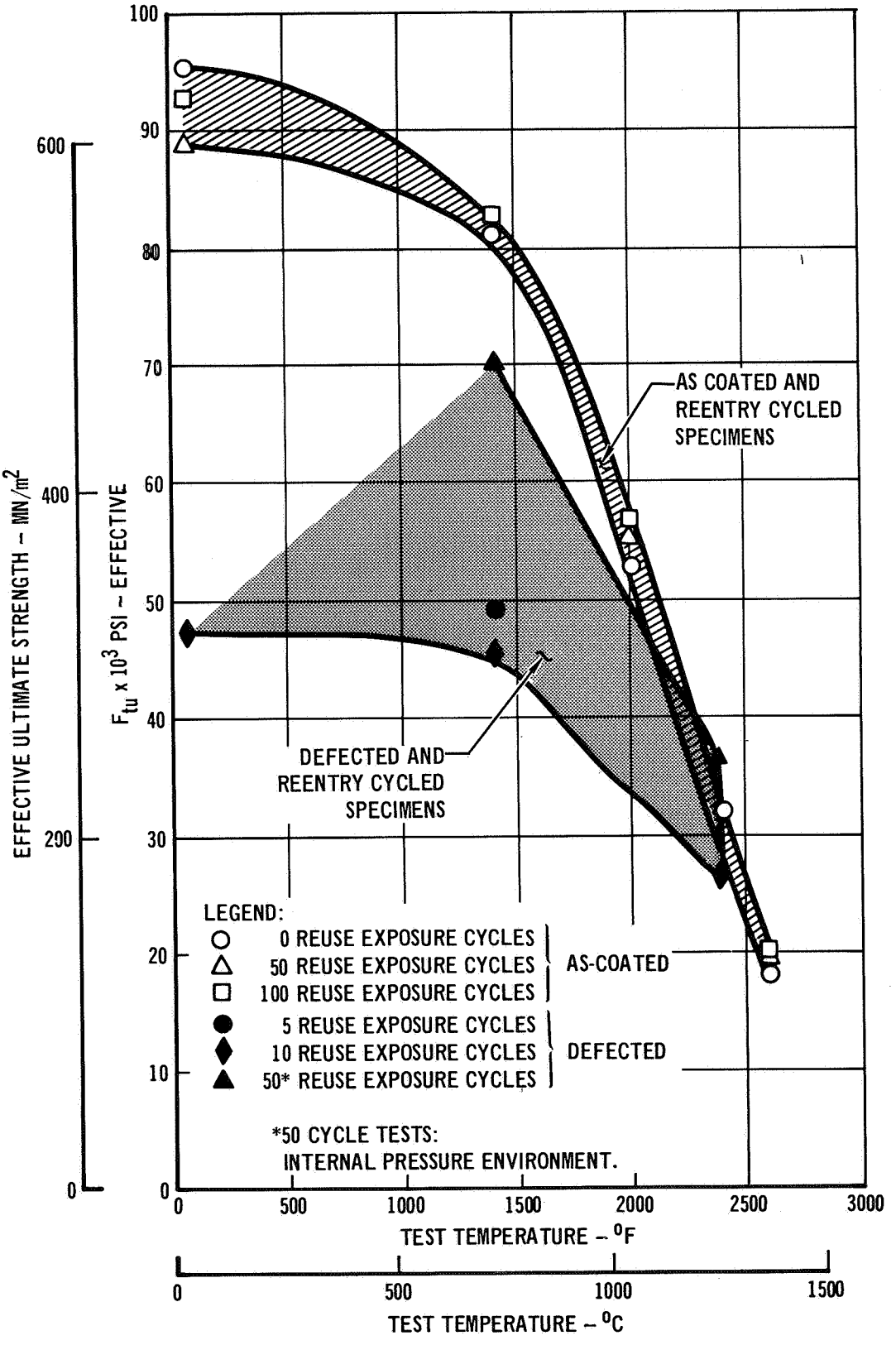

R-512E COATED B-66: EFFECTIVE ULTIMATE TENSILE STRENGTH AS A FUNCTION OF REUSE AND COATING DAMAGE

FIGURE 5-17

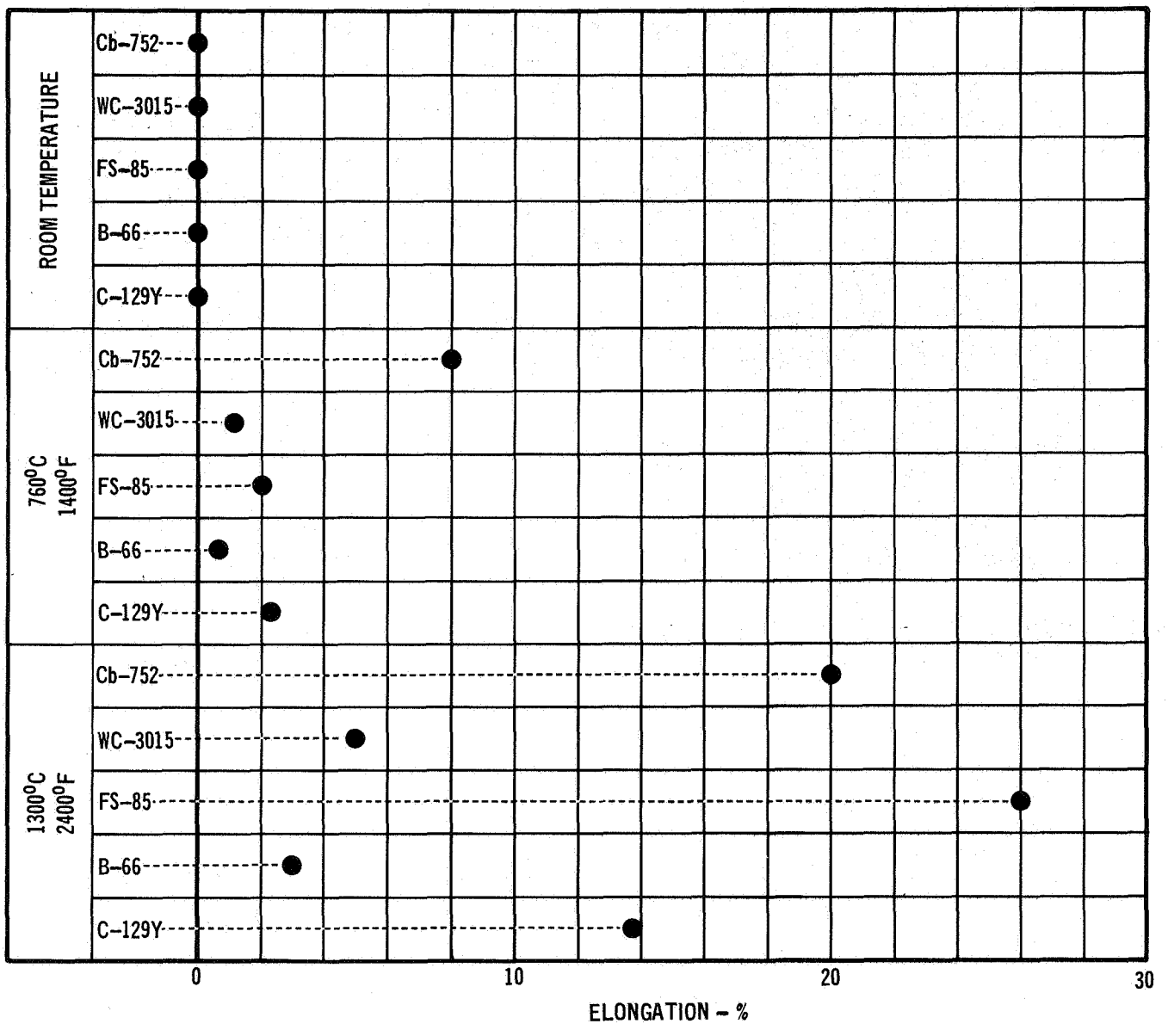

EFFECTS OF COATING DAMAGE ON TENSILE ELONGATION AFTER EXPOSURE TO 10 REENTRY CYCLES

FIGURE 5-18

exposed to 10 reentry cycles (external pressure). The reduced availability of oxygen at the lower internal pressures evidently reduced the rate of strength deterioration.

Overall, Cb-752 and C-129Y tend to offer the highest tolerance to coating damage effects. The difference between the FS-85 and B-66 is subtle.

5.2.4 Summary - Alloy Selection on the Basis of Strength and Reuse Properties - The selection of the three best performing alloys was made on the basis of properties such as: ultimate tensile and yield strength, tensile elongation, reuse and coating damage effects. The information concerning the effects of these factors is summarized in Table 5-3.

The test data presented in Table 5-3 show that the Cb-752, FS-85 and C-129Y have overall properties superior to those of the WC-3015 and B-66 alloys. Although the WC-3015 exhibited the greatest room temperature ultimate strength, this strength was more rapidly degraded with increasing temperature, reuse and coating damage.

The coated B-66 alloy had approximately the same tensile strength as Cb-752, FS-85 and C-129Y, but like the WC-3015 alloy, the B-66 alloy exhibited a low room temperature tensile elongation in the "as coated" condition. This is an indication of embrittlement as a result of diffusion reactions associated with the R-512E coating.

The Cb-752, FS-85 and C-129Y alloys performed in a similar manner throughout the testing series. However, it should be noted that the Cb-752 alloy specimens showed oxidation failures after 50 and 100 reentry exposures prior to tensile test.

Cb-752, FS-85, and C-129Y were selected as the three alloys for evaluation on miniature heat shield panels on the basis of their performances in mechanical property reuse evaluation. The WC-3015 was not chosen because of its high ductile to brittle transition temperature and the large and erratic changes in properties under reuse conditions. The B-66 was not selected primarily because of the poorer performance in defect sensitivity tests and secondarily because of the lack of availability.

TABLE 5-3

COMPARISON OF R-512E COATED COLUMBIUM ALLOYS ON THE BASIS OF STRENGTH AND REUSE

PROPERTIES \ ALLOYS	Cb-752	FS-85	C-129Y	WC-3015	B-66
R.T. Δ L/L CHANGE DUE TO COATING BARE ALLOY.	HIGH	HIGH	HIGH	LOW (EMBRITTLED)	LOW
F_{tu} AND F_{ty} (R.T.)	COMPARABLE	COMPARABLE	COMPARABLE	HIGH	COMPARABLE
F_{tu} AND F_{ty} ($2400^{o}F$)($1300^{o}C$)	COMPARABLE	COMPARABLE	COMPARABLE	COMPARABLE	COMPARABLE
REUSE EFFECTS ON STRENGTH (50,100 CYCLES)	COMPARABLE	COMPARABLE	COMPARABLE	HIGHER REDUCTION IN STRENGTH	COMPARABLE
REUSE EFFECTS ON OXIDATION FAILURE(50,100 CYCLES)	1/3 SPECIMENS FAILED	NONE	NONE	NONE	NONE
F_{tu} AND F_{ty} (R.T., DEFECTED)	COMPARABLE	COMPARABLE	COMPARABLE	COMPARABLE	COMPARABLE
F_{tu} AND F_{ty} ($2400^{o}F$, ($1300^{o}C$) DEFECTED)	COMPARABLE	COMPARABLE	COMPARABLE	COMPARABLE	COMPARABLE

6.0 CONSPECTUS OF COATING STUDY FOR COLUMBIUM ALLOYS C-129Y AND FS-85

The object of this study was to select a coating chemistry for the C-129Y and FS-85 alloys that would offer better protection than the R-512E (Si-20Cr-20Fe) coating. The R-512E composition was "optimized" for D-43 and Cb-752 type alloys and might not provide equivalent protection to the other alloys which differ markedly in chemistry.

Seven basic compositions (Si-20Cr-20Fe; Si-20Cr-5Ti; Si-40Cr-20Fe; Si-20Cr-10Mo; Si-20Cr-10W; Si-20Ti-10M; Si-20Ti-3V) were formulated and applied to batches of 10 of each alloy-coating combination by spraying. The unit weight of coating applied was adjusted to yield coatings having equivalent silicon contents of about 16.5 mg/cm^2. All samples were given a standard fusion-diffusion treatment for one hour at 2580°F (1420°C). Two hundred ten specimens were processed.

The Cb-752/Si-35Cr-20Fe system gave the overall best performance based on the test criteria employed. Almost equivalent results were recorded for the Cb-752/Si-40Cr-20Fe system. The best performing coating on FS-85 was Si-40Cr-20Fe and the best performing coating on C-129Y was Si-35Cr-20Fe.

The decision was made not to change to the 35 or 40 Cr content coatings for the remainder of the program because the improvement in life was not considered significant enough to warrant a change. Details of the test procedure and test results (oxidation and metallography) are given in Volume II.

7.0 CONSPECTUS OF SELECTION OF OPTIMUM COLUMBIUM ALLOY FOR REUSABLE HEAT SHIELD APPLICATIONS

The effects of multiple cycle reuse on coating emittance, coating chemistry and structure, and heat shield panel structural integrity were investigated to provide a broader performance base for optimum alloy selection.

A new technique for making total normal emittance measurements on sheet material without using a thermocouple attachment was developed. Changes in emittance due to reuse up to 100 simulated reentries were determined. The effect of reuse on emittance of all five alloy/coating systems was small. Most alloy/coating systems showed an initial drop in emittance of about 5% up to the first 15 to 20 cycles, then a gradual increase until all of the loss had been recovered by 100 cycles. Differences in emittance between alloys were very subtle. The FS-85/R-512E system showed the largest increase in emittance from one cycle to 100 cycles.

Coating chemistry and changes in chemistry, both surface and body, were examined utilizing x-ray diffraction, x-ray fluorescence, and electron microprobe techniques. The specimens used for the examinations performed under this effort of the program were portions of the tensile specimens which were used for determining the effects of reuse on mechanical properties. The portion of the specimens used was the area between the loading hole and the reduced cross section. Specimens, their reentry cycle history, and the analytical tests that were performed on each, are shown in the Table 7-1, Test Matrix. The R-512E coated FS-85 appeared to have the most stable coating structure with respect to reentry cycling.

The emittance and coating chemistry studies were used in conjunction with the mechanical property data from Section 5.0 to select Cb-752, FS-85, and C-129Y as the alloys to be used in heat shield structural integrity studies.

The miniature 1" x 4" (2.5 cm x 10 cm) panel specimen selected (Figure 7-34) was one employed in past coating evaluations (Reference 2) which fit into an existing test facility.

The panels were coated with the R-512E coating by HiTemCo and subjected to temperature-pressure-stress profile conditions typical of those for a Space Shuttle reentry (see Figure 4-1). Temperature and pressure conditions were provided by a resistance heated tube furnace while stress on the panels was provided simultaneously from a scissors-type loading fixture.

The four point loading fixture was fabricated from FS-85 columbium alloy and protected with the R-512E coating. The loading fixture and the bending moment distribution it produced are shown in Figure 7-1.

Miniature rib stiffened heat shield panels of the three alloys were subjected to temperature, pressure, and stress profile testing to determine coating reusability, and structural performance. The panels were subjected to temperature-pressure-stress profile conditions typical of those for a Space Shuttle reentry. A total of 1200 reentry cycles was performed. Seven panels were exposed for 100 cycles each. Three of the seven 100 cycle panels were exposed in the internal pressure environment. The testing on five panels was terminated prior to reaching 100 cycles due to equipment malfunctions and operator problems. The two remaining panels, which were the C-129Y alloy, failed structurally after 87 cycles each in the external pressure environment. The structural failures were brought about by coating failures on the ribs. The reason for the coating failures on the C-129Y panels is explained by a very thin coating on the rib edges. However, the coating failures on the C-129Y panels did demonstrate that the occurrence of a coating failure does not mean immediate catastrophic structural failure. In this particular case the coating failures occurred in the most highly tension stressed area; a minimum of 50 reentry cycles, after noticeable oxidation, was required before structural integrity was affected.

TABLE 7-1

TEST MATRIX FOR CHEMISTRY AND STRUCTURE STUDIES

SPECIMEN	NO. OF CYCLES	COMPOSITION (NOMINAL)	XRD EXAM	XRF EXAM	ELECTRON PROBE LINE SCANS							
					Si	Cr	Fe	Nb	W	Zr	Ta	Hf
C-62	0	5 Zr, 10 W, BAL. Nb	–	–	X	X	X	X	X	X	–	–
C-27	50	5 Zr, 10 W, BAL. Nb	X	X	X	X	X	X	X	X	–	–
C-89	100	5 Zr, 10 W, BAL. Nb	X	X	X	X	X	X	X	X	–	–
F-70	0	11W, 28 Ta,1Zr,BAL.Nb	–	–	X	X	X	X	X	–	X	–
F-77	50	11W, 28 Ta,1Zr,BAL.Nb	X	X	X	X	X	X	X	–	X	–
F-84	100	11W, 28 Ta,1Zr,BAL.Nb	X	X	X	X	X	X	X	–	X	–
Y-43	0	10W,10Hf,0.1Y,BAL.Nb	–	–	X	X	X	X	X	–	–	X
Y-12	50	10W,10Hf,0.1Y,BAL.Nb	X	X	X	X	X	X	X	–	–	X
Y-18	100	10W,10Hf,0.1Y,BAL.Nb	X	X	X	X	X	X	X	–	–	X
B-38	50	5Mo, 5V,1 Zr,BAL.Nb	X	X	–	–	–	–	–	–	–	–
B-81	100	5Mo, 5V,1 Zr, BAL. Nb	X	X	–	–	–	–	–	–	–	–
W-8	50	30 Hf 4Ti,15W BAL.Nb	X	X	–	–	–	–	–	–	–	–
W-4	100	30 Hf 4Ti ,15W BAL.Nb	X	X	–	–	–	–	–	–	–	–

Based on the results of reuse testing of the miniature heat shield panels, there was not a clear cut choice of the best alloy for reentry heat shield panels. The results of all screening tests performed were reviewed and the FS-85 alloy was selected for the coating/alloy evaluations to be performed in the remainder of the program.

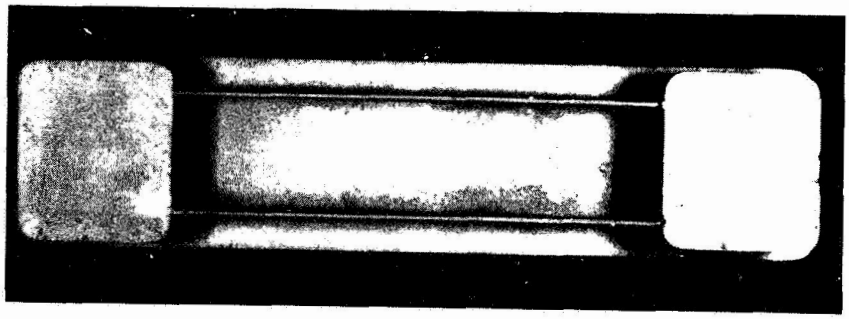

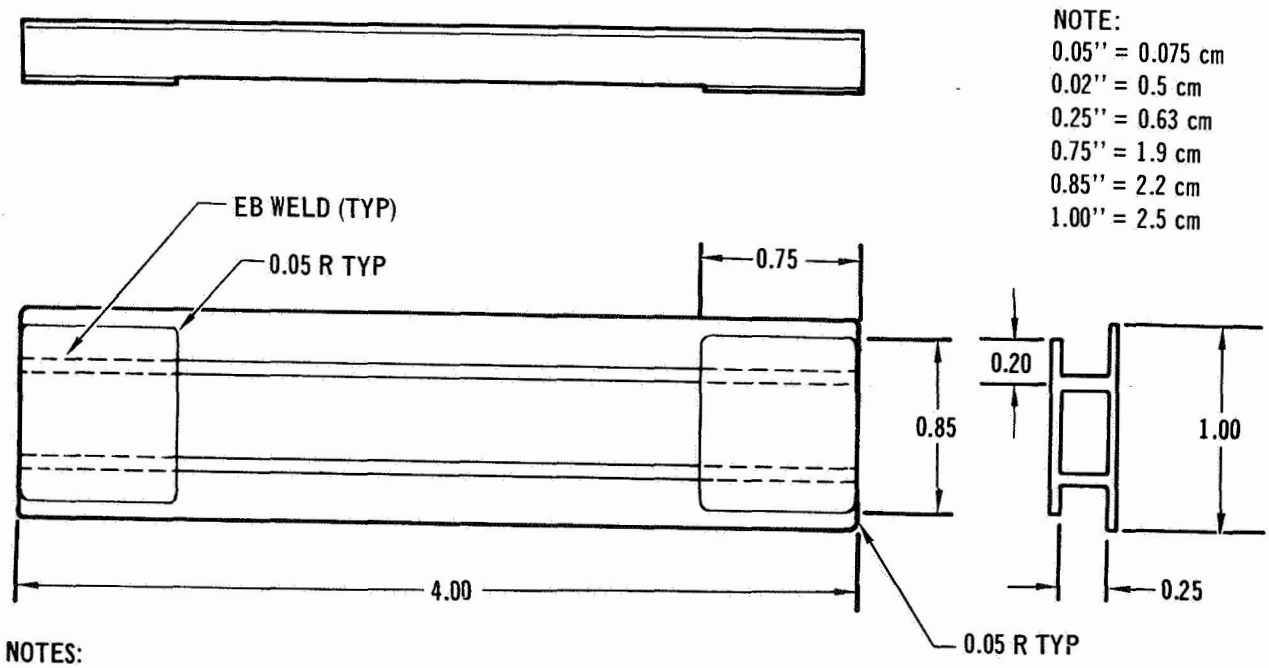

NOTES:
(1) PANEL SKIN 0.008" (0.02 cm) AFTER COATING
(2) PANEL RIBS 0.016" (0.04 cm) AFTER COATING
(3) ALL DIMENSIONS ARE IN INCHES.

457-1154

RIB STIFFENED PANEL SPECIMEN

FIGURE 7-1

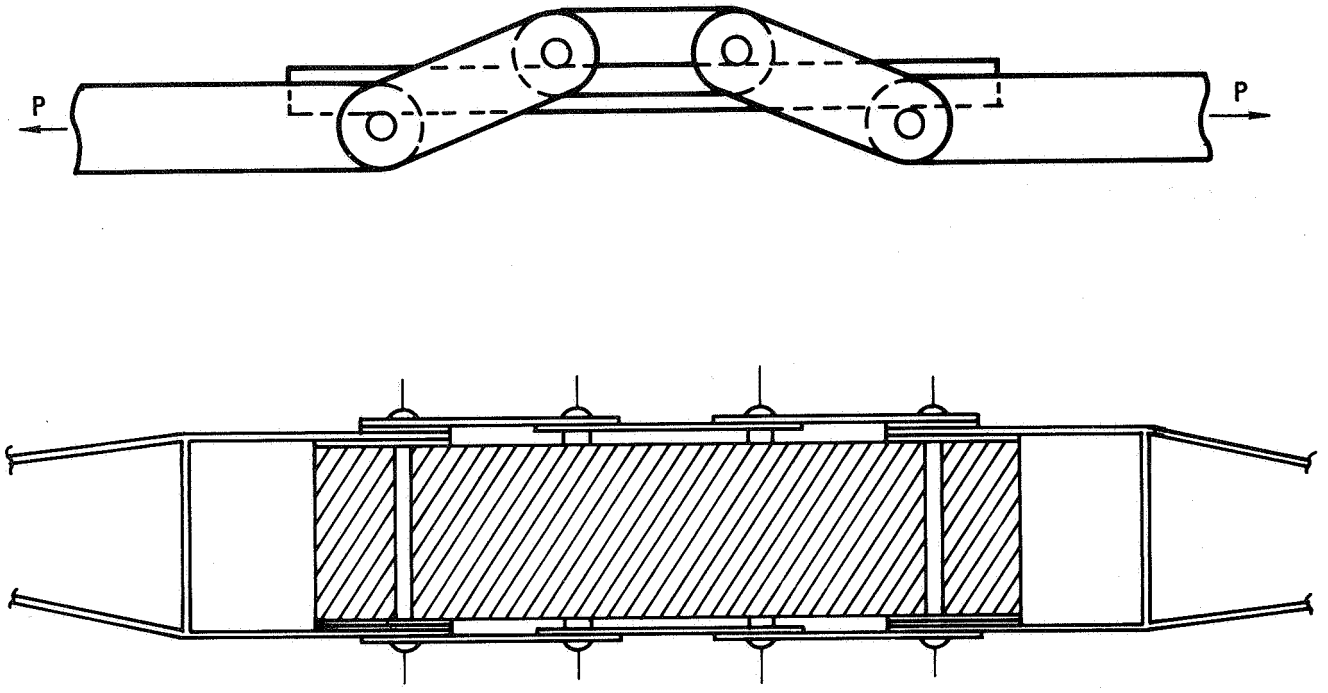

457-1155

Four Point Loading Fixture

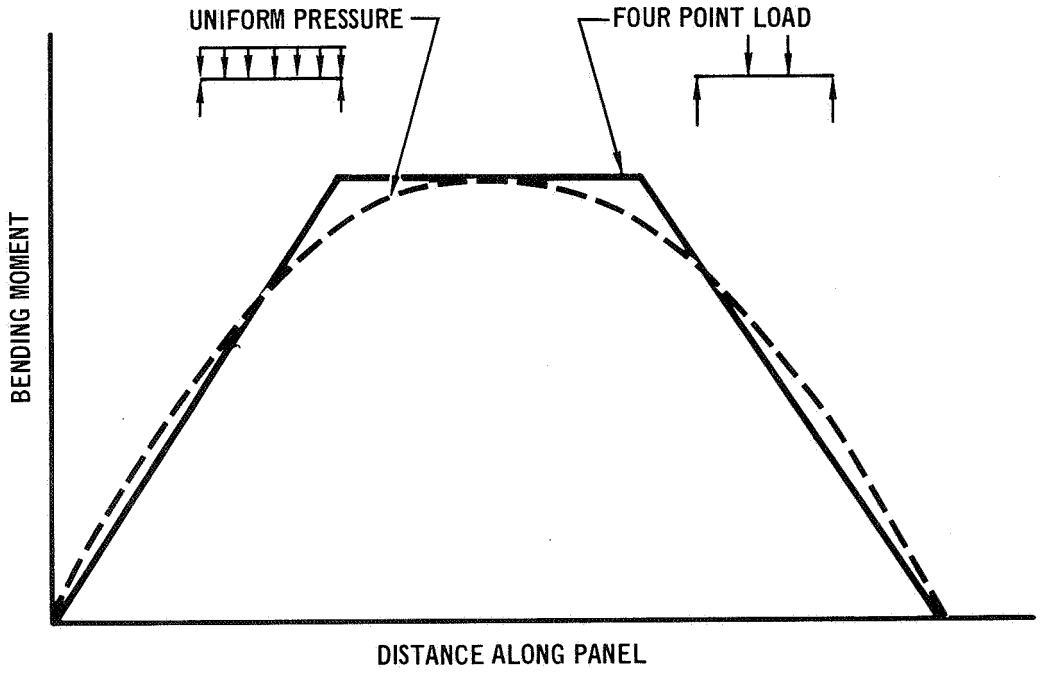

457-1156

Panel Bending Moment Distribution

FIGURE 7-2

8.0 CONSPECTUS OF COATING PROCESS OPTIMIZATION AND SCALE-UP STUDIES FOR RIB STIFFENED HEAT SHIELD PANELS

8.1 Process Development - The objective of this study was to optimize coating slurries, using a lacquer and an acrylic based vehicle, so that full size 20" x 20" (50 cm x 50 cm) heat shield panels could be coated uniformly and reproducibly. The same basic R-512E, Si-20Cr-20Fe, metal powder composition was used throughout the program. Various additives were made to the slurries to give them thixotropic properties, primarily to promote suspension of the metal particles and also to prevent caking when settling occurs after long periods of nonuse. Materials used and the sources of supply are listed in Table 8-1.

The L-18 nitrocellulose lacquer has been used as the basic vehicle for the R-512E slurry coating system since its inception; it was adopted because it is a low residue material with good "green" strength and it has a history of practical use in glass-to-metal seals and other applications at HiTemCo.

During a previous scale-up program (Reference 3) with Sn-Al slurry coatings for tantalum alloys and early work with the R512 system coatings "in-house," certain qualitative relationships were established between slurry properties and coating deposition rate and uniformity. In dip-coating, slurry viscosity and withdrawal rates were found proportional to coating thickness. Viscosity could be increased by thixotropic additives or by increased metal powder ratios and decreased by increasing ambient temperatures.

TABLE 8-1

MATERIALS USED FOR SLURRY PREPARATION

MATERIAL IDENTIFICATION	SUPPLIER
1. L-18 LACQUER	RAFFE AND SWANSON
2. B-66 ACRYLIC	ROHN AND HAAS
3. MPA 60	BAKER CHEMICAL CO.
4. THIXATROL ST	BAKER CHEMICAL CO
5. HIGH FLASH NAPHTHA (HFN)	HOGAN CHEMICAL
6. LACQUER THINNER (LT)	HOGAN CHEMICAL
7. XYLENE	HOGAN CHEMICAL
8. SILICON POWDER (-325)	UNION CARBIDE
9. CHROMIUM POWDER (ELCHROME)	UNION CARBIDE
10. IRON POWDER (K291)	GLIDDEN COMPANY

It was found in general that withdrawal rates of approximately 1.0-6.0 in/min (0.40-2.4 mm/sec) were most practical. Also, that temperatures above 80°F (27°C) drastically decreased the stabilizing effect on thixotropic additives. Accordingly, these findings and experience were used as a guide in the present program.

Tables 8-2 and 8-3 list the slurry compositions screened and some of the typical dipping data obtained. Altogether 32 slurries were investigated. The results were evaluated on the basis of dipping and drying rates, coating thickness, coating uniformity top to bottom, streaking, sagging, and edge pull back.

Six compositions selected from both systems were prepared to allow coating of 2" x 20" (5 cm x 50 cm) strips prior to selection of the slurries for full size scale-up.

The C-5 nitrocellulose based slurry and A-22 acrylic based slurry were selected for further study and large batches were prepared for study on 20" x 20" (50 x 50 cm) specimens.

Concurrent with this study, another study was made to determine the latitude in the fusion furnace cycle and the additive effects on the oxidation protection of the coatings.

This study is summarized now. In general, longer processing times at temperature gave decreased protection. Paradoxically there also appears some tendency toward increased life with higher processing temperature. However, there are probably several competing systems at work. On the negative side are the coating weight losses which increase with time and temperature. The lost material is probably high in chromium and iron. Structurally, this increases the amount of $CbSi_2$ at the outermost surface. On the positive side, the coating diffusion zone grows with time and temperature which probably improves reliability by giving more protection at crack roots in thin coating areas. The interpretation and correlation of the quantitative results obtained from optimizing the coating fusion cycle was not deemed as important as development of an improved and consistent edge coating technique. If anything, this work illustrated that fairly effective protection could be obtained over a broad range of processing time and temperature. Accordingly, for the balance of the program, no attempt was made to change the fusion cycle, particularly since a considerable data base had been obtained in the industry for the standard cycle.

The possible effects on coating structure and performance caused by the use of the various binders and thixotropic additives were investigated by coating and evaluating Cb-752 specimens. The coating structures obtained, failed to show any

TABLE 8–2

ACRYLIC BASE SCREENING SURRIES

SLURRY NO.	AMT. OF VEHICLE (CC)	MPA WT (g)	THIXATROL WT. (g)	POWDER WT (g) R512E	VISCOSITY CP x 10^2 (Nsec/m^2)	AMBIENT TEMP ^oF (^oC)	DIPPING SPEED IN/MIN (mm/sec)		COATING WT. mg/cm^2
A. VEHICLE IS HFN PLUS 8 V/O B–66 ACRYLIC									
A–1	200	20	0	500	36 (3.6)	80 (27)	1	(0.4)	23.5
A–2	400	20	0	600	9 (0.9)	85 (29)	2.5	(1.0)	9.0
A–3	200	0	0	500	26 (2.6)	78 (26)	1	(0.4)	19.8
A–4	200	10	0	500	14 (1.4)	76 (24)	4.5	(1.8)	12
A–5	200	10	0	600	24 (2.4)	80 (27)	6	(2.4)	17
A–6	200	10	5	600	35 (3.5)	78 (26)	6	(2.4)	32
A–7	300	10	5	600	18 (1.8)	74 (23)	8	(3.2)	16
A–8	200	16	0.25	500	16 (1.6)	78 (26)	6	(2.4)	15
A–9	200	16	0.75	500	28 (2.8)	74 (23)	4	(1.6)	25
A–10	200	16	0.75	550	37 (3.7)	74 (23)	6	(2.4)	13
B. VEHICLE IS HFN + LACQUER THINNER + 8V/O B–66 ACRYLIC									
A–11	200 (50% HFN)	7.5	0	530	24 (2.4)	76 (24)	5	(2.0)	20
A–12	200 (50% HFN)	7.5	0	630	26 (2.6)	75 (24)	4	(1.6)	21
A–13	200 (60% HFN)	7	0.3	600	24 (2.4)	79 (26)	3	(1.6)	19.4
A–14	200 (60% HFN)	7	0.5	700	20 (2.0)	74 (23)	6	(2.4)	22
A–15	200 (85% HFN)	7	0.4	600	15 (1.5)	74 (23)	5	(2.0)	18
A–16	200 (85% HFN)	7	0.6	600	27 (2.7)	73 (23)	7	(2.8)	24
A–17	200 (85% HFN)	9	0.4	600	24 (2.4)	70 (21)	4	(1.6)	17
B–1	200 (100% LT	20	0	500	19 (1.9)	80 (27)		(0.4)	21
B–2	400 (100% LT)	20	0	600	15 (1.5)	78 (26)	2.5	(1.0)	25
B–3	200 (100% LT)	5	0	500	17 (1.7)	76 (24)	2.5	(1.0)	15
B–4	220 (100% LT)	5	0	560	14 (1.4)	80 (27)	6	(2.4)	22
B–5	200 (50% HFN)	7.5	0	600	30 (3.0)	78 (26)	4	(1.6)	24
B–6	200 (50% HFN)	7.5	1.0	600	23 (2.3)	79 (26)	6	(2.4)	20
C. VEHICLE IS XYLENE + 8 V/O B–66 ACRYLIC									
X–1	200	7	0	600	26 (2.6)	76 (24)	7	(2.8)	22
X–2	200	7	0	650	25 (2.5)	74 (23)	6	(2.4)	20
X–3	200	7	0.4	650	24 (2.4)	76 (24)	6	(2.4)	18
X–4	200 (50% HFN)	7	0.4	600	23 (2.3)	74 (23)	4	(1.6)	20

significant differences attributable to the various binders or additives. The effects of these binders and additives on oxidation life in the accelerated air slow cyclic test, were also studied. The results failed to show any significant differences attributable to the various binders or additives. This result was anticipated because the binders and additives are reported to be residue-free and to decompose early in the diffusion cycle. It appeared feasible, therefore, to use these binders as additives in preparation of slurries for the large scale panels.

TABLE 8-3
NITROCELLULOSE (L-18) LACQUER SLURRIES

SLURRY NO.	AMT OF VEHICLE (g)	MPA WT (g)	THIXOTROL WT (g)	POWDER R512 WT (g)	VISCOSITY CP x 10^2 (Nsec/m^2)	AMBIANT TEMP, ^oF (^oC)	DIPPING SPEED IN/MIN (mm/sec)	COATING WT. mg/cm^2
C-1	200	16	0.25	500	15 (1.5)	79 (26)	4 (1.6)	18.5
C-2	200	16	0.75	500	13 (1.3)	73 (23)	6 (2.4)	16.5
C-3	200	16	0.75	600	20 (2.0)	75 (24)	0.75 (0.3)	18
C-4	200	16	0	600	18 (1.8)	74 (23)	2 (0.8)	20.1
C-5	200	16	1.0	600	21 (2.1)	73 (23)	2 (0.8)	21.1

As indicated above, the C-5 nitrocellulose lacquer and A-22 acrylic based slurries were selected for scale-up evaluation. Several steel dipping tanks 3" (7.5 cm) wide x 23" (58 cm) long x 27" (69 cm) high were constructed and used for these trials and eventually for full scale panel dipping. Sheets of stainless steel 0.018" x 20" x 20" (0.5 cm x 50 cm x 50 cm) were used as panel mockups to check the uniformity of the coating thickness and slurry chemistry.

A large batch (20 gal. (0.076 m^3)) of C-5 nitrocellulose base slurry was made up; it performed similarly to previous smaller batches after a minor viscosity adjustment was made. Figure 8-1 shows the coating uniformity obtained on one of the 20" x 20" (50 cm x 50 cm) panels. The average coating thickness was 20.5 mg/cm^2 and the Dermitron showed a thickness variation of 18 to 22 mg/cm^2. This converts to a green coating thickness of 5.5 mils (140 μm) with a range of 5.0 to 6.0 mils (127 to 152 μm). After fusion, the finished coating is approximately one-half the green coating thickness. These values were well within the program goals.

Evaluation of the large batch of acrylic based slurry A-22 indicated that there were problems with settling and aging. In order to obtain uniform coatings, it is necessary for the viscosity of the slurry at the surface of the batch to be constant for the time required to coat the hardware. The viscosity of the A-22 slurry was

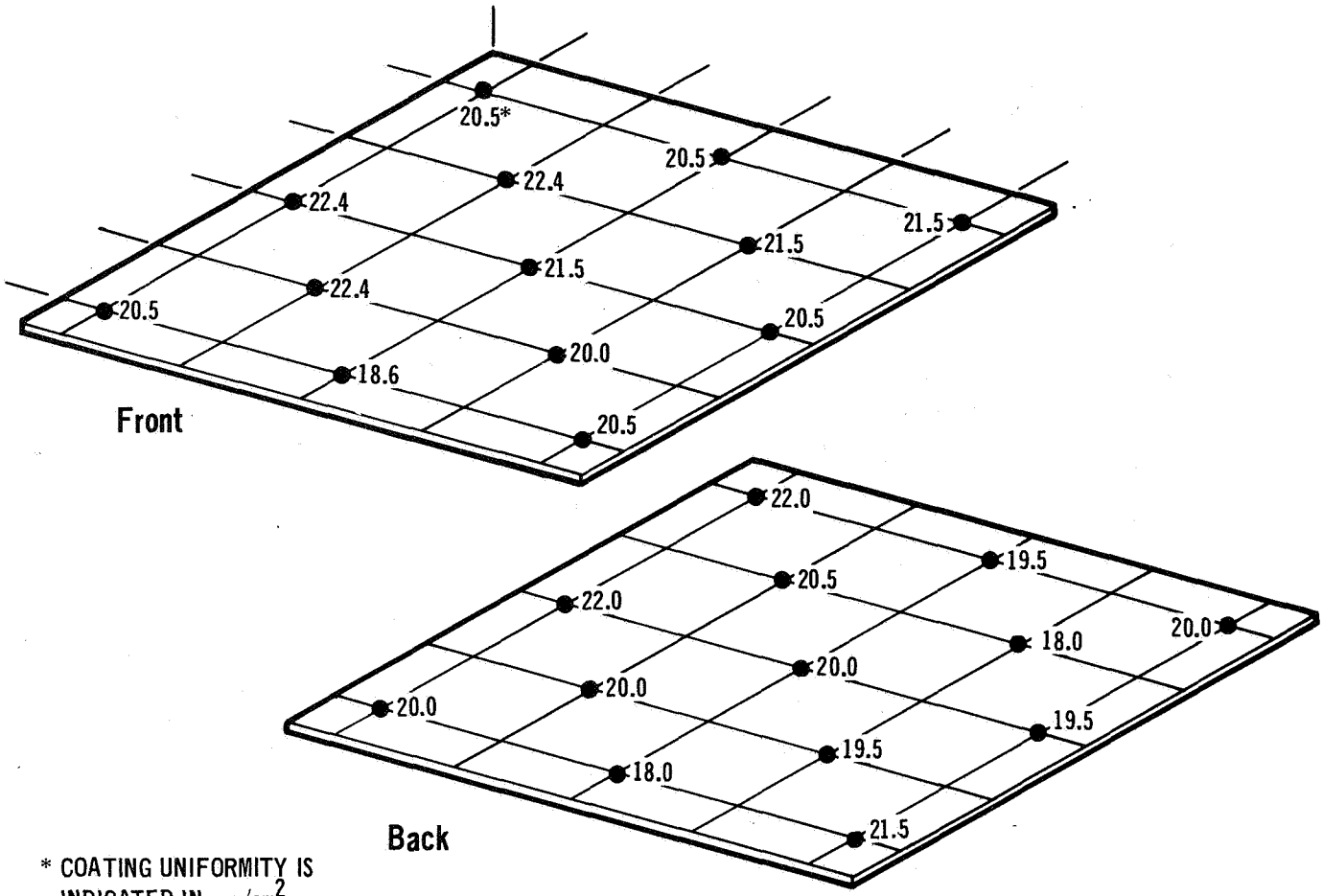

COATING UNIFORMITY STUDIES ON 20" x 20" (50 CM x 50 CM) FLAT PANEL MOCKUP

FIGURE 8-1

determined just below the surface of the batch and compared to similar data on the C-5 slurry. The results of this test are shown in Figure 8-2. The C-5 slurry shows a constant viscosity whereas the A-22 slurry shows a considerable decrease with time. This change in viscosity indicates the lack of effectiveness of the viscosity control additives employed. In order to avoid major program delays, studies on the A-22 slurry were suspended and optimization studies were continued with the C-5 slurry.

The possible variations in coating chemistry obtained in this process at the slurry stage, were determined by coating a 20" x 20" (50 cm x 50 cm) flat stainless mockup in the C-5 slurry. The green coating was then selectively removed from 2" (5 cm) square areas in nine locations on the panel. The coating powder obtained was analyzed for Cr and Fe by x-ray fluorescence techniques, the results of which are shown in Figure 8-3. Silicon contents were determined by difference.

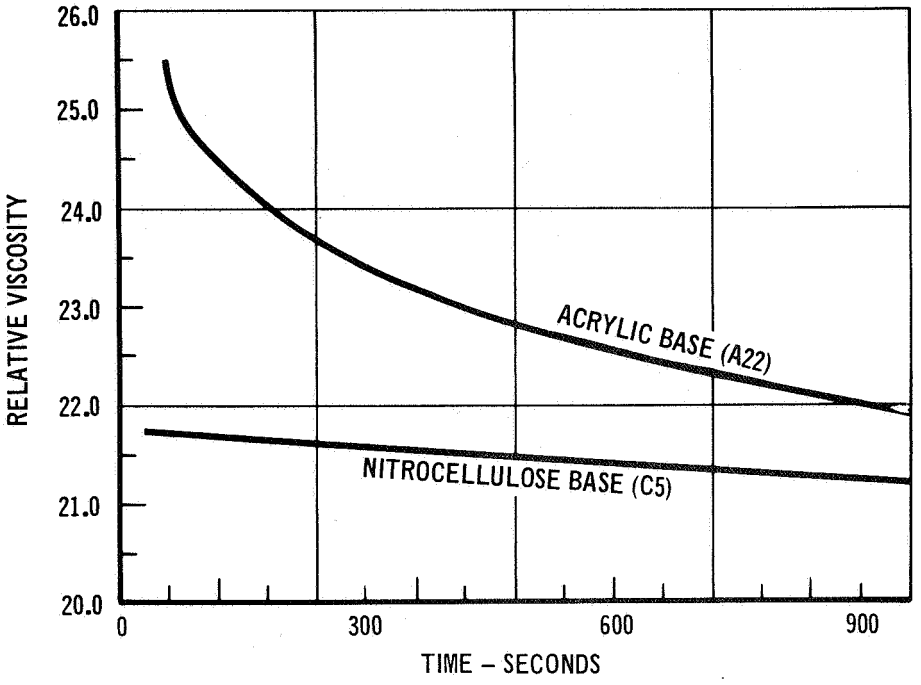

EFFECT OF SETTLING ON VISCOSITY 1/4 IN. (0.6 CM) BELOW SURFACE FOR ACRYLIC BASE (A22) AND NITROCELLULOSE BASE (C5) SLURRIES

FIGURE 8–2

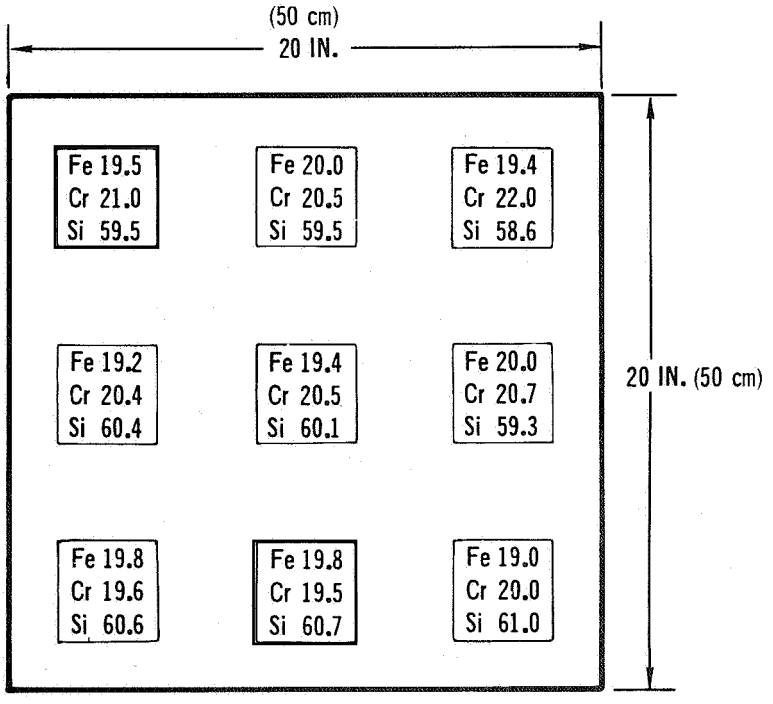

COATING COMPOSITION UNIFORMITY FROM C–5 SLURRY ON 20 IN. X 20 IN. (50 CM X 50 CM) FLAT STAINLESS MOCKUP

FIGURE 8–3

The effects of geometry were investigated by dip-coating a 20" x 20" (50 cm x 50 cm) electron beam welded rib stiffened stainless steel panel in the same batch of slurry used for the 20" x 20" (50 cm x 50 cm) sheet. The panel picked up an average weight of 20.8 mg/cm^2 (the range was 19 to 22 mg/cm^2). The average green coating thickness was 5.6 mils (142 μm). The front or skin side of the panel had an average coating thickness of 5.3 mils (135 μm), while the back side of the skin between the ribs was 5.7 mils (145 μm), and the ribs were 5.7 mils (145 μm). Green coating thickness distributions on the panel are shown in Figure 8-4. The coating uniformity (excluding edge coverage) was considered excellent for dipping and, in a fused state, would give a coating with a plus or minus variation in thickness of 0.3 mil (7.6 μm).

8.2 Edge Coverage and Coating Reproducibility - The normal coating procedure prior to this program included the application of additional coating to the edges of specimens by spraying with an air brush. Although excellent reproducibility was obtained on specimens supplied for evaluation programs by this coating method, it is a manual process and subject to operator error. It appeared desirable therefore to develop methods for improving slurry application at edges.

Double cycle coating application was investigated first in an effort to improve the edge coverage. The first processing sequence investigated consisted of two separate dip and fire cycles.

The second processing sequence consisted of 2 green slurry coats followed by a single diffusion treatment. The first cycle dip was applied from the C-5 nitrocellulose based lacquer (13 mg/cm^2); and, after thorough drying, additional coating (9 mg/cm^2) was applied by dipping in an acrylic based slurry. These samples failed to show any significant improvement over either single cycle or the double diffusion coatings previously described.

Eventually a method for applying a bead of slurry directly to the edge was developed. A miniature paint striping tool was obtained as shown in Figure 8-5, and found to be adequate for applying the bead of slurry to the edge. Samples of Cb-752 were then dip coated and evaluated by NDT (thermoelectric) and by slow cycle oxidation testing at one atmosphere in the as-dipped, oversprayed, and beaded-edge conditions. The results of these tests are shown in Table 8-4. Bead coating of edges greatly reduces the problem of premature coating failure at edges which was one of the major limitations to long life.

8.3 Process Verification - Rib stiffened panels, 3 by 12" (7.5 x 30 cm) were required to verify effectiveness and reproducibility of the optimized coating.

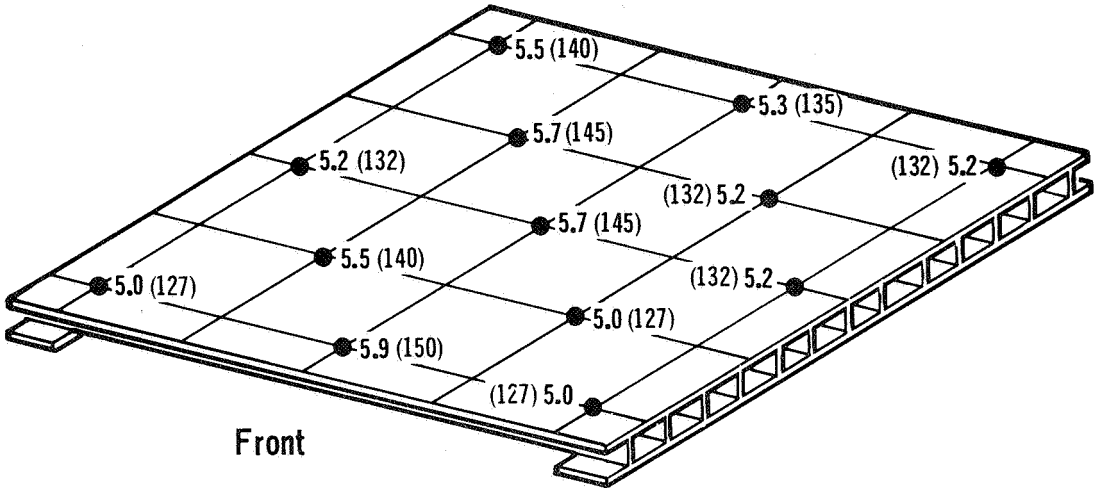

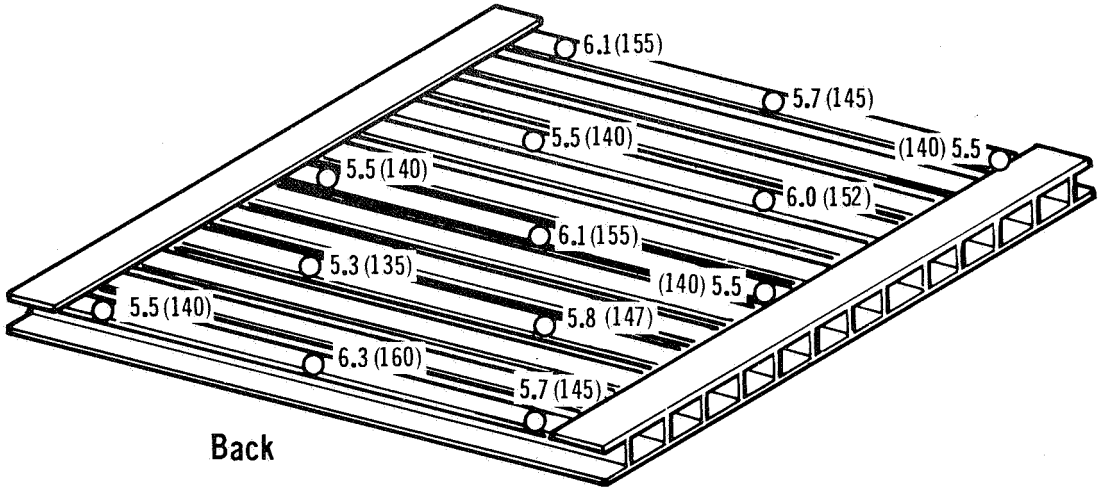

Ribs

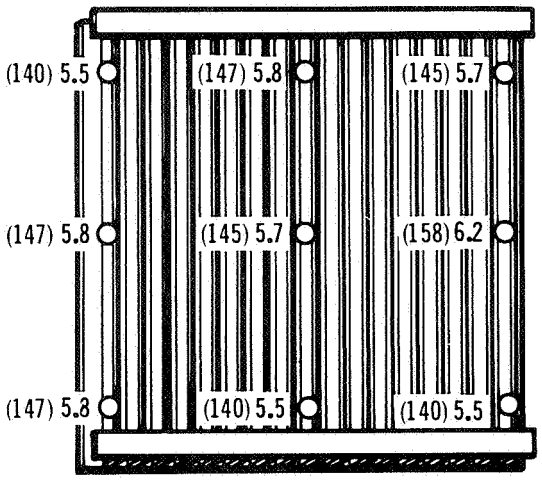

COATING UNIFORMITY STUDY ON 20 IN. x 20 IN. (50 CM x 50 CM) RIB STIFFENED MOCKUP
Slurry Thickness is in Mils (μm)

FIGURE 8-4

The design is representative of a full-size rib stiffened panel in all respects except the overall dimensions, which were selected to fit into a load fixture used in conjunction with a 7" (18 cm) diameter tube furnace.

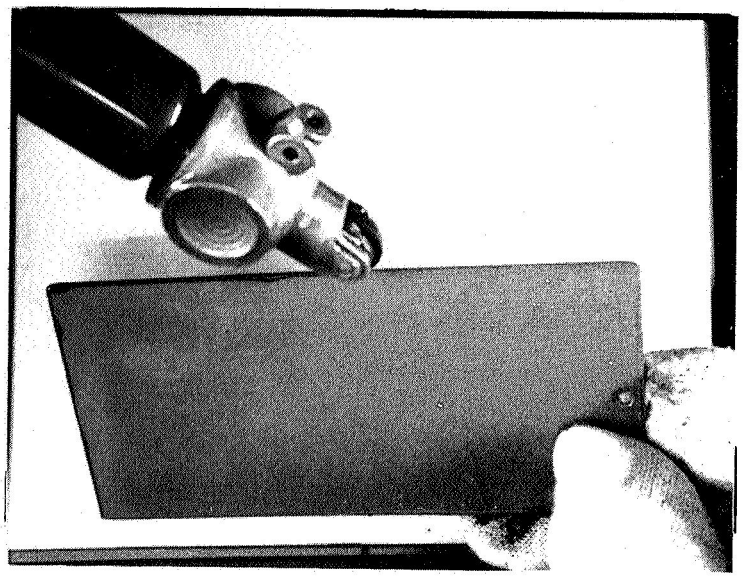

SLURRY BEAD APPLIED TO EDGE AFTER DIP COATING

FIGURE 8-5

TABLE 8-4

EFFECT OF EDGE COATING METHOD ON PERFORMANCE OF R-512E COATING

CONDITION	EDGE THICKNESS NDT (MILLIVOLTS) COPPER PROBE	1 ATMOSPHERE SLOW CYCLIC OXIDATION LIFE
AS DIPPED	-0.2	2 CYCLES
AS DIPPED AND OVERSPRAYED	+0.2	20-50 CYCLES
AS DIPPED AND SLURRY BEADED	+0.4	75-150 CYCLES

Five subsize heat shield panels were subjected to simultaneous simulation of temperature, pressure, and stress profiles and acoustic exposures representative of a Space Shuttle reentry flight.

The temperature, pressure and stress conditions are those that were presented in Section 4.0, Figure 4-2, for subsize panel testing. A total of 412 reentry cycles were conducted; three panels were exposed for 100 cycles each. Creep and elastic deflection measurements were made prior to and during testing.

Results of creep and elastic deflection measurements are shown in Table 8-5. Creep deflections are expressed in average deflection rate (mils/cycle and μm/cycle)

for each group of cycles conducted per panel and in cumulative average deflection rate (mils/cycle and μm/cycle) for each group of cycles conducted per panel. Elastic deflection measurements are shown in inches and centimeters measured at the center of an 11" (28 cm) span.

TABLE 8-5

DEFLECTION MEASUREMENTS FOR SUB-SIZE RIB STIFFENED PANELS

PANEL NO.	PRESSURE	CYCLE NO.	DEFLECTION MEASUREMENTS		
			CREEP		ELASTIC
			GROUP RATE MILS(μm)/CYCLE	CUMULATIVE AVERAGE RATE MILS(μm)/CYCLE	AFTER EACH GROUP REENTRY CYCLES IN. (cm)
1	EXTERNAL	0			
		14	0.71 (18)	0.71 (18)	
		28	0.22 (5.6)	0.46 (11.7)	
		41	0.15 (3.8)	0.38 (9.7)	
		57	0.57 (14.5)	0.40 (10.2)	
		70	0.54 (13.7)	0.43 (11)	
		86	0.50 (12.7)	0.43 (11)	
		100	0.43 (11)	0.43 (11)	
2	EXTERNAL	0			
		13	0.61 (15.5)	0.61 (15.5)	
		28	- 0.27 (-6.9)	0.14 (3.6)	
		40	0.17 (4.3)	0.15 (3.8)	
		56	0.75 (19)	0.32 (8.1)	
		70	0.50 (12.7)	0.36 (9.2)	
		86	0.38 (9.7)	0.36 (9.2)	
		100	0.50 (12.7)	0.38 (9.7)	
5	EXTERNAL	0			0.107 (0.272)
		15	1.30 (33)	1.30 (33)	0.083 (0.210)
		30	0.67 (17)	0.97 (24.6)	0.082 (0.208)
		45	0.33 (8.4)	0.76 (19.3)	
3	INTERNAL	0			0.091 (0.230)
		22	0.73 (18.5)	0.73 (18.5)	0.076 (0.193)
		47	0.60 (15.2)	0.66 (16.8)	0.075 (0.190)
		71	0.00 (0)	0.43 (11)	0.075 (0.190)
		86	0.33 (8.4)	0.42 (10.7)	0.076 (0.193)
		100	0.50 (12.7)	0.43 (11)	
4	INTERNAL	0			0.092 (0.234)
		25	0.80 (20.2)	0.80 (20.2)	0.082 (0.208)
		45	0.05 (1.3)	0.47 (12)	0.089 (0.226)
		67	0.09 (2.3)	0.34 (8.6)	

The reuse evaluation testing was also designed to determine structural performance under service conditions which would be expected on Space Shuttle vehicles for 100 flights. From this aspect the coating and panel were treated as an integral unit. The failure criterion was structural life. There were no structural failures due to the application of flight loads; the structural failures

were induced by acoustic exposure. However, acoustic environment simulation was designed to produce fatigue failures in 100 flights. Reasons for this are explained in Section 1.0, Volume II. In actual practice, heat shield panel design factors would include allowances for fatigue life in order to obtain reliable structural performance for 100 flights.

Two full size 20" x 20" (50 cm x 50 cm) rib stiffened heat shield panels were fabricated from FS-85 alloy sheet. Material gages, rib spacing and height were the same as those utilized on the subsize panels. Fabrication procedures were also identical, except that the full size panels were subjected to a creep flattening procedure to remove the skin distortion between the welds. The undesirable skin distortion was caused by shrinkage of the electron beam fusion weld which joined the ribs to the skin. The creep flattening was successfully performed using machined molybdenum tooling and a vacuum heat cycle of one hour (36 h sec) at 2700°F (1480°C).

The 20" x 20" (50 cm x 50 cm) rib stiffened panels were coated by the process developed on this program, and a significant improvement in coating uniformity, edge coverage and slurry stability were demonstrated. The process specification for application of the R-512E coating to rib stiffened panels using the C-5 slurry and the details of this study are presented in Volume II. The full size coated panels are shown in Figure 8-6 with a closeup view in Figure 8-7.

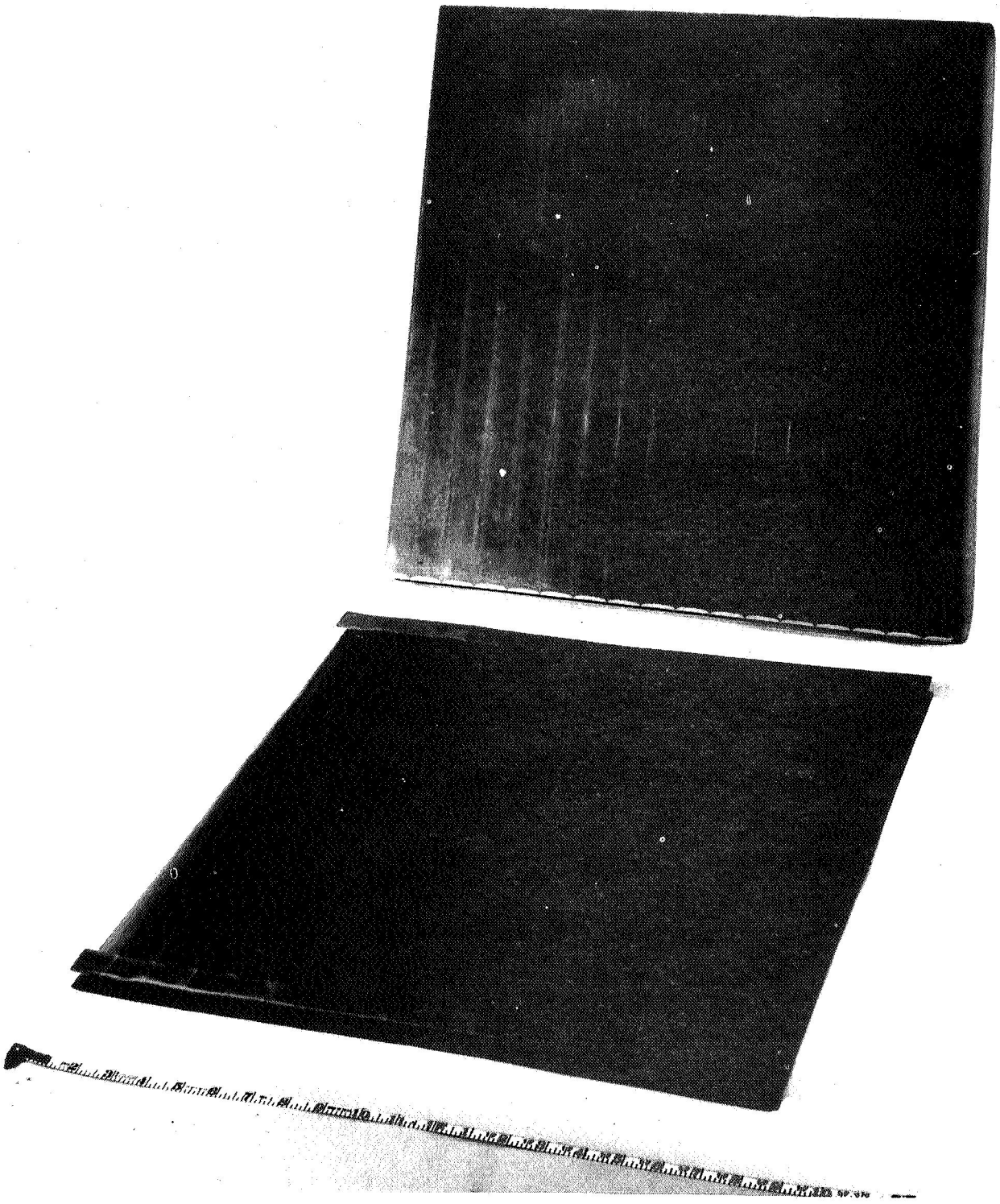

20" x 20" (50 CM x 50 CM) RIB STIFFENED FS85 ALLOY HEAT SHIELD PANEL

FIGURE 8-6

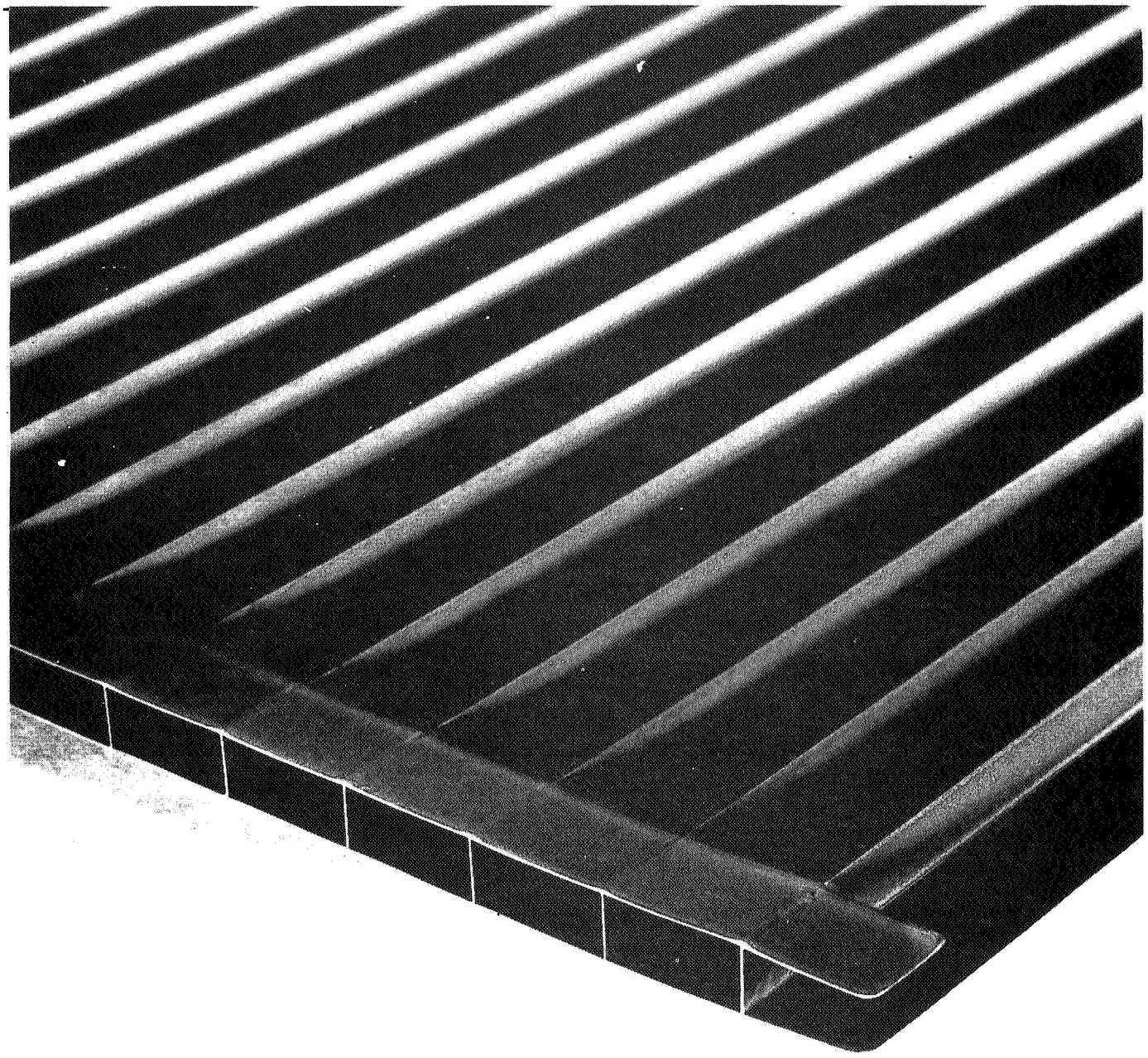

CORNER DETAIL OF 20" x 20" (50 CM x 50 CM) RIB STIFFENED FS85 ALLOY HEAT SHIELD PANEL

FIGURE 8–7

9.0 CONSPECTUS OF COATING PROCESS OPTIMIZATION AND SCALE-UP STUDIES FOR CORRUGATION STIFFENED HEAT SHIELD PANELS

9.1 Process Development - The use of corrugation stiffening of structural skins to improve efficiency has been a popular design for some time. Past hardware programs utilizing refractory metals have used corrugation stiffening almost exclusively for heat shielding. The rib stiffened heat shield design was selected as the initial configuration for this program because it offered increased inspectability which is considered important in 100 multimission reuse. However, the strength to weight efficiency of the corrugation design cannot be overlooked because of the important role that weight plays in space vehicle systems. The corrugation design will undoubtedly be utilized in future columbium hardware systems, and because of this it was considered important to optimize and scale-up the fused slurry coating process for corrugation stiffened heat shield panels.

It was anticipated that one of the major problems would be to get equal coating thickness on the inside and outside of the corrugations. Due to restricted access of air, the drying rate of the slurry is lower on the inside. There were also some questions regarding the general effect the geometry would have on coating uniformity.

To verify this behavior and to develop a base on which improvements could be made, an 18" (46 cm) long electron beam welded single faced corrugated FS-85 specimen was coated with the C-5 nitrocellulose base slurry which was optimized for the rib stiffened design. The coating thickness taper from top to bottom on the inside or outside was not of a magnitude to be considered a significant problem. However, there was an interior coating thickness distribution range of 1.2 mils (30.5 μm) to 2.7 mils (68.6 μm) for the top location. The thinning occurred as the coating approached the acute angle at the weld.

Because of the above problem with the nitrocellulose slurry and the desire to obtain a high green slurry strength, it was decided to further the development of an acrylic based slurry having long term stability. Initial efforts performed during processing studies for rib stiffened panels, failed to produce an acrylic slurry which did not degrade within a few weeks. It was discovered that by using a high solids content slurry and by substituting more acrylic resin for the thixotropic agents, the slurries become more stable. A list of the slurry compositions used in the balance of the program is shown in Table 9-1.

TABLE 9-1

MODIFIED AND SCALED UP ACRYLIC BASE SLURRY COMPOSITIONS (Vehicle is HFN Plus B-66)

SLURRY NO.	MPA WT (G)	R-512E METAL POWDERS WT (G)	VEHICLE	
			TOTAL WT (G)	% B-66 ACRYLIC RESIN
28	50	3600	1140	43
29	50	3860	1140	43
30	50	3600	1190	43
31	100	3600	1240	38
32	150	3600	1190	39

Figure 9-1 shows the slurry viscosity as a function of time for the optimized C-5 nitrocellulose based slurry and the acrylic slurries, A-22 and A-28. The A-22 slurry is based on a resin content of 4.0% and thixotropic additives MPA and Thixatrol ST. The A-28 is based on an acrylic resin content of 40% and minor amount of MPA as an agglomerate preventative.

The weight loss on the acrylic based slurry during the diffusion treatment is approximately 7 mg/cm^2 compared to 2 mg/cm^2 for the nitrocellulose slurry, C-5. This is due to the higher resin content in the dried film. It is therefore necessary to apply 27-29 mg/cm^2 green instead of 22-24 mg/cm^2 to obtain a coating of the desired final thickness.

At the desired coating weights, significant coating taper was produced with the A-28 slurry. The A-28 slurry was modified to increase its viscosity by increasing the solids content. Excellent uniformity at the desired coating thickness was obtained.

9.2 Process Verification - As seen in Figure 9-2 the fused slurry silicide coating applied using the A-29 acrylic base slurry to subsize corrugation stiffened heat shield panels utilizing optimized processing techniques developed in this program was of excellent uniformity.

Subsize, 3" x 12" (7.5 cm x 30 cm) corrugation stiffened heat shields were utilized in flight simulation testing to demonstrate the effectiveness of the optimized fused slurry coating and to determine the reuse capability of the heat shield. Five panels were subjected simultaneously to temperature, pressure, and

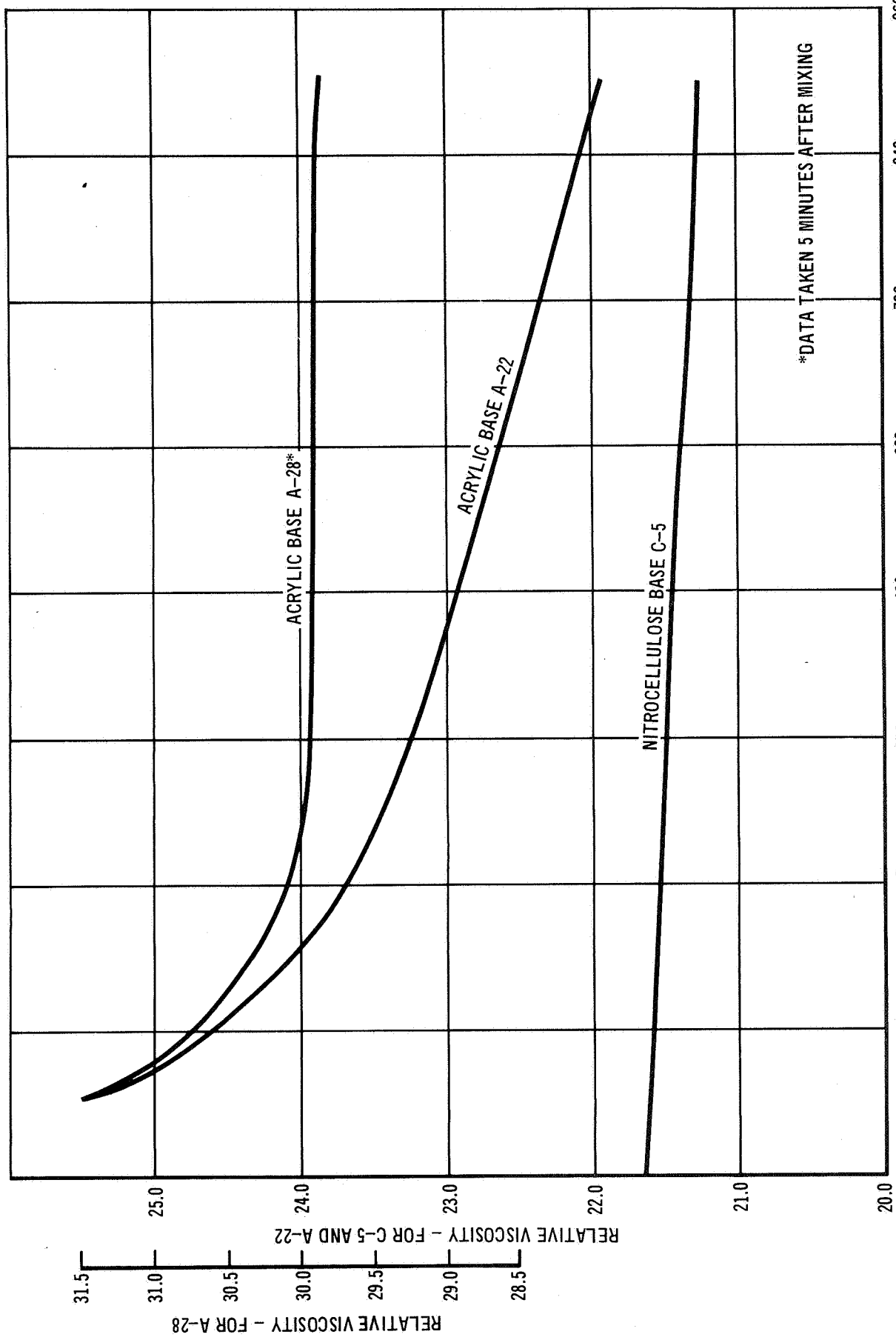

EFFECT OF SETTLING ON VISCOSITY 1/4" (0.6 CM) BELOW SURFACE FOR ACRYLIC BASE A-22, A-28 AND NITROCELLULOSE BASE C-5 SLURRIES

FIGURE 9-1

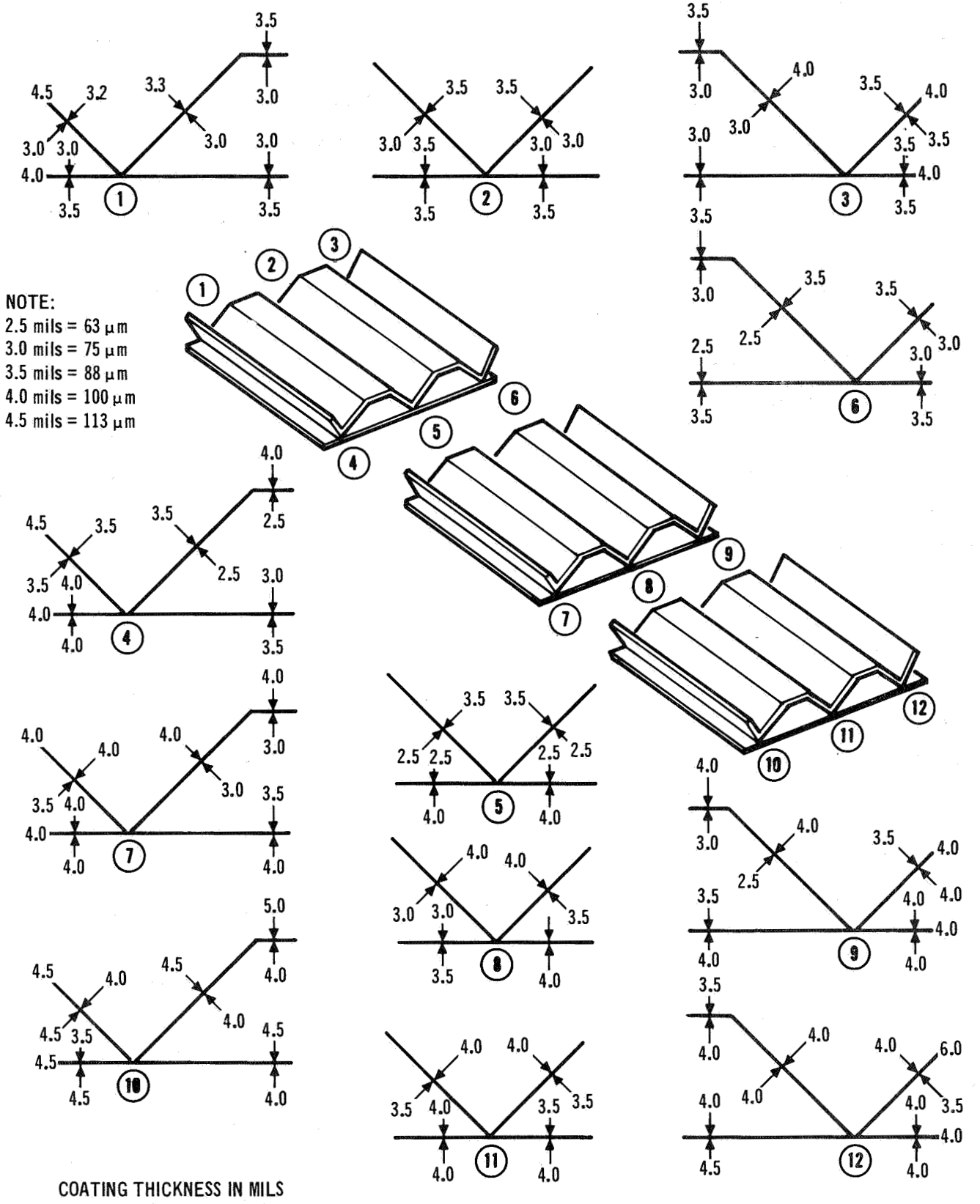

COATING UNIFORMITY STUDY ON SUB-SIZE CORRUGATED HEAT SHIELD PANEL

FIGURE 9-2

stress profiles and acoustic exposures representative of a Space Shuttle flight. The temperature, pressure and stress conditions are the same as those that were utilized for the rib stiffened panels; they were presented in Section 4.0.

Good coating quality was evidenced by the low incidence of coating failures; four of the five panel tests were conducted for 100 reentry cycles. A total of 488 reentry cycles were conducted; four panels were exposed for 100 cycles each. Elastic and creep deflection measurements were made under four-point loading of the panels at a load of 216 lbs (98.5 kg) which produced a stress in the outermost portion of the corrugation equal to 77% of room temperature yield. Creep deflection measurements made with a straight bar and micrometer over an 11" (28 cm) span were also recorded for each panel at various intervals during cycling.

Results of creep and elastic deflection measurements are shown in Table 9-2. Creep deflections are expressed in deflection rate (mils (μm)/cycle) for each group of cycles conducted per panel and in cumulative average deflection rate (mils (μm)/cycle) for each group of cycles conducted per panel. Elastic deflection measurements are shown in inches and centimeters measured at the center of an 11" (28 cm) span.

The creep deflection rate for the corrugation stiffened panels was approximately three times the creep rate of the rib stiffened panels. Both types of panels were loaded to the same stress level in the outermost portion of the stiffeners (the edge of the ribs for the rib stiffened panels and the flat of the corrugations for the corrugation stiffened panels). To achieve the same stress level in the outermost portion of the stiffeners, the corrugation design required a load 53% higher than for the rib stiffened design. The difference in amount of creep experienced for one design versus the other design can be attributed to different stress distributions within the panels, which are generated simply by the different cross-sectional geometries. The rib stiffened design has a tension to compression neutral axis that is much closer to the skin than the corrugation design. This means higher stresses in the skin for the corrugation design. Compressive stresses contribute just as much to creep strain as the tensile stresses. Thus the corrugation design should show a higher creep deflection.

The general appearance of the two (20" x 20") panels after coating is illustrated in Figures 9-3 and 9-4. Both have uniform texture over all surfaces with a slight exception. On the bottom half of each panel (dipping direction), in the valleys between corrugations, which correspond to the weld line, the coating is somewhat shiny. Under a low power microscope it appears the coating

TABLE 9-2

DEFLECTION MEASUREMENTS FOR SUB-SIZE CORRUGATION STIFFENED HEAT SHIELD PANELS

PANEL NO.	PRESSURE	CYCLE NO.	DEFLECTION MEASUREMENTS		
			CREEP		ELASTIC
			GROUP RATE MILS(μm)/CYCLE	CUMULATIVE AVERAGE RATE MILS (μm)/CYCLE	AFTER EACH GROUP REENTRY CYCLES IN. (cm)
2	EXTERNAL	0			0.118(0.300)
		22	2.04(52)	2.04(52)	0.095(0.242)
		44	1.68(43)	1.86(47)	0.102(0.259)
		66	1.55(39)	1.75(45)	0.102(0.259)
		88	1.32(33)	1.65(42)	0.103(0.262)
		100	2.42(61)	1.64(42)	
5	EXTERNAL	0			0.112(0.284)
		22	1.59(40)	1.59(40)	0.090(0.228)
		44	1.45(37)	1.52(39)	0.099(0.252)
		66	1.23(31)	1.42(36)	0.104(0.264)
		88	1.09(28)	1.34(34)	
7	INTERNAL	0			0.114(0.290)
		22	1.86(47)	1.86(47)	0.092(0.234)
		44	1.18(30)	1.52(39)	–
		66	1.23(31)	1.42(36)	0.091(0.232)
		88	1.00(25)	1.32(33)	0.092(0.234)
		100	1.25(32)	1.31(33)	
10	INTERNAL	0			0.106(0.269)
		22	1.14(29)	1.14(29)	0.106(0.232)
		44	0.18(5.0)	0.66(17)	0.088(0.224)
		66	1.59(40)	0.97(25)	0.090(0.228)
		88	1.45(37)	1.09(28)	0.099(0.252)
		100	1.25(32)	1.11(28)	
12	INTERNAL	0			0.122(0.310)
		22	1.77(45)	1.77(45)	0.096(0.244)
		44	1.00(25)	1.57(40)	0.094(0.239)
		66	1.55(39)	1.44(37)	0.098(0.249)
		88	1.64(42)	1.49(38)	0.101(0.256)
		100	1.08(27)	1.44(37)	

may be somewhat thicker here than in other areas.

In summary the coating process utilizing the acrylic based vehicle can be used to obtain good, adherent, uniform and reproducible coatings on corrugated panels. The process specification for application of the R-512E coating using the A-32 slurry and details of this study are presented in Volume II.

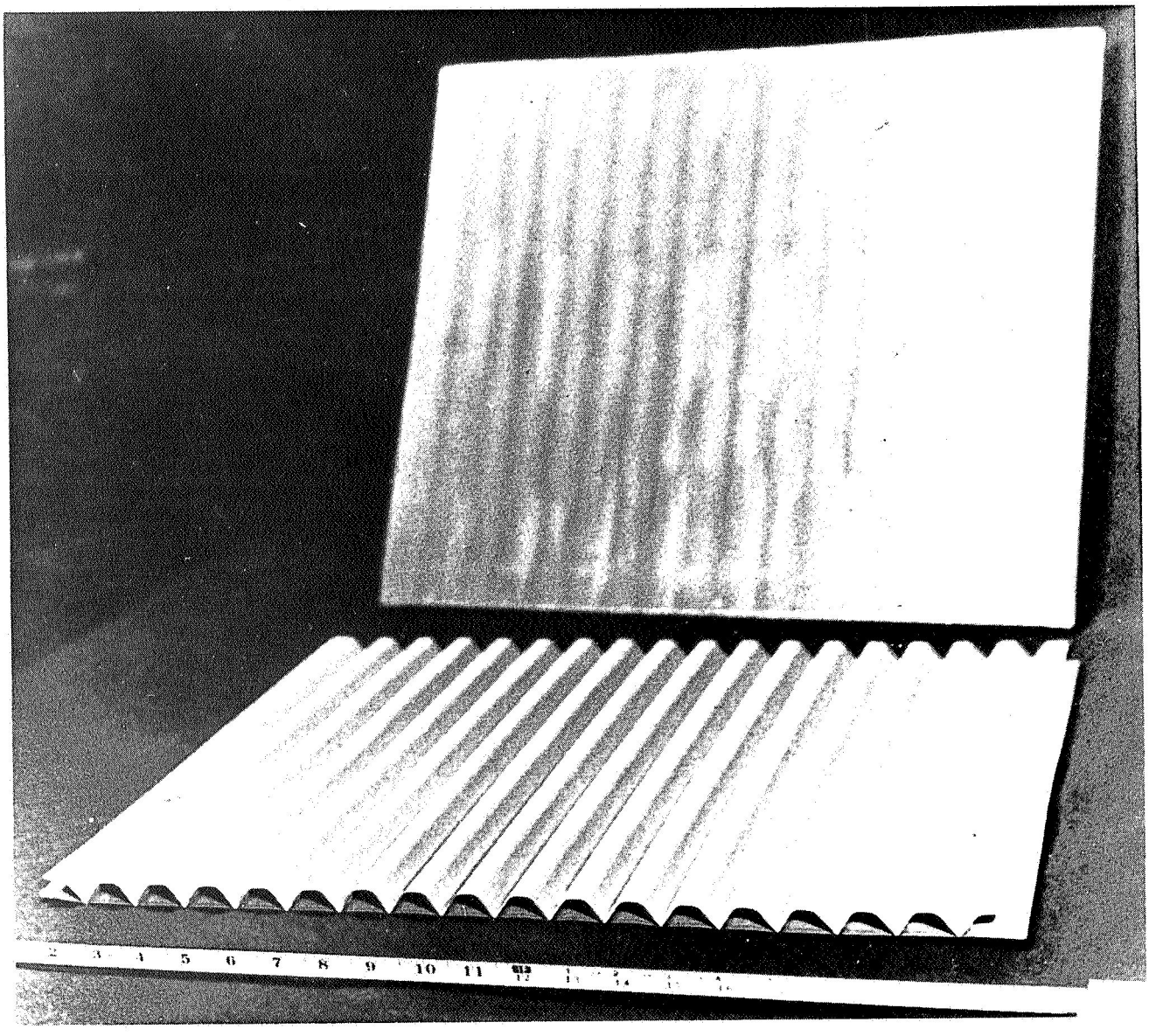

GENERAL APPEARANCE OF PANELS F-1 AND F-2 AFTER COATING

FIGURE 9-3

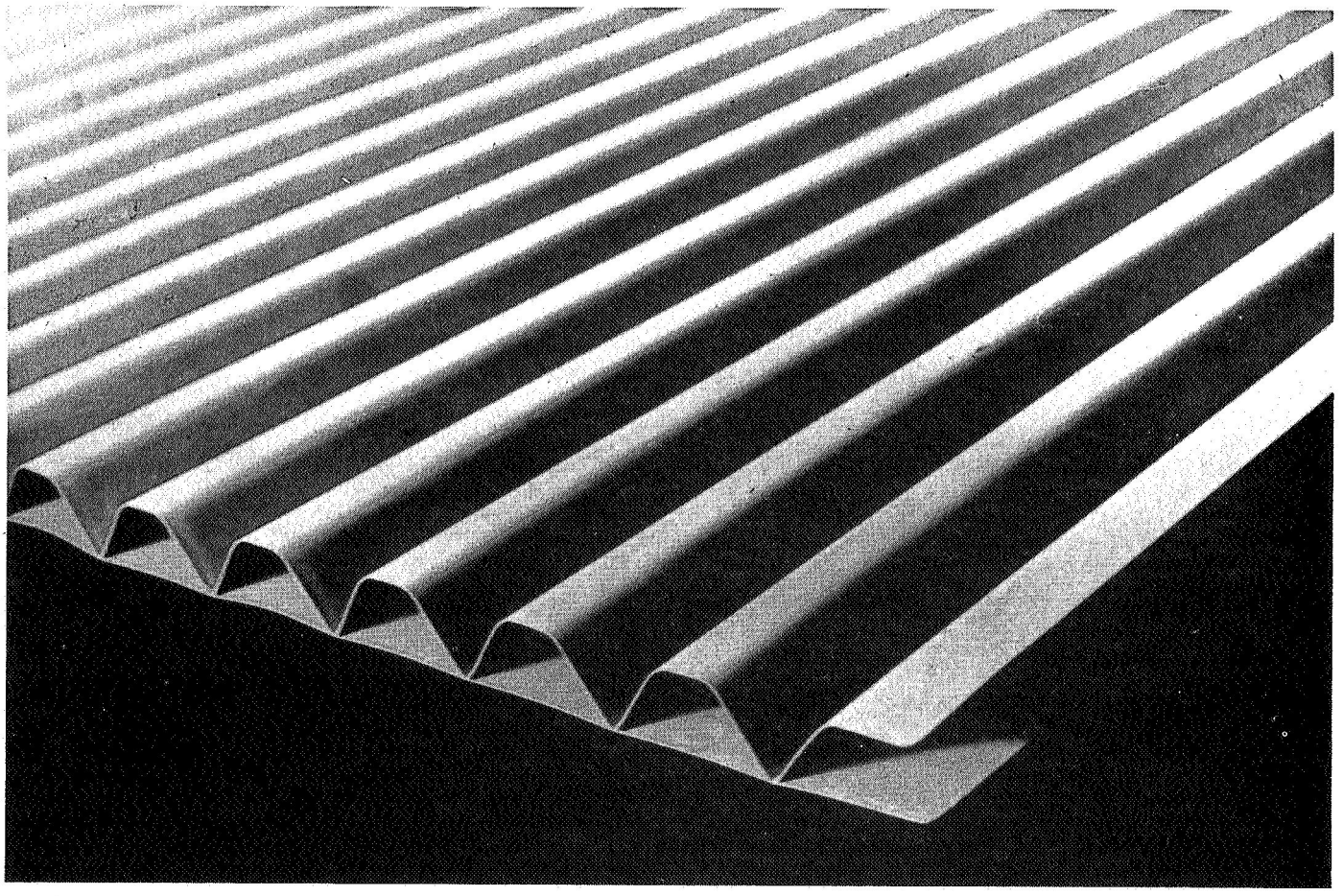

CLOSEUP VIEW OF CORNER AREA OF PANEL F-1 AFTER COATING

FIGURE 9-4

10.0 STRUCTURAL PERFORMANCE OF REPRESENTATIVE PANELS WITH INTENTIONAL COATING DAMAGE

The effect of local coating damage on the structural integrity of coated refractory metal hardware is an important consideration in any actual flight program and one which has been largely overlooked to date. Because coated refractory metal structures are required to perform multimissions, the ability to judge structural adequacy in relation to local coating damage becomes even more important.

Two main points must be considered with respect to the effect of coating damage on the structural integrity of columbium alloys. The first is the contamination of the columbium substrate with oxygen and nitrogen and the embrittlement which this causes. The initial effect is strengthening of the substrate with an accompanying loss of ductility, followed by deterioration of the strength. The second consideration is the oxidation of columbium leading to a reduction in the load bearing cross section. The first consideration, contamination, is probably the more important aspect in a reduced pressure environment. The loss of columbium cross section due to gross oxidation is small compared to the depth of contamination which is usually several times greater in volume. In both damage considerations, the atmosphere must come in contact with the substrate by passing through the coating or by the coating being totally absent. For this program, coating damage was induced by mechanically removing the coating in a local area so that the variables of defect size and location could be precisely defined.

The specimens used in this study were subsize 3" x 12" (7.5 cm x 30 cm) FS-85 columbium alloy rib and corrugation stiffened heat shield panels, identical in size and construction with the panels utilized in Sections 8.0 and 9.0. The rib stiffened panels were coated by HiTemCo with a nominal 3.0 mil (75 μm) R-512E coating applied using the C-5 nitrocellulose based slurry. The corrugation stiffened panels were also coated by HiTemCo with a nominal 3.0 mil (7.5 μm) R-512E coating applied using the A-32 acrylic based slurry.

Prior to reentry simulation, each panel was intentionally defected, to simulate coating damage, by grit blasting to remove an area of coating approximately 1/8" (0.3 cm) in diameter. The surrounding coating was protected during the grit blasting operation by masking with a metal template. The number and location of defects varied from one to three and from skin side to stiffener side, respectively.

The subsize defected panels were subjected to simultaneous simulation of temperature, pressure, and stress profiles representative of a Space Shuttle reentry

flight. Pressure conditions representative of both internal and external surfaces were simulated. Flight simulations were accomplished using the modified Astro tube furnace and the loading fixture which were shown in Section 8.0, Figure 8-20. The temperature, pressure and stress conditions are the same as those established in Section 4.0 for subsize panel tests. These defected panels were also subjected to acoustic exposures to simulate the noise environment experienced during lift-off for a Space Shuttle flight. The level of acoustic exposure was such as to create a stress level of 10,000 psi (69 MN/m^2) in the outer portion of the stiffeners. This was the same acoustic exposure condition that was utilized for testing nondefected rib and corrugation subsize panels in Section 8.0 and Section 9.0, respectively.

10.1 Test Results for Rib Stiffened Panels - Five subsize rib stiffened heat shield panels were exposed to reentry simulation including acoustic testing. Three panels were exposed to external pressure conditions and two panels were exposed to internal pressure conditions. Elastic deflection measurements were made at room temperature prior to and during testing under four-point loading of the panels at a load of 141 lb (64 kg) which produced a stress in the outer portion of the ribs equal to 77 percent of room temperature yield. Creep deflection measurements were made with a straight bar and micrometer over an 11" (28 cm) span and recorded for each panel at various intervals during cycling.

Results of creep and elastic deflection measurements are shown in Table 10-1. Creep deflections are expressed in deflection rate (mils/cycle and μm/cycle) for each group of cycles conducted per panel and in cumulative average deflection rate (mils/cycle, and μm/cycle) after each group of cycles. Elastic deflection measurements are shown in inches and centimeters measured at the center of an 11" (28 cm) span. The higher deflection rates (creep and elastic) for the first group of cycles for all panels compared to the deflection rates of subsequent groups of cycles were again experienced, as they were for the nondefected panels. The elastic deflection after the initial decrease from the first group of cycles showed a gradual increase with time. It was thought that the defected panels would show a decrease in elastic deflection with time as a result of contamination which would increase modulus. This may still be a valid theory which occurs and is then overshadowed by the loss of cross-sectional area due to defect growth. This change may have occurred within the 22-cycle span before deflection measurements were made. Such strengthening might have been revealed, had measurements been made after every cycle.

TABLE 10-1

DEFLECTION MEASUREMENTS, SUB-SIZE RIB STIFFENED PANELS

PANEL NO.	PRESSURE	DEFECT	CYCLE NO.	DEFLECTION MEASUREMENTS		
				CREEP		ELASTIC
				GROUP RATE MILS(μm)/CYCLE	CUMULATIVE AVERAGE RATE MILS(μm)/CYCLE	AFTER EACH GROUP REENTRY CYCLES IN. (cm)
2-A	EXTERNAL	2-1/8" (0.32 cm)	0			0.118(0.300)
		DEFECTS	16	1.25(31.8)	1.25(31.8)	0.084(0.214)
		BETWEEN	31	0.60(15.2)	0.94(23.8)	0.086(0.217)
		RIBS	47	0.56(14.2)	0.81(20.6)	0.090(0.228)
			62	0.20(5.1)	0.65(16.5)	0.091(0.230)
			77	0.67(17.0)	0.66(16.8)	0.091(0.230)
			100	0.44(11.2)	0.61(15.5)	
1-A	EXTERNAL	1-1/8" (0.32 cm)	0			0.113(0.287)
		DEFECT	13	0.69(17.5)	0.69(17.5)	0.087(0.221)
		ABOVE	29	0.56(14.2)	0.62(15.8)	0.085(0.216)
		CENTER	45	0.25(6.4)	0.49(12.4)	0.088(0.224)
		RIB	60	0.13(3.3)	0.40(10.2)	
6	EXTERNAL	3-1/8" (0.32 cm)	0			0.122(0.310)
		DEFECT	16	0.81(20.6)	0.81(20.6)	0.081(0.206)
		ABOVE	32	0.44(11.2)	0.63(16.0)	0.089(0.226)
		EACH RIB	47	0.20(5.1)	0.49(12.4)	0.102(0.259)
			60	0.54(13.7)	0.50(12.7)	
7X	INTERNAL	1-1/8" (0.32 cm)	0			
		DEFECT ON	22	0.18(4.6)	0.18(4.6)	0.085(0.216)
		CENTER				
		RIB				
8X	INTERNAL	1-1/8" (0.32 cm)	0			0.082(0.208)
		(0.3200)	5	0	0	0.067(0.170)
		DEFECT ON	10	1.8(46)	0.9(23)	0.077(0.196)
		CENTER	15	-0.6(-15.2)	0.4(10)	0.076(0.193)
		RIB	20	1.0(25)	0.55(14)	

Creep deflections versus number of reentry cycles for the defected rib stiffened panels tested in both the external and internal pressure environments are shown in Figure 10-1. Also shown is a line representing the average creep deflection rate for nondefected panels tested in Section 8.0. Creep deflections for the defected panels were erratic but generally higher than those for the nondefected panel average. The loss in cross-sectional area due to consumption from oxidation caused higher deflections but these were offset some, by the increased strength due to oxygen and nitrogen contamination. The location of the defect site and the subsequent consumption and contamination have some effect on the creep deflections. It is not possible to determine the effects of pressure environment on deflections because the defect locations are different for the internal pressure environment tests.

Table 10-2 presents the results of nondestructive coating thickness measurements made on the five subsize heat shield panels before and after reentry cycling. The Dermitron eddy current device was used for thickness measurements. Excellent coating uniformity for each panel is revealed for the as-coated condition. Thickness change due to cycling in the external pressure environment agrees very well with that for the rib stiffened panels tested in Section 8.0. The panels (7X and 8X) tested in the internal pressure environment showed thickness increases after about 20 cycles that were twice the increases for panels (3 and 4) exposed for 70 to 100 cycles in Section 8.0. Since the coatings and test environments are the same, this implies that there is an initial thickness increase due to formation of a coating oxide which is then gradually depleted with continued reentry exposure.

Defected panels 1-A, 2-A and 6 which were tested in the external pressure environment, had defect sites 1/8" (0.3 cm) in diameter located on the skin side of the panels, one directly above the center rib for Panel No. 1-A and one above each of the three ribs for Panel No. 6, and two between the ribs for panel 2-A. The location, size and growth of these defects can be observed in Figures 10-2, 10-3 and 10-4. Panels 1-A and 6 showed structural lives of 60 reentry cycles which were approximately 40 percent shorter than the nondefected panels. The two factors responsible for the major portion of the reduced life are loss of panel cross-section due to consumption by oxidation and premature crack formation and propagation in the contaminated columbium substrate. Structural failure for both panels occurred during acoustic testing. The 1/8" (0.3 cm) defects had grown to 0.6" (1.5 cm) diameter and had consumed approximately 1/3 of the rib cross-section. This amount of reduction in cross-section would lead to considerably higher

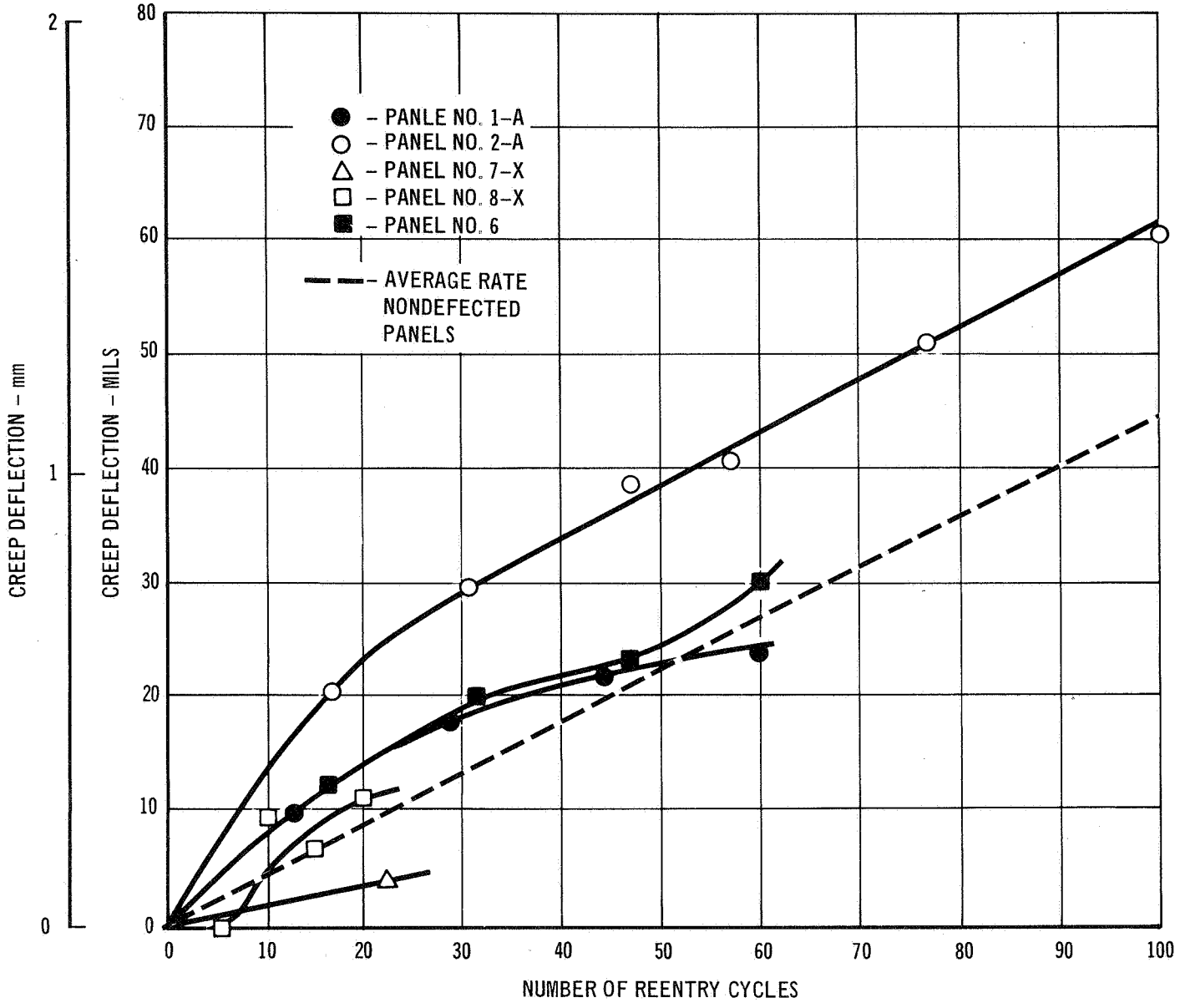

INTENTIONALLY DEFECTED SUB-SIZE RIB STIFFENED HEAT SHIELD
PANEL CREEP DEFLECTIONS

FIGURE 10–1

TABLE 10-2

NDT DERMITRON COATING THICKNESS ON R-512E COATED FS-85 SUB-SIZE RIB STIFFENED PANELS

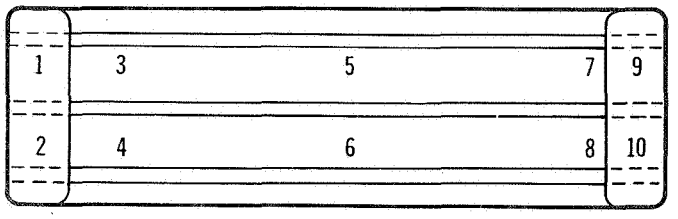

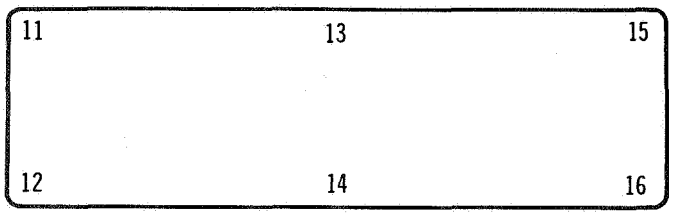

PANEL NO.	REENTRY CYCLES (NO.)	COATING THICKNESS MILS/μm AT LOCATION															
		1	2	3	4	5	6	7	8	9	10	11	12	13	14	15	16
1-A	0	3.1/79	3.3/84	2.9/74	4.3/109	3.1/79	3.1/79	3.5/89	2.7/69	3.2/81	3.3/84	3.7/94	3.3/84	3.2/81	3.5/89	3.2/81	3.1/79
	60			3.9/99	3.9/99	4.4/111	4.5/114	3.7/94	3.5/89			4.3/109	4.9/125	4.5/114	4.8/121	4.3/109	4.7/119
2-A	0	3.1/79	3.1/79	3.2/81	4.0/101	3.5/89	3.4/84	3.2/81	4.3/109	3.2/81	3.5/89	3.9/99	4.0/101	3.2/81	3.5/89	3.2/81	3.2/81
	100			4.4/111	5.2/133		4.5/114	4.3/109	4.0/101			5.5/141	6.1/157	4.5/114		3.5/89	4.0/101
6	0	3.2/81	3.3/84	3.7/94	3.6/91	3.1/79	3.2/81	3.5/89	3.2/81	3.2/81	3.3/84	3.6/91	3.5/89	3.5/89	3.5/89	3.2/81	3.3/84
	60			4.3/109	4.0/101	4.3/109	3.7/94	3.7/94	3.5/89			4.3/109	4.0/101	3.6/91	4.0/101	3.7/94	3.7/94
7X	0	2.8/71	2.7/69	3.3/84	3.3/84	3.2/81	3.1/79	2.8/71	2.9/74	3.1/79	2.9/74	3.1/79	3.1/79	3.1/79	3.2/81	2.9/74	2.9/74
	22			4.1/104	4.1/104	4.0/101	3.7/94	3.9/99	3.9/99			3.6/91	3.6/91	3.5/89	3.5/89	3.6/91	3.5/89
8X	0	2.7/69	2.7/69	2.9/74	2.9/74	3.2/81	3.1/79	3.1/79	3.1/79	3.1/79	2.9/74	2.9/74	3.1/79	2.9/74	3.1/79	2.9/74	2.8/71
	20			4.0/101	4.0/101	3.7/94	4.0/101	4.1/104	4.1/104			3.3/84	3.5/89	3.6/91	3.6/91	3.6/91	3.2/81

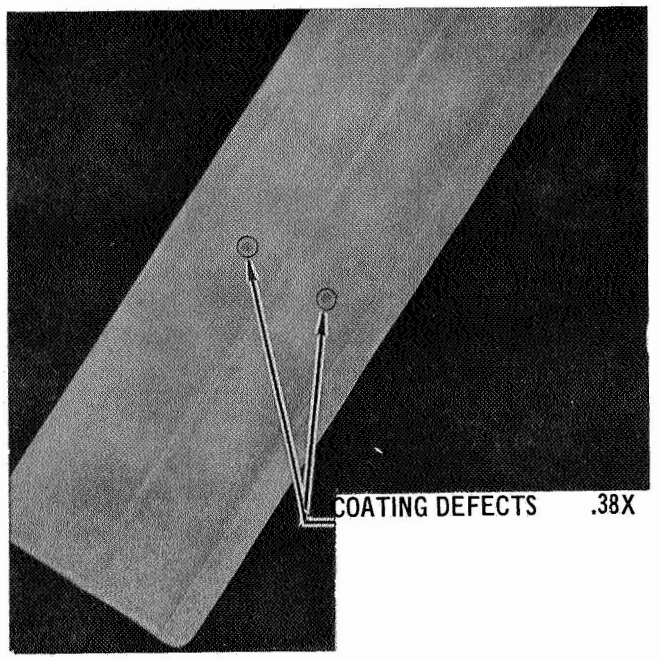

A) AS DEFECTED PRIOR TO TESTING

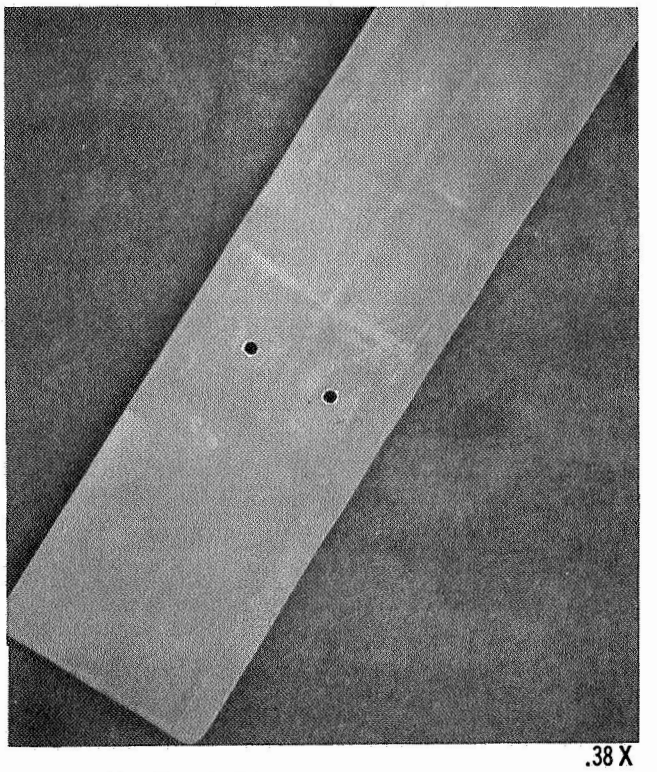

.38 X

B) AFTER 16 REENTRY AND ACOUSTICS CYCLES

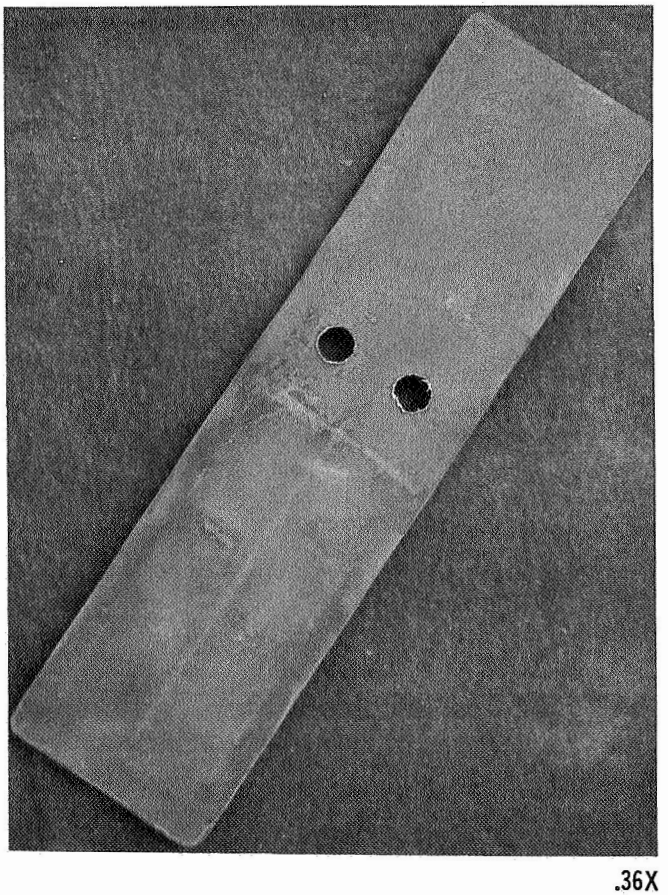

.36X

C) AFTER 100 REENTRY CYCLES AND 77 ACOUSTIC CYCLES

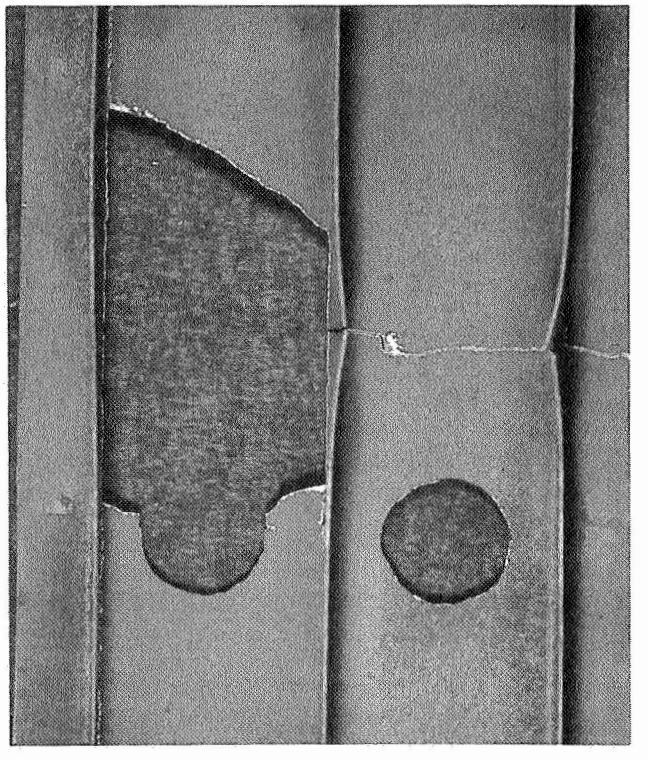

1X

D) AFTER 100 REENTRY AND ACOUSTIC CYCLES

FLIGHT SIMULATION TESTING OF PANEL NO. 2-A

FIGURE 10-2

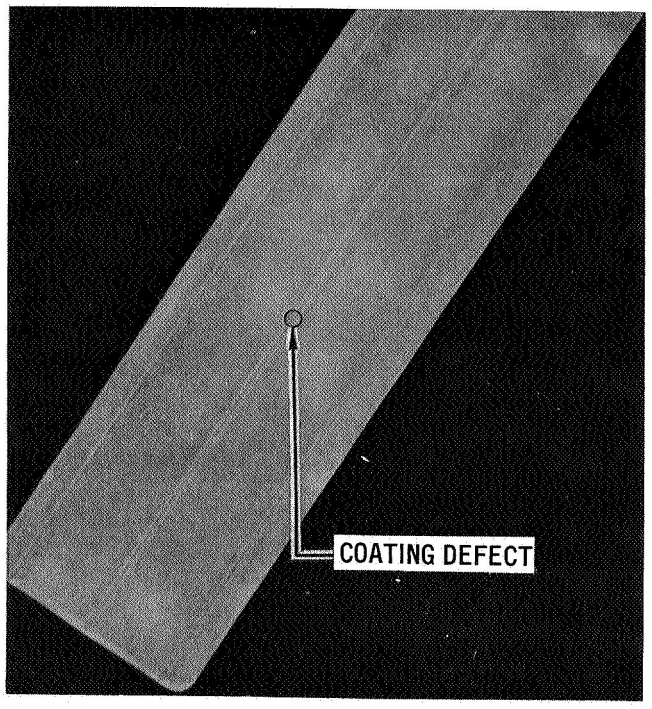

.38X

A) AS DEFECTED PRIOR TO TESTING

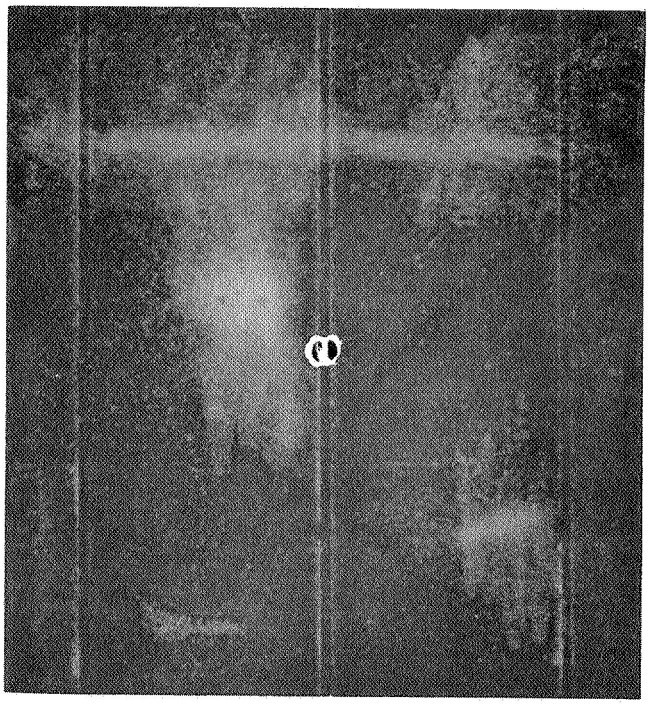

1X

B) AFTER 13 REENTRY AND ACOUSTIC CYCLES

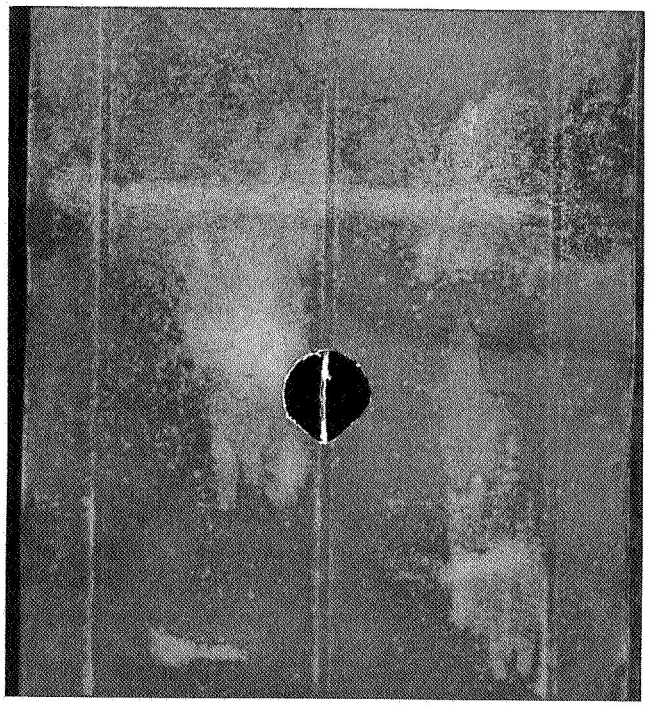

.93X

C) AFTER 60 REENTRY CYCLES AND 45 ACOUSTIC CYCLES

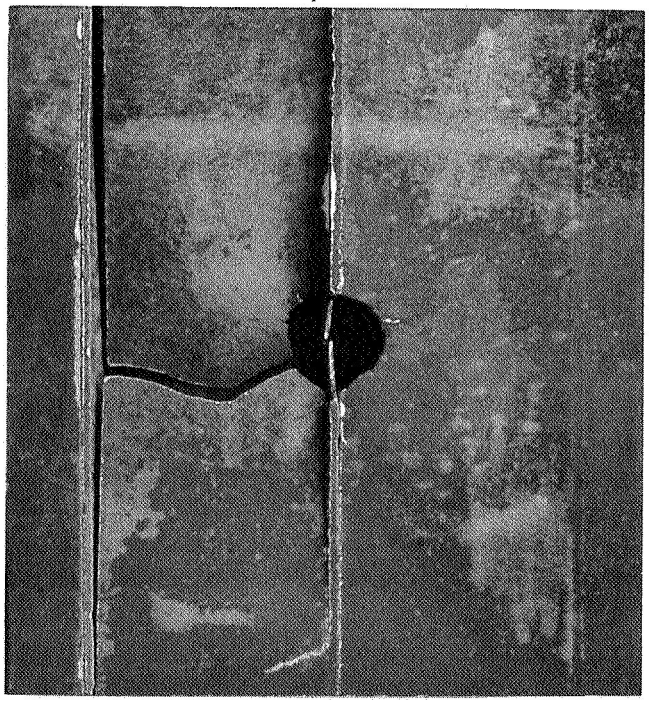

1X

D) AFTER 60 REENTRY AND ACOUSTIC CYCLES

FLIGHT SIMULATION TESTING OF PANEL NO. 1-A

FIGURE 10-3

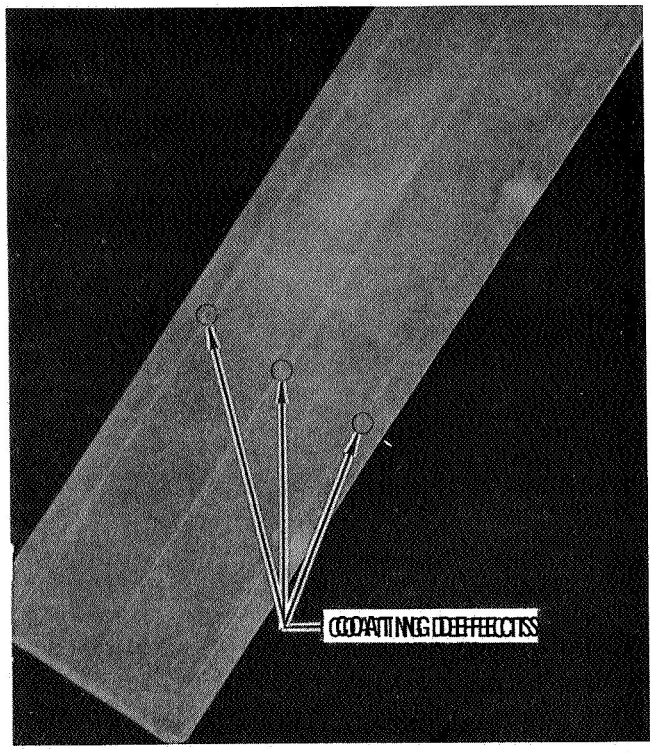

.38X

A) AS DEFECTED PRIOR TO TESTING

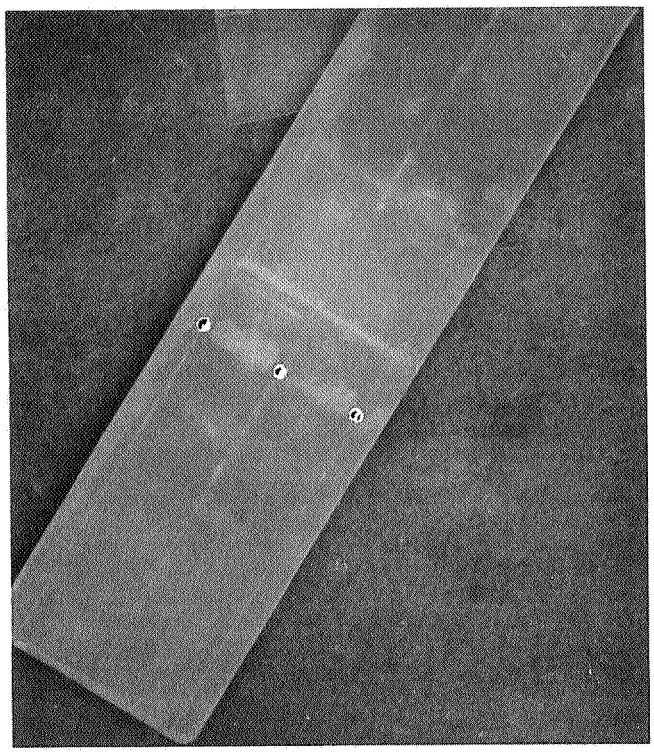

.37X

B) AFTER 16 REENTRY AND ACOUSTIC CYCLES

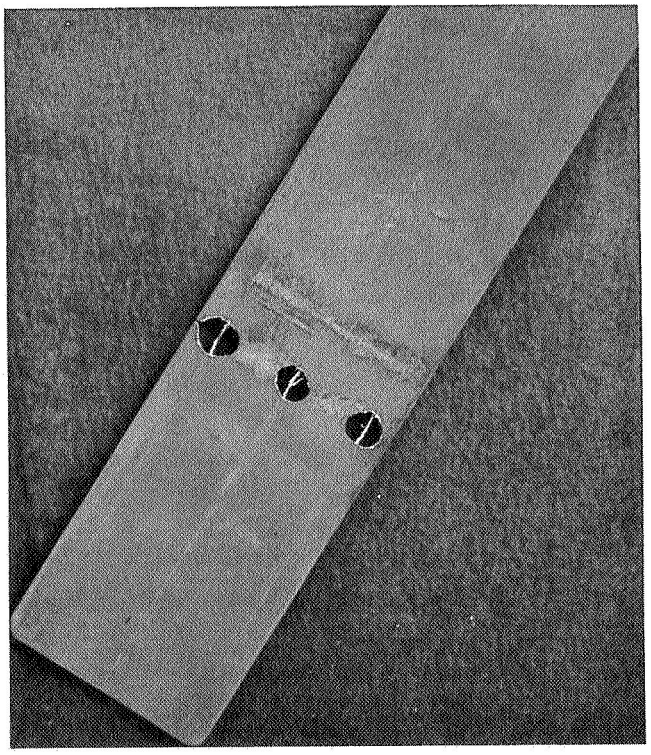

.36X

C) AFTER 60 REENTRY CYCLES AND 47 ACOUSTIC CYCLES

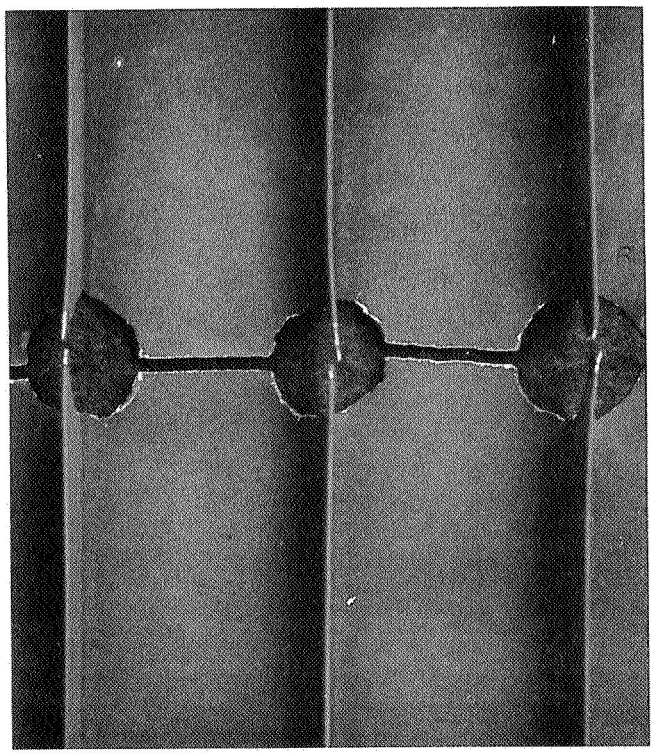

1X

D) AFTER 60 REENTRY AND ACOUSTIC CYCLES

FLIGHT SIMULATION TESTING OF PANEL NO. 6

FIGURE 10-4

stresses during flight and acoustic loading. Panel 2-A which had defects between the ribs did not show any reduced structural integrity up to 100 reentry cycles, where testing was terminated, because the critical load carrying rib stiffeners were not affected by the oxidation.

One defected panel, 7X, tested in the internal pressure environment, had one defect on the stiffener side on top of the center rib. This can be seen in Figure 10-5. This panel structurally failed in acoustics after it had been reentry cycled 22 times. This defect is located in the most critical area on the panel, where the highest stresses are experienced. To determine structural life more closely, another panel, 8X, with the same type of defect was cycled in increments of 5 cycles. Twenty (20) cycles were completed before structural failure. It must be remembered that the acoustic environment utilized for these panel tests was designed to cause failure of nondefected panels in 100 flights. Most of the nondefected panels withstood acoustic exposures that represented 88-100 reentry flight cycles. It is understandable that the defected panels with the oxidation and contamination they developed would not survive as much acoustic exposure. A true feel for structural life was not revealed by these tests, because of the the life dependency on acoustic environment and defect size, which were somewhat arbitrarily selected and did not represent true simulation of flight conditions.

True simulation of naturally occurring or accidental, mechanically-induced, coating damage sites would be impossible. Choosing a defect size of 1/8" (0.3 cm) was arbitrary but it was felt to be rather severe considering that the panel area of the subsize panels utilized is less than 1/10 that of full size 20" x 20" (50 cm x 50 cm) panels.

Since the same acoustic environment was utilized for both nondefected and defected panels, the relative effect of coating damage could be assessed. The structural life in the external pressure environment was reduced from 0 to 40 percent, depending on location, for damage sites on the skin. The structural life in the internal pressure environment was reduced by about 80 percent when the damage site was located on the most critical area (edge of rib stiffener).

All of the structural failures in the defected rib stiffened panel tests were fatigue failures generated by the acoustic exposures. All panels withstood the static design loads (room temperature and elevated temperature) just prior to generation of fatigue failures.

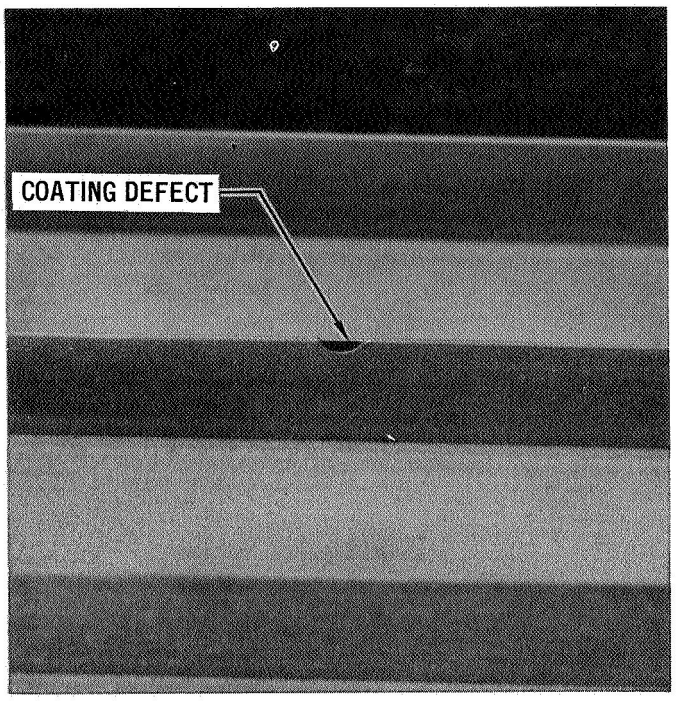

1X

A) AS DEFECTED PRIOR TO TESTING

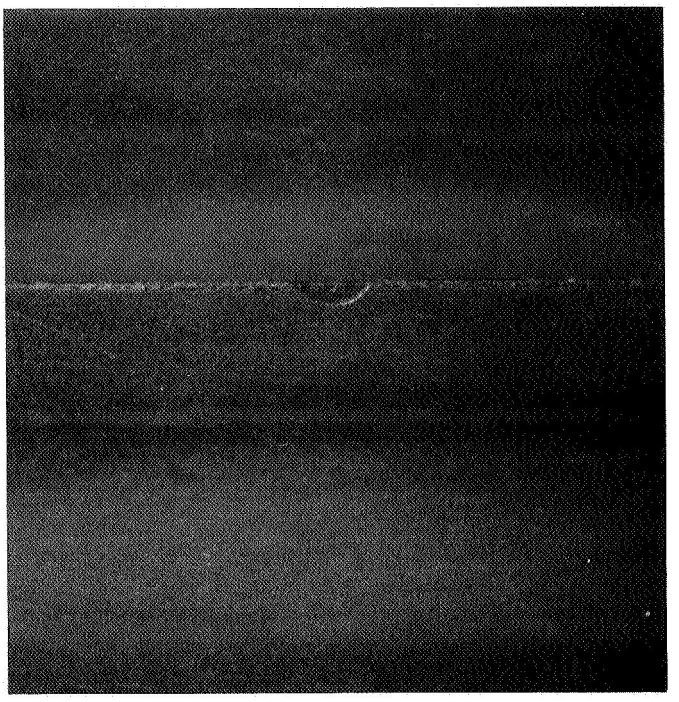

1.5X

B) AFTER 22 REENTRY CYCLES AND BEFORE ACOUSTIC TESTING

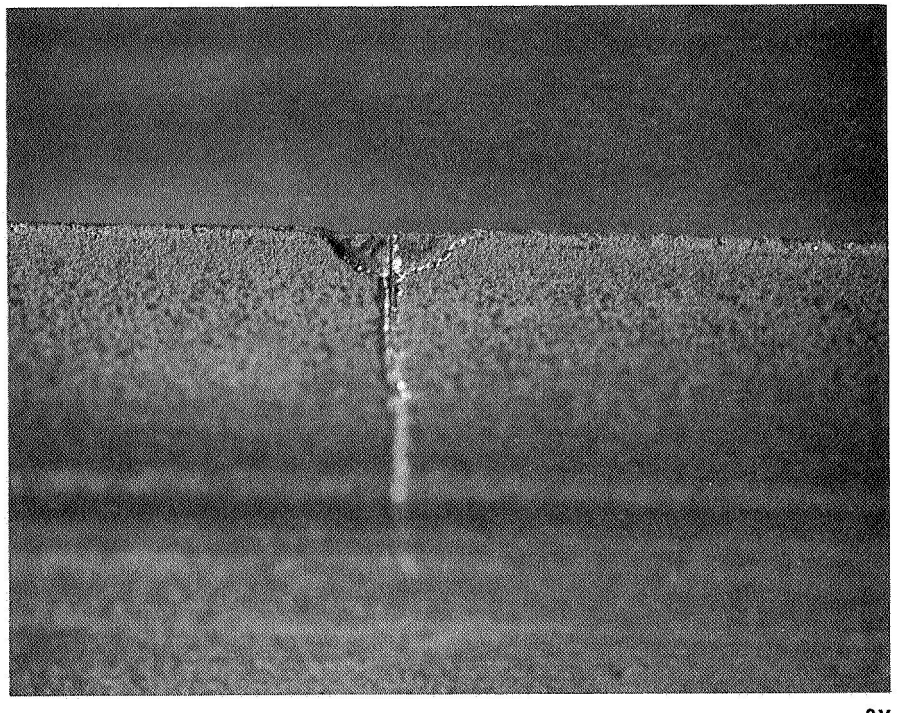

3X

C) AFTER 22 REENTRY AND ACOUSTIC CYCLES

FLIGHT SIMULATION TESTING OF PANEL NO. 7X

FIGURE 10-5

In order to have a reliable heat shield, fatigue life must be considered in the design. The possibility of coating damage to the critical edge of the rib stiffener must also be considered. The tests conducted in this investigation indicate a fatigue life of about 160,000 cycles at 10,000 psi (69 MN/m^2), should coating damage to the rib stiffener occur. This is considered quite a short life for a metallic material at such a low stress level. This suggests that fatigue strength may very well become the critical design factor for coated columbium heat shields.

10.2 Test Results for Corrugation Stiffened Panels - Five subsize corrugation stiffened heat shield panels were exposed to reentry simulation including acoustic testing. Three panels were exposed to reentry simulation under external pressure conditions and two panels were exposed to reentry simulation under internal pressure conditions. Elastic deflection measurements were made at room temperature prior to and during testing under four-point loading of the panels at a load of 216 lb (98.5 kg) which produced a stress in the outer portion of the corrugations equal to 77 percent of room temperature yield strength. Creep deflection measurements were made with a straight bar and micrometer over an 11" (28 cm) span and recorded for each panel at various intervals during testing. These test conditions and deflection measurement procedures were the same as those employed for the defected rib stiffened panels.

Results of creep and elastic deflection measurements are shown in Table 10-3. Creep deflections are expressed in deflection rate, mils (μm)/cycle, for each group of cycles conducted per panel and in cumulative average deflection rate, mils (μm)/cycle, after each group of cycles. Elastic deflection measurements are shown in inches and centimeters measured at the center of an 11" (28 cm) span.

The deflection rates (creep and elastic) for the defected corrugation stiffened panels compared very favorably to the rates for nondefected panels. The effect of defects and defect location on creep deflections showed the same trends as the rib stiffened panels. Creep deflections versus number of reentry cycles for the defected corrugation stiffened panels tested in both the external and internal pressure environments are shown in Figure 10-6. Also shown in this figure is a line representing the average creep deflection rate for nondefected corrugated panels tested as described in Section 9.0. In general, creep deflections were higher for the defected panels. As occurred with the rib stiffened panels, loss of cross-section due to consumption by oxidation would produce higher creep deflections.

TABLE 10–3

DEFLECTION MEASUREMENTS, SUB-SIZE CORRUGATION STIFFENED PANELS

PANEL NO.	PRESSURE	DEFECT	CYCLE NO.	DEFLECTION MEASUREMENTS		
				CREEP		ELASTIC
				GROUP RATE MILS(μm)/CYCLE	CUMULATIVE AVERAGE RATE MILS(μm)/CYCLE	AFTER EACH GROUP REENTRY CYCLES IN. (cm)
6	EXTERNAL	2-1/8"	0			0.122(0.310)
		(0.32 cm)	22	2.27(57.6)	2.27(57.6)	0.077(0.246)
		DEFECTS	44	1.59(40)	1.94(49)	0.108(0.274)
		BETWEEN	66	1.45(37)	1.77(45)	0.105(0.266)
		WELDS ON	88	–0.45(–11.5)	1.22(31)	0.117(0.298)
		SKIN SIDE	100	–0.17(–4.2)	1.05(26.6)	
3	EXTERNAL	1-1/8"	0			0.109(0.277)
		(0.32 cm)	22	1.64(41.6)	1.64(41.6)	0.092(0.234)
		DEFECT ON	44	1.36(34.2)	1.50(38)	0.100(0.254)
		CENTER WELD	66	1.32(33)	1.44(37)	0.124(0.315)
		SKIN SIDE	88	0.82(20.8)	1.28(32.6)	
4	EXTERNAL	3-1/8"	0			0.112(0.284)
		(0.32 cm)	22	1.82(46)	1.83(46)	0.096(0.244)
		DEFECTS ON	44	1.50(38)	1.66(42)	
		EACH WELD				
8	INTERNAL	1-1/8"	0			0.116(0.295)
		(0.32 cm)	22	1.86(47.3)	1.86(47.3)	
		DEFECT ON				
		TOP OF				
		CORRUGATION				
11	INTERNAL	1-1/8"	0			0.112(0.284)
		(0.32 cm)	5	4.8(122)	4.8(122)	0.095(0.242)
		DEFECT ON	10	–1.2(–30)	1.8(46)	0.094(0.239)
		TOP OF	15	2.8(71)	2.1(54)	0.098(0.249)
		CORRUGATION	20	1.6(41)	2.2(56)	0.101(0.256)
			25	0.4(10)	1.8(46)	

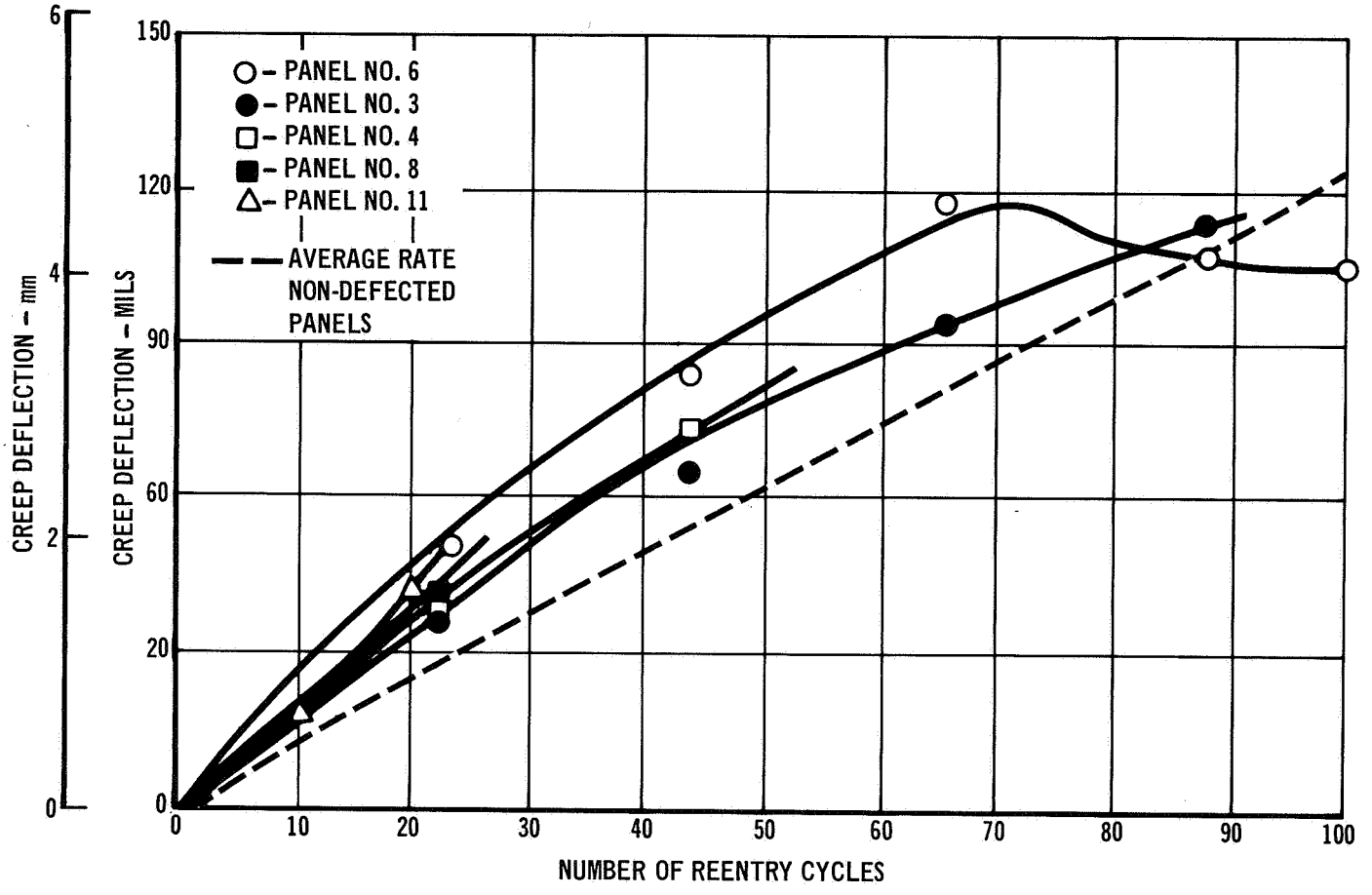

INTENTIONALLY DEFECTED SUB-SIZE CORRUGATION STIFFENED HEAT SHIELD PANEL CREEP DEFLECTIONS

FIGURE 10-6

Defect locations for the corrugation stiffened panels were in approximately the same areas as they were for the rib stiffened panels. The response of two different designs was very similar when defects were located in approximately the same areas as shown in Figures 10-1 and 10-6.

Table 10-4 presents the results of nondestructive coating thickness measurements made on the five subsize heat shield panels before and after reentry cycling. The panels show excellent coating uniformity and the thickness changes due to cycling agree very closely with those for the corrugated panels evaluated in Section 9.0.

Defected panels 3, 4, and 6 which were tested in the external pressure environment, had defect sites 1/8" (0.3 cm) diameter located on the skin side of the panels directly on the welds for panel Nos. 3 and 4, and between the welds for panel No. 6. The location, size, and growth of these defects can be observed in Figures 10-7, 10-8, and 10-9. Panel No. 3 with one defect and panel No. 4, with three defects, showed structural lives that were shorter by 12 and 56 percent, respectively, compared with lives for the nondefected panels described in Section 9.0. Structural failures occurred with both panels during acoustic testing. Panel No. 6 which had two defects on the skin between the welds did not show any reduced structural life prior to termination of the testing at 100 cycles. Cross-sectional photomicrographs of panel No. 6 are shown in Figures 10-10 and 10-11, after 100 cycles of exposure. Uniform coating coverage can be observed as well as typical coating oxidation.

Panel No. 8 tested in the internal pressure environment had one defect on the stiffener side of the panel on the top of the corrugation. This can be seen in Figure 10-12. This panel structurally failed in acoustics after it had been reentry cycled 22 times. In order to determine more closely what structural life was, another panel, No. 11 with the same type of defect was reentry cycled in increments of 5 cycles. Thirty reentry cycles were complete before failure occurred, again, during acoustic testing that followed Panel No. 11 is shown in Figure 10-13.

The almost identical performance of the defected corrugated panels and defected rib stiffened panels certainly suggests that neither design has a reuse advantage when the coating has been damaged. The equivalent performance of the corrugation and rib stiffened panels in the internal pressure environment with defects located on the maximum stress area of the stiffeners was somewhat surprising. Since failures were fatigue failures, it was thought that the defect located

TABLE 10–4

NDT DERMITRON COATING THICKNESS ON R–512E COATED FS–85 SUB-SIZE CORRUGATION STIFFENED PANELS

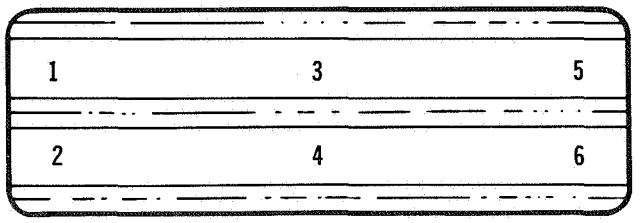

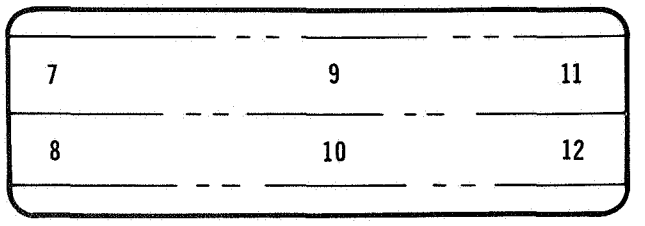

PANEL NO.	NO. OF REENTRY CYCLES	COATING THICKNESS MILS/μm AT LOCATION											
		1	2	3	4	5	6	7	8	9	10	11	12
3	0	2.8 71	2.9 74	2.9 74	2.9 74	2.9 74	3.1 79	2.9 74	2.9 74	2.9 74	2.8 71	2.9 74	3.1 79
	88	4.8 121	4.5 114	4.1 104	4.0 101	3.9 99	3.9 99	4.7 119	4.4 111	4.7 119	4.7 119	4.0 101	4.3 109
4	0	2.9 74	2.8 71	2.9 74	2.8 71	2.9 74	2.9 74	2.9 74	2.9 74	2.9 74	2.8 71	2.9 74	2.9 74
	44	3.6 91	3.5 89	3.3 84	3.5 89	3.6 91	3.6 91	3.7 94	3.9 99	3.3 84	3.9 99	4.1 104	3.7 94
6	0	2.8 71	2.8 71	2.8 71	2.8 71	2.9 74	2.9 74	2.8 71	3.1 79	2.8 71	2.9 74	2.8 71	2.8 71
	100	4.4 111	4.5 114	3.6 91	3.6 91	4.3 109	4.0 101	4.7 119	4.4 111	4.0 101	3.9 99	4.0 101	4.4 111
8	0	2.9 74	2.8 71	2.9 74	2.9 74	2.9 74	2.9 74	2.9 74	3.1 79	2.9 74	3.1 79	2.9 74	2.9 74
	22	3.3 84	3.3 84	3.3 84	3.5 89	3.5 89	3.5 89	3.2 81	3.2 81	3.3 84	3.3 84	3.3 84	3.6 91
11	0	2.8 71	2.8 71	2.9 74	2.8 71	2.8 71	2.9 74	2.9 74	2.8 71	2.9 74	2.8 71	2.9 74	2.9 74
	30	3.3 84	3.5 89	3.6 91	3.6 91	3.5 89	3.5 89	3.5 89	3.5 89	3.2 81	3.5 89	4.0 101	3.3 84

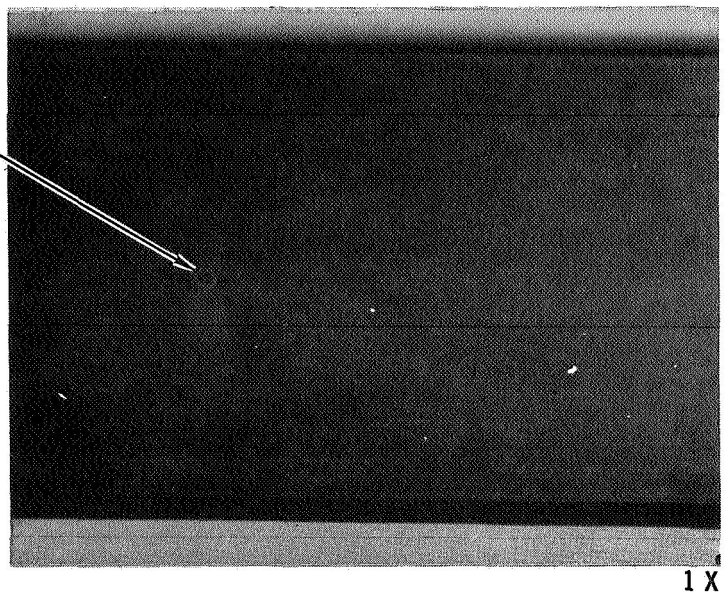

(A) As Defected Prior to Testing

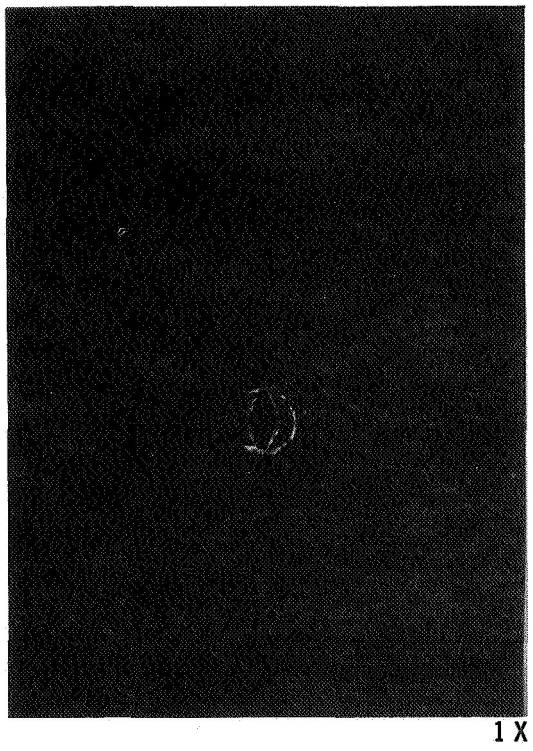

(B) After 44 Reentry and Acoustic Cycles

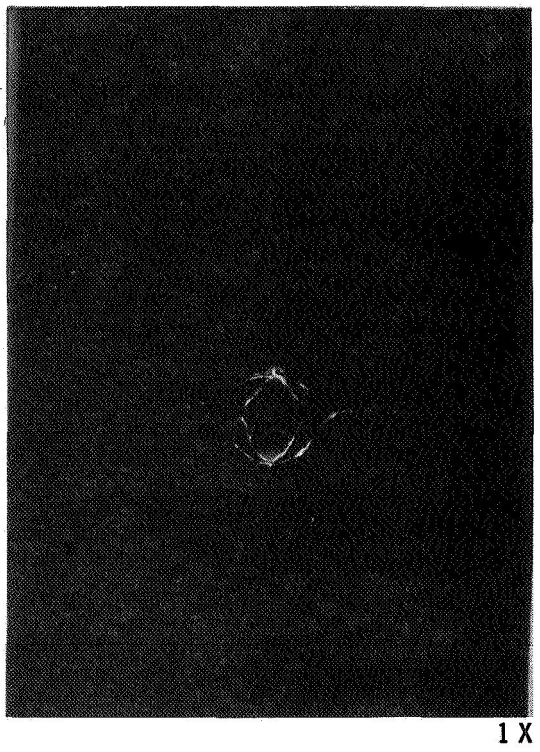

(C) After 88 Reentry and Acoustic Cycles

FLIGHT SIMULATION TESTING OF PANEL NO. 3

FIGURE 10-7

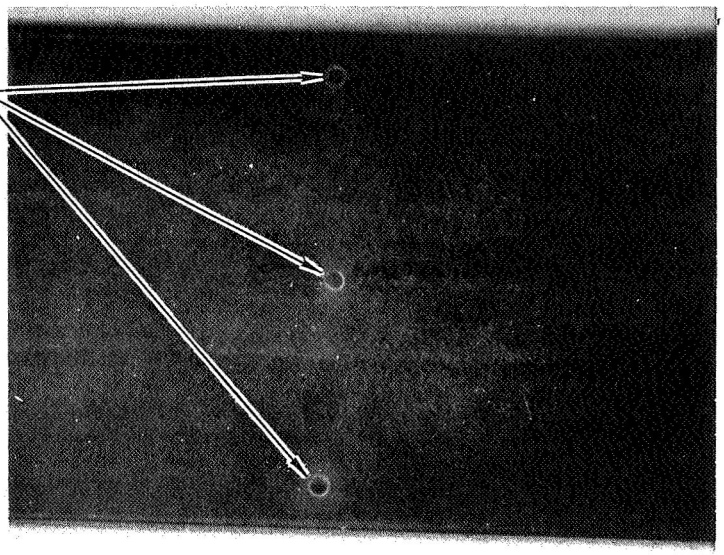

1 X

(A) As Defected Prior to Testing

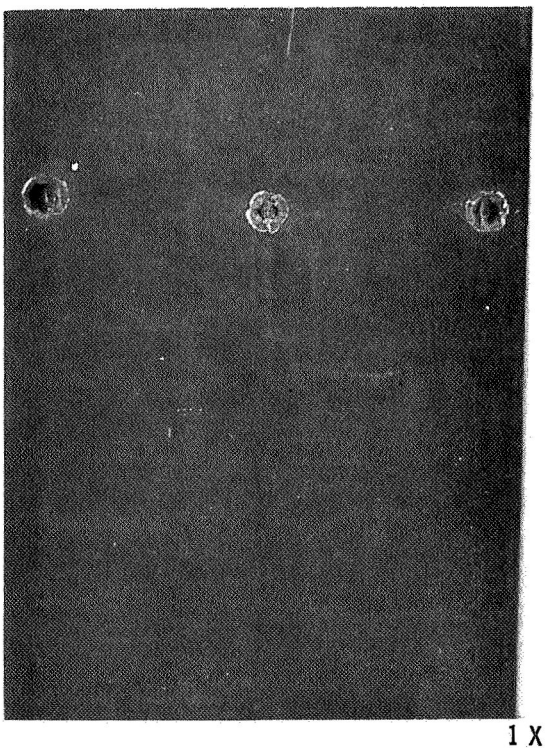

1 X

(B) After 22 Reentry and Acoustic Cycles

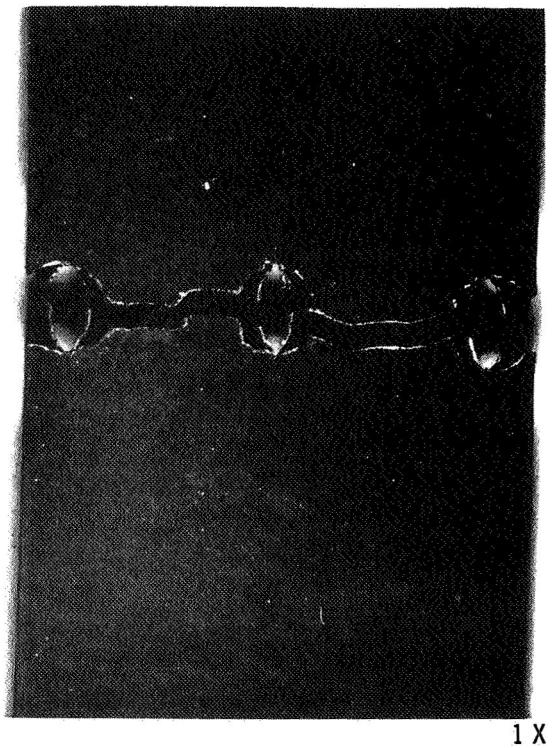

1 X

(C) After 44 Reentry and Acoustic Cycles

FLIGHT SIMULATION TESTING OF PANEL NO. 4

FIGURE 10–8

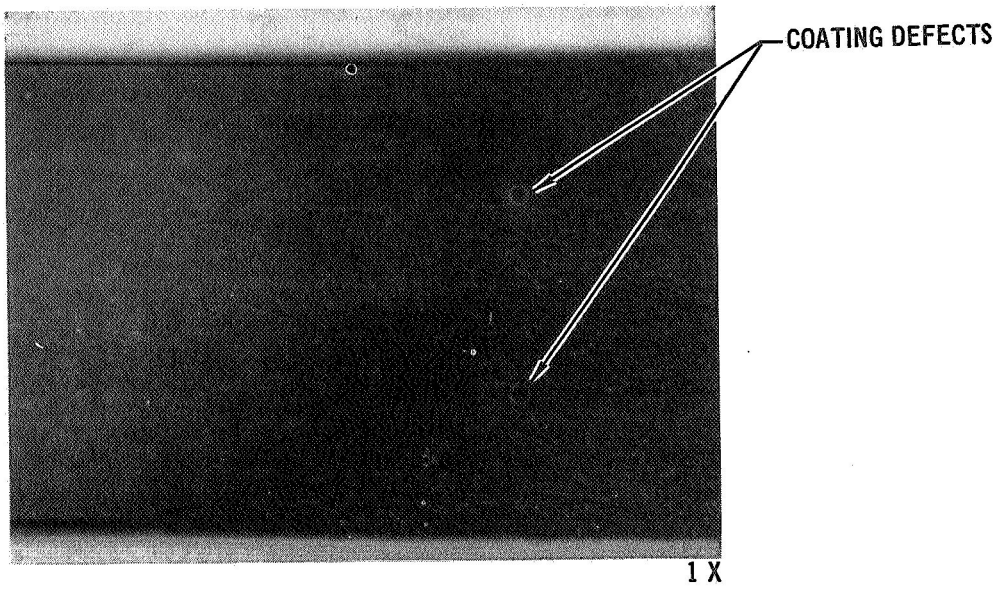

(A) As Defected Prior to Testing

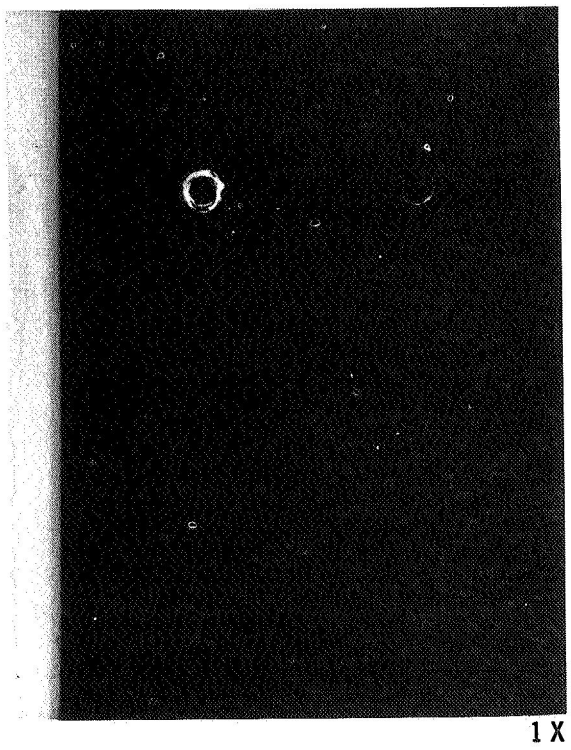

(B) After 22 Reentry and Acoustic Cycles

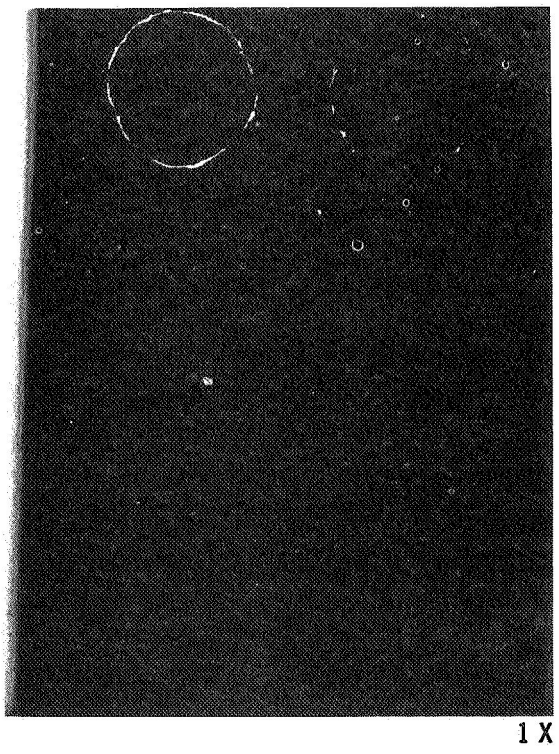

(C) After 100 Reentry and Acoustic Cycles

FLIGHT SIMULATION TESTING OF PANEL NO. 6

FIGURE 10–9

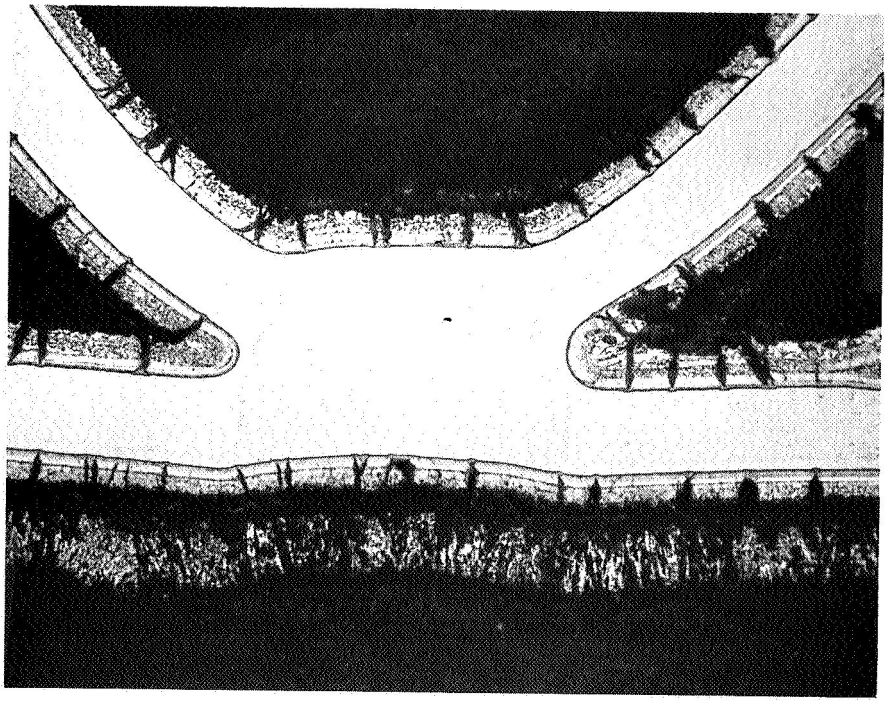

50 X

CORRUGATION-SKIN JOINT OF PANEL NO. 6 AFTER 100 REENTRY CYCLES – EXTERNAL PRESSURE ENVIRONMENT

FIGURE 10–10

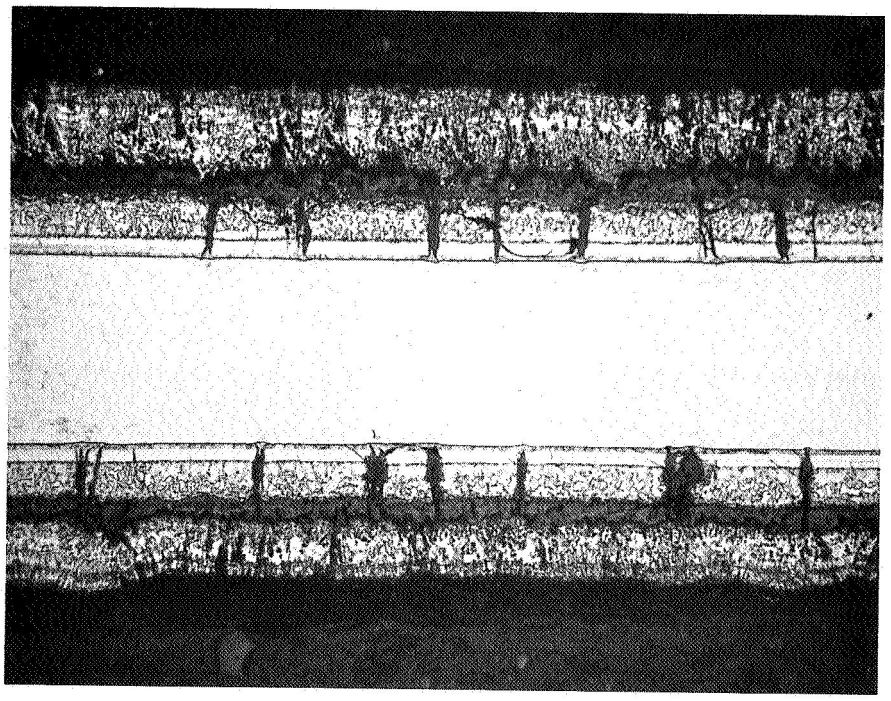

100 X

SKIN CROSS-SECTION BETWEEN WELDS OF PANEL NO. 6 AFTER 100 REENTRY CYCLES – EXTERNAL PRESSURE ENVIRONMENT

FIGURE 10–11

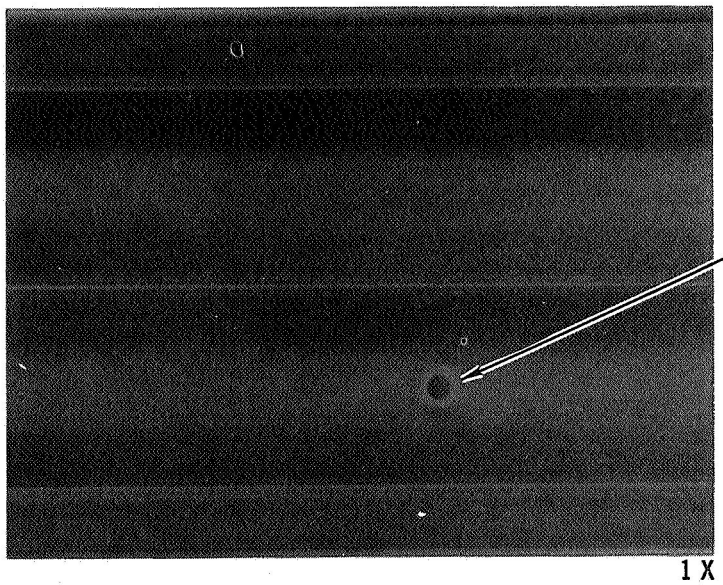

(A) As Defected Prior to Testing

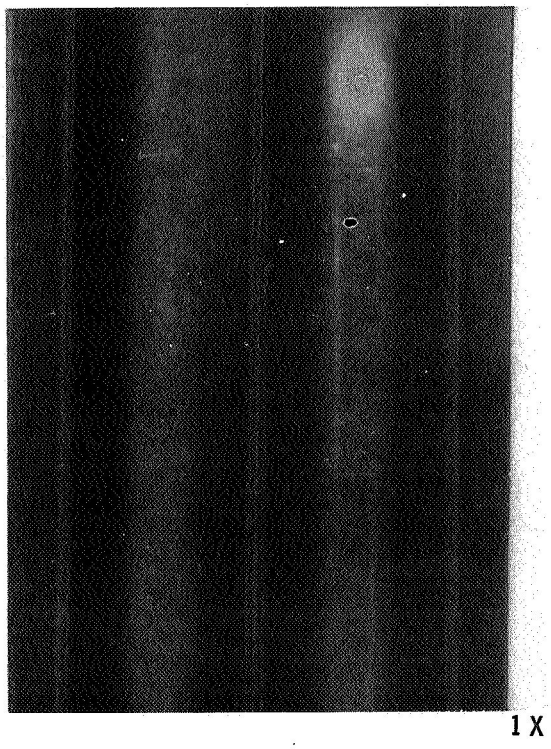

(B) After 22 Reentry Cycles

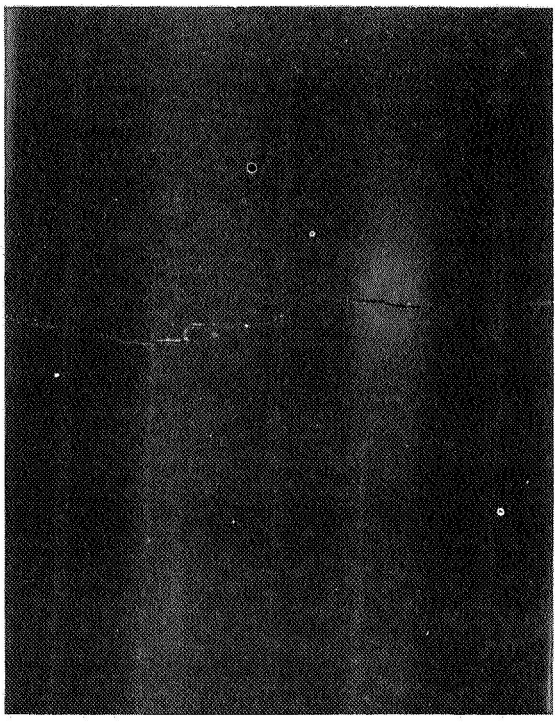

(C) After 22 Reentry and Acoustic Cycles

FLIGHT SIMULATION TESTING OF PANEL NO. 8

FIGURE 10-12

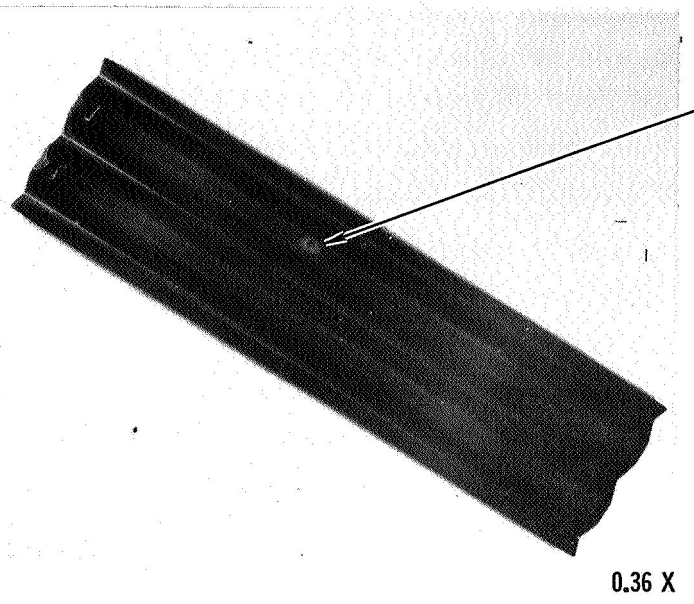

(A) After 10 Reentry and Acoustic Cycles

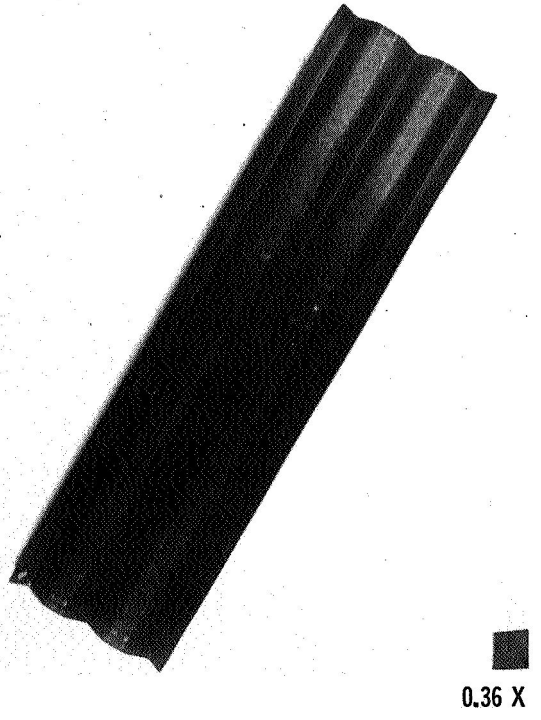

(B) After 30 Reentry and 25 Acoustic Cycles

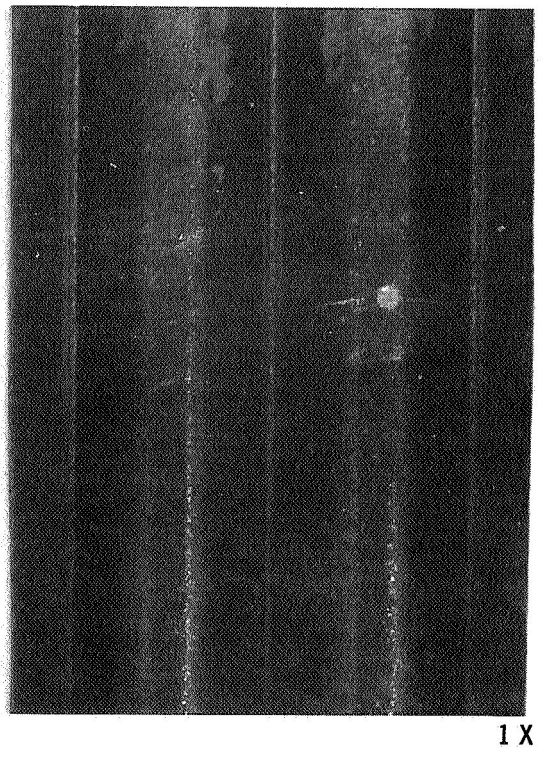

(C) After 30 Reentry and Acoustic Cycles

FLIGHT SIMULATION TESTING OF PANEL NO. 11

FIGURE 10–13

on the edge of the rib stiffener would lead to a failure earlier than the one located on the flat of the corrugation. It would seem that the thin edge of the rib would be more likely to provide a site for generation of a fatigue crack, but this was not the case as both panels (rib and corrugation) showed failures at very nearly the same number of cycles. It should be noted that in actual practice the edge of the rib stiffener is much more likely to sustain coating damage than the flat of the corrugation stiffener.

The performance of all defected panels (rib and corrugation) considering the acoustic conditions and defect size utilized revealed that FS-85 columbium heat shields are quite tolerant of local coating damage. There were no immediate catastrophic failures. Even under the severe acoustic conditions, a minimum capability of 20 reentry flights were shown for defected heat shields. Fears that micrometeoroid damage during flight would jeopardize reentry are no longer justified.

11.0 REUSE LIFE STUDIES OF R-512E COATED FS-85 COLUMBIUM ALLOY HEAT SHIELD PANELS

The objective of this additional work was to fabricate, coat and test subsize columbium alloy heat shield panels to determine their total structural life and to establish how long after incipient coating degradation they maintain structural integrity.

11.1 Fabrication of Heat Shield Panels - The rib stiffened heat shield panel was designed, optimized, and sized for the basic program assuming that it was radiative and behaved as a secondary structure which carries pressure loads only and not primary body loads. Also, the minimum structural gage allowable was approximately 0.010" (0.025 cm) when handling, welding, and coating are considered. This same rationale was used for the heat shield panels used in this phase of the study. The 3" x 12" (7.5 cm x 30 cm) rib stiffened panels were utilized and are basically the same as those used earlier in the program for coating evaluations.

The FS-85 columbium alloy was used for panel fabrication. Starting gages were 0.025" (0.063 cm) for rib stock and 0.012" (0.03 cm) for skin stock. The skin was joined to the ribs by EB welding through the skin to produce a joint that is free of faying surfaces. Nine panels were fabricated using established fabrication techniques.

11.2 Coating of Heat Shield Panels - The R-512E coating was applied by HiTemCo using the optimized nitrocellulose slurry (C-5) and processing parameters developed in Section 8.0. The technique of applying a bead of slurry to all panel edges to improve coating reliability was employed. Average coating weight for the nine panels was 21.2 mg/cm^2 (determined by weighing). The scatter in average coating weight between panels was within $\pm$0.5 mg/cm^2, (by weight) and the ranges on individual panels was within $\pm$3 mg/cm^2 (determined by Dermitron NDT). The average coating weight of 21.2 mg/cm^2 is equivalent to 3 mils (7.5 μm) of coating thickness per side.

11.3 Testing of Heat Shield Panels - Test conditions represented Earth reentry for a long cross range Space Shuttle flight and included simulated reentry profiles established in Section 4.0. Bending loads were applied to the subsize panels by a scissors fixture, and temperature and air pressure were provided and controlled by a 7" (18 cm) diameter Astrotube Furnace. The entire panel was placed in the testing furnace and subjected to the external pressure environment of reentry flight. These are the same test conditions and facilities which were utilized for testing the subsize ((3" x 12")(2.5 cm x 30 cm)) panels in Sections 8.0, 9.0, and 10.0.

A part of the flight simulation which was performed on each subsize rib stiffened panel was acoustic exposure to simulate the noise environment experienced during lift-off. Acoustic simulation was accomplished after each group of reentry cycles. Since acoustic loading produces fatigue which is a cumulative condition, it was felt that grouping the acoustic tests was satisfactory and since the level of exposure was constant, the total time was the most important factor in the simulation. The reasons and rationale for the level of acoustic exposures selected were presented in Section 4.0 for testing of the subsize ((3" x 12")(7.5 cm x 30 cm)) panels utilized in Sections 8.0, 9.0 and 10.0. Fatigue failures were generated at a stress level of 10,000 psi (69 MN/m^2) in approximately 2860 sec (the acoustic environment associated with 100 reentry cycles). The 10,000 psi (69 MN/m^2) stress level was considerably higher than that expected in flight and was designed to produce fatigue in 100 reentry cycles.

Since the objective of this study was to determine total structural life or a minimum of 200 reentry exposures for each panel, the acoustic exposure conditions had to be changed to achieve the reentry exposure desired. Because the stress level dictates the fatigue life, it was decided to lower the stress level to 7500 psi (52 MN/m^2) in order to allow 200 reentry cycles without fatiguing the panels. The stress level selected was somewhat arbitrary and was selected considering the fact that a small decrease in stress can produce orders of magnitude increases in fatigue life.

11.4 Test Results - Eight (8) subsize rib stiffened heat shield panels were exposed to reentry simulation including acoustic testing. A total of 1600 reentry cycles were conducted; each of the 8 panels was exposed for 200 cycles. Elastic and creep deflection measurements were made prior to and at intervals during testing. Elastic deflection measurements were made under four-point loading of the panels at a load (141 lb (64 kg)) which produced a stress in the outer portion of the ribs equal to 77% of room temperature yield for coated FS-85 columbium alloy. Creep deflection measurements were made with a straight bar and micrometer over an 11" (28 cm) span for each panel.

Results of creep and elastic deflection measurements are shown in Table 11-1. The creep measurements shown are cumulative deflections from time 0 cycles. The elastic deflections shown are the results measured after each group of reentry cycles. The creep and elastic deflection results are presented graphically in Figures 11-1 and 11-2. The creep deflection rate for the first 100-120 cycles is

TABLE 11-1

DEFLECTION MEASUREMENTS, SUBSIZE RIB STIFFENED HEAT SHIELD PANELS

PANEL NO.	CYCLE NO.	DEFLECTION MEASUREMENTS			
		CUMULATIVE CREEP		ELASTIC	
		(MILS)	(MM)	(MILS)	(MM)
1	0	0	0	70	1.8
	22	12	0.3	70	1.8
	44	21	0.5	71	1.8
	66	33	0.8	76	1.9
	88	33	0.8	68	1.7
	110	43	1.1	74	1.9
	132	48	1.2	81	2.0
	154	44	1.1	83	2.1
	176	42	1.1	78	2.0
	200	47	1.2	77	1.9
2	0	0	0	66	1.7
	22	13	0.3	68	1.7
	44	18	0.4	69	1.7
	66	32	0.8	72	1.8
	88	36	0.9	70	1.8
	110	42	1.1	75	1.9
	132	47	1.2	76	1.9
	154	55	1.4	80	2.0
	176	52	1.3	72	1.8
	200	–	–	70	1.8
3	0	0	0	74	1.9
	22	13	0.3	72	1.8
	44	17	0.4	76	1.9
	66	28	0.7	77	1.9
	88	37	0.9	74	1.9
	110	41	1.0	76	1.9
	132	45	1.1	79	2.0
	154	45	1.1	80	2.0
	176	48	1.2	76	1.9
	200	64	1.6	75	1.9
5	0	0	0	77	1.9
	22	9	0.2	71	1.8
	44	14	0.4	73	1.8
	66	23	0.6	74	1.9
	88	27	0.7	78	2.0
	110	39	1.0	78	2.0
	132	41	1.0	82	2.1
	154	42	1.1	76	1.9
	176	42	1.1	77	1.9
	200	–	–	72	1.8
6	0	0	0	70	1.8
	22	10	0.3	66	1.7
	44	16	0.4	72	1.8
	66	24	0.6	70	1.8
	88	35	0.9	75	1.9
	110	38	1.0	73	1.8
	132	42	1.1	78	2.0
	154	37	0.9	75	1.9
	176	41	1.0	74	1.9
	200	41	1.0	73	1.8
7	0	0	0	65	1.6
	22	13	0.3	65	1.6
	44	25	0.6	71	1.8
	66	32	0.8	66	1.7
	88	34	0.9	70	1.8
	110	41	1.0	76	1.9
	132	53	1.3	76	1.9
	154	60	1.5	78	2.0
	176	59	1.5	77	1.9
	200	–	–	75	1.9
8	0	0	0	68	1.7
	50	21	0.5	75	1.9
	100	49	1.2	86	2.2
	150	51	1.3	77	1.9
	200	65	1.6	73	1.8
9	0	0	0	70	1.8
	50	20	0.5	70	1.8
	100	34	0.9	75	1.9
	150	38	1.0	78	2.0
	200	43	1.1	75	1.9

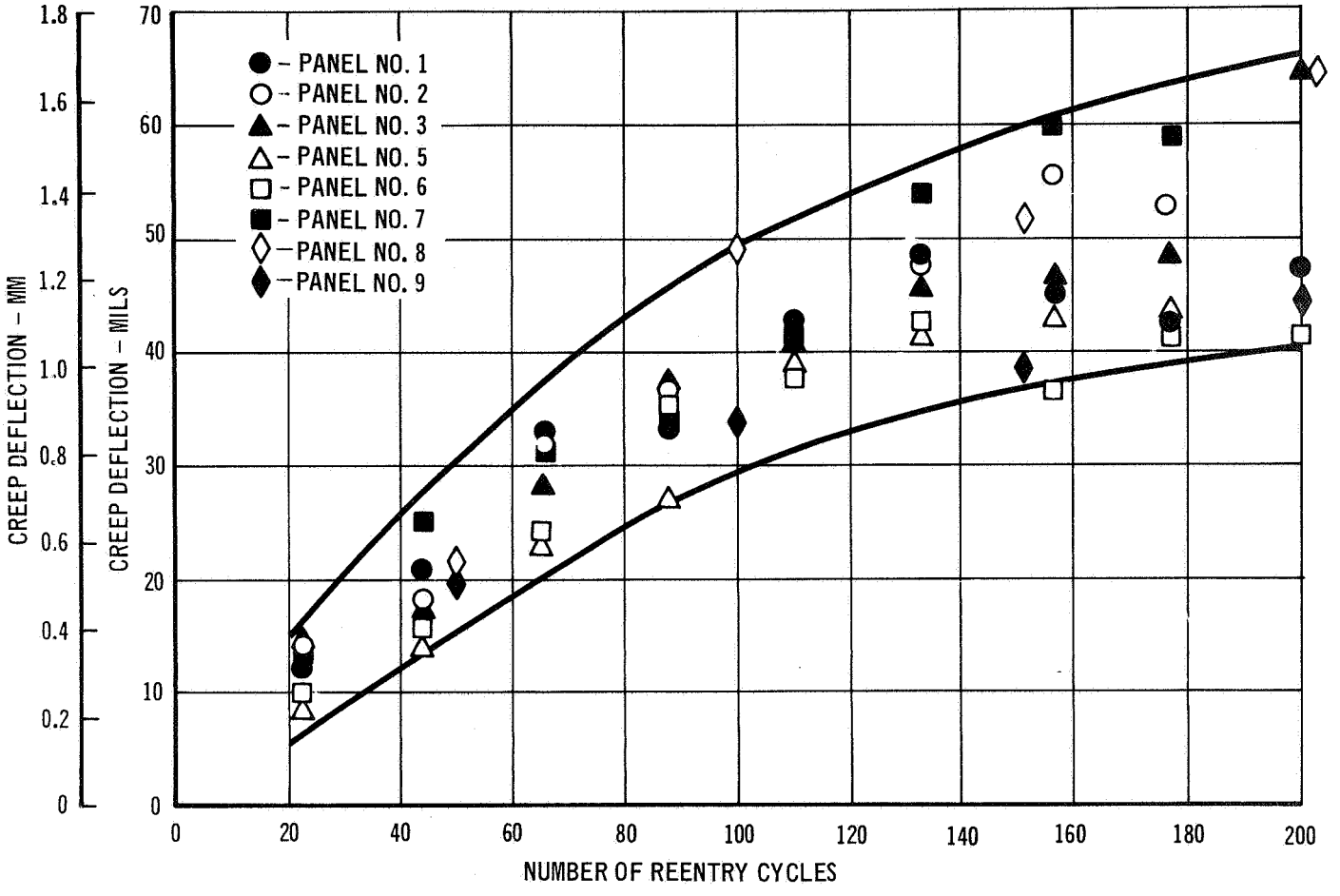

EFFECT OF REENTRY CYCLING ON CREEP DEFLECTION OF RIB STIFFENED HEAT SHIELD PANELS

457-3192

FIGURE 11-1

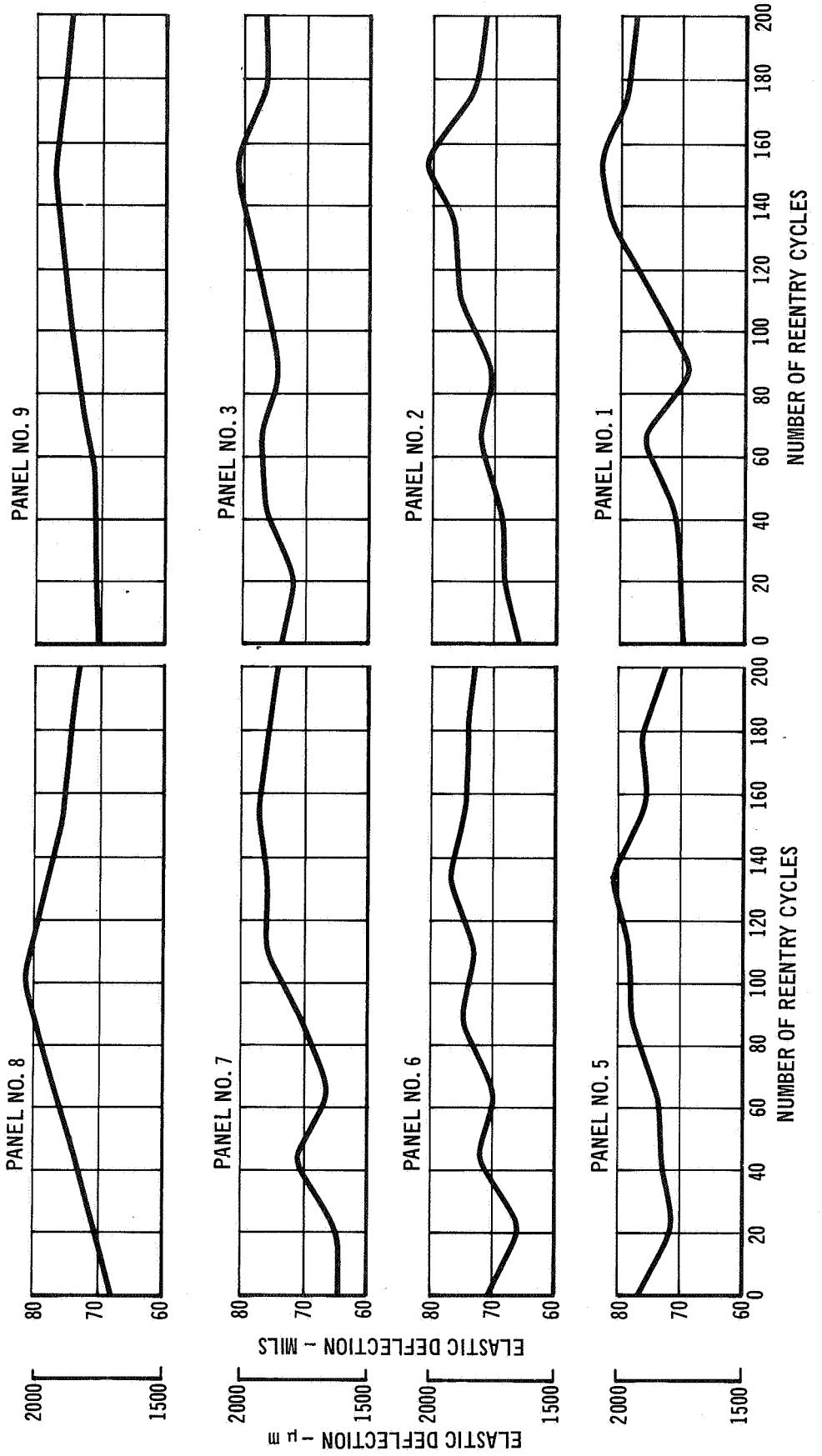

EFFECT OF REENTRY CYCLING ON ELASTIC DEFLECTION OF RIB STIFFENED HEAT SHIELD PANELS

FIGURE 11-2

about 0.4 mil/cycle (10 μm/cycle) which compares very favorably to the creep rate of 0.45 mil/cycle (11.4 μm/cycle) determined for the rib stiffened panels evaluated in Section 8.0. After 100-120 cycles the creep deflection rate decreased to about 0.2 mil/cycle (5 μm/cycle). Examination of the elastic deflections (Figure 11-2) reveals a change in elastic deflection after about the same number (120) of reentry cycles. The elastic deflections increase from 0 cycles and reach a peak around 100-150 cycles with decreasing deflections on up to 200 cycles where testing was terminated. It would seem that continued base metal consumption due to inter-diffusion of the coating and base metal as reentry exposure time increases would lead to increasing elastic and creep deflection because of reduced metal cross section. The base metal consumption due to reentry cycling to 2400°F (1300°C) should be about 0.5 mil (12.5 μm)/side after 100 reentry cycles. This trend is evident in the elastic deflections for the first 100-150 cycles but of course is not discernible in the creep deflections. The creep rate changes from 0.4 mil (10 μm)/cycle to 0.2 mil (5 μm)/cycle and the decrease in elastic deflections after 100-150 reentry cycles can best be explained by a strengthening of the substrate by slight increases in the interstitial content. This increase in contaminants occurs because oxidation of the coating has progressed to the point where total protection is not being provided. This contamination and coating oxidation can be observed in Figure 11-3, which shows cross section photomicrographs of a panel after 200 reentry cycles.

11.4.1 Incipient Coating Breakdown - The reproducibility of the optimized fused slurry silicide coating process and the coating quality were demonstrated to be exceptionally good. The first incipient coating failures for the 8 panels tested did not occur until after 66 reentry cycles had been completed. Two panels showed no evidence of coating failures until after 200 cycles had been completed.

Photographs of each of the eight panels are shown at various stages of testing in Figures 11-4 through 11-11. Some of the panels look well used, but at least 95% of the damage that was incurred happened during the last 25 cycles. The appearance of the panels after 176 reentry cycles was vastly different. Withstanding 176 simulated reentry flights and maintaining good appearance is considered a great achievement.

The times to incipient coating failure were examined statistically utilizing a Weibull analysis. The Weibull distribution is one of the more common and versatile mathematical probability density functions to which empirical life data can be fitted.

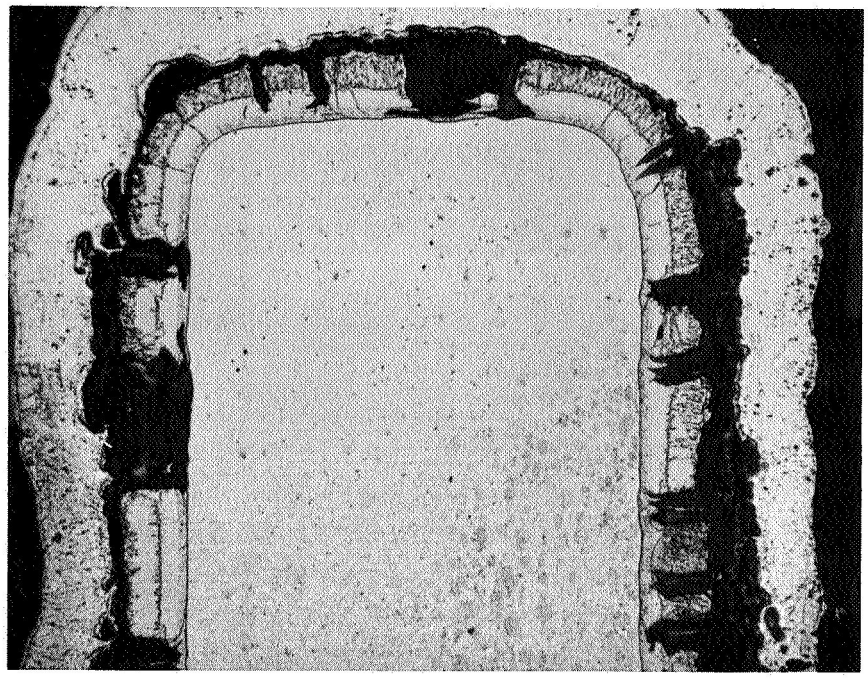

100X

(a) Cross–Section of Upper Portion of Rib

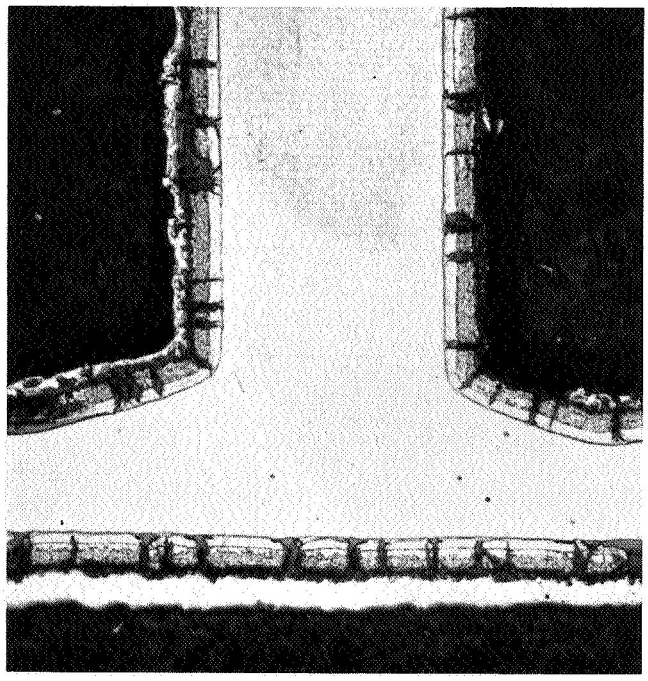

50X

(b) Cross–Section of Rib–Skin Joint

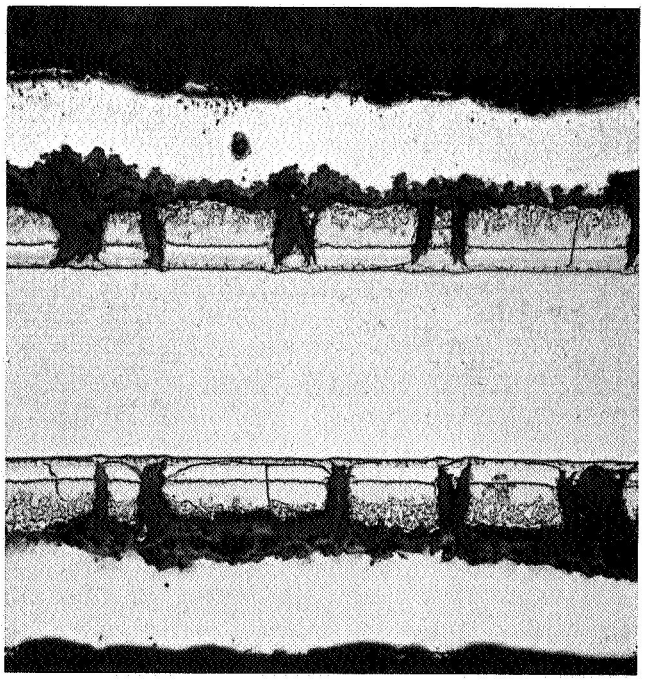

100X

(c) Cross–Section of Skin Between Ribs

HEAT SHIELD PANEL NO. 7 AFTER 200 FLIGHT SIMULATION CYCLES – EXTERNAL PRESSURE ENVIRONMENT

FIGURE 11–3

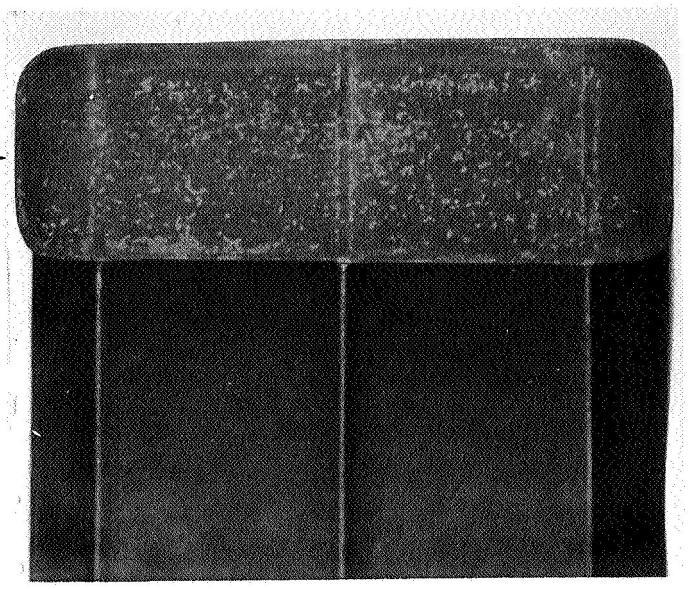

1X

(a) After 66 Reentry and Acoustic Cycles

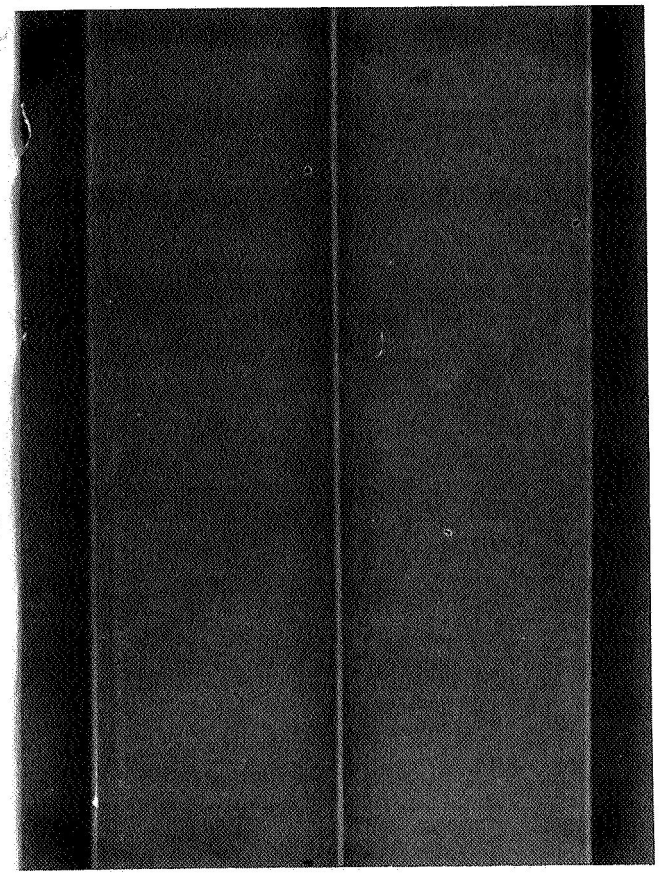

1X

(b) After 176 Reentry and Acoustic Cycles

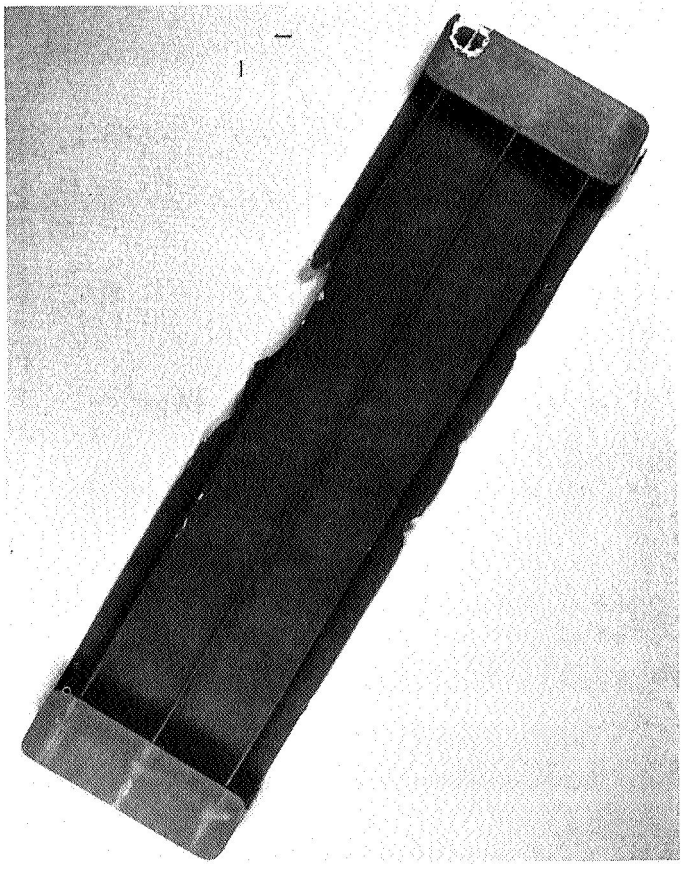

0.36X

(c) After 200 Reentry and Acoustic Cycles

FLIGHT SIMULATION TESTING OF PANEL NO. 1

FIGURE 11-4

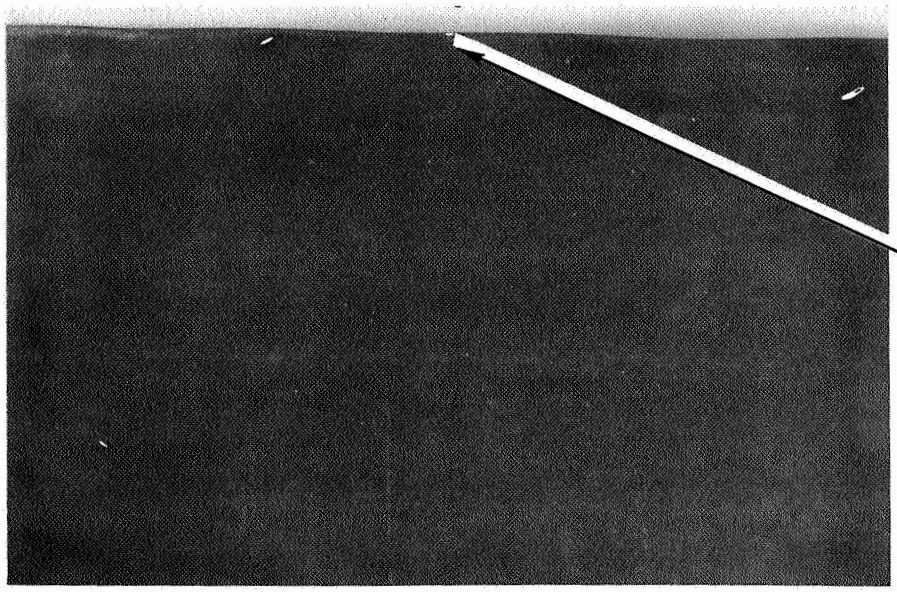

PANEL CENTER SECTION–SKINSIDE 1X

(a) After 176 Reentry and Acoustic Cycles

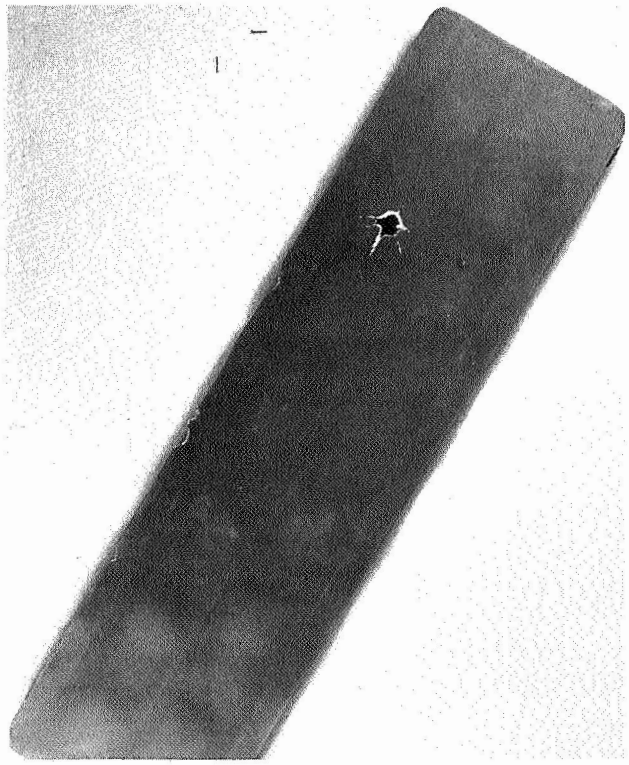

(b) After 200 Reentry and 176 Acoustic Cycles 0.36X

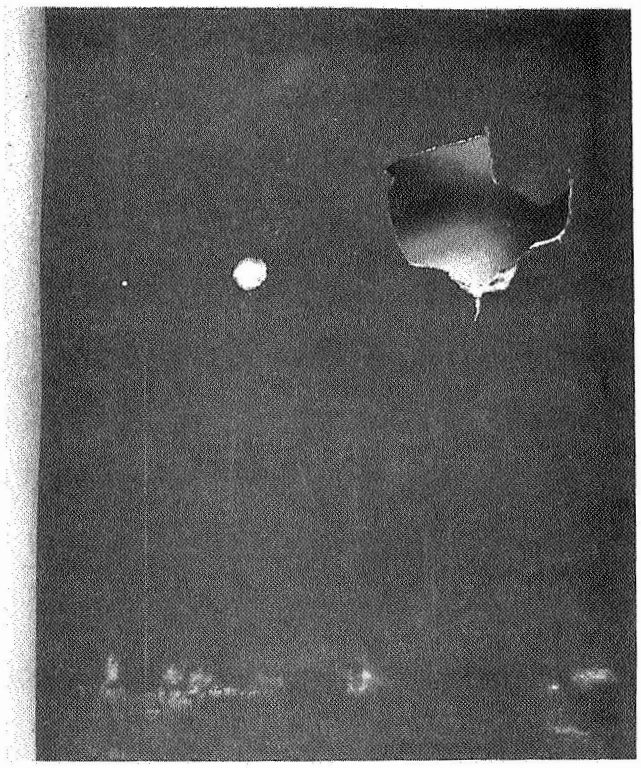

(c) After 200 Reentry and Acoustic Cycles 1X

FLIGHT SIMULATION TESTING OF PANEL NO. 2

FIGURE 11–5

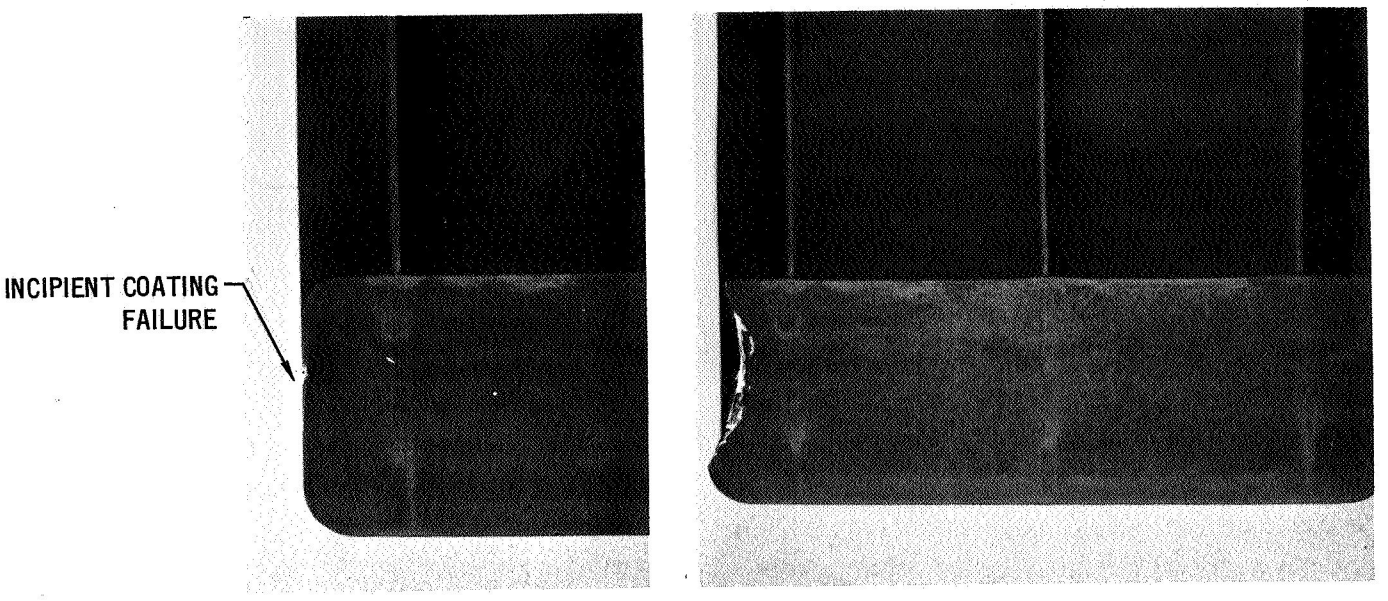

1.2X

(a) After 66 Reentry and Acoustic Cycles

1X

(b) After 132 Reentry and Acoustic Cycles

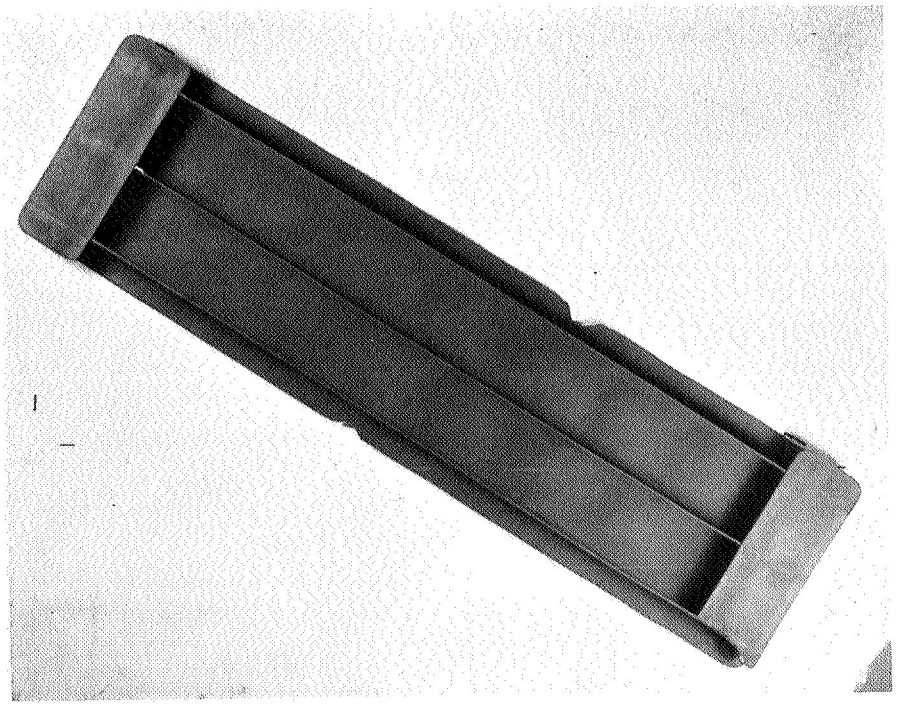

0.36X

(c) After 200 Reentry and Acoustic Cycles

FLIGHT SIMULATION TESTING OF PANEL NO. 3

FIGURE 11-6

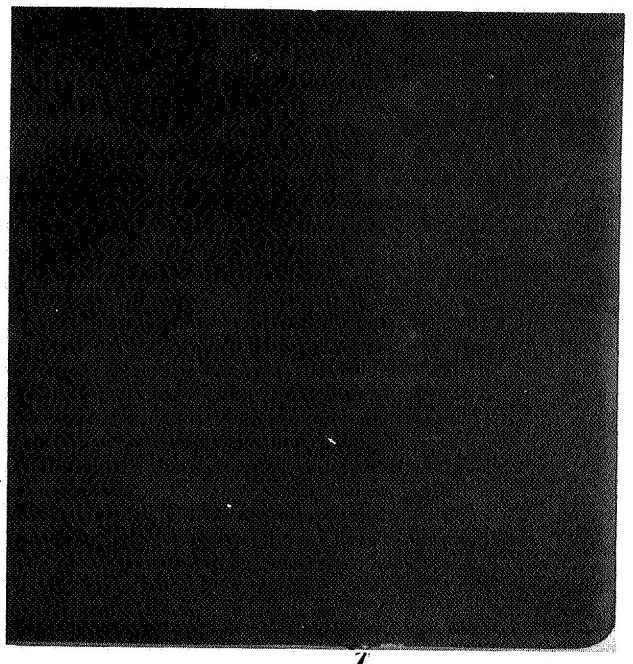

1.2X

(a) After 110 Reentry and Acoustic Cycles

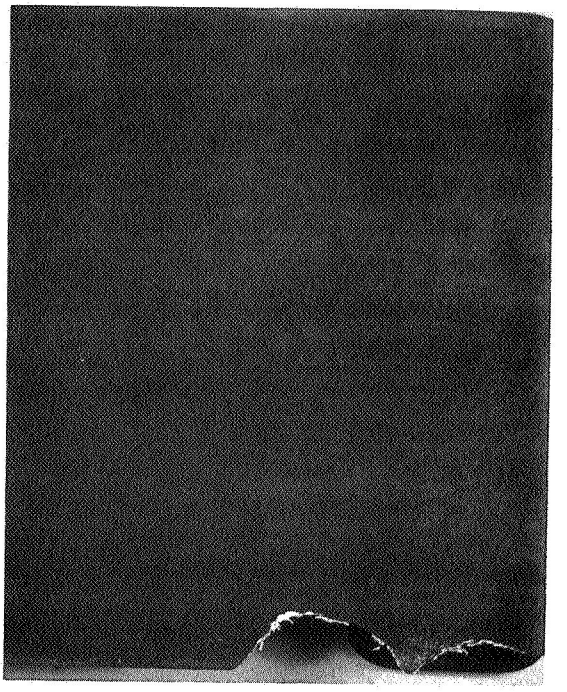

1.2X

(b) After 176 Reentry and Acoustic Cycles

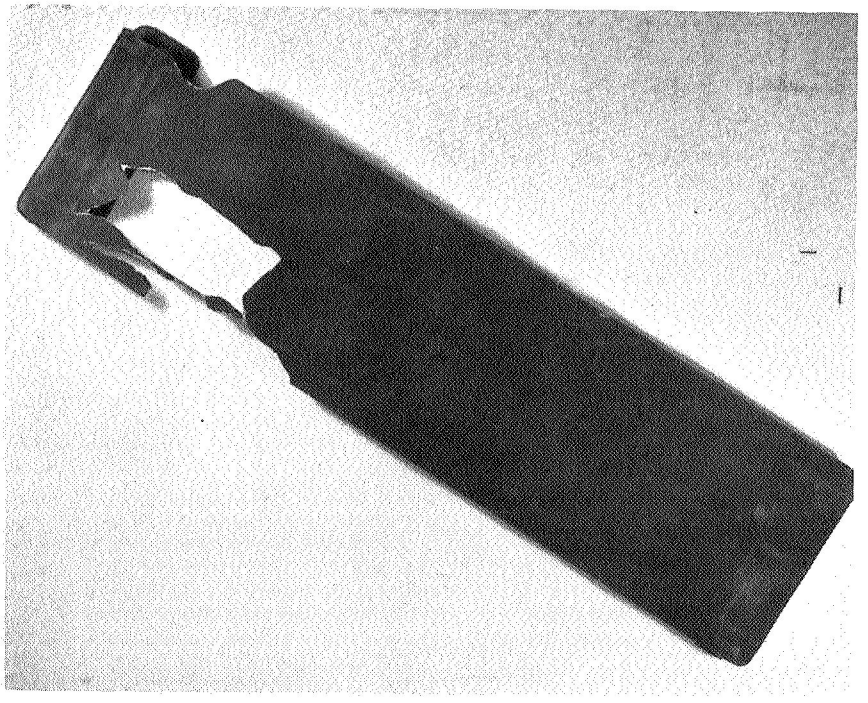

0.38X

(c) After 200 Reentry and Acoustic Cycles

FLIGHT SIMULATION TESTING PANEL NO. 5

FIGURE 11-7

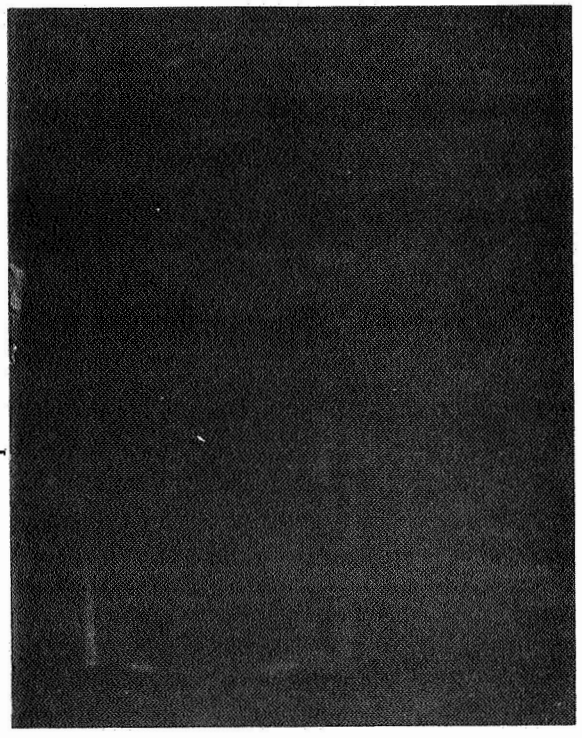

1X

(a) After 154 Reentry and Acoustic Cycles

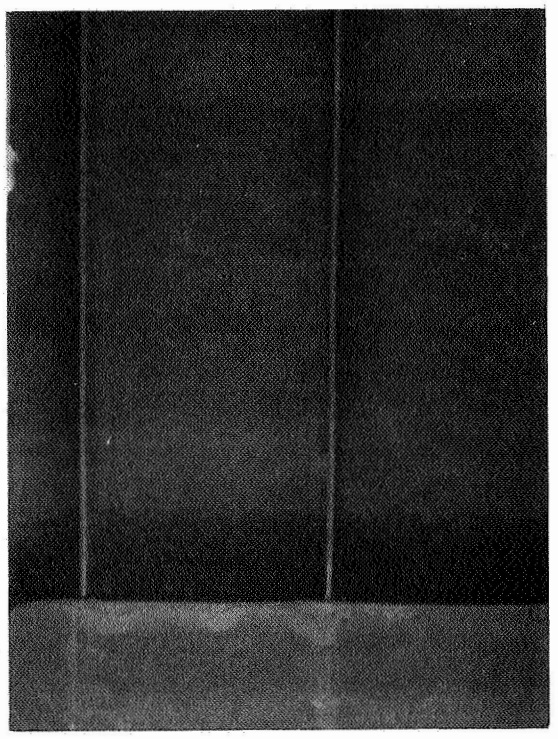

1X

(b) After 176 Reentry and Acoustic Cycles

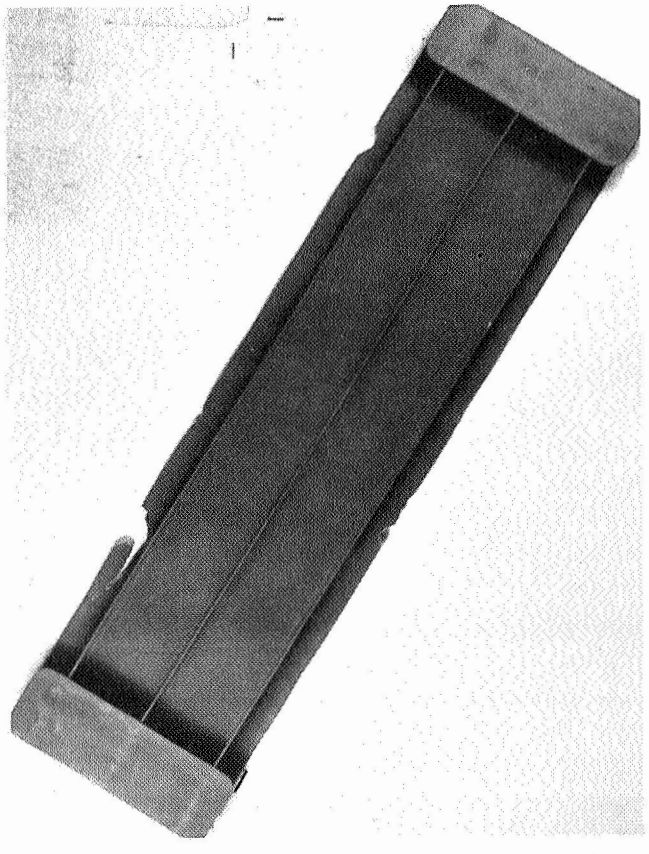

(c) After 200 Reentry and Acoustic Cycles 0.36X

FLIGHT SIMULATION TESTING OF PANEL NO. 6

FIGURE 11-8

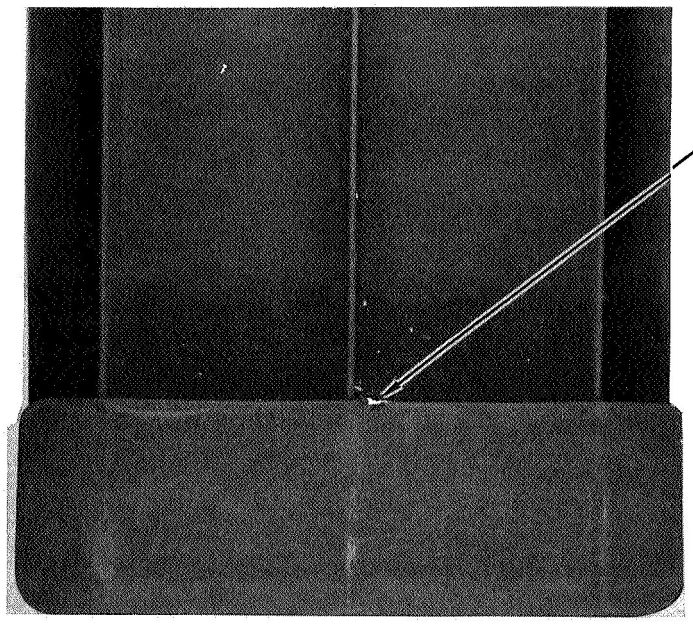

(a) After 66 Reentry and Acoustic Cycles 1X

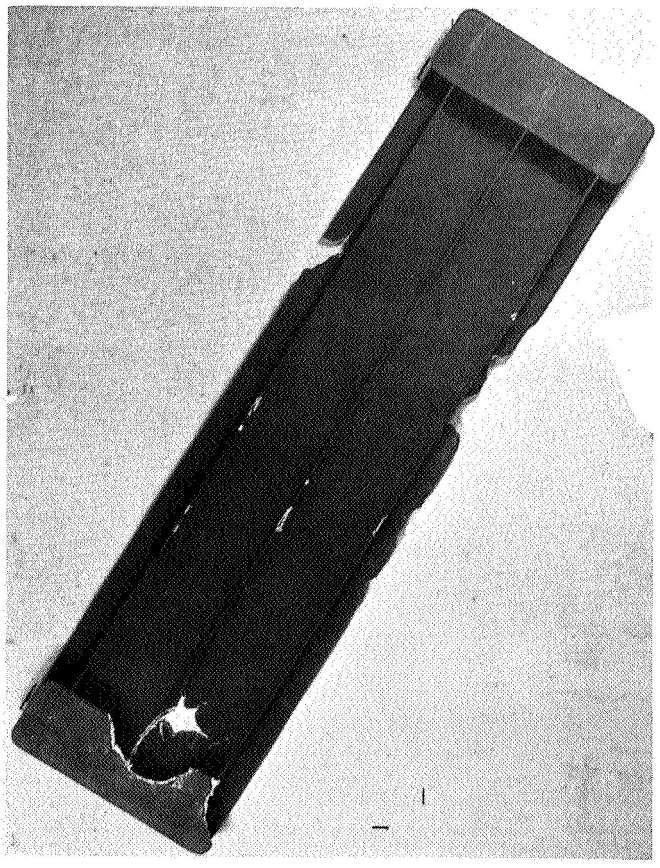

0.36X

(b) After 200 Reentry and 176 Acoustic Cycles

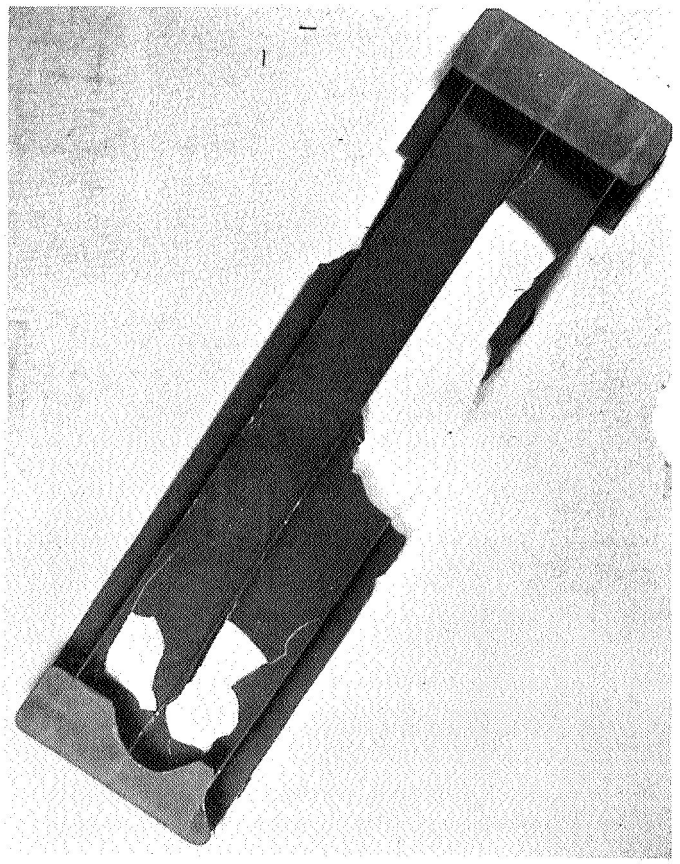

0.36X

(c) After 200 Reentry and Acoustic Cycles

FLIGHT SIMULATION TESTING OF PANEL NO. 7

FIGURE 11-9

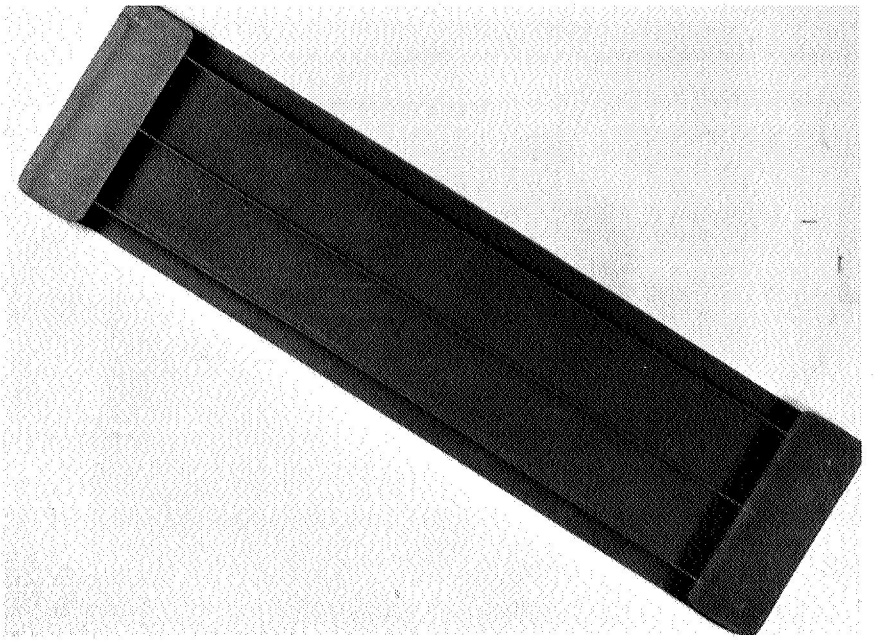

(a) After 50 Reentry and Acoustic Cycles 0.36X

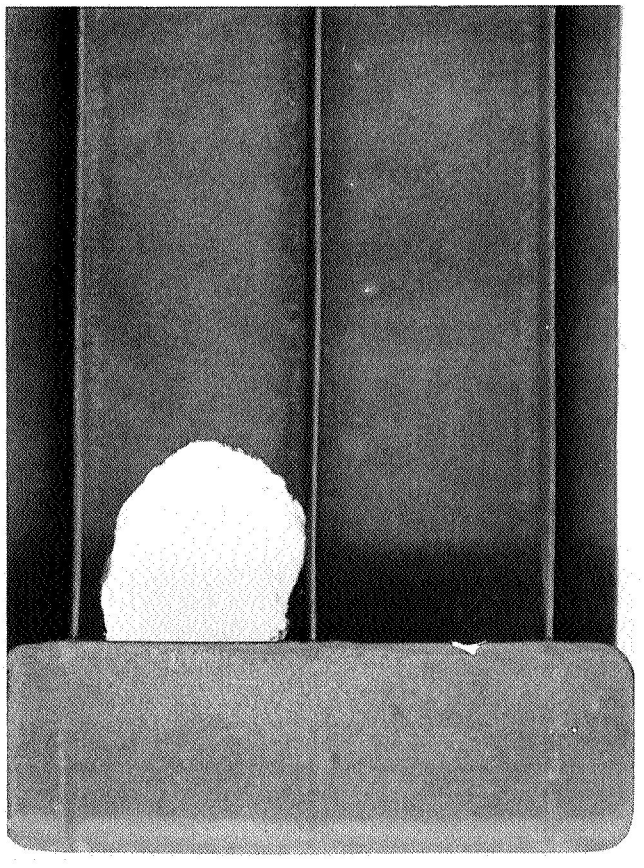

1X

(b) After 200 Reentry and 150 Acoustic Cycles

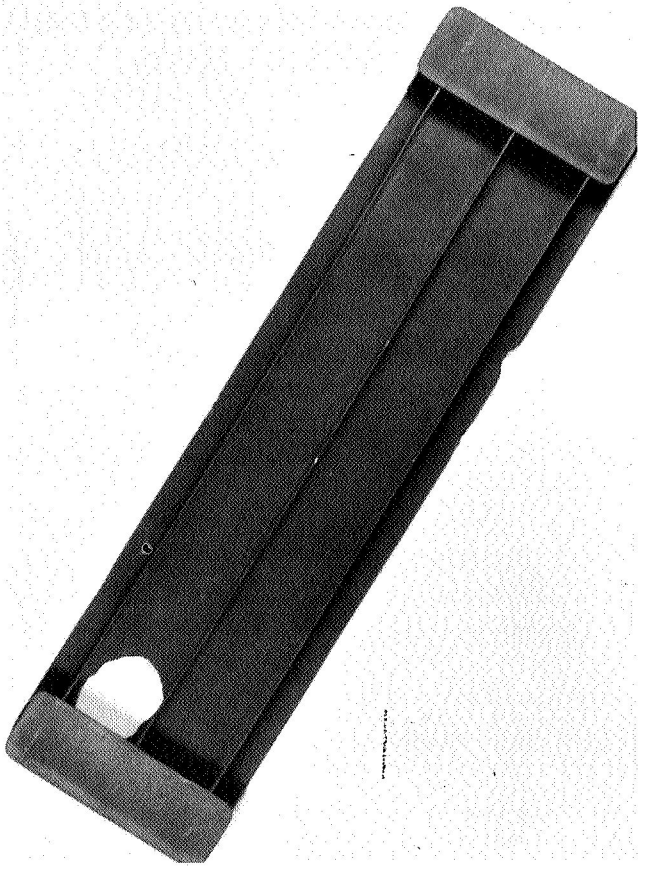

0.36X

(c) After 200 Reentry and Acoustic Cycles

FLIGHT SIMULATION TESTING OF PANEL NO. 8

FIGURE 11-10

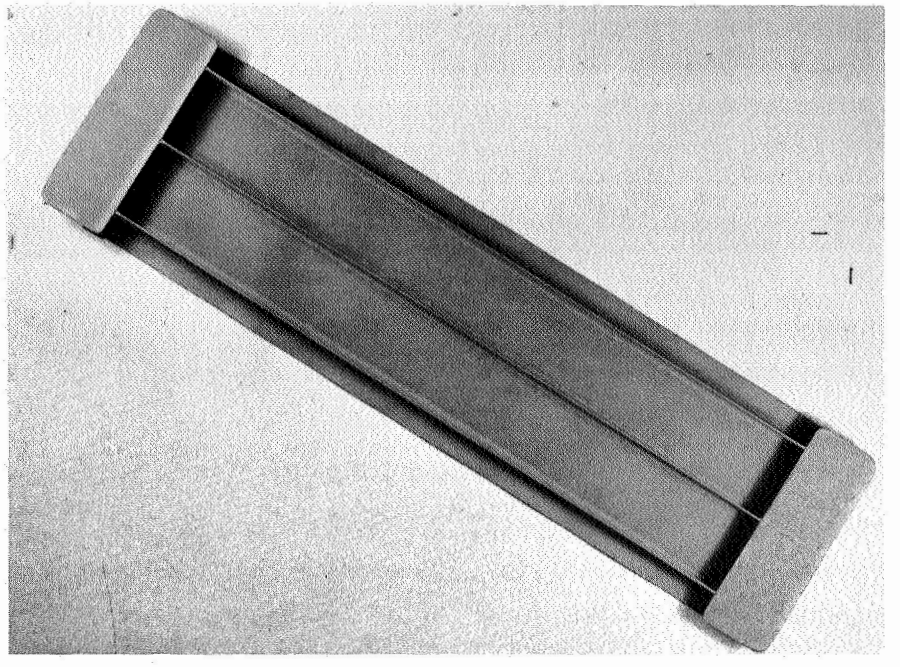

(a) As Coated Prior to Testing 0.36X

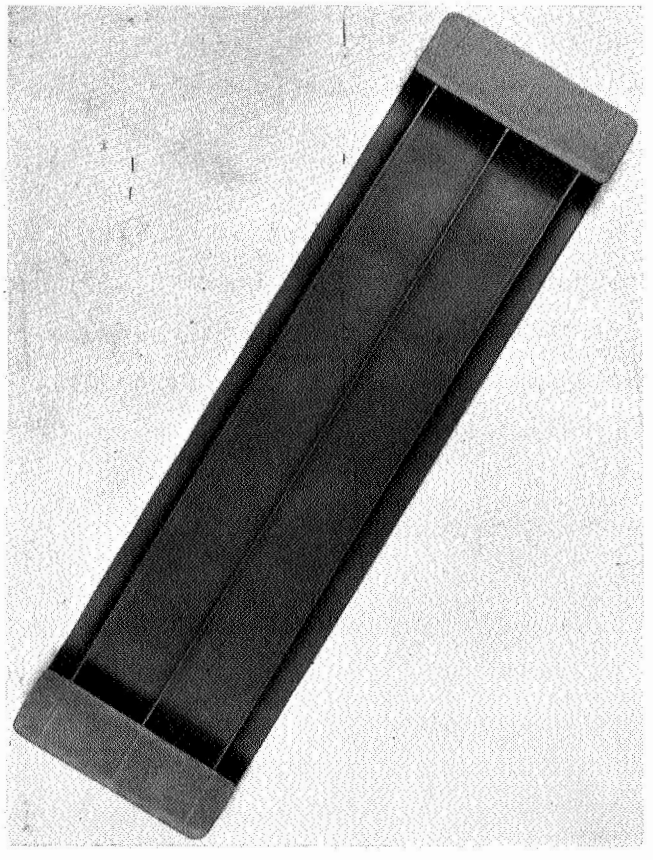

RIB SIDE 0.36X

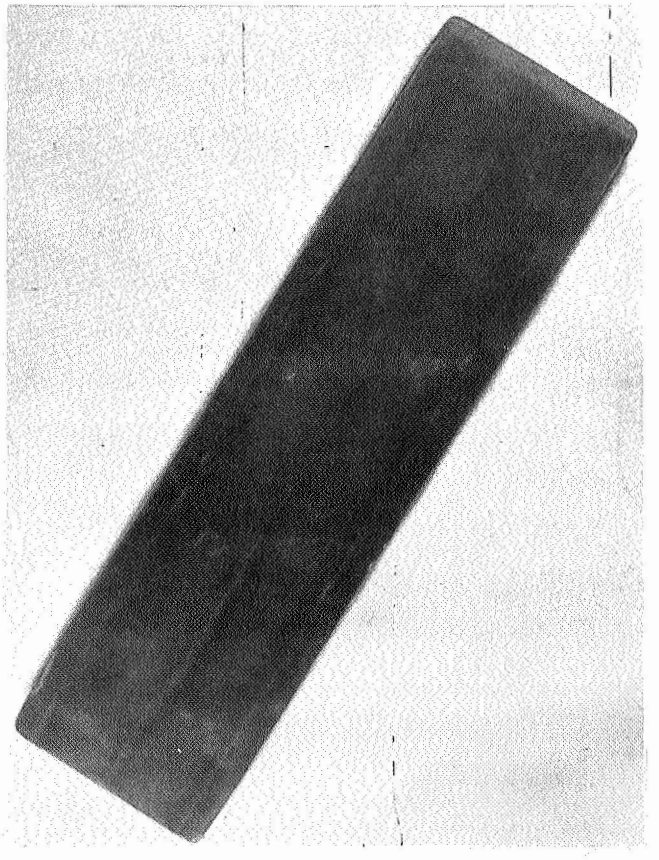

SKIN SIDE 0.36X

(b) After 200 Reentry and Acoustic Cycles

FLIGHT SIMULATION TESTING OF PANEL NO. 9

FIGURE 11-11

The Weibull cumulative frequency function is expressed by the mathematical relationship:

$$F(t) = 1 - \exp\ (-5 + \alpha/\theta)^{\beta}$$

Where F(t) = the cumulative failures expressed as a fraction of the original sample lot:

t = time

α = the threshold or location parameter

θ = the time to failure of 63.2 percent of the sample population

β* = the shape parameter (b > 0).

*For β = 1.0 the distribution is exponential; for β = 3.34 the normal distribution is approximated.

Where the number of test samples is less than fifty, the risk that the entire population is not represented by the test increases substantially. To minimize this risk, rank tables are available from a solution of the multinominal theorem of joint probabilities (Reference 1). These tables relate the cumulative failures within a given sample size to the percentage values which would be obtained had an infinite number of samples been tested. Ranks have been calculated for the 50 percent level (median) in which a given cumulative failure percentage has an equal probability of being either greater or smaller if the total population were tested, the 95 percent level at which all but 5 percent of the total population would rank below the specified level, and the 5 percent level above which 95 percent of the total population would be ranked. With these tables, which are shown in Tables 11-2, 11-3, and 11-4, bands encompassing 90 percent of the total population of test data can be generated from tests of relatively small numbers of samples.

Examination of times to incipient coating failure for the 8 panel specimens revealed the following data:

PANEL SPECIMEN NO.	TIME TO INCIPIENT COATING FAILURES (CYCLES)
1	66
2	66
3	66
5	110
6	154
7	176
8	200
9	200

TABLE 11-2

MEDIAN RANKS

	1	2	3	4	5	6	7	8	9	10	11	12	13	14	15	16	17	18	19	20
1	.5000	.2929	.2063	.1591	.1294	.1091	.0943	.0830	.0741	.0670	.0611	.0561	.0519	.0483	.0452	.0424	.0400	.0378	.0358	.0341
2		.7071	.5000	.3864	.3147	.2655	.2295	.2021	.1806	.1632	.1489	.1368	.1266	.1178	.1101	.1034	.0975	.0922	.0874	.0831
3			.7937	.6136	.5000	.4218	.3648	.3213	.2871	.2594	.2366	.2175	.2013	.1873	.1751	.1644	.1550	.1465	.1390	.1322
4				.8409	.6853	.5782	.5000	.4404	.3935	.3557	.3244	.2982	.2760	.2568	.2401	.2254	.2125	.2009	.1905	.1812
5					.8706	.7345	.6352	.5596	.5000	.4519	.4122	.3789	.3506	.3263	.3051	.2865	.2700	.2553	.2421	.2302
6						.8909	.7705	.6787	.6065	.5481	.5000	.4596	.4253	.3958	.3700	.3475	.3275	.3097	.2937	.2793
7							.9057	.7979	.7129	.6443	.5878	.5404	.5000	.4653	.4350	.4085	.3850	.3641	.3453	.3283
8								.9170	.8194	.7406	.6756	.6211	.5747	.5347	.5000	.4695	.4425	.4184	.3968	.3774
9									.9259	.8368	.7634	.7018	.6494	.6042	.5650	.5305	.5000	.4728	.4484	.4264
10										.9330	.8511	.7825	.7240	.6737	.6300	.5915	.5575	.5272	.5000	.4755
11											.9389	.8632	.7987	.7432	.6949	.6525	.6150	.5816	.5516	.5245
12												.9439	.8734	.8127	.7599	.7135	.6725	.6359	.6032	.5736
13													.9481	.8822	.8249	.7746	.7300	.6903	.6547	.6226
14														.9517	.8899	.8356	.7875	.7447	.7063	.6717
15															.9548	.8966	.8450	.7991	.7579	.7207
16																.9576	.9025	.8535	.8095	.7698
17																	.9600	.9078	.8610	.8188
18																		.9622	.9126	.8678
19																			.9642	.9169
20																				.9659

TABLE 11-3

95% RANKS

	1	2	3	4	5	6	7	8	9	10	11	12	13	14	15	16	17	18	19	20
1	.9500	.7764	.6316	.5271	.4507	.3930	.3482	.3123	.2831	.2589	.2384	.2209	.2058	.1926	.1810	.1726	.1642	.1559	.1475	.1391
2		.9747	.8646	.7514	.6574	.5818	.5207	.4707	.4291	.3942	.3644	.3387	.3163	.2967	.2794	.2640	.2525	.2411	.2296	.2182
3			.9830	.9024	.8107	.7287	.6587	.5997	.5496	.5069	.4701	.4381	.4101	.3854	.3634	.3438	.3262	.3129	.2995	.2862
4				.9873	.9236	.8468	.7747	.7108	.6551	.6076	.5644	.5273	.4946	.4657	.4398	.4166	.3956	.3767	.3621	.3475
5					.9898	.9371	.8713	.8071	.7486	.6965	.6502	.6091	.5726	.5400	.5107	.4844	.4605	.4389	.4191	.4036
6						.9915	.9466	.8889	.8312	.7776	.7287	.6848	.6452	.6096	.5774	.5483	.5219	.4978	.4758	.4556
7							.9926	.9532	.9032	.8500	.7993	.7535	.7117	.6737	.6392	.6078	.5792	.5540	.5289	.5068
8								.9935	.9590	.9127	.8637	.8176	.7745	.7348	.6984	.6650	.6458	.6063	.5804	.5566
9									.9943	.9632	.9200	.8755	.8329	.7918	.7541	.7195	.6869	.6571	.6297	.6043
10										.9949	.9667	.9281	.8873	.8473	.8091	.7733	.7399	.7088	.6799	.6531
11											.9935	.9693	.9335	.8953	.8576	.8214	.7872	.7551	.7251	.6971
12												.9957	.9719	.9389	.9033	.8679	.8336	.8010	.7702	.7413
13													.9960	.9737	.9426	.9090	.8753	.8425	.8113	.7817
14														.9963	.9755	.9464	.9146	.8827	.8525	.8215
15															.9966	.9773	.9501	.9203	.8901	.8604
16																.9968	.9784	.9534	.9239	.8949
17																	.9970	.9795	.9548	.9275
18																		.9971	.9806	.9571
19																			.9972	.9817
20																				.9974

TABLE 11-4

5% RANKS

	1	2	3	4	5	6	7	8	9	10	11	12	13	14	15	16	17	18	19	20
1	.0500	.0253	.0170	.0127	.0102	.0085	.0074	.0065	.0057	.0051	.0047	.0043	.0040	.0037	.0034	.0032	.0030	.0029	.0028	.0026
2	-----	.2236	.1354	.0976	.0764	.9629	.0534	.0468	.0410	.0368	.0333	.0307	.0281	.0263	.0245	.0227	.0216	.0205	.0194	.0183
3	----------	----------	.3684	.2486	.1893	.1532	.1287	.1111	.0978	.0873	.0800	.0719	.0665	.0611	.0574	.0536	.0499	.0476	.0452	.0429
4	----------	----------	----------	.4729	.3426	.2713	.2253	.1929	.1688	.1500	.1363	.1245	.1127	.1047	.0967	.0910	.0854	.0797	.0761	.0725
5	----------	----------	----------	----------	.5493	.4182	.3413	.2892	.2514	.2224	.2007	.1824	.1671	.1527	.1424	.1321	.1247	.1173	.1099	.1051
6	----------	----------	----------	----------	----------	.6070	.4793	.4003	.3449	.3035	.2713	.2465	.2255	.2082	.1909	.1786	.1664	.1575	.1485	.1396
7	----------	----------	----------	----------	----------	----------	.6518	.5293	.4504	.3934	.3498	.3152	.2883	.2652	.2459	.2267	.2128	.1990	.1887	.1785
8	----------	----------	----------	----------	----------	----------	----------	.6877	.5709	.4931	.4356	.3909	.3548	.3263	.3016	.2805	.2601	.2449	.2298	.2183
9	----------	----------	----------	----------	----------	----------	----------	----------	.7169	.6058	.5299	.4727	.4274	.3904	.3608	.3350	.3131	.2912	.2749	.2587
10	----------	----------	----------	----------	----------	----------	----------	----------	----------	.7411	.6356	.5619	.5054	.4600	.4226	.3922	.3542	.3429	.3201	.3029
11	----------	----------	----------	----------	----------	----------	----------	----------	----------	----------	.7616	.6613	.5899	.5343	.4893	.4517	.4208	.3937	.3703	.3469
12	----------	----------	----------	----------	----------	----------	----------	----------	----------	----------	----------	.7791	.6837	.6146	.5602	.5156	.4781	.4460	.4196	.3957
13	----------	----------	----------	----------	----------	----------	----------	----------	----------	----------	----------	----------	.7942	.7033	.6366	.5834	.5395	.5022	.4711	.4434
14	----------	----------	----------	----------	----------	----------	----------	----------	----------	----------	----------	----------	----------	.8074	.7206	.6562	.6044	.5611	.5242	.4932
15	----------	----------	----------	----------	----------	----------	----------	----------	----------	----------	----------	----------	----------	----------	.8190	.7360	.6738	.6233	.5809	.5444
16	----------	----------	----------	----------	----------	----------	----------	----------	----------	----------	----------	----------	----------	----------	----------	.8274	.7475	.6871	.6379	.5964
17	----------	----------	----------	----------	----------	----------	----------	----------	----------	----------	----------	----------	----------	----------	----------	----------	.8358	.7589	.7005	.6525
18	----------	----------	----------	----------	----------	----------	----------	----------	----------	----------	----------	----------	----------	----------	----------	----------	----------	.8441	.7704	.7138
19	----------	----------	----------	----------	----------	----------	----------	----------	----------	----------	----------	----------	----------	----------	----------	----------	----------	----------	.8525	.7818
20	----------	----------	----------	----------	----------	----------	----------	----------	----------	----------	----------	----------	----------	----------	----------	----------	----------	----------	----------	.8609

Regrouping these data in terms of failure time and cumulative failures with the corresponding rank levels for an eight-sample test yields the following:

TIME TO FAILURE (CYCLES)	CUMULATIVE FAILURES	RANK		
		MEDIAN	95%	5%
66	3	32	60	11
110	4	44	71	19
154	5	56	81	29
176	6	68	89	40
200	8	92	99	69

These data are shown plotted on Weibull probability paper in Figure 11-12. In constructing this plot the median rank points were fitted with straight lines and the 95% and 5% bands located from these lines with smooth curves. The Weibull plot clearly shows a mixed distribution consisting of two segments. The slope of the first segment is very near unity indicating random occurrence of failures in this region. At approximately 156 reentry cycles, wearout becomes the predominant mechanism of failure. The proportion of the population (60%) which showed random failures is estimated by dropping a vertical line from the upper bound of the

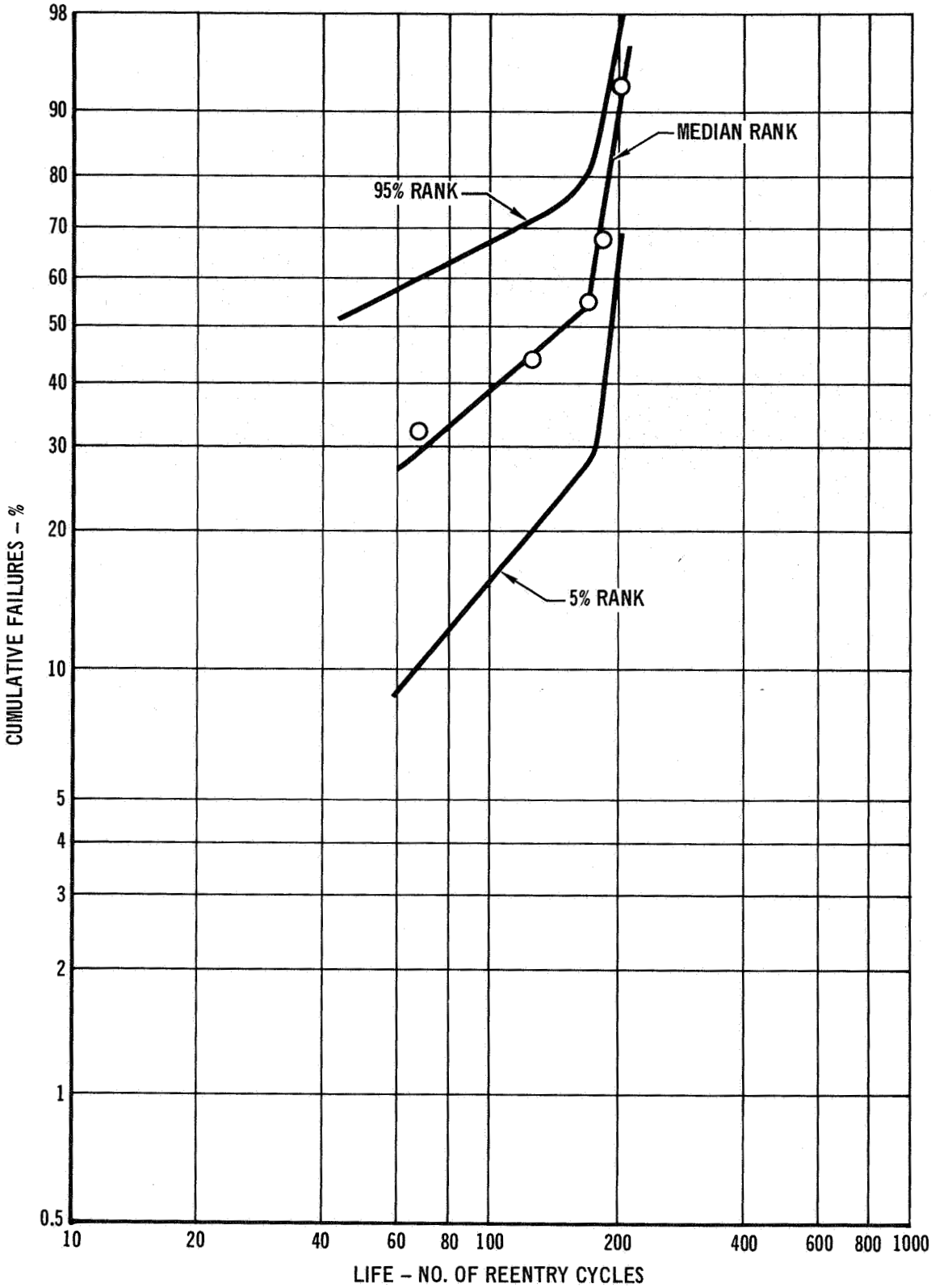

WEIBULL PLOT OF INCIPIENT COATING FAILURES

FIGURE 11–12

wearout distribution line to the intersection of the extrapolated random distribution line and reading the proportion from this point off the cumulative distribution scale. The threshold parameter represents the time at which wearout failures would initiate if there were no random failures and is estimated by extrapolating the wearout curve to the lower boundary of the graph. In this case the threshold parameter is 80 cycles. The randomly occurring incipient coating failures probably represent weak areas such as thin spots or cracks, which fail prior to the onset of general coating degradation. All incipient coating failures, except one, occurred at the edges of panel skins, ribs, or straps. The relatively high percentage of random incipient coating failures indicates that a significant increase in reliability could be realized if the edge coating process were further improved.

11.4.2 Structural Performance - As conceived, the evaluation testing in this study would determine the time to incipient coating failure and the time after incipient coating failure during which structural integrity would be maintained. A time limit of 200 reentry cycles was imposed in order to control costs, but also it was felt that 200 cycles would be sufficient time to determine structural life.

Flight simulation testing of all eight panels was terminated after 200 cycles of exposure. Seven of the eight panels were structurally capable of supporting design loads after 200 cycles. One panel (No. 7) had structural deterioration, which resulted from fatigue caused by the acoustic simulation. The fatigue failure and resulting fracture of this panel occurred through a coating failure site on the edge of one of the rib stiffeners. The incipient coating failure site on this panel (rib-loading strap junction) which occurred after 66 cycles was not the fatigue fracture site. The coating failure site which led to fatigue failure occurred somewhere between 154 and 176 reentry cycles. It was shown in the coating damage studies that coating failure or damage sites located on the edge of the rib stiffeners would lead to fatigue failures at 10,000 psi (69 MN/m^2) induced by acoustic loading in about 20 cycles. The 7500 psi (52 MN/m^2) loading induced by acoustics in these tests did not cause fatigue failure until 25-45 cycles. The rib coating failure on Panel No. 7 was the only rib coating failure that had progressed by oxidation to a point to affect structural integrity. Only one other panel (No. 1) had any rib coating failure and this was after 176 cycles. It was a very small site and did not progress to a point to cause any structural damage.

Other incipient coating failures of the combined group of panels were found at most edge locations. None of these incipient coating failures led to loss of

structural integrity of the panel. Some failures occurred at 66 reentry cycles which means that more than 134 additional reentry cycles are required before structural integrity is affected. All of the incipient coating failures associated with the skin on the panels caused holes, by consumption due to oxidation, which would become unacceptable because of aerodynamic considerations long before structural integrity was affected. Only the edges of the rib stiffeners presented an area that was structurally critical in an acoustic environment which generates 7500 psi (52 MN/m^2) should early coating failures occur. The 7500 psi (52 MN/m^2) is still considered well above anticipated acoustic generated stress levels for full size columbium heat shield panels. Based on the results of the eight panels tested, a 100 flight structural life is a certainty.

11.4.3 NDT Coating Thickness Data - Table 11-5 presents the results of non-destructive coating thickness measurements made on the eight heat shield panels before and after flight simulation for 200 cycles. The Dermitron eddy current device was used for the thickness measurements. Excellent coating uniformity was revealed for all panels in the "as coated" condition.

Thickness measurements made after 200 reentry cycles were made with some considerable difficulty because of the wrinkled or warped condition of the skin. The warped condition of the skin existed prior to reentry cycling, but was made worse because of the compressive forces in the skin from reentry load simulation. Coating thickness increase due to cycling for 200 times was increased from 75 to 100% on the average. This compares to a 30 to 50% average increase for R-512E coated FS-85 panels exposed for 100 reentry cycles. Backside (stiffener side) of the panels showed a slightly larger increase in coating thickness than the skin side. This could be due to greater air flow exposure, thus more coating oxide, or to lower compression stresses which would cause less spalling of the coating oxide.

TABLE 11-5

NDT DERMITRON COATING THICKNESS ON R-512E COATED FS-85 SUBSIZE PANELS

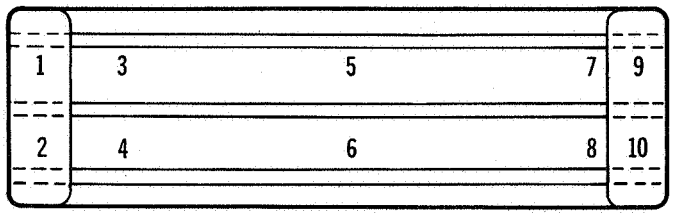

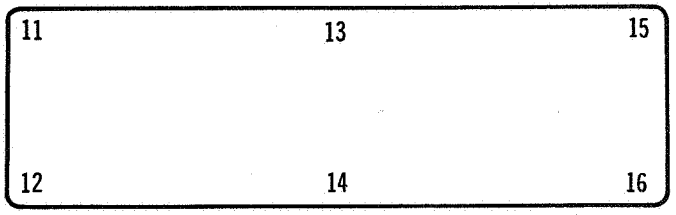

PANEL NO.	REENTRY CYCLES (NO.)	COATING THICKNESS MILS/μm AT LOCATION															
		1	2	3	4	5	6	7	8	9	10	11	12	13	14	15	16
1	0	3.3/84	3.2/81	3.2/81	3.7/94	3.3/84	3.3/84	3.7/94	3.9/99	3.2/81	3.3/84	3.2/81	3.3/84	3.2/81	3.7/94	3.1/79	3.1/79
	200			6.1/157	5.6/143	6.1/157	6.1/157	5.3/136	5.2/133			4.7/119	4.0/101	5.1/130	5.2/133	3.9/99	4.1/104
2	0	3.1/79	3.1/79	3.9/99	3.5/89	3.3/84	3.1/79	3.2/81	3.5/89	3.3/84	3.5/89	3.3/84	3.3/84	3.6/91	3.1/79	3.2/81	3.3/84
	200			6.9/177	7.1/182	5.9/151	5.7/146	5.1/130	5.3/136			6.1/157	5.6/143	5.1/130	5.5/141	3.7/94	3.9/99
3	0	2.9/74	3.1/79	3.2/81	3.5/89	3.3/84	3.3/84	3.7/94	3.6/91	3.1/79	3.1/79	3.1/79	3.2/81	3.2/81	3.3/84	2.9/74	2.8/71
	200			7.3/187	7.1/182	5.6/143	5.9/151	4.8/121	4.5/114			5.7/146	6.0/154	7.3/187	5.9/151	4.4/111	4.7/119
5	0	3.1/79	3.2/81	3.6/91	3.6/91	3.5/89	3.3/84	3.6/91	3.6/91	3.2/81	3.3/84	3.2/81	3.3/84	3.6/91	3.2/81	3.1/79	3.3/84
	200			–	6.1/157	6.9/177	5.9/151	5.6/143	5.6/143			5.1/130	–	5.9/151	5.6/143	3.6/91	3.9/99
6	0	3.2/81	3.5/89	3.6/91	3.3/84	3.3/84	3.3/84	3.2/81	3.6/91	3.2/81	3.3/84	3.3/84	3.2/81	3.5/89	3.5/89	3.3/84	3.5/89
	200			6.5/167	6.7/172	5.6/143	5.9/151	5.9/151	5.6/143			5.5/141	5.5/141	5.9/151	4.8/121	3.7/94	3.9/99
7	0	3.1/79	2.9/74	3.3/84	3.6/91	3.7/94	3.5/89	3.5/89	3.2/81	3.3/84	3.2/81	3.2/81	3.2/81	3.2/81	3.5/89	3.1/79	3.1/79
	200	NOT MEASURED															
8	0	3.1/79	3.1/79	3.5/89	3.3/84	3.3/84	3.3/84	3.3/84	3.6/91	3.1/79	3.2/81	3.3/84	3.3/84	3.1/79	3.5/89	2.9/74	3.2/81
	200			6.3/162	6.4/164	5.9/151	5.3/136	4.3/109	4.4/111			5.9/151	5.3/136	5.3/136	4.5/114	3.7/94	3.7/99
9	0	3.2/81	3.2/81	3.6/91	3.9/99	3.2/81	3.2/81	3.2/81	3.5/89	3.1/79	3.2/81	3.3/84	3.5/89	3.5/89	3.6/91	3.3/84	3.2/81
	200			6.1/157	6.1/157	5.5/141	5.6/143	5.6/143	5.3/136			4.9/125	4.8/121	4.8/121	5.3/136	4.4/111	4.4/111

IV

DISCUSSION OF RESULTS

This program had a two fold objective of:

(1) Characterization and evaluation of fused slurry silicide coated columbium alloys for Space Shuttle heat shield applications with 100 flight reuse capability, and

(2) Fused slurry silicide coating process optimization and scale-up development for uniform and reproducible coating of full size columbium alloy heat shield panels.

The 100 reentry flight structural reuse capability of fused slurry silicide coated columbium alloy reentry heat shields was demonstrated and with a considerable margin of safety. Also the uniform and reproducible coating of rib and corrugation stiffened heat shield panels was verified by the coating and testing of 30 subsize panels and by coating 4 full size panels.

The results of experimental activities conducted during pursuit of the program objectives are discussed in the following paragraphs.

Characterization and Evaluation of Columbium Alloys - Five columbium alloys were evaluated in a series of evaluation tests to determine the optimum alloy for Space Shuttle heat shields. Evaluations included a weldability test, ductile to brittle transition temperature test, and mechanical property changes due to coating and reuse.

All five alloys successfully passed a welding test in which a circular weld was made on a restrained sheet of material and visually examined for cracking. The test as conducted was not severe because the thin gage sheet used warped thus relieving created weld stresses.

Ductile to brittle transition temperature (DBTT) tests were conducted as a measure of fabricability. The DBTT is the temperature below which a metal fails in a brittle manner and above which it fails in a ductile manner. Because of the many factors which can cause increases in DBTT, a low DBTT is desired. When the DBTT is room temperature, or above, fabrication requiring bending and welding becomes very difficult and at times almost impossible. The high DBTT for the WC-3015 alloy would make fabrication and handling of thin gage heat shields very difficult. The moderately low DBTT for the B-66 alloy is not as low as desired because slight variations in chemistry or annealing temperature could raise the DBTT above room temperature. The other three alloys, Cb-752, FS-85, and C-129Y,

have DBTT's that are low enough to allow variations in the parameters that affect DBTT and still remain below room temperature.

The effects of coating and reuse on the mechanical properties of the five columbium alloys were determined. The coating caused no loss of ultimate or yield strength for any of the five alloys. There was a loss in tensile elongation for all alloys, but the only drastic losses were for WC-3015 and B-66 which were 80 and 90%, respectively. The WC-3015 was the only alloy to show a large loss ($\sim$ 35%) in strength due to reentry cycling. The room temperature strength of the WC-3015 decreased to the same strength levels as the other alloys after reentry cycling. Defecting produced a loss of strength at room temperature on the average of about 30% for all alloys except the WC-3015 which showed essentially no loss due to defecting and reentry cycling up to the exposure times (50 cycles) used in these tests. The loss in R.T. strength due to defecting and subsequent reentry cycling for Cb-742, FS-85, C-129Y, and B-66 was gradually restored with increasing test temperature to 2400°F (1300°C) where defected and nondefected strengths were approximately the same. This restoration of strength must be related to ductility which increases with temperature. The lack of strength reduction, due to defecting for the WC-3015, is a very desirable property in an alloy. If ductility could be improved without losing the desirable attribute of defect tolerance, this alloy should receive more consideration for heat shield utilization.

Cb-752, FS-85, and C-129Y alloys were selected for further evaluation as miniature heat shield panels on the basis of their performance in the mechanical property reuse evaluation. The WC-3015 was not chosen because it has a high DBTT and a low tensile elongation after reuse cycling. The B-66 was not selected primarily because of the poorer performance in defect sensitivity tests; secondarily because of lack of availability.

Coating Study For Columbium Alloy C-129Y and FS-85 - This study was performed to select a coating chemistry for the C-129Y and FS-85 alloys that would offer better protectiveness than the R-512E (Si-20Cr-20Fe) coating which was developed for Cb-752. The basic conclusion was that the coating compositions which showed the most promist for increased life involved the chromium-iron modified coatings with higher than 20% chromium content. The best performing coating on FS-85 was Si-40Cr-20Fe and the best performing coating on C-129Y was Si-35Cr-20Fe. The decision was made not to change to the 35 or 40% Cr content coatings for the remainder of the program because the improvement in life was not considered

significant enough to warrant a change. Some chromium is lost during firing which reduces the life of the R-512E coating. Lower firing temperatures, shorter firinf times, higher pressures in the firing furnace and coverings or shields for parts during firing to prevent direct vapor loss of chromium are a few possibilities for reducing this loss.

Selection of Optimum Columbium Alloy for Reusable Heat Shield Applications - Selection of the optimum columbium alloy for reusable heat shields was made based on studies of the effects of multiple cycle reuse on coating emittance, coating chemistry and structure and structural integrity of heat shield panels. Results of emittance and coating chemistry/structure studies were used in conjunction with mechanical property data to make the preliminary selection of three alloys for heat shield structural studies.

Because of difficulties encountered in attaching thermocouples directly to the thin sheet samples, a new method using ultraviolet pyrometry was developed to determine the emittance. Temperature and emittance were calculated by iteration from the thermocouple infrared detector and the optical pyrometer outputs. Emittance was affected very slightly by reentry cycling or reuse. There is however an initial trend of lower emittance with increasing reuse but this stops around 20 cycles and increases from this point with continued cycling. Other emittance tests were conducted to determine if R-512E coatings applied from acrylic base slurries and modified (higher chromium content) coatings would affect emittance under reuse conditions. The coating produced from an acrylic based slurry showed the same emittance response to reentry cycling as the coating produced from the nitrocellulose base slurry. The modified R-512E (45Si-35Cr-20Fe) coating had a slightly lower emittance for the first 25 reentry cycles than the normal R-512E (60Si-20Cr-20Fe) coating. After 25 cycles the emittances were basically the same. It was thought that the higher chromium content would produce a coating with a higher emittance. The chromium content alone is apparently not totally responsible for any increases in emittance. It may well be the iron content or the combined chromium and iron content.

R-512E coated Cb-752, FS-85, C-129Y, B-66 and WC-3015 were examined with x-ray diffraction and x-ray fluorescence techniques to study the effects of reuse on coating surface chemistry. The major observation from the x-ray fluorescence studies was that the FS-85/R-512E system showed an increase in the chromium and iron coating modifiers on the surface while the C-129Y/R-512E system showed a

decrease in the modifiers. The other alloy/coating systems did not reveal much change in the surface concentration of the coating modifiers. $CrCb0_4$ was the only compound clearly identified by x-ray diffraction that was present on the surface of all alloy/coating systems. The B-66 and FS-85/R-512E system showed large increases in the $CrCb0_4$ concentration due to reentry exposure from 50 to 100 cycles. The Cb-752/R-512E system was the only alloy/coating system in which SiO_2 could be clearly detected. Electron microprobe examinations were limited to the FS-85, Cb-752, and C-129Y/R-512E systems. The major conclusion that can be drawn from the electron microprobe analysis is the excellent stability of the elements in the R-512E coating on FS-85 with respect to reentry cycling. This coating/alloy system should provide longer life because of this stability. The R-512E coating on Cb-752 showed the most shifting and moving of elements due to reentry cycling.

Test results from mechanical property studies, coating chemistry optimization studies, chemistry and structure studies, and emittance studies were reviewed to choose the three alloys most suitable for heat shield panel applications. The three columbium alloys selected were FS-85, Cb-752, and C-129Y. These alloys were coated with the R-512E coating and evaluated in the form of miniature, 1" x 4" (2.5 cm x 10 cm), rib stiffened heat shield panels to determine the alloy with the best reuse capability. The panels were subjected to temperature-pressure-stress profile conditions typical of those for a Space Shuttle reentry. A total of 1200 reentry cycle tests were performed. Seven panels were exposed for 100 cycles each. Three of the seven 100 cycle panels were exposed in the internal pressure environment. The testing on five panels was terminated prior to reaching 100 cycles due to equipment malfunctions and operator problems. The two remaining panels, which were the C-129Y alloy, failed structurally after 87 cycles each in the external pressure environment. The structural failures were brought about by coating failures on the ribs. The reason for the coating failures on the C-129Y panels is explained by a very thin coating on the rib edges. However, the coating failure does not mean immediate catastrophic structural failure. In this particular case the coating failures occurred in the most highly tension stressed area and a minimum of 50 reentry cycles, after noticeable oxidation, was required before structural integrity was affected. A comparison of panel average creep deflection rates showed the panels to have acceptable creep resistance. Panel deflection rates were determined from the portions of the testing of each panel which were not affected by overloading, operator error, or coating failures.

Based on the results of reuse testing of the miniature heat shield panels, there was not a clear cut choice of the best alloy for reentry heat shield panels. The results of all screening tests performed were reviewed and the FS-85 alloy was selected for the coating/alloy evaluations to be performed in the remainder of the program.

Structural Performance of Representative Panels With Intentional Coating Damage - The specimens used in this investigation were subsize FS-85 columbium alloy rib and corrugation stiffened heat shield panels. The panels were coated with a nominal 3.0 mils (75 μm) of R-512E coating; and, prior to reentry simulation, each panel was intentionally defected to simulate coating damage. An area of coating approximately 1/8" (0.32 cm) in diameter was removed by grit blasting. The number of defect sites varied from one to three per panel.

Most of the panels experienced fatigue failures prior to 100 reentry flights. Defecting on the stiffener side of the panels in the areas where the highest stresses are experienced and then exposing the panel to internal pressure reentry cycling was more critical than defecting on the skin and exposing the panel to external pressure reentry cycling. This is most likely due to tension stress and crack propagation versus compressive stresses that are predominant in the skin. All panels withstood static design loads (room and elevated temperature) just prior to the start of fatigue failures.

In order to have a reliable heat shield, fatigue life must be considered and allowed for in the design. The possibility of coating damage to the critical stiffening ribs must be considered. Should coating damage occur, a fatigue life of as low as 160,000 cycles at 10,000 psi (69 NM/m^2), (which is considered quite low) is possible. This suggests that fatigue strength, or life, may well become the critical design factor for coated columbium heat shielding.

The performance of all of the defected panels, considering the acoustic condition and defect size utilized, showed that FS-85 columbium alloy heat shields are quite tolerant of local coating damage. No immediate catastrophic failures occurred. Even under the severe acoustic conditions and worst case defect location, the defected heat shields survived a minimum of 20 reentry flights.

Reuse Life Studies of R-512E Coated FS-85 Columbium Alloy Heat Shield Panels - This study was performed to determine the total structural life of columbium alloy (FS-85) rib stiffened heat shield panels and to establish how long the panels would maintain structural integrity after incipient coating degradation.

Subsize 3 x 12" (7.5 x 30 cm) rib stiffened FS-85 columbium alloy heat shield panels coated with 3.0 mils (75 μm) of R-512E coating, were utilized in this reuse

life study. Profile test conditions of temperature, pressure, and stress represented reentry flight for a Space Shuttle Orbiter.

Eight panels were subjected to flight simulation; each of the panels was exposed for 200 cycles. Creep and elastic deflections were monitored during testing; the creep rate decreased 50% after about 120 cycles. The elastic deflections started to decrease at about the same time. The decrease in elastic and creep deflections indicates a strengthening of the base metal which can best be explained by slight increases in the interstitial content, resulting from slight leakage of oxygen through the coating at the base of the coating microcracks.

The reproducibility of the optimized fused slurry silicide coating process and coating quality were demonstrated to be excellent. Evidence of the first incipient coating failure for the eight panels tested did not become apparent until after 66 flight simulation cycles. Two panels showed no evidence of coating failures until after 200 flight simulation cycles had been completed. All incipient coating failures, which occurred prior to 176 flight simulation cycles, were edge failures. One surface failure occurred after 176 flight simulation cycles.

Times to incipient coating failures were examined statistically utilizing Weibull distribution. Rank tables were used because of the small sample size.

Median rank values for the incipient times to failure were plotted on Weibull probability paper. The Weibull plot clearly shows a mixed distribution consisting of two segments. The first segment indicating random occurrence of failures and at approximately 156 reentry cycles coating wearout becomes the predominant mechanism of failure. The proportion of the population which showed random failures is estimated at 60%. The estimated time at which wearout failures would initiate if there were no random failures is 80 reentry cycles. The relatively high percentage of random incipient coating failures indicates that a significant increase in reliability could be realized if the edge coating process were further improved.

Structural life for seven of the eight panels exceeded 200 reentry cycles for the test conditions employed. The one structural failure was a fatigue failure which occurred during the last acoustic exposure after the panel had been reentry cycled 200 times. The panel had successfully passed 176 complete flight simulations. The fatigue failure started at a coating failure site on one of the rib stiffeners. This coating failure site was first evident after 176 reentry cycles. Other edge incipient coating failures (some of which occurred at 66 reentry cycles), had no effect on structural integrity up to 200 reentry cycles. Based on the results of

the eight panels tested, 100 flight structural life for R-512E coated FS-85 rib stiffened heat shield panels is a certainty.

Coating Process Optimization and Scale-Up Studies for Rib Stiffened Heat Shield Panels - This study was conducted to optimize a slurry, or slurries, so that full size 20 x 20" (50 x 50 cm) rib stiffened panels could be coated uniformly and reproducibly. The basic R-512E (Si-20Cr-20Fe) metal powder composition was used throughout the study.

Thirty-two slurry compositions were evaluated, using 6" (12.2 cm) long stainless steel strips on the basis of dripping and drying rates, coating thickness, coating uniformity top to bottom, streaking, sagging, and edge pull back. Twenty-seven of the slurries used an acrylic resin for a binder and five slurries used the nitrocellulose lacquer. The nitrocellulose lacquer based slurries were closely related to the system utilized prior to this program. They were found to be more consistent and satisfactory in their behavior than those which used the acrylics. The acrylic resin base slurries offered higher green strength, faster dipping rates, and were subject to less edge pull back. The thirty-two compositions were screened to six: three acrylic based and three nitrocellulose based. The six slurries were evaluated on the same basis as the thirty-two, but using larger 2" x 20" (5 cm x 50 cm) long, stainless steel strips. Slurry stability problems were discovered with the acrylic based slurries. The viscosity was found to change significantly with time and appeared to related to a reaction between the acrylic binder and thixotropic additives. Other additives were evaluated for the acrylic slurries, and slurry evaluations were continued on large 20" x 20" (50 cm x 50 cm) specimens. The stability problem still existed, and a nitrocellulose based slurry designated C-5 was chosen for further study on full size panel mockups.

The possible variations in coating chemistry at the slurry stage obtained with the dipping process and C-5 slurry were determined by coating a 20 x 20" (50 x 50 cm) flat stainless steel mockup. The green coating was then selectively removed from 2" (5 cm) square areas in nine locations on the panel. The coating powder obtained was analyzed for chromium and iron by x-ray fluorescence techniques. The iron content was found to vary from 19.0 to 20.0%, chromium from 19.5 to 22%, and silicon from 58.6 to 61.0%. Since the normal slurry composition is 60% Si, 20% Cr, and 20% Fe, the analyzed values indicate the effectiveness of the viscosity additives in minimizing relative settling of the metal powders.

A full size rib stiffened stainless steel panel which was dip coated in the

C-5 slurry picked up an average weight of 20.8 mg/cm^2; this was within the goal of 19 $\pm$3 mg/cm^2. The weight range, as determined by Dermitron NDT, was 19 to 22 mg/cm^2. Uniformity was further studied using columbium alloy (Cb-752) rib stiffened panel segments. These segments were dip coated, diffusion treated, and examined for coating uniformity. Uniformity was good except for the edges. Edge coating methods were evaluated, and eventually a method of applying a bead of slurry directly to the edges was developed. A paint striping tool was found to be adequate for applying the bead of slurry. Cb-752 samples were dip coated and evaluated by slow cycle oxidation testing at one atmosphere in the as-dipped, oversprayed edge, and beaded edge conditions. The results of these tests showed a life improvement factor of 50 for the edge beaded specimens. Columbium alloy (Cb-752) panel segments which were evaluated using the edge bead coating were found to have slow cycle, one atmosphere lives in excess of 100 cycles.

Five subsize, 3 x 12" (7.5 x 30 cm), rib stiffened FS-85 heat shield panels were used to verify the effectiveness and reproducibility of the coating produced from the optimized C-5 slurry and application process. These panels were evaluated by simultaneous simulation of temperature, pressure, and stress conditions representing a Space Shuttle Orbiter reentry. Acoustic simulation of the lift-off environment was also performed. Panels were evaluated up to 100 reentry flight cycles. There was not one breakdown of coating produced by the environment to which the panels were subjected. Structural failures were experienced on all panels from fatigue resulting from the acoustic testing. The acoustic environment was designed to cause fatigue failures at approximately 100 flight cycles. Based on the results of the test, the fatigue life at 10,000 psi (69 MN/m^2) is between 650,000 and 760,000 cycles.

As final verification of the coating application process, two full size 20 x 20" (50 x 50 cm) rib stiffened FS-85 columbium alloy heat shield panels were coated. An average green coating weight of 24 mg/cm^2 was achieved with a range as determined by Dermitron NDT of 21 to 27 mg/cm^2. The edges of the panels were coated by the edge beading technique and diffusion treated for one hour at 2580°F (36h sec at 1420°C). After firing the panels, the coating was found to have local thickness variations that were within the program goal of $\pm$3 mg/cm^2. This is better than a 50% reduction in the $\pm$7 mg/cm^2 variation typical prior to this process optimization study.

Coating Process Optimization and Scale-Up Studies for Corrugation Stiffened Heat Shield Panels - This study was conducted to optimize a slurry or slurries so that full size 20 x 20" (50 x 50 cm) corrugation stiffened panels could be coated

uniformly and reproducibly. The basic R-512E (Si-20Cr-20Fe) metal powder composition was used throughout the study. Because of the restricted access of air to the inside of the corrugation, slurry drying rates between the outside and inside were different, thus a problem of unequal coating thickness was encountered. Other than some geometry considerations, this was the basic difference in coating between the rib stiffened panels and the corrugation stiffened panels.

The C-5 slurry was evaluated on a corrugated specimen and was found to produce a nonuniform coating on the interior of the corrugation, particularily near the acute angle at the weld.

During the time sub and full size rib stiffened panels were being coated with the C-5 slurry, the stability problem with the acrylic base slurry was solved by using a high solids content slurry and by substituting acrylic resin for the thixotropic agents. An acrylic based slurry with a resin content of 40% and with only a minor amount of MPA as an agglomerate preventive was developed which was stable and produced excellent coating uniformity results on 2 x 20" (5 x 50 cm) long stainless steel strips. Single faced stainless steel corrugated specimens 2.4" wide x 18" long (6 x 46 cm) with a corrugation pitch of 1.2" (3 cm) and a corrugation height of 0.55" (1.4 cm) were used for further evaluation of the acrylic slurry. Poor coating uniformity and unequal thickness from inside to outside was revealed. The use of vacuum drying was evaluated as a means to accelerate drying of the slurry in the interior of the corrugations to improve coating thickness. Vacuum drying produced excellent results.

Other slurry control methods were investigated in an attempt to eliminate the vacuum drying. Higher MPA concentrations and additions of wetting agents to improve coating uniformity were evaluated. A wetting agent "Post 4" essentially eliminated coating uniformity problems, but caused excessive slurry stability problems; the ability of the slurry to suspend the coating powders was completely lost in less than one week. The higher MPA concentration greatly improved coating uniformity; but even with some flow-out, which occurred during firing, the uniformity was considered marginal and the procedure of vacuum drying was retained.

Single faced corrugated FS-85 panel segments 3 x 4" (7.5 x 10 cm) were coated with an acrylic slurry designated A-32, examined and found to have excellent coating uniformity. Slow cycle one atmosphere oxidation tests were conducted using these panel segments. There were no signs of coating failures on the insides of the corrugations, indicating good coating coverage.

Five subsize, 3 x 12" (7.5 x 30 cm), corrugation stiffened FS-85 heat shield panels were used to verify the effectiveness and reproducibility of the coating produced from the A-32 slurry and application process. Some difficulties were encountered with the vacuum drying procedure: blistering occurred because it was more difficult to control the vacuum when larger quantity of parts were processed. The vacuum drying was dropped in favor of longer air drying with the corrugations in a horizontal position.

These five panels were tested under the same conditions as the rib stiffened panels. Two small areas of coating breakdown occurred on the weld of one panel after 44 cycles of reentry testing but did not lead to, or cause any, structural failure of the panel. There were no indications of coating breakdown on the interior of the corrugations. The fatigue life of the corrugated panels was slightly better than that of the rib stiffened panels, but still falling under 760,000 cycles at 10,000 psi (69 MN/m^2). This difference might be expected because the thin edge of the rib stiffener would surely offer a better site for initiation of a fatigue crack than the flat continuous portion of the corrugation.

As final verification of the coating application process, two full size 20 x 20" (50 x 50 cm) corrugation stiffened FS-85 columbium alloy heat shield panels were coated. An average green coating weight of 27.7 mg/cm^2 was achieved with a range, as determined by Dermitron NDT, of 26 mg/cm^2 to 29 mg/cm^2. The side edges of the panels were coated using the edge beading process while the ends were redipped to a depth of approximately 1/8" (0.32 cm). The panels were diffusion treated for one hour at 2580°F (36h/sec at 1420°C). After firing, the panels had coating thickness distributions, that ranged from 20 mg/cm^2 to 23 mg/cm^2, well within the program goal of ± 3 mg/cm^2.

V

CONCLUSIONS

(1) The R-512E(Si-20Cr-20Fe) fused slurry silicide coating has repeatedly demonstrated the ability to provide reliable protection on columbium specimens and panels when exposed to 100 simulated reentry cycles.

(2) Beyond the initial small change in mechanical properties due to coating, the R-512E coated columbium alloy's mechanical properties are not affected significantly by 100 simulated reuse cycles.

(3) R-512E coated FS-85 specimen mechanical properties and panel structural integrity are not hypersensitive to the local removal of coating but the strength properties and life are reduced with exposure and are dependent on location.

(4) R-512E coated FS-85 demonstrated better overall reuse properties than R-512E coated Cb-752, C-129Y, B-66 or WC-3015.

(5) The total hemispherical emittance on the five R-512E coated columbium alloys studied in this program was not significantly affected by 100 simulated reentry cycles.

(6) Coating processes were developed so that either nitrocellulose lacquer or acrylic resin based slurries can be used for the uniform application of R-512E coating to specimens and full size columbium heat shield panels.

(7) R-512E hardware coating uniformity of $\pm$15% is now possible compared to $\pm$30% prior to slurry and process optimization.

(8) Improved R-512E coating life can be achieved by using a slightly higher processing temperature 2620°F and a shorter processing time, 30 minutes instead of the normal 1 hour at 2580°F and by increasing the chromium content of the R-512E coating from 20 to 40%.

(9) Application of a bead of slurry to the edges of columbium specimens and structural configurations prior to firing increases the life before incipient coating failure by several times and changes the failure mode from predominantly edge to one of wear out.

(10) A 200 plus simulated reentry and lift-off cycle life has been demonstrated for coated FS-85 which represents a sizable safety margin beyond the 100 reentry reuse requirement established at the beginning of the program.

VI

RECOMMENDATIONS

Following is a list of areas discovered during the course of this program which need more investigation and are recommended here for future studies.

(1) Determination of the effects of high gas flow rates on the emittance of fused slurry silicide coated columbium under multiple reuse conditions.

(2) Develop design fatigue properties for fused slurry silicide coated columbium and determine the fatigue requirements for coated columbium heat shielding.

(3) Further explore methods or techniques of application of slurry edge coating for improved reliability.

(4) Improve or develop columbium heat shield designs and/or thermal protection systems for multiple reuse hypersonic vehicles which will be more tolerant of the degradation associated with local coating failures.

VII

REFERENCES

1) Johnson, L. G., "The Median Ranks of Sample Values in their Population with an Application to Certain Fatigue Studies," Research Laboratories, General Motors Corporation, Detroit, Michigan.

APPENDIX A
MECHANICAL PROPERTY DATA

Appendix A contains the mechanical property data for each specimen used in determining the effect of coating, coating damage, and reuse.

Cb-752 COLUMBIUM ALLOY

SPECIMEN NUMBER	SURFACE CONDITION	REENTRY EXPOSURE (CYCLES)	TENSILE TEST TEMPERATURE (°F)/(°C)	ELONGATION	BASELINE (1)		EFFECTIVE (2)		BASELINE (1)		EFFECTIVE (2)	
					Ftu (PSI)	Fty (PSI)	Ftu (PSI)	Fty (PSI)	Ftu MN m^2	Fty MN m^2	Ftu MN m^2	Fty MN m^2
C86	BARE	0	R.T.	28.0	79,000	64,500			545	445		
C67			R.T.	28.0	80,000	60,500			552	417		
C41			R.T.	28.0	79,000	59,500			545	410		
				AVERAGE	79,300	61,500			547	424		
C12			2000/1100	37.0	30,700	23,900			212	165		
C64			2000/1100	38.0	34,000	22,800			234	157		
C76			2000/1100	51.0	31,000	22,500			214	155		
				AVERAGE	31,900	23,100			220	159		
C59	COATED		R.T.	20.0	70,378	51,866	82,415	60,688	485	358	568	418
C62			R.T.	18.5	69,389	51,104	81,249	59,907	478	352	560	413
C80			R.T.	20.5	68,453	49,980	80,548	58,710	472	345	555	405
				AVERAGE	69,400	51,000	81,400	59,800	479	352	561	412
C63			1400/760	9.0	42,264	27,124	49,540	31,794	291	187	342	219
C70			1400/760	9.0	45,868	30,364	53,908	35,686	316	209	372	246
C74			1400/760	8.5	41,217	23,462	48,256	27,469	284	162	333	189
				AVERAGE	43,100	27,000	50,600	31,700	297	186	349	219
C65			2000/1100	11.0	31,967	24,934	37,428	29,194	220	172	258	201
C71			2000/1100	13.0	31,375	23,760	36,636	27,744	216	164	253	191
C75			2000/1100	10.0	34,379	24,167	40,923	28,767	237	167	282	198
				AVERAGE	32,600	24,300	38,300	28,600	225	168	264	197
C92			2400/1300	13.0	23,301	20,235	27,088	23,524	161	140	187	162
C72			2400/1300	7.0	24,345	24,345	28,295	28,295	168	168	195	195
C78			2400/1300	-	21,491	20,262	25,039	23,608	148	140	173	163
				AVERAGE	23,000	21,600	26,800	25,100	159	149	185	173
C69			2600/1425	17.0	17,537	16,545	20,695	19,524	121	114	143	135
C73			2600/1425	47.5	15,294	13,109	17,820	15,275	105	90	123	105
C79			2600/1425	47.5	16,142	12,727	18,873	14,880	111	88	130	103
				AVERAGE	16,300	14,100	19,100	16,600	112	97	132	114

(1) PROPERTIES BASED ON BEFORE COATING DIMENSIONS
(2) PROPERTIES BASED ON REMAINING BASE METAL

Cb-752 COLUMBIUM ALLOY

SPECIMEN NUMBER	SURFACE CONDITION	REENTRY EXPOSURE (CYCLES)	TENSILE TEST TEMPERATURE (°F)/(°C)	ELONGATION	BASELINE (1)		EFFECTIVE (2)		BASELINE (1)		EFFECTIVE (2)	
					Ftu (PSI)	Fty (PSI)	Ftu (PSI)	Fty (PSI)	Ftu MN m^2	Fty MN m^2	Ftu MN m^2	Fty MN m^2
C22	COATED	50	R.T.	19.0	64.083	49.005	82.961	63.440	442	338	572	437
C11			R.T.	37.0	65.433	48.852	87.735	65.503	451	337	605	451
C27			R.T.	18.0	65.342	49.165	84.600	63.655	450	339	583	439
				AVERAGE	65.000	49.000	85.100	64.200	448	338	587	443
C15			1400/760	11.0	38.384	21.049	49.478	27.133	265	145	341	187
C23			1400/760	10.0	42.276	25.366	55.357	33.214	291	175	381	229
C45			1400/760	10.0	42.511	26.451	55.035	34.244	293	182	379	236
				AVERAGE	41.100	24.300	53.300	31.500	283	168	368	217
C17			2000/1100	8.5	29.371	20.113	38.192	26.154	203	139	263	180
C24			2000/1100	11.0	30.874	22.399	39.553	28.696	213	154	272	198
C52			2000/1100	9.0	25.974	19.881	33.777	25.854	179	137	233	178
				AVERAGE	28.700	20.800	37.200	26.900	198	143	256	185
C19			2400/1300	14.0	18.568	17.076	24.318	22.365	128	118	168	154
C25			2400/1300	12.0	17.813	16.443	23.683	21.862	123	113	163	151
C53			2400/1300		19.462	17.604	25.037	22.652	134	121	173	156
				AVERAGE	18.600	17.000	24.400	22.300	128	117	168	154
C21			2600/1425	21.0	13.824	12.749	17.818	16.432	95	88	123	113
C26			2600/1425	21.0	14.003	12.024	18.046	15.496	97	83	124	107
C61			2600/1425	30.0	17.606	13.834	22.654	17.799	121	95	156	123
				AVERAGE	15.100	12.900	19.500	16.600	104	89	134	114
C28		100	R.T.	18.0	63.429	48.194	86.157	65.462	437	332	594	451
C88			R.T.	–	–	–	–	–	–	–	–	–
C89			R.T.	–	–	–	–	–	–	–	–	–
				AVERAGE	63.429	48.200	86.200	65.500	437	332	594	451
C14			1400/760	10.0	39.598	24.419	55.011	33.923	273	168	379	234
C29			1400/760	10.0	39.334	26.017	53.163	35.163	271	179	367	242
C31			1400/760	10.0	38.227	24.682	51.052	32.962	264	170	352	227
				AVERAGE	39.100	25.000	53.100	34.000	270	172	366	234
C13			2000/1100	10.0	23.103	17.483	31.463	23.810	159	120	217	164
C85			2000/1100	8.5	30.023	20.823	41.012	28.444	207	144	283	196
C87			2000/1100	10.0	28.995	22.552	39.606	30.804	200	155	273	212
				AVERAGE	27.400	20.300	37.400	27.700	189	140	258	191
C30			2400/1300	15.0	18.547	15.555	24.822	20.819	128	107	171	144
C60			2400/1300	13.0	20.227	15.960	27.621	21.795	139	110	190	150
C82			2400/1300	13.0	21.743	18.119	30.032	25.027	150	125	207	173
				AVERAGE	20.200	16.500	27.500	22.500	139	113	190	155
C81			2600/1425		14.877	12.290	20.431	16.877	103	85	141	116
C83			2600/1425	–	13.712	12.755	18.727	17.420	95	88	129	120
C84			2600/1425	–	14.072	12.473	19.271	17.081	97	86	133	118
				AVERAGE	14.200	12.500	19.500	17.100	98	85	134	118

(1) PROPERTIES BASED ON BEFORE COATING DIMENSIONS
(2) PROPERTIES BASED ON REMAINING BASE METAL

Cb-752 COLUMBIUM ALLOY

SPECIMEN NUMBER	SURFACE CONDITION	REENTRY EXPOSURE (CYCLES)	TENSILE TEST TEMPERATURE (°F)/(°C)	ELONGATION	BASELINE (1)		EFFECTIVE (2)		BASELINE (1)		EFFECTIVE (2)	
					Ftu (PSI)	Fty (PSI)	Ftu (PSI)	Fty (PSI)	Ftu MN m^2	Fty MN m^2	Ftu MN m^2	Fty MN-m^2
C1	COATING & DEFECTED	5	R.T.	2.0	52,040	48,630	60,990	57,000	359	335	420	393
C2			R.T.	1.0	47,990	47,990	56,780	56,780	331	331	391	391
C3			R.T.	1.0	49,940	48,900	58,840	57,620	344	337	406	397
				AVERAGE	50,000	48,500	58,900	57,100	345	334	406	394
C34			1400/760	9.0	44,509	23,474	51,913	27,379	307	162	358	189
C36			1400/760	9.0	44,825	24,450	53,124	28,977	309	169	366	200
C50			1400/760	9.0	40,779	23,815	48,054	28,064	281	164	331	194
				AVERAGE	43,400	23,900	51,000	28,100	299	165	352	194
C4			2000/1100	1.0	26,560	24,860	29,130	31,120	183	171	201	215
C6			2000/1100	1.0	26,430	24,270	28,440	30,980	182	167	196	214
C7			2000/1100	2.0	28,890	24,600	28,950	33,990	199	169	200	234
				AVERAGE	27,300	24,500	28,800	32,000	188	169	199	221
C35			2400/1300	17.0	17,847	16,360	20,720	18,994	123	113	143	131
C49			2400/1300	18.0	19,899	18,345	23,267	21,449	137	126	160	148
C56			2400/1300	17.0	19,582	17,950	23,075	21,152	135	124	159	146
				AVERAGE	19,100	17,600	22,400	20,500	132	121	154	141
C96		10	R.T.	0	31,063	31,027	47,916	46,471	214	214	330	320
C98			R.T.	0	30,491	30,003	46,352	45,610	210	207	320	314
C99			R.T.	0	31,637	31,247	47,603	47,016	218	215	328	324
				AVERAGE	31,100	30,800	47,300	46,400	214	212	326	320
C51			1400/760	8.0	42,925	26,750	52,641	32,805	296	184	363	226
C54			1400/760	8.0	41,853	25,376	51,964	31,506	289	175	358	217
C35			1400/760	8.0	41,980	23,859	51,154	29,073	289	165	353	200
				AVERAGE	42,300	25,300	51,900	31,100	292	174	358	214
C8			2000/1100	8.0	30,530	23,870	37,960	29,690	211	165	261	205
C9			2000/1100	11.0	30,420	24,240	37,420	29,820	210	167	258	206
C10			2000/1100	9.0	29,470	22,180	36,440	27,430	203	153	251	189
				AVERAGE	30,100	23,400	37,300	28,000	208	161	257	200
C38			2400/1300	18.0	20,503	19,345	25,598	24,153	141	133	176	167
C39			2400/1300	18.0	18,419	17,103	22,372	20,774	127	118	154	143
C40			2400/1300	24.0	18,140	16,576	22,318	20,394	125	114	154	141
				AVERAGE	19,000	17,675	23,400	21,800	131	122	161	150

Cb-752 COLUMBIUM ALLOY

SPECIMEN NUMBER	SURFACE CONDITION	REENTRY* EXPOSURE (CYCLES)	TENSILE TEST TEMPERATURE (°F)/(°C)	ELONGATION	BASELINE (1)		EFFECTIVE (2)		BASELINE (1)		EFFECTIVE (2)	
					Ftu (PSI)	Fty (PSI)	Ftu (PSI)	Fty (PSI)	Ftu MN/m^2	Fty MN/m^2	Ftu MN/m^2	Fty MN/m^2
C11	COATED & DEFECTED	50	R.T.	1.0	49,490	47,760	64,340	62.090	341	329	444	428
C12		50	R.T.	1.0	44,180	44,180	57,180	57,180	305	305	394	394
C13		50	R.T.	2.0	53,620	47,590	69,400	66,600	370	328	479	425
				AVERAGE	49,100	46,500	63,600	60,300	339	321	439	416
C32		50	1400/760	3.0	36,309	25,983	47,780	34,191	250	179	329	236
C42		50	1400/760	1.0	35,577	31,130	35,993	31,494	245	215	248	217
C47		50	1400/760	2.0	30,604	26,280	40,084	34,420	245	215	248	217
				AVERAGE	34,200	27,800	41,300	33,700	236	192	285	232
C14		50	2000/1100	7.0	30,590	23,640	39,600	30,600	211	163	273	211
C15		50	2000/1100	7.0	29,640	23,530	38,540	29,980	204	162	266	207
C16		50	2000/1100	8.0	29,670	22,460	39,030	29,554	205	155	269	204
				AVERAGE	30,000	23,200	39,100	30,040	207	160	269	207
C33		50	2400/1300	11.0	20,210	18,906	26,404	24,700	139	130	182	170
C46		50	2400/1300	16.0	20,375	18,465	27,255	24,700	140	127	188	170
C48		50	2400/1300	–	20,558	18,237	26,987	23,941	142	126	186	165
				AVERAGE	20,400	18,500	26,900	24,400	140	128	185	168

(1) PROPERTIES BASED ON BEFORE COATING DIMENSIONS

(2) PROPERTIES BASED ON REMAINING BASE METAL

*INTERNAL PRESSURE EXPOSURE

C-129Y COLUMBIUM ALLOY

SPECIMEN NUMBER	SURFACE CONDITION	REENTRY EXPOSURE (CYCLES)	TENSILE TEST TEMPERATURE (°F)/(°C)	ELONGATION	BASELINE (1)		EFFECTIVE (2)		BASELINE (1)		EFFECTIVE (2)	
					Ftu (PSI)	Fty (PSI)	Ftu (PSI)	Fty (PSI)	Ftu MN/m^2	Fty MN/m^2	Ftu MN/m^2	Fty MN/m^2
Y14	BARE	0	R.T.	24.0	90,000	67,000		-	621	462		-
Y24			R.T.	23.0	90,000	70,500		-	621	486		-
Y79			R.T.	24.0	91,000	70,500		-	627	486		-
				AVERAGE	90,300	69,300			623	488		
Y21			2000/1100	23.0	33,100	25,900			228	179		
Y89			2000/1100	23.0	35,100	26,200			230	174		
Y97			2000/1100	15.0	33,300	25,300			230	174		
				AVERAGE	33,800	25,800			233	178		
Y39	COATED		R.T.	18.0	78,033	60,269	93,503	72,218	538	416	645	498
Y45			R.T.	18.0	77,823	58,871	93,440	70,565	537	406	644	487
Y51			R.T.	16.5	78,013	59,271	93,431	71,131	538	409	644	490
				AVERAGE	77,900	59,500	93,400	71,300	538	410	644	492
Y38			1400/760	10.0	54,027	33,523	65,038	40,355	373	231	448	278
Y43			1400/760	10.0	52,863	33,320	63,441	39,987	364	230	437	276
Y48			1400/760	8.0	53,686	33,515	64,050	33,985	370	231	442	234
				AVERAGE	53,500	33,400	64,200	38,100	369	231	442	263
Y40			2000/1100	3.0	35,949	29,237	43,013	35,089	248	202	297	242
Y44			2000/1100	3.0	35,906	29,921	42,961	35,800	248	206	291	247
Y49			2000/1100	3.5	34,865	27,575	41,777	33,042	240	190	288	228
				AVERAGE	35,600	28,900	42,600	34,600	245	199	294	239
Y41			2400/1300	2.0	26,688	22,457	32,127	27,034	184	155	222	186
Y46			2400/1300	2.5	25,141	23,324	29,870	27,710	173	161	206	191
Y50			2400/1300	1.5	26,907	24,874	32,147	29,718	186	171	222	205
				AVERAGE	26,200	23,600	31,400	28,200	181	163	217	194
Y42			2600/1425	36.0	17,308	16,667	20,771	20,002	119	115	143	138
Y47			2600/1425	57.0	17,143	16,190	20,542	19,400	118	112	142	134
Y52			2600/1425	40.0	15,867	14,597	19,012	17,491	109	101	131	121
				AVERAGE	16,800	15,800	20,100	19,000	116	109	139	131

(1) PROPERTIES BASED ON BEFORE COATING DIMENSIONS
(2) PROPERTIES BASED ON REMAINING BASE METAL

C-129Y COLUMBIUM ALLOY

SPECIMEN NUMBER	SURFACE CONDITION	REENTRY EXPOSURE (CYCLES)	TENSILE TEST TEMPERATURE (°F)/(°C)	ELONGATION	BASELINE (1)		EFFECTIVE (2)		BASELINE (1)		EFFECTIVE (2)	
					Ftu (PSI)	Fty (PSI)	Ftu (PSI)	Fty (PSI)	Ftu MN m^2	Fty MN m^2	Ftu MN m^2	Fty MN m^2
Y12	COATED	50	2600/1425	16.0	73,317	58,795	92,628	73,324	506	405	639	506
Y36			2600/1425	16.0	75,229	60,020	94,558	75,441	519	414	652	520
Y58			2600/1425	16.0	74,375	59,595	92,767	74,332	513	411	640	513
				AVERAGE	74,600	59,500	93,300	74,400	514	410	643	513
Y13			1400/760	10.0	48,720	31,497	60,624	39,137	336	217	418	270
Y37			1400/760	10.0	50,648	32,717	63,054	40,730	349	226	435	281
Y59			1400/760	9.0	52,381	35,238	65,333	43,951	361	243	450	303
				AVERAGE	50,600	33,200	63,000	41,300	349	229	434	285
Y15			2000/1100	8.0	30,174	24,302	37,632	31,556	208	174	259	218
Y54			2000/1100	8.0	29,155	24,189	36,433	30,227	201	167	251	208
Y60			2000/1100	7.5	33,237	26,394	41,696	33,111	229	182	287	228
				AVERAGE	30,900	25,300	38,600	31,600	213	174	266	218
Y16			2400/1300	10.0	24,245	22,969	30,351	28,754	167	158	209	198
Y55			2400/1300	13.0	24,063	22,969	29,902	28,453	166	158	206	197
Y61			2400/1300	12.0	21,533	20,795	26,482	25,575	148	143	183	176
				AVERAGE	23,300	22,200	28,900	27,600	160	153	199	190
Y35			2600/1425	50.0	17,422	17,099	21,853	21,448	120	118	151	148
Y56			2600/1425	62.0	16,774	16,129	21,002	20,194	116	111	145	139
Y62			2600/1425	56.0	17,867	17,554	22,243	21,852	123	121	153	151
				AVERAGE	17,400	16,900	21,700	21,200	120	117	150	146
Y18		100	R.T.	10.0	72,415	58,697	93,571	75,846	499	405	645	523
Y63			R.T.	11.0	72,516	58,510	93,088	75,110	500	403	642	518
Y69			R.T.	11.0	71,125	59,532	91,498	76,584	490	410	631	528
				AVERAGE	72,000	58,900	92,700	75,800	496	406	639	523
Y20			1400/760	6.0	46,854	30,392	60,408	39,184	323	210	417	270
Y64			1400/760	7.0	48,673	33,482	62,353	42,892	336	231	430	296
Y91			1400/760	7.0	48,973	30,016	63,139	38,698	338	207	435	267
				AVERAGE	48,200	31,300	62,000	40,300	332	216	427	278
Y22			2000/1100	9.0	35,550	28,534	45,637	36,629	245	197	315	253
Y65			2000/1100	8.0	34,118	27,356	43,617	34,972	235	189	301	291
Y92			2000/1100	9.0	35,078	27,092	45,126	34,852	242	187	311	240
				AVERAGE	34,900	27,700	44,800	35,500	241	191	309	245
Y23			2400/1300	18.0	23,635	21,559	30,541	27,857	163	149	211	192
Y67			2400/1300	24.0	22,013	19,261	28,085	24,574	152	133	194	169
Y93			2400/1300	22.0	23,496	21,487	30,099	27,525	162	148	208	190
				AVERAGE	23,000	20,800	29,600	26,700	159	143	204	184
Y25			2600/1425	47.0	17,090	14,833	22,085	19,168	118	102	152	132
Y68			2600/1425	67.0	15,623	13,308	19,668	16,754	108	92	136	116
Y94			2600/1425	74.0	16,449	13,919	21,208	17,945	113	96	146	124
				AVERAGE	16,400	14,000	21,000	18,000	113	97	145	124

(1) PROPERTIES BASED ON BEFORE COATING DIMENSIONS

(2) PROPERTIES BASED ON REMAINING BASE METAL

C-129Y COLUMBIUM ALLOY

SPECIMEN NUMBER	SURFACE CONDITION	REENTRY EXPOSURE (CYCLES)	TENSILE TEST TEMPERATURE (°F)/(°C)	ELONGATION	BASELINE (1)		EFFECTIVE (2)		BASELINE (1)		EFFECTIVE (2)	
					Ftu (PSI)	Fty (PSI)	Ftu (PSI)	Fty (PSI)	Ftu MN m^2	Fty MN m^2	Ftu MN m^2	Fty MN m^2
Y1	COATED	5	R.T.	3.0	51,210	48,150	61,950	58,250	353	332	427	402
Y2			R.T.	2.0	53,160	50,240	63,690	60,190	367	346	439	415
Y3			R.T.	2.0	50,610	44,390	60,640	53,190	349	306	418	367
				AVERAGE	51,700	47,600	62,110	57,200	356	328	428	394
Y26			1400/760	2.0	40,882	34,494	49,133	41,455	282	238	339	286
Y28			1400/760	4.0	48,071	36,132	57,598	43,292	331	249	397	298
Y81			1400/760	2.0	35,106	30,091	42,062	36,053	242	207	290	249
				AVERAGE	41,400	33,600	49,600	40,300	285	232	342	278
Y4			2000/1100	–	–	–	–	–	–	–	–	–
Y6			2000/1100	1.0	32,280	29,850	38,850	35,940	223	206	268	248
Y7			2000/1100	1.0	27,180	26,210	32,710	31,540	187	181	226	217
				AVERAGE	29,700	28,000	35,800	33,740	205	193	247	232
Y27			2400/1300	8.0	21,519	18,671	25,822	22,404	148	129	178	154
Y80			2400/1300	14.0	24,003	22,898	28,803	27,476	166	158	199	189
Y82			2400/1300	16.0	24,247	21,915	29,008	26,219	167	151	200	181
				AVERAGE	23,300	21,200	27,900	25,400	161	146	192	175
Y83		10	R.T.	0	45,158	44,227	65,308	63,962	311	305	450	441
Y84			R.T.	0	45,179	44,161	65,473	63,998	312	304	451	441
Y85			R.T.	0	45,272	44,728	65,481	64,695	312	308	451	446
				AVERAGE	45,200	44,400	65,400	64,200	312	306	451	443
Y29			1400/760	3.0	45,523	35,806	53,017	43,616	300	247	366	301
Y31			1400/760	2.0	38,143	36,540	46,779	44,813	263	252	323	309
Y74			1400/760	2.0	36,634	33,420	45,005	41,057	253	230	310	283
				AVERAGE	39,400	35,300	48,300	43,200	272	243	333	298
Y8			2000/1100	1.0	24,190	24,020	29,830	29,670	167	166	206	205
Y9			2000/1100	3.0	32,740	29,240	40,080	35,800	226	202	276	247
Y10			2000/1100	3.0	32,800	26,180	40,520	32,340	226	181	279	223
				AVERAGE	29,900	26,500	36,800	32,600	206	183	254	225
Y30			2400/1300	11.0	22,722	19,298	27,680	23,509	157	183	191	162
Y73			2400/1300	16.0	24,319	21,634	29,772	26,485	168	149	205	183
Y75			2400/1300	14.0	23,653	22,875	28,860	27,911	163	158	199	192
				AVERAGE	23,600	21,300	28,800	26,000	163	147	199	179

(1) PROPERTIES BASED ON BEFORE COATING DIMENSIONS
(2) PROPERTIES BASED ON REMAINING BASE METAL

C-129Y COLUMBIUM ALLOY

SPECIMEN NUMBER	SURFACE CONDITION	REENTRY EXPOSURE* (CYCLES)	TENSILE TEST TEMPERATURE (°F)/(°C)	ELONGATION % – IN.	BASELINE (1)		EFFECTIVE (2)		BASELINE (1)		EFFECTIVE (2)	
					Ftu (PSI)	Fty (PSI)	Ftu (PSI)	Fty (PSI)	Ftu MN/m^2	Fty MN/m^2	Ftu MN/m^2	Fty MN/m^2
Y11	COATED & DEFECTED	50	R.T.	2.0	45,760	41,840	56,760	51,890	315	288	391	358
Y12		50	R.T.	1.0	46,880	46,880	59,290	59,290	323	323	409	409
Y13		50	R.T.	2.0	45,710	45,710	57,330	57,330	315	315	395	395
				AVERAGE	46,120	44,810	57,790	56,170	318	309	398	387
Y33		50	1400/760	1.5	31,758	30,796	39,759	38,554	219	212	274	266
Y71		50	1400/760	1.5	32,886	31,320	41,012	39,059	227	216	283	269
Y72		50	1400/760	1.5	32,311	31,370	40,295	39,122	223	216	278	270
				AVERAGE	32,300	31,200	40,400	38,900	223	215	278	268
Y14		50	2000/1100	5.0	34,700	27,440	43,280	34,230	239	189	298	236
Y15		50	2000/1100	4.0	34,940	28,320	44,100	35,740	241	195	304	246
Y16		50	2000/1100	3.0	36,700	30,130	45,950	37,720	253	208	317	260
				AVERAGE	35,450	28,130	44,440	35,930	244	194	306	248
Y70		50	2400/1300	–	20,973	19,739	26,060	24,527	145	136	180	169
Y32		50	2400/1300	22.0	23,672	19,354	29,636	24,229	163	133	204	167
Y34		50	2400/1300	22.0	22,332	20,066	26,931	24,199	154	138	186	167
				AVERAGE	22,300	19,700	27,500	24,300	154	136	190	168

(1) PROPERTIES BASED ON BEFORE COATING DIMENSIONS
(2) PROPERTIES BASED ON REMAINING BASE METAL
*INTERNAL PRESSURE EXPOSURE

FS-85 COLUMBIUM ALLOY

SPECIMEN NUMBER	SURFACE CONDITION	REENTRY EXPOSURE (CYCLES)	TENSILE TEST TEMPERATURE (°F)/(°C)	ELONGATION	BASELINE (1)		EFFECTIVE (2)		BASELINE (1)		EFFECTIVE (2)	
					Ftu (PSI)	Fty (PSI)	Ftu (PSI)	Fty (PSI)	Ftu MN/m^2	Fty MN/m^2	Ftu MN/m^2	Fty MN/m^2
F16	BARE	0	R.T.	21.0	90,000	70,000			621	483		
F13			R.T.	21.0	91,500	71,500			631	493		
F3			R.T.	21.0	88,500	67,500			610	465		
				AVERAGE	90,000	69,700			621	481		
F15			2000/1100	30.0	34,200	25,000			236	172		
F36			2000/1100	33.0	31,300	24,500			216	169		
F83			2000/1100	31.0	33,600	24,500			232	169		
				AVERAGE	33,000	24,700			228	170		
F58	COATED		R.T.	17.0	75,549	56,513	90,589	67,764	521	390	625	467
F65			R.T.	16.0	77,522	57,983	93.959	70,084	535	400	648	483
F72			R.T.	17.0	77,090	57,856	92,666	69,408	532	399	639	479
				AVERAGE	76,700	57,500	92,700	69,100	529	396	639	476
F59			1400/760	10.0	54,086	31,033	64,761	37,158	373	214	447	256
F63			1400/760	9.0	55,329	31,525	67,172	38,273	381	217	463	264
F68			1400/760	9.0	55,870	32,281	67,452	38,941	385	223	465	268
				AVERAGE	55,100	31,600	66,500	38,100	380	218	459	263
F60			2000/1100	10.0	35,703	25,277	43,271	30,634	246	174	298	211
F64			2000/1100	9.0	36,077	25,503	43,521	30,765	249	176	300	212
F69			2000/1100	10.0	37,684	26,501	45,454	31,966	260	183	313	220
				AVERAGE	36,500	25,800	44,100	31,100	252	178	304	214
F61			2400/1300	9.0	26,599	26,140	31,991	31,439	183	180	221	217
F66			2400/1300	7.5	26,434	23,053	31,839	27,767	182	159	220	191
F70			2400/1300	6.5	26,122	24,256	31,559	29,305	180	167	218	202
				AVERAGE	26,400	24,500	31,800	29,500	182	169	219	203
F67			2600/1425	50.0	17,416	15,239	21,072	18,438	120	105	145	127
F71			2600/1425	72.0	18,235	15,652	21,931	18,824	126	108	151	130
F62			2600/1425	47.0	17,151	12,942	20,722	15,635	118	89	143	108
				AVERAGE	17,600	14,600	21,200	17,600	121	101	146	121

(1) PROPERTIES BASED ON BEFORE COATING DIMENSIONS

(2) PROPERTIES BASED ON REMAINING BASE METAL

FS-85 COLUMBIUM ALLOY

SPECIMEN NUMBER	SURFACE CONDITION	REENTRY EXPOSURE (CYCLES)	TENSILE TEST TEMPERATURE (°F)/(°C)	ELONGATION	BASELINE (1)		EFFECTIVE (2)		BASELINE (1)		EFFECTIVE (2)	
					Ftu (PSI)	Fty (PSI)	Ftu (PSI)	Fty (PSI)	Ftu MN m^2	Fty MN m^2	Ftu MN m^2	Fty MN m^2
F26	COATED	50	R.T.	16.5	74,791	58,898	93,880	73,930	516	406	647	510
F31			R.T.	16.5	71,998	56,134	90,192	70,319	496	387	622	485
F74			R.T.	15.5	72,983	55,669	91,778	70,000	503	384	633	483
				AVERAGE	73,300	56,900	91,900	71,400	505	392	634	492
F27			1400/760	9.0	43,456	28,367	54,335	35,469	300	196	375	245
F32			1400/760	9.0	43,807	28,555	55,648	36,274	302	197	384	250
F76			1400/760	8.0	44,963	29,469	56,224	36,849	310	203	388	254
				AVERAGE	44,100	28,800	55,400	36,200	304	199	382	250
F28			2000/1100	15.0	29,246	25,286	36,571	31,619	202	174	252	218
F34			2000/1100	11.0	29,525	23,871	37,272	30,135	204	165	257	208
F77			2000/1100	11.0	30,416	24,333	38,034	30,438	210	168	262	210
				AVERAGE	29,700	24,500	37,300	30,700	205	169	257	212
F29			2400/1300	43.0	17,033	12,984	20,941	15,963	117	90	144	110
F56			2400/1300	47.0	19,045	15,299	23,995	19,275	131	105	165	133
F78			2400/1300	40.0	20,293	18,708	25,620	23,619	140	129	177	163
				AVERAGE	18,800	15,700	23,500	19,600	130	108	162	135
F30			2600/1425	40.0	20,529	17,924	25,718	22,455	142	124	177	155
F73			2600/1425	69.0	16,577	15,349	20,804	19,263	114	106	143	133
F79			2600/1425	31.0	17,220	14,669	21,783	18,556	119	101	150	128
				AVERAGE	18,100	16,000	22,800	20,100	125	110	157	139
F52		100	R.T.	15.0	69,454	52,017	88,955	66,612	479	359	613	459
F81			R.T.	15.0	71,491	53,776	93,159	70,075	493	371	642	483
F100			R.T.	15.0	72,282	54,212	93,353	70,015	498	374	644	483
				AVERAGE	71,100	53,300	91,800	68,900	490	368	633	475
F51			1400/760	7.5	43,994	27,173	57,471	35,497	303	187	396	245
F80			1400/760	7.0	41,740	24,597	53,291	31,403	288	170	367	217
F86			1400/760	7.0	43,490	27,936	57,098	36,678	300	193	394	253
				AVERAGE	43,100	26,600	56,000	34,500	297	183	386	238
F50			2000/1100	9.0	28,520	21,080	36,994	27,343	197	145	255	189
F55			2000/1100	11.0	29,516	22,361	37,880	28,697	204	154	261	198
F85			2000/1100	10.0	29,597	22,651	38,141	29,190	204	156	263	201
				AVERAGE	29,200	22,000	37,700	28,400	202	152	260	196
F49			2400/1100	19.0	22,669	21,007	29,213	27,071	156	145	201	186
F54			2400/1100	18.0	21,181	19,953	27,413	25,824	146	138	189	178
F84			2400/1100	16.5	22,605	21,650	29,524	28,277	156	149	204	195
				AVERAGE	22,200	20,900	28,700	27,000	153	144	198	186
F48			2600/1425	50.0	15,957	12,046	20,656	15,593	110	83	142	108
F53			2600/1425	43.0	16,702	13,720	21,436	17,608	115	95	148	121
F82			2600/1425	54.0	15,465	14,297	19,693	18,206	107	99	136	126
				AVERAGE	16,000	13,400	20,600	17,100	111	92	142	118

(1) PROPERTIES BASED ON BEFORE COATING DIMENSIONS

(2) PROPERTIES BASED ON REMAINING BASE METAL

FS-85 COLUMBIUM ALLOY

SPECIMEN NUMBER	SURFACE CONDITION	REENTRY EXPOSURE (CYCLES)	TENSILE TEST TEMPERATURE (°F)/(°C)	ELONGATION	BASELINE (1)		EFFECTIVE (2)		BASELINE (1)		EFFECTIVE (2)	
					Ftu (PSI)	Fty (PSI)	Ftu (PSI)	Fty (PSI)	Ftu MN m^2	Fty MN m^2	Ftu MN m^2	Fty MN m^2
F1	COATED & DEFECTED	5	R.T.	2.0	46,070	42,890	56,400	52,510	318	296	389	362
F2			R.T.	1.0	47,350	40,590	58,170	49,860	327	280	401	344
F3			R.T.	2.0	45,680	43,450	56,430	53,670	315	300	389	370
				AVERAGE	46,400	42,300	57,000	42,200	320	292	393	360
F14			1400/760	2.0	29,871	28,362	36,389	34,550	206	196	251	238
F21			1400/760	2.5	32,111	29,908	39,444	36,737	221	206	272	253
F25			1400/760	–	–	–	–	–	–	–	–	–
				AVERAGE	31,000	29,100	37,900	35,600	214	201	261	245
F4			2000/1100	–	22,110	22,110	27,070	27,070	152	152	187	187
F6			2000/1100	–	18,320	18,320	22,500	22,500	126	126	155	155
F7			2000/1100	–	18,320	18,320	22,510	22,510	126	126	155	155
				AVERAGE	19,600	19,600	24,080	24,080	135	135	165	165
F12			2400/1300	35.0	15,088	12,102	18,503	14,841	104	83	128	102
F17			2400/1300	13.0	18,228	17,260	22,510	21,315	126	119	155	147
F24			2400/1300	14.0	19,000	16,975	23,298	20,815	131	117	161	144
				AVERAGE	17,400	15,500	21,400	19,000	120	107	148	131
F87		10	R.T.	0	35,594	35,591	50,949	50,949	245	245	351	351
F88			R.T.	0	34,264	34,264	49,242	49,242	236	236	340	340
F89			R.T.	0	37,234	37,234	54,583	54,583	257	257	376	376
				AVERAGE	35,400	35,400	51,600	51,600	244	244	356	356
F9			1400/760	2.0	31,291	28,635	38,122	34,885	216	197	263	241
F11			1400/760	1.0	31,735	30,194	38,977	37,085	219	208	269	256
F19			1400/760	2.0	32,901	30,729	40,478	37,805	227	212	279	261
				AVERAGE	32,000	29,900	39,200	36,600	221	206	270	252
F8			2000/1100	–	18,560	12,560	15,590	15,590	87	87	107	107
F9			2000/1100	–	23,430	23,430	29,200	29,200	162	162	201	201
F10			2000/1100	–	22,630	22,630	28,150	28,150	156	156	194	194
				AVERAGE	19,500	19,500	24,300	24,300	134	134	168	168
F10			2400/1300	26.0	21,628	18,964	26,656	23,372	149	131	184	161
F18			2400/1300	27.0	22,279	18,922	27,361	23,238	154	130	189	160
F20			2400/1300	3.0	17,442	17,131	21,495	21,111	120	118	148	146
				AVERAGE	20,500	18,300	25,200	22,600	141	126	174	156

(1) PROPERTIES BASED ON BEFORE COATING DIMENSIONS

(2) PROPERTIES BASED ON REMAINING BASE METAL

FS-85 COLUMBIUM ALLOY

SPECIMEN NUMBER	SURFACE CONDITION	REENTRY EXPOSURE* (CYCLES)	TENSILE TEST TEMPERATURE (°F)/(°C)	ELONGATION	BASELINE (1)		EFFECTIVE (2)		BASELINE (1)		EFFECTIVE (2)	
					Ftu (PSI)	Fty (PSI)	Ftu (PSI)	Fty (PSI)	Ftu MN/m^2	Fty MN/m^2	Ftu MN/m^2	Fty MN/m^2
F11	COATING & DEFECTED	50	R.T.	1.0	57,640	54,150	72,770	68,360	397	373	502	471
F12		50	R.T.	–	52,670	52,670	66,900	66,900	363	363	461	461
F13		50	R.T.	5.0	66,170	55,480	83,880	70,320	456	383	578	485
				AVERAGE	58,800	54,100	74,500	68,500	406	373	514	472
F1		50	1400/760	1.0	27,334	25,626	33,713	31,606	188	177	232	218
F4		50	1400/760	1.0	29,217	27,771	36,041	34,256	201	191	249	236
F6		50	1400/760	1.0	35,638	30,060	44,732	37,730	246	207	308	260
				AVERAGE	30,600	27,800	38,200	34,500	211	192	263	238
F14		50	2000/110	–	–	–	–	–	–	–	–	–
F15		50	2000/1100	4.0	32,090	25,300	40,520	31,940	221	174	279	220
F16		50	2000/1100	–	–	–	–	–	–	–	–	–
				AVERAGE	32,100	25,300	40,500	31,940	221	174	279	220
F2		50	2400/1300	18.0	20,096	17,225	25,373	21,748	139	119	175	150
F5		50	2400/1300	–	19,311	17,728	24,334	22,340	133	122	168	154
F7		50	2400/1300	22.0	19,050	–	23,865	–	131	–	–	–
				AVERAGE	19,500	17,500	24,500	22,000	134	121	169	152

(1) PROPERTIES BASED ON BEFORE COATING DIMENSIONS

(2) PROPERTIES BASED ON REMAINING BASE METAL

*INTERNAL PRESSURE EXPOSURE

B-66 COLUMBIUM ALLOY

SPECIMEN NUMBER	SURFACE CONDITION	REENTRY EXPOSURE (CYCLES)	TENSILE TEST TEMPERATURE (°F)/(°C)	ELONGATION	BASELINE (1)		EFFECTIVE (2)		BASELINE (1)		EFFECTIVE (2)	
					Ftu (PSI)	Fty (PSI)	Ftu (PSI)	Fty (PSI)	Ftu MN/m^2	Fty MN/m^2	Ftu MN/m^2	Fty MN/m^2
B93	BARE	0	R.T.	27.0	99,500	80,000	–	–	686	552	–	–
B94			R.T.	27.0	99,000	79,000	–	–	683	545	–	–
B95			R.T.	27.0	99,500	79,500	–	–	686	548	–	–
				AVERAGE	99,300	79,500			685	548		
B83			2000/1100	44.0	37,200	34,900	–	–	256	241	–	–
B85			2000/1100	48.0	36,200	31,900	–	–	250	220	–	–
B89			2000/1100	47.0	36,600	31,900	–	–	252	220	–	–
				AVERAGE	36,700	32,900			253	227		
B16	COATED		R.T.	3.5	77,931	62,412	96,635	77,393	537	430	666	534
B29			R.T.	1.5	74,300	63,710	92,362	79,474	512	439	637	548
B30			R.T.	3.0	77,247	64,163	95,680	79,456	533	442	660	548
				AVERAGE	76,500	63,400	94,900	78,800	527	437	654	543
B17			1400/760	10.0	65,111	42,170	80,740	52,292	449	291	557	361
B21			1400/760	11.0	65,319	41,750	80,995	51,770	450	288	558	357
B25			1400/760	10.0	65,370	41,823	81,889	52,391	451	288	565	361
				AVERAGE	65,200	41,900	81,200	52,200	450	289	560	360
B18			2000/1100	8.0	40,143	37,133	49,683	45,957	277	256	343	317
B22			2000/1100	7.5	41,126	36,595	51,307	45,654	284	252	354	315
B26			2000/1100	8.0	42,102	37,231	52,630	45,540	290	257	363	314
				AVERAGE	41,100	37,000	51,200	46,100	284	255	353	315
B19			2400/1300	6.5	25,444	22,730	31,553	28,187	175	157	218	194
B23			2400/1300	4.0	24,910	23,914	30,772	29,541	172	165	212	204
B27			2400/1300	6.5	26,529	25,132	33,163	31,417	183	173	229	217
				AVERAGE	25,600	23,900	31,800	29,700	176	165	219	205
B20			2600/1425	17.0	13,898	12,203	17,235	15,133	96	84	119	104
B24			2600/1425	15.0	15,536	12,726	19,191	15,720	107	88	132	108
B28			2600/1425	24.0	13,901	11,271	17,697	14,349	96	78	122	99
				AVERAGE	14,400	12,100	18,000	15,100	99	83	124	104

(1) PROPERTIES BASED ON BEFORE COATING DIMENSIONS

(2) PROPERTIES BASED ON REMAINING BASE METAL

B-66 COLUMBIUM ALLOY

SPECIMEN NUMBER	SURFACE CONDITION	REENTRY EXPOSURE (CYCLES)	TENSILE TEST TEMPERATURE (°F)/(°C)	ELONGATION	BASELINE (1)		EFFECTIVE (2)		BASELINE (1)		EFFECTIVE (2)	
					Ftu (PSI)	Fty (PSI)	Ftu (PSI)	Fty (PSI)	Ftu MN m^2	Fty MN m^2	Ftu MN m^2	Fty MN m^2
B38	COATED	50	R.T.		63,844	62,119	84,122	81,848	440	428	580	564
B43			R.T.	1.0	68,988	62,871	90,657	82,619	476	433	625	570
B69			R.T.	1.0	70,196	62,135	91,787	81,247	484	428	633	560
				AVERAGE	67,700	62,400	88,900	81,900	467	430	613	565
B39			1400/760	9.0	59,445	36,446	78,961	48,410	410	251	544	334
B44			1400/760	9.0	61,577	39,952	82,746	53,686	425	275	570	370
B70			1400/760	9.0	62,353	38,287	83,783	51,446	430	264	578	355
				AVERAGE	61,100	38,200	81,800	51,200	421	263	564	353
B40			2000/1100	8.0	40,980	35,442	55,235	47,770	283	244	381	329
B45			2000/1100	8.0	42,015	36,849	55,499	48,675	290	254	383	337
			2000/1100		42,230	33,358	56,247	44,431	291	230	389	306
				AVERAGE	41,700	35,200	55,700	47,000	287	243	384	324
B41			2400/1300	17.0	23,305	22,565	31,413	30,415	161	156	217	210
B67			2400/1300	20.0	25,590	24,566	33,629	32,284	176	169	232	223
B72			2400/1300	18.0	18,915	18,239	24,794	23,908	130	126	171	165
				AVERAGE	22,600	21,800	29,400	28,900	157	150	203	199
B42			2600/1425	35.0	14,567	14,212	19,403	18,929	100	98	134	131
B68			2600/1425	39.0	15,428	14,889	20,608	19,889	106	103	142	137
B73			2600/1425	43.0	14,200	13,017	18,659	17,104	98	90	129	118
				AVERAGE	14,700	14,000	19,600	18,600	101	97	135	128
B47		100	R.T.	1.0	66,234	60,120	88,849	80,647	457	415	613	556
B58			R.T.	2.0	70,451	61,955	96,173	84,574	486	427	663	583
B81			R.T.	1.0	66,887	60,966	93,492	85,258	461	420	645	588
				AVERAGE	67,900	61,000	92,800	83,500	468	421	640	576
B48			1400/760	9.0	59,961	39,746	80,880	53,612	413	274	558	370
B59			1400/760	11.0	60,771	38,024	83,771	52,483	419	262	578	362
B82			1400/760	11.0	62,506	41,104	84,073	55,287	431	283	580	381
				AVERAGE	61,100	39,500	82,900	53,800	421	272	572	371
B49			2000/1100	7.0	40,064	32,051	56,202	44,962	276	221	388	310
B60			2000/1100	7.0	42,576	35,891	57,943	48,845	294	247	400	337
B84			2000/1100	7.0	40,915	35,271	55,684	48,003	282	243	384	331
				AVERAGE	41,200	34,400	56,600	47,300	284	237	390	326
B50			2400/1300	17.0	24,953	24,250	33,959	33,002	172	167	234	228
B51			2400/1300	20.0	22,366	22,006	30,728	30,232	154	152	212	208
B86			2400/1300	18.0	21,183	20,087	29,199	27,688	138	138	201	191
				AVERAGE	22,800	22,100	31,300	30,300	157	152	216	209
B57			2600/1425	35.0	13,826	13,489	18,546	18,093	95	93	128	125
B80			2600/1425	38.0	15,223	14,161	20,781	19,331	105	98	143	133
B88			2600/1425	32.0	14,385	13,307	19,701	18,224	99	92	136	126
				AVERAGE	14,500	13,700	19,700	18,500	100	94	136	128

(1) PROPERTIES BASED ON BEFORE COATING DIMENSIONS
(2) PROPERTIES BASED ON REMAINING BASE METAL

B-66 COLUMBIUM ALLOY

SPECIMEN NUMBER	SURFACE CONDITION	REENTRY EXPOSURE (CYCLES)	TENSILE TEST TEMPERATURE (°F)/(°C)	ELONGATION	BASELINE (1)		EFFECTIVE (2)		BASELINE (1)		EFFECTIVE (2)	
					Ftu (PSI)	Fty (PSI)	Ftu (PSI)	Fty (PSI)	Ftu MN/m^2	Fty MN/m^2	Ftu MN/m^2	Fty MN/m^2
B11	COATED & DEFECTED	5	1400/760	0	40,168	36,048	50,007	44,878	277	249	345	309
B13		5	1400/760	0	38,667	37,937	48,872	47,950	267	262	337	331
B35		5	1400/760	1.0	39,534	37,845	49,024	46,929	273	261	338	323
				AVERAGE	39,500	37,300	49,300	46,600	272	257	340	321
B34		5	2400/1300	4.0	22,835	21,430	28,606	26,845	157	148	197	185
B36		5	2400/1300	2.5	23,175	22,483	28,910	28,047	160	155	199	193
B12		5	2400/1300	17.0	23,149	21,725	29,063	27,275	160	150	200	188
				AVERAGE	23,000	21,900	28,900	27,400	159	151	199	189
B76		10	R.T.	0	29,918	29,918	45,617	45,617	206	206	315	315
B77		10	R.T.	0	31,797	31,797	48,608	48,608	219	219	335	335
B78		10	R.T.	–	30,544	30,544	48,077	48,077	211	211	331	331
				AVERAGE	30,800	30,800	47,400	47,400	212	212	327	327
B14		10	1400/760	0	37,762	34,801	49,633	45,740	260	240	342	315
B52		10	1400/760	0	33,218	32,526	42,872	41,979	229	224	296	289
B31		10	1400/760	2.0	33,069	32,697	43,465	42,977	228	225	300	296
				AVERAGE	34,700	33,300	45,300	43,600	239	230	312	301
B15		10	2400/1300	3.0	19,873	19,530	25,587	25,145	137	135	176	173
B51		10	2400/1300	3.5	22,430	22,080	29,091	28,636	155	152	201	197
B53		10	2400/1300	2.5	20,360	19,307	26,406	25,040	140	133	182	173
				AVERAGE	20,900	20,300	27,000	26,300	144	140	186	181
B32		50*	1400/760	1.0	32,060	32,060	42,826	42,826	221	221	295	295
B55		50*	1400/760	11.0	64,815	39,683	84,538	51,758	447	274	583	357
B66		50*	1400/760	10.0	63,198	40,340	82,836	52,874	436	278	571	365
				AVERAGE	53,400	37,400	70,100	49,200	368	258	483	339
B33		50*	2400/1300	14.0	24,811	23,925	33,047	31,867	171	165	228	220
B37		50*	2400/1300	11.0	25,455	25,273	34,103	33,860	176	174	235	233
B54		50*	2400/1300	11.0	32,401	30,505	42,691	40,193	223	210	294	277
				AVERAGE	27,600	26,600	36,600	35,300	190	183	252	243

(1) PROPERTIES BASED ON BEFORE COATING DIMENSIONS
(2) PROPERTIES BASED ON REMAINING BASE METAL
* INTERNAL PRESSURE EXPOSURE

WC-3015 COLUMBIUM ALLOY

SPECIMEN NUMBER	SURFACE CONDITION	REENTRY EXPOSURE (CYCLES)	TENSILE TEST TEMPERATURE (°F)/(°C)	ELONGATION	BASELINE (1)		EFFECTIVE (2)		BASELINE (1)		EFFECTIVE (2)	
					Ftu (PSI)	Fty (PSI)	Ftu (PSI)	Fty (PSI)	Ftu MN m^2	Fty MN m^2	Ftu MN m^2	Fty MN m^2
W41	BARE	0	R.T.	23.0	144,000	141,000			993	972		
W50			R.T.	23.0	142,000	135,000			979	931		
W44			R.T.	23.0	144,000	134,000			993	924		
				AVERAGE	143,300	136,700			988	943		
W47			2000/1100	90.0	38,500	37,900			265	261		
W72			2000/1100	75.0	43,400	–			299	–		
W94			2000/1100	92.0	40,000	36,800			276	254		
				AVERAGE	40,600	37,400			280	258		
W56	COATED		R.T.	–	119,407	110,030	156,544	144,250	823	759	1079	995
W57			R.T.	–	113,034	110,610	146,862	143,712	779	763	1013	991
W74			R.T.	6.0	113,550	104,452	151,904	139,734	783	720	1047	963
				AVERAGE	115,300	108,400	151,800	142,300	795	747	1046	981
W52			1400/760	2.0	78,136	60,984	103,166	80,520	539	420	711	555
W58			1400/760	2.5	69,655	65,302	89,389	83,802	480	450	616	578
W62			1400/760	3.0	74,701	64,448	96,057	82,873	515	444	662	571
				AVERAGE	74,200	63,600	96,200	82,400	512	438	663	568
W53			2000/1100	0	40,714	37,851	53,886	50,097	281	261	371	345
W59			2000/1100	0	28,218	–	37,261	–	195	–	257	–
W63			2000/1100	0	35,432	–	45,935	–	244	–	317	–
				AVERAGE	34,800	–	45,700	–	240	–	315	–
W54			2400/1300	0	28,254	–	37,217	–	195	–	257	–
W91			2400/1300	1.5	27,959	24,782	26,829	32,644	193	171	185	225
W64			2400/1300	1.0	28,230	–	36,372	–	195	–	251	–
				AVERAGE	28,100	24,800	36,800	32,600	194	171	254	225
W55			2600/1425	24.0	13,752	13,453	17,792	17,405	95	93	123	120
W61			2600/1425	17.0	12,318	11,994	16,307	15,878	85	83	112	109
W100			2600/1425	16.0	13,628	13,311	17,830	17,416	94	92	123	120
				AVERAGE	13,200	12,900	17,300	16,900	91	89	119	116

(1) PROPERTIES BASED ON BEFORE COATING DIMENSIONS
(2) PROPERTIES BASED ON REMAINING BASE METAL

WC-3015 COLUMBIUM ALLOY

SPECIMEN NUMBER	SURFACE CONDITION	REENTRY EXPOSURE (CYCLES)	TENSILE TEST TEMPERATURE (°F)/(°C)	ELONGATION	BASELINE (1)		EFFECTIVE (2)		BASELINE (1)		EFFECTIVE (2)	
					Ftu (PSI)	Fty (PSI)	Ftu (PSI)	Fty (PSI)	Ftu MN m^2	Fty MN m^2	Ftu MN m^2	Fty MN m^2
W32	COATED	50	R.T.	0	59,208	-	80,644	-	408	-	556	-
W39			R.T.	0	81,880	-	114,379	-	565	-	789	-
				AVERAGE	68,800		97,500		474		672	
W7			1400/760	1.0	68,504	57,809	92,149	77,763	472	399	635	536
W38			1400/760	2.0	69,892	66,911	98,549	94,345	481	461	679	651
W45			1400/760	1.0	66,099	64,729	95,118	93,147	456	446	656	642
				AVERAGE	68,200	63,100	95,300	88,400	470	435	657	610
W8			2000/1100	0	31,551	-	44,346	-	218	-	306	-
W34			2000/1100	0	23,132	-	31,589	-	159	-	218	-
W43			2000/1100	0	24,389	-	33,301	-	168	-	230	-
				AVERAGE	26,400		36,400		182		251	
W9			2400/1300	19.0	19,063	17,951	26,544	24,995	131	124	183	172
W35			2400/1300	0	18,694	-	25,399	-	129	-	175	-
W42			2400/1300	1.5	18,818	18,191	25,979	25,112	130	125	179	173
				AVERAGE	18,900	18,100	26,000	25,100	130	125	179	173
W33			2600/1425	52.0	12,251	11,937	16,914	16,480	84	82	117	114
W36			2600/1425	67.0	12,262	11,970	16,497	16,104	85	83	114	111
W40			2600/1425	58.0	10,624	10,302	14,795	14,347	73	71	102	99
				AVERAGE	11,700	10,900	16,100	15,600	81	75	111	108
W1		100	R.T.	0	63,000	-	93,618	-	434	-	645	-
W46			R.T.	0	71,838	-	109,426	-	495	-	754	-
W67			R.T.	0	74,964	-	110,561	-	517	-	767	-
				AVERAGE	69,900		104,500		482		721	
W2			1400/760	1.5	60,048	58,493	86,714	85,156	414	403	598	587
W48			1400/760	-	-	-	-	-	-	-	-	-
W69			1400/760	0	58,008	-	82,985	-	400	-	572	-
				AVERAGE	59,000	58,493	84,800		407	403	585	
W3			2000/1100	0	23,087	-	32,349	-	159	-	223	-
W49			2000/1100	0	17,197	-	25,260	-	119	-	174	-
W70			2000/1100	0	21,893	-	31,617	-	151	-	218	-
				AVERAGE	20,700		29,700		143		205	
W4			2400/1300	1	25,559	24,635	36,674	35,348	176	170	253	244
W65			2400/1300	-	-	-	-	-	-	-	-	-
W71			2400/1300	0	26,270	25,659	37,575	36,701	181	177	259	253
				AVERAGE	25,900	25,100	37,100	36,000	179	173	256	248
W6			2600/1425	87.0	15,176	14,569	21,640	20,775	105	100	149	143
W66			2600/1425	47.0	16,002	14,746	23,110	22,204	110	107	159	153
W73			2600/1425	-	-	-	-	-	-	-	-	-
				AVERAGE	15,600	14,600	22,400	21,500	108	101	154	148

(1) PROPERTIES BASED ON BEFORE COATING DIMENSIONS
(2) PROPERTIES BASED ON REMAINING BASE METAL

WC-3015 COLUMBIUM ALLOY

SPECIMEN NUMBER	SURFACE CONDITION	REENTRY EXPOSURE (CYCLES)	TENSILE TEST TEMPERATURE (°F)/(°C)	ELONGATION	BASELINE (1)		EFFECTIVE (2)		BASELINE (1)		EFFECTIVE (2)	
					Ftu (PSI)	Fty (PSI)	Ftu (PSI)	Fty (PSI)	Ftu MN/m^2	Fty MN/m^2	Ftu MN/m^2	Fty MN/m^2
W21	COATED & DEFECTED	5	1400/760	1.5	62,649	-	85,278	----	432	-	588	-
W22		5	1400/760	2.5	60,923	57,612	81,484	77,056	420	397	562	531
W25		5	1400/760	2.0	60,209	57,444	78,240	74,647	415	396	539	515
				AVERAGE	61,300	57,500	81,700	75,900	423	396	563	523
W20		5	2400/1300	27.0	23,721	23,417	30,952	30,555	164	161	213	211
W23		5	2400/1300	26.0	22,444	20,906	29,227	27,224	155	144	202	188
W24		5	2400/1300	0.5	24,632	24,295	33,129	32,675	170	168	228	225
				AVERAGE	23,600	22,900	31,100	30,100	163	158	214	208
W76		10	R.T.	0	37,045	37,045	58,953	-	255	255	406	406
W84		10	R.T.	0	63,460	63,460	101,026	-	438	438	697	697
W99		10	R.T.	0	34,766	34,766	55,931	-	240	240	386	386
				AVERAGE	45,100	45,100	72,000		311	311	496	496
W15		10	1400/760	1.5	63,015	62,375	84,924	84,924	434	430	592	586
W18		10	1400/760	1.0	56,762	56,128	76,458	75,618	391	387	527	521
W27		10	1400/760	1.5	60,652	60,039	81,301	80,480	418	414	561	555
				AVERAGE	59,900	59,500	81,200	80,300	413	410	560	554
W16		10	2400/1300	7.0	25,022	24,118	33,379	32,172	173	166	230	222
W26		10	2400/1300	6.5	26,312	25,700	35,269	34,449	181	177	243	238
W28		10	2400/1300	2.0	26,432	25,727	37,226	36,233	182	177	257	250
				AVERAGE	25,900	25,200	35,300	34,300	179	174	243	236
W11		50*	1400/760	1.0	59,101	56,044	84,170	79,810	408	386	580	550
W13		50*	1400/760	2.0	70,748	-	98,522	-	488	-	679	-
W14		50*	1400/760	1.0	58,655	56,224	92,131	88,310	404	389	635	609
				AVERAGE	62,800	56,100	91,600	84,060	433	387	632	580
W29		50*	2400/1300	-	21,475	-	29,317	-	148	-	202	-
W30		50*	2400/1300	0	21,134	-	30,305	-	146	-	209	-
W31		50*	2400/1300	0	24,881	-	33,890	-	172	-	234	-
				AVERAGE	22,500		31,200		155		215	

(1) PROPERTIES BASED ON BEFORE COATING DIMENSIONS

(2) PROPERTIES BASED ON REMAINING BASE METAL

*INTERNAL PRESSURE EXPOSURE